Society of Vertebrate Paleontology Memoir 8
Journal of Vertebrate Paleontology
Volume 27, Supplement to Number 2: 32–102, June 2007

CRANIOFACIAL ANATOMY OF *MAJUNGASAURUS CRENATISSIMUS* (THEROPODA: ABELISAURIDAE) FROM THE LATE CRETACEOUS OF MADAGASCAR

SCOTT D. SAMPSON*[,1] and LAWRENCE M. WITMER[2]
[1]Utah Museum of Natural History and Department of Geology and Geophysics, University of Utah, 1390 East Presidents Circle, Salt Lake City, UT 84112-0050; ssampson@umnh.utah.edu
[2]Department of Biomedical Sciences, College of Osteopathic Medicine, Ohio University, Athens, Ohio, 45701; witmer@oucom.ohiou.edu

ABSTRACT —Recent fieldwork in the Upper Cretaceous (Maastrichtian) Maevarano Formation, northwest Madagascar, has yielded important new skull material of the abelisaurid theropod, *Majungasaurus crenatissimus*. One of these specimens in particular—a virtually complete, disarticulated, and well preserved skull—greatly elucidates the craniofacial osteology of abelisaurids. Herein we describe the skull and lower jaws of this mid-sized theropod dinosaur. A number of features of the facial skeleton and cranium (as well as the postcranium) appear to result from increased levels of mineralization and ossification, which, at least in some instances, can be related directly to specific soft-tissue structures; examples include lacrimal-postorbital contact dorsal to the orbit, suborbital processes of the lacrimal and postorbital, presence of a mineralized interorbital septum, fused interdental plates, and mineralization of the overlying integument. Autapomorphic features include a highly derived nasal—greatly thickened and fused to its counterpart, with a large interior pneumatic chamber—and a median, 'dome'-like thickening of the frontals, which appear to have been variably pneumatized by a paranasal air sac. *Majungasaurus* also possesses a derived suite of skull morphologies, including: a rostrocaudally abbreviated, dorsoventrally deep, and transversely broad skull; an expanded occiput, likely associated with expanded cervical musculature; short-crowned dentition; and an enlarged external mandibular fenestra consistent with a moderate degree of intramandibular movement or accommodation. A number of characters, present on both the skull and postcranial skeleton, suggest a divergent mode of predation relative to other, non-abelisaurid theropods.

MALAGASY ABSTRACT (FAMINTINANA) —Ireo asa fikarohana natao tao amin'ny Fiforonanana Maevarano tamin'ny vanim-potoana Cretaceous Ambony (Maastrichtian) tany amin'ny faritra avaratr'andrefan'i Madagasikara dia nahitana taolan-karan-doha vaovao tena sarobidy tokoa izay an'ny abelisaurid theropod, *Majungasaurus crenatissimus*. Iray tamin'ireo taolana ireo dia nisongadina satria saika feno tanteraka na tsy nitambatra tsara intsony aza dia tena voatahiry tsara io taolan-doha io, ka nahahana nampiseho mazava tsara ny fiforonan'ny taolan'ny loha sy ny tavan'ny abelisaurids. Koa eto izahay dia manazava ny taolan-doha sy ny valan-dranon'ny theropod dia ireo theropod dinozaoro izay manana vatana tsy lehibe nefa tsy kely koa. Maro amin'ireo toetran'ny taolan'ny endrika sy ny loha (sy ny aorinan'ny loha) dia ohatry ny vokatry ny fitombon'ny fivontoan'ny mineraly sy ny taolana, izay, farafahakeliny ho an'reo karazany sasany, dia azo heverina ho misy fifandraisany amin'ny firafitr'ireo rakotra malefaka miavaka; ohatra ny fifandraisan'ny lacrimal-postorbital aoriana amin'ny lavaky ny maso, ny vohitry ny suborbital-n'ny lacrimal sy ny postorbital, ny fisian'ny fvontosan'ny mineraly interorbital septum, fitambaran'ny taolam-pisaka manelana ny nify, ary fivontosan'ny mineraly tegument anatiny mipetraka ambony. Ireo toetra autapomorphic dia ahitana ireo taolan'orona nisy fivoarana be, izay manome endrika matevina sy mitambatra amin'ny lafiny mifanila aminy, ka ny endrika anatiny dia malalaka afaka hitoeran'ny rivotra, sy mitondra vohitra afovoany toa mampitombo ny fahatevenan'ny taolan'andrina, izay toa milaza fa toa afaka nitoeran'ny rivotra noho ny paranasal izay kitapon-drivotra. *Majungasaurus* koa dia manana endriky ny fivoaran'ny karan-doha, ka anisan'izany ny fihenan'ny rostro aoriana, lalina ny faritra afovoany-aoriana, sy mivelatra ny sisin'ny karan-doha, mivelatra ny occiput, izay mampiseho ny toetra mafonja ny hozatry ny loha; boribory-fohy ny nify; ary mivelatra ny mandibular fenestra ivelany mifanaraka amin'ny fahafahan'ny fihetsehana na fandraisana ihany koa ny intramandibular. Maro amin'ireo toetra hita amin'ny karan-doha sy ny taolan'ny vatana dia afahana mamantatra ireo karazana fomba fihazana raha ampitahaina amin'ieo hafa dia ireo tsy abelisaurid theropods.

INTRODUCTION

Prior to the initiation of the joint Stony Brook University/University of Antananarivo Mahajanga Basin Project (MBP) in 1993, little was known of the skull of the abelisaurid theropod here referred to as *Majungasaurus crenatissimus*. Depéret (1896) erected a new theropod taxon, *Megalosaurus crenatissimus*, on the basis of six isolated specimens, including two teeth, all found in the Berivotra field area of the Mahajanga Basin, northwestern Madagascar. Lavocat (1955) described a partial theropod dentary from the Berivotra area, which he assigned to the same species, *M. crenatissimus*, while erecting a new genus, *Majungasaurus*.

Much later, Sues and Taquet (1979; see also Sues, 1980) described an oddly ornamented partial skull roof with domed frontals (MNHN.MAJ 4) recovered from these same deposits in the Mahajanga Basin. Based on the frontal 'dome,' these authors referred this specimen to Pachycephalosauria, erecting a new genus and species, *Majungatholus atopus*. Not only was *Majungatholus* the first pachycephalosaur to be recognized from Madagascar, it was also the only pachycephalosaur identified from a Gondwanan landmass. All other known pachycephalosaurs are restricted to Northern Hemisphere landmasses (Asia, Europe,

*Corresponding author.

and North America). Subsequent examinations of MNHN.MAJ 4 (Sampson et al., 1996a) identified several features not present in any pachycephalosaur (e.g., lack of radiating trabeculae in the 'dome;' 'dome' occurring wholly within the frontals rather than also incorporating the parietals; rugose ornamentation). Moreover, other derived characteristics (e.g., long, rostrally divided olfactory tract cavity) supported the notion that this fragmentary specimen is instead referable to Theropoda (Sampson et al., 1998).

The initial expedition of the MBP in 1993 yielded an isolated theropod premaxilla (FMNH PR 2008) with teeth indistinguishable from those previously assigned to *Majungasaurus crenatissimus* (Sampson et al., 1996b). Sampson and colleagues (1996b) documented several derived features on this specimen shared with Late Cretaceous Indian materials referred to Abelisauridae, and argued that *Majungasaurus* was referable to this clade. Several fragmentary Late Cretaceous theropod specimens from landmasses other than Madagascar have also been purported to resemble those of *M. crenatissimus*. These include isolated teeth and terminal phalanges from Egypt (Gemmellaro, 1921; Stromer and Weiler, 1930), isolated teeth from Argentina (Bonaparte and Powell, 1980), an incomplete tooth from India (Mathur and Srivastava, 1987), and a partial dentary from Morocco (Russell, 1996); a full list of referred specimens is included in Krause and colleagues' article (this volume).

MBP field efforts in 1996 resulted in a nearly complete, exceptionally preserved skull of a medium-sized abelisaurid theropod (FMNH PR 2100; Sampson et al., 1998; Fig. 1). The teeth in the premaxilla, maxilla, and dentary of this specimen are indistinguishable from the hundreds of isolated teeth recovered previously (Smith, this volume), and the premaxilla closely matches that of FMNH PR 2008. More significantly, a small, median 'dome' projecting dorsally from the fused frontals provides conclusive evidence that *Majungatholus atopus* is not a pachycephalosaur, as previously posited, but rather a theropod. Sampson and colleagues (1998) referred this new skull to *Majungatholus atopus*, retaining MNHN.MAJ 4 as the holotype. As detailed in Krause and colleagues (this volume), a reassessment of known abelisaurid materials has led us to resurrect the neotype dentary described by Lavocat (1955) and refer all known abelisaurid materials from the Maevarano Formation to *Majungasaurus crenatissimus*.

Although abelisaurid theropods had a broad geographic distribution, including India, Madagascar, South America, and Africa (Novas, 1997; Sampson et al, 1998; Carrano et al., 2002; Sereno et al., 2002, 2004; Wilson et al., 2003; Novas et al., 2004), the group remains poorly understood. Other than the specimens described herein, nearly complete skulls of abelisaurids are known only for the Late Cretaceous Argentine taxa *Abelisaurus* (Bonaparte and Novas, 1985), *Carnotaurus* (Bonaparte et al., 1990), and *Aucasaurus* (Coria et al., 2002). Sereno and colleagues (2004) briefly described a new abelisaurid taxon, *Rugops primus*, from the Cenomanian of Niger, northern Africa. The partial skull of *Rugops* includes the premaxilla, maxilla, nasal, lacrimal, prefrontal, frontal, and partial parietal. Numerous isolated craniofacial elements of abelisaurids have been reported from the Late Cretaceous of India (Huene and Matley, 1933; Chatterjee, 1978a; Chatterjee and Rudra, 1996), but, other than the holotype braincases, it has been difficult to ascribe these elements to a particular taxon since all were recovered as isolated finds. Novas and colleagues (2004) re-evaluated much of the Huene and Matley (1933) collection, and likewise concluded that, although specimens assigned to *Indosaurus* and *Indosuchus* certainly pertain to abelisaurids, the number of taxa and their taxonomy remain difficult to resolve. Wilson and colleagues (2003) described a partial skull and postcranium from India, erecting a new taxon, *Rajasaurus narmadensis*. Unfortunately, skull materials for *Rajasaurus* are limited to a single fragmentary braincase. In order to avoid confusion, for the purposes of this discussion we will refer to the Indian abelisaurid materials simply as the 'Lameta abelisaurids.' The names *Indosaurus*, *Indosuchus* and *Rajasaurus* will be used only when referring to the holotypic specimen in each case.

The present contribution reviews in detail the craniofacial anatomy of *Majungasaurus crenatissimus*, including element-by-element descriptions for the entire skull and lower jaws. In addition, we address several aspects that relate to specific soft-tissue systems—such as the brain endocast, inner ear, and pneumaticity—revealed by 3D visualization of CT scanning as well as more conventional bony correlates. The assessment of soft anatomy further encompasses mineralization of soft-tissue structures that are generally not preserved in theropod dinosaurs; these include the interorbital septum and, in a number of instances, overlying integumentary structures such as the dermis. Finally, we consider some of the functional implications of the highly derived skull anatomy of this basal theropod.

Institutional abbreviations—**AMNH**, American Museum of Natural History, New York, NY; **BMNH**, British Museum (Natural History), London; **BSP**, Bayerische Staatssammlung für Paläontologie und historische Geology, München, Germany; **BYU-VP**, Brigham Young University, Vertebrate Paleontology, Provo, UT; **CM**, Carnegie Museum, Pittsburgh, PA; **CV**, Sichuan Museum, Sichuan Province, China; **DINO**, Dinosaur National Monument, Utah; **FMNH**, Field Museum of Natural History, Chicago, IL; **GSI-IM**, Geological Survey of India, Calcutta; **IVPP**, Institute for Vertebrate Paleontology and Paleoanthropology, Beijing, China; **MACN**, Museo Argentino de Ciencias Naturales, Buenos Aires, Argentina; **MB**, Humboldt Museum für Naturkunde, Berlin; **MC**, Museo de Cipoletti, Rio Negro, Argentina; **MCF-PVPH**, Museo Municipal Carmen Funes, Paleontologia de Vertebrados, Plaza Huincul, Argentina; **MCZ**, Museum of Comparative Zoology, Harvard University, Cambridge, MA; **MNHN**, Muséum National de l'Histoire Naturelle, Paris; **MNN**, Musée National de Niger, Niamey; **MOR**, Museum of the Rockies, Bozeman, MT; **MUCPv**, Museo de Ciencias Naturales de la Universidad Nacional de Comahue, Neuquén, Argentina; **MUO**, Museum of the University of Oklahoma, Norman, OK; **MWC**, Museum of Western Colorado, Fruita, CO; **OUM**, Oxford University Museum, Oxford, UK; **OUVC**, Ohio University Vertebrate Collections, Athens, OH; **PVSJ**, Museo Provincial de San Juan, Argentina; **PVL**, Fondación Miguel Lillo, Tucumán, Argentina; **QG**, National Museum of Natural History, Bulawayo, Zimbabwe; **UA**, Université d'Antananarivo, Antananarivo, Madagascar; **SGM**, Société Geologique de Morocco, Rabat; **SMU**, Southern Methodist University, Dallas, TX; **TATE**, Tate Geological Museum, Casper, WY; **UCMP**, University of California Museum of Paleontology, Berkeley, CA; **UMNH**, Utah Museum of Natural History, Salt Lake City, UT; **USNM**, National Museum of Natural History, Smithsonian Institution, Washington, DC; **YPM**, Yale Peabody Museum, New Haven, CT.

Comparative Taxa and Specimens—The following specimens of theropod taxa were examined for the comparisons mentioned in this paper. All specimens were examined firsthand or as casts, except those indicated by an asterisk (of which only published materials and photographs were studied): *Abelisaurus comahuensis* (MC 11908); *Acrocanthosaurus atokensis* (MUO 8-0-S9; SMU 74646); *Allosaurus fragilis* (CM 11844, 21703; MCZ 3897; MOR 693; USNM 4734; UMNH VP 5814, 6000, 18046, 18047, 18048, 18050, 18055); *Aucasaurus garridoi* (MCF-PVPH 236); *Baryonyx walkeri* (BMNH R9951); *Carnotaurus sastrei* (MACN-CH 894); *Ceratosaurus dentisulcatus* (UMNH VP 5278; likely synonymous with *C. nasicornis*); *Ceratosaurus magnicornis* (MWC 1.1; likely synonymous with *C. nasicornis*); *Ceratosaurus nasicornis* (USNM 4735; BYU-VP 4838, 4853, 4908); *Carcharodontosaurus saharicus* (BSP 1922 X-46*; SGM Din-1, Din-3);

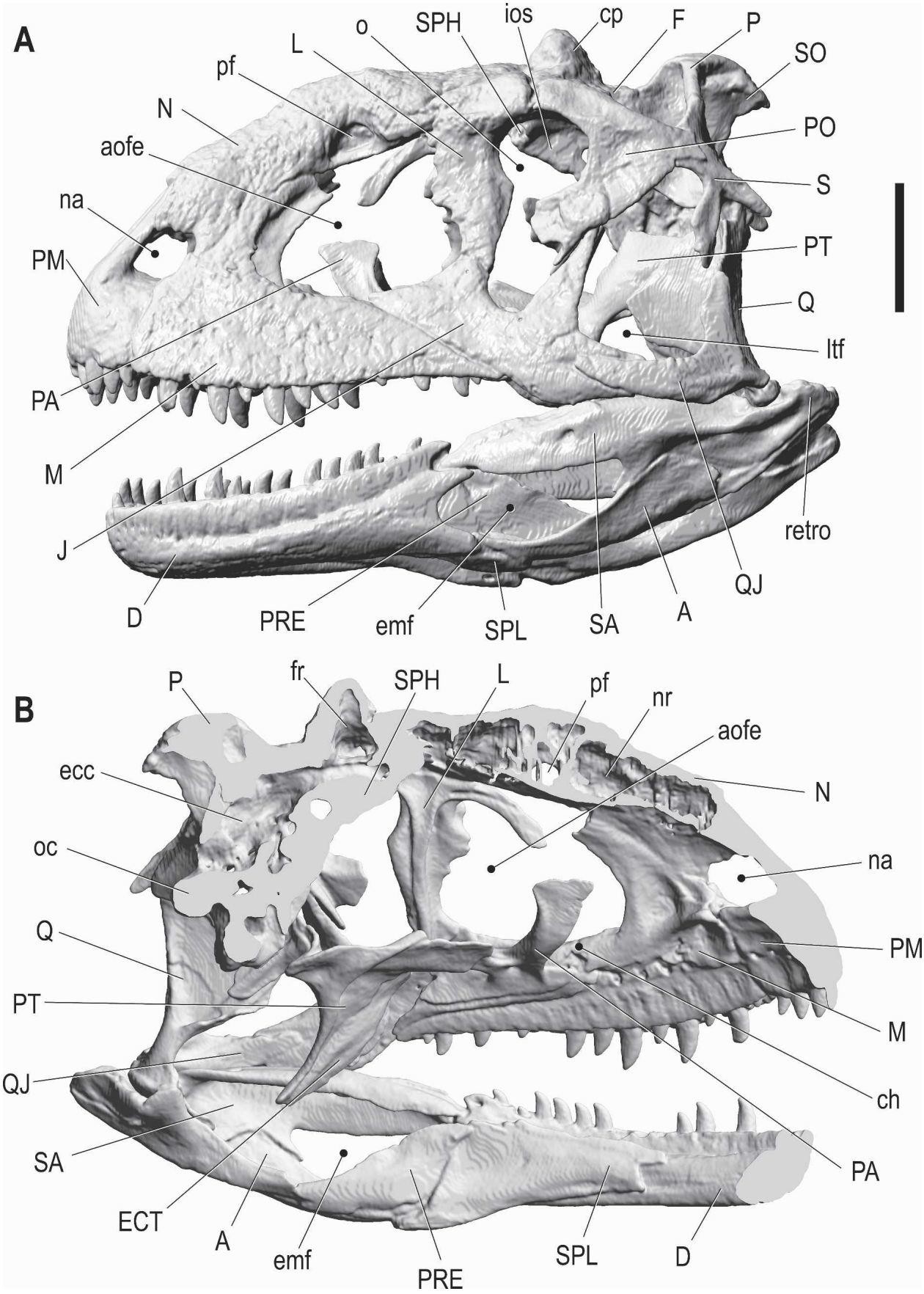

FIGURE 1. Skull and lower jaws of *Majungasaurus crenatissimus* (FMNH PR 2100) in the following views: **A**, **G**, left lateral; **B**, **I**, medial (of left side in sagittal section); **C**, **K**, dorsal; **D**, **L**, ventral; **E**, **M**, caudal; **F**, **N**, rostral; **H**, right lateral; **J**, dorsal of mandibles. **G–N** are stereopairs. Images derived from reconstructed axial CT scans of cast skull. Scale bars equal 10 cm. See Appendix 1 for abbreviations.

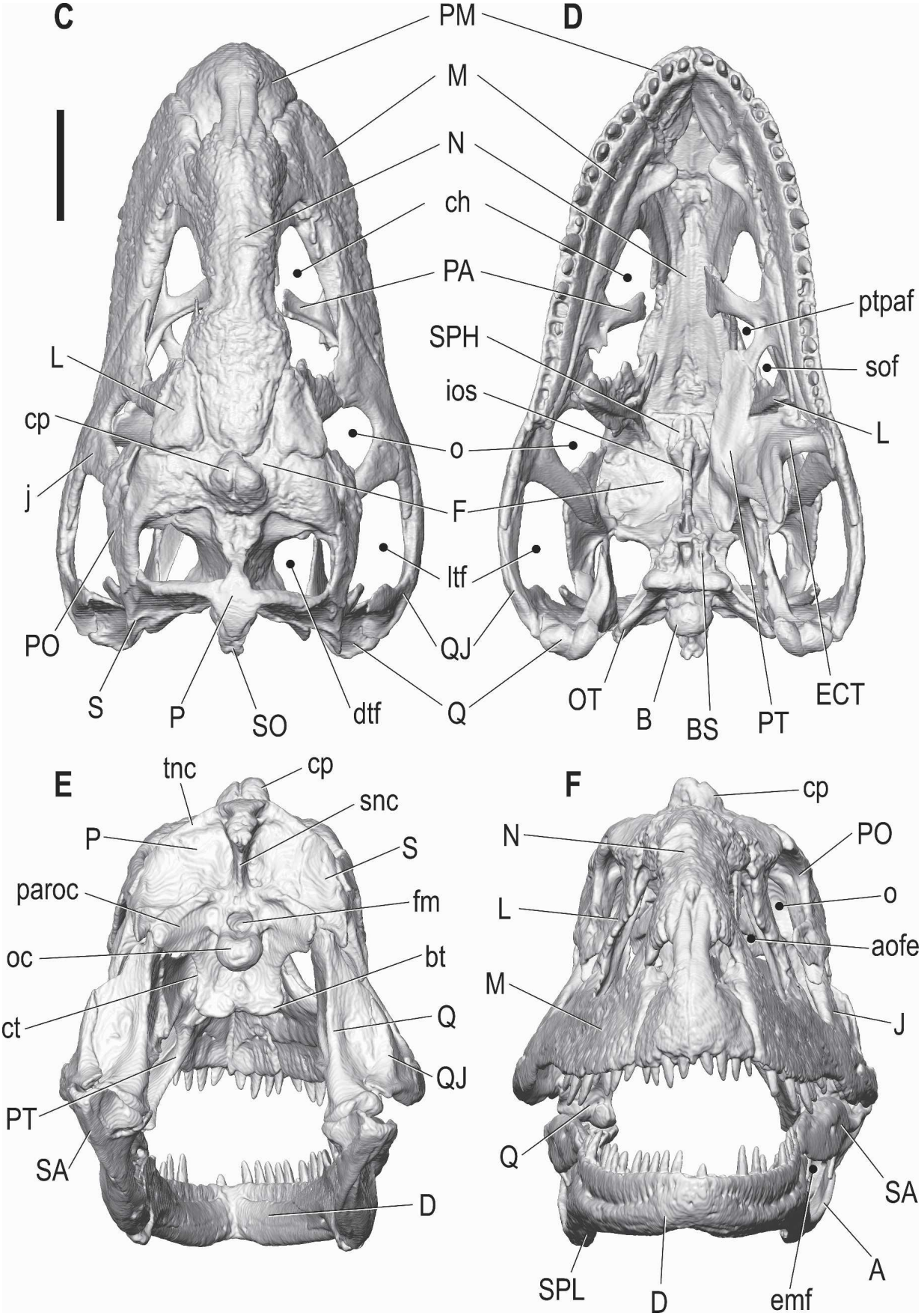
C
PM
M
N
ch
PA
L
cp
j
o
F
ltf
QJ
PO
S
P
SO
dtf
Q
D
ptpaf
SPH
sof
ios
L
OT
B
BS
PT
ECT
E
tnc
cp
snc
P
S
paroc
fm
oc
bt
ct
Q
QJ
PT
SA
D
F
cp
N
PO
o
L
aofe
M
J
Q
SA
A
SPL
D
emf

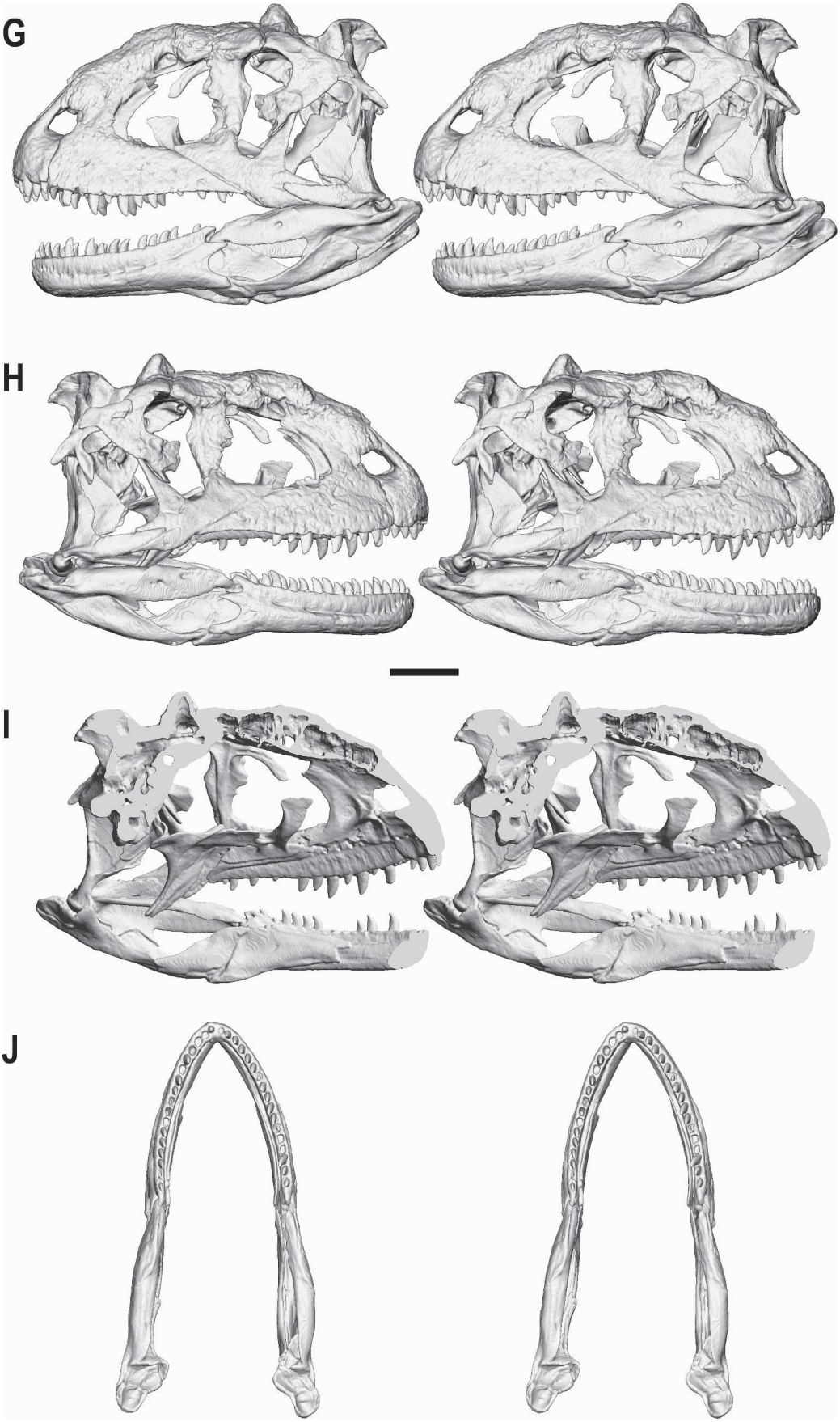
G
H
I
J

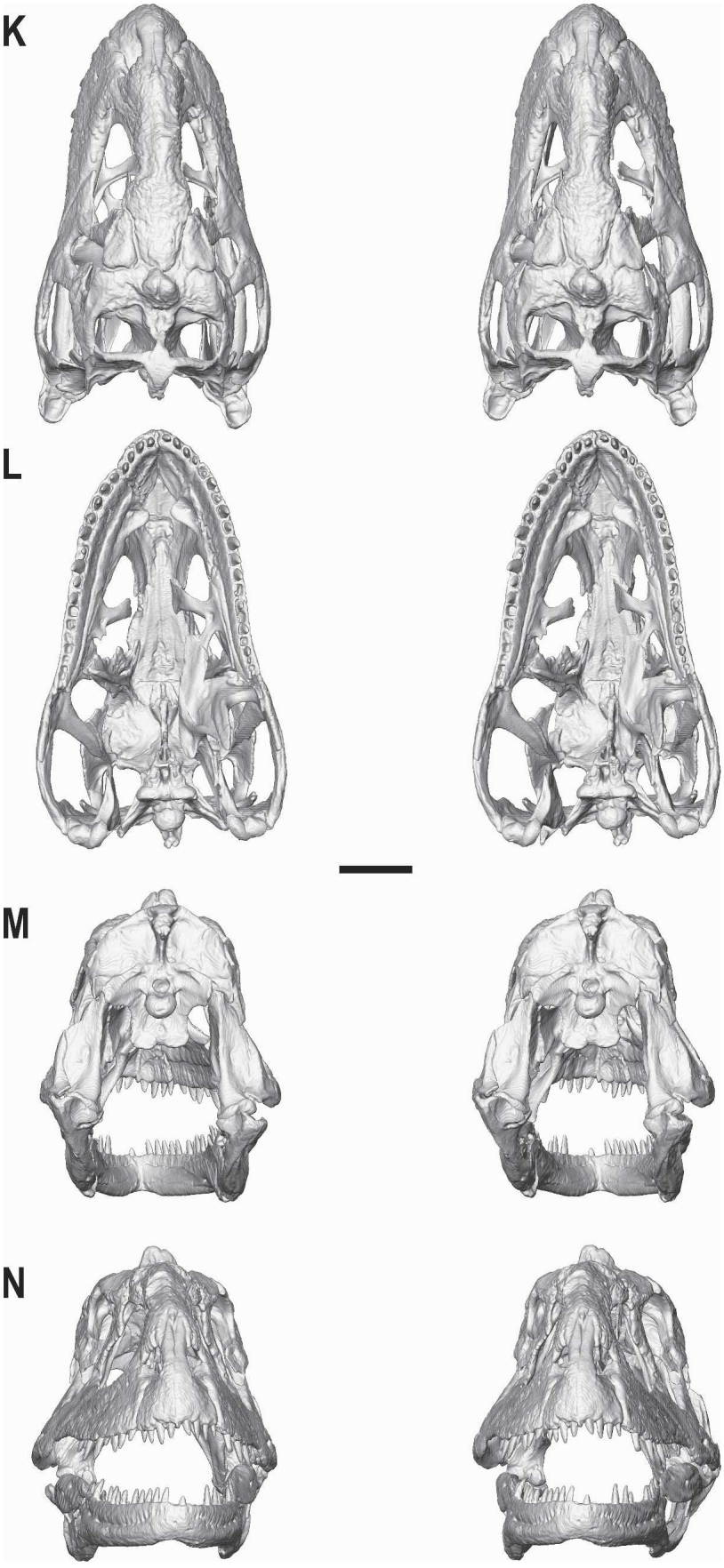
K
L
M
N

Coelophysis bauri (AMNH 2701-8, 2715-53, 7243, 7246; MCZ 4326, 4331); *Deinonychus antirrhopus* (YPM 5205; MCZ 4371; MOR 747-1/2); *Dilophosaurus wetherilli* (UCMP 37302–03, 77270); *Edmarka rex* (TATE 1002, 1005-06); *Eoraptor lunensis* (PVSJ 512); *Eustreptospondylus oxoniensis* (OUM J13558); *Giganotosaurus carolinii* (MUCPv-CH-1); *Herrerasaurus ischigualastensis* (MCZ 7063, 7064; PVSJ 53, 373, 407); *Ilokelesia aguadagrandensis* (MCF-PVPH 35); *Indosaurus matleyi* (GSI-IM K27/565); *Indosuchus raptorius* (GSI-IM K27/685*); Indeterminate Lameta abelisaurids (GSI-IM K20/619, 548*, 21141/1-33, GSI-IM K20/350*, AMNH 1955, 1960, 1753); *Liliensternus liliensterni* (MB R.1291-92); *Marshosaurus bicentesimus* (DINO 343); *Masiakasaurus knopfleri* (FMNH PR 2108-2182; UA 8680-8696); *Megalosaurus bucklandi* (OUM J13506); *'Megalosaurus' hesperis* (BMNH R.332); *Monolophosaurus jiangi* (IVPP 84019*); *Noasaurus leali* (PVL 4061); *Rajasaurus narmadensis* (GSI-IM 21141*); *Rugops primus* (MNN IGU1*); *Sinraptor dongi* (IVPP 10600); *Suchomimus tenerensis* (MNN GDF 500; MNHN GDF 365); *Syntarsus rhodesiensis* (QG 1, 203, 208, 302, 691); *Torvosaurus tanneri* (BYU-VP 2002); *Tyrannosaurus rex* (AMNH 5117) *Yangchuanosaurus shangyouensis* (CV 00215; CV 00216).

Methods—Throughout the text, the genus name of a given taxon is generally used rather than the full binomen and/or an abbreviation of the genus designation. Exceptions are made in instances where there is more than one species within the genus, and for those species exhibiting variation in the characteristic being described. Given that most theropod genera are monospecific and typically referred to with the genus designation, this convention both reduces text and facilitates readability. The bulk of taxonomic comparisons are made with other basal (non-coelurosaurian) theropods, since an ancillary goal is to provide a sufficiently detailed description that will aid efforts to elucidate phylogenetic relationships. The Introduction lists comparative specimens used in this study for all taxa discussed in the text. In order to simplify description, unless otherwise specified, the general term 'theropod' as applied herein is synonymous with 'nonavian theropod.' The term 'basal theropod' is used throughout to refer to non-coelurosaurian theropods.

A number of the elements were subjected to X-ray computed tomographic (CT) imaging at O'Bleness Memorial Hospital in Athens, Ohio, using General Electric HiSpeed FX-i and LightSpeed Ultra Multislice helical CT scanners. All elements were scanned using a bone algorithm, yielding transverse (axial) slices. The following elements were scanned, and the scan parameters are provided: MNHN.MAJ 4 (120 kV, 120 mA); UA 8709 (articulated skull roof; 140 kV, 110 mA); FMNH PR 2099 (120 kV, 100 mA), UA 8719 (120 kV, 90 mA), UA 8718 (140 kV, 120 mA); and the following elements from FMNH PR 2100: braincase (120 kV, 170 mA), nasals (120 kV, 170 mA), both lacrimals (140 kV, 120 mA), and left dentary (140 kV, 120 mA). Slice thicknesses for all elements were 1 mm, except for the nasals, which were scanned at 2 mm, and a second medical scan of the braincase, which was scanned at 0.625 mm. Data were exported in DICOM format using eFilm (v. 1.5.3, Merge eFilm, Toronto). Part of the braincase unit of FMNH PR 2100 was scanned again at the Center for Quantitative Imaging, Pennsylvania State University, State College, Pennsylvania, using an Omni-X Pantak industrial high-energy system at 160 kV, 0.3 mA, and a slice thickness of 0.179 mm; data were exported as 16-bit TIFF images. Analysis, postprocessing, and 3D visualization employed the software packages eFilm (v. 2.0), Amira (v. 3.0 and 3.1.1, TGS, Inc., San Diego), and SolidView/Pro (v. 2004.2, Solid Concepts, Inc., Valencia). In general, CT scanning provided excellent resolution of bone and rock matrix. Complicating scanning was the presence of isolated nodules of mineral precipitates within the bone substance in a number of places. Although the precipitates resulted in some 'streaking,' the problems fortunately were minor and never obscured critical features. A 'virtual endocast' (Witmer et al., 2003) was generated from the CT dataset, and a hardcopy was rapid-prototyped using a Stratasys Dimension BST (Eden Prairie, Minnesota) at Ohio University, Athens.

SYSTEMATIC PALEONTOLOGY

DINOSAURIA Owen, 1842
SAURISCHIA Seeley, 1888
THEROPODA Marsh, 1881
CERATOSAURIA Marsh 1884
ABELISAUROIDEA (Bonaparte and Novas, 1985)
ABELISAURIDAE Bonaparte and Novas, 1985
MAJUNGASAURUS Lavocat, 1955
MAJUNGSAURUS CRENATISSIMUS (Depéret, 1896) Lavocat, 1955

Type Specimen—MNHN.MAJ 1, nearly complete right dentary of subadult individual (Lavocat, 1955).

Referred Specimens—See complete listing in Krause and colleagues (this volume).

Revised Diagnosis— See Krause and colleagues (this volume).

Age and Distribution—All specimens assigned to *Majungasaurus crenatissimus* were recovered from deposits surrounding the village of Berivotra, Mahajanga Basin, northwestern Madagascar. They were concentrated in the uppermost white sandstone unit (Anembalemba Member) of the Maevarano Formation, which has been dated as Maastrichtian. For an overview of the stratigraphy, see Rogers and colleagues (2000, this volume), and for a full listing of localities see Krause and colleagues (this volume).

Described Material—The following description of the skull of *Majungasaurus crenatissimus* is based on several specimens representing putative subadult and adult age classes. In addition to the holotype, specimens referred to *Majungasaurus* preserving skull elements include: FMNH PR 2008 – right premaxilla from locality MAD93-33; FMNH PR 2099 – partial skull roof including partially fused frontals with small median cornual process, or 'horncore,' of immature individual from MAD93-33; FMNH PR 2100 – nearly complete, exquisitely preserved, disarticulated skull from MAD96-01; FMNH PR 2278 – near-adult partial skull including partially fused left and right premaxillae, left and right maxillae, left jugal, left quadratojugal, left ectopterygoid, left quadrate, left surangular, left angular, left prearticular, and left articular from MAD99-26; MNHN.MAJ 4 – partial skull roof with portions of partially fused frontals (with rounded median cornual process), parietals, caudal process of right lacrimal, sphenethmoid, and laterosphenoids from unspecified locality in the 'Majunga District'; UA 8678 – incomplete and disarticulated skull (including left splenial, left prearticular, right surangular, and right squamosal) of subadult individual from MAD96-21; UA 8709 – nearly complete, articulated, but poorly preserved skull (including maxillae, nasals, frontals, jugals, lacrimals, right postorbital and squamosal, pterygoids, ectopterygoids, right palatine, and partial braincase) and both lower jaws from MAD99-33; UA 8716 – right premaxilla from MAD99-33; UA 8717 – right and left premaxillae from MAD99-33; UA 8718 – partial left lacrimal from MAD 93-01; UA 8719 – partial skull roof from MAD01-05; UA 8782 – distal portion of left quadrate from MAD93-01. A complete listing of referred specimens, including postcranial elements, is included in Krause and colleagues (this volume). Comparative specimens from other basal theropods used in this study are listed in the Introduction above.

The description focuses on FMNH PR 2100 (Fig. 1), consisting of a nearly complete skull recovered in association with most of the caudal vertebral series (Sampson et al., 1998). The skull was found disarticulated, spread over an area of less than 2 m^2. The

only missing skull elements are the left premaxilla, right pterygoid, right ectopterygoid, epipterygoids, vomers, and columellae (stapes). Several of the referred specimens suggest that FMNH PR 2100 does not represent the maximum size of *Majungasaurus*. For example, MNHN.MAJ 4 (a skull roof) is approximately 25% larger than that of FMNH PR 2100. This evidence suggests a maximum skull length in the range of 60–70 cm and a total body length of 8–11 m, approximately equivalent to the holotype skeleton of *Carnotaurus sastrei*. Efforts have been taken to describe and figure elements in anatomical position, thereby resulting in some non-traditional orientations (e.g., Fig. 11). FMNH PR 2100 exhibits extraordinary preservation, enabling detailed descriptions of many distinctive morphological features otherwise unknown among abelisaurids. However, it must be noted that, at least in some instances, this distinctiveness may be due to preservational effects rather than taxonomic uniqueness. That is, the detailed information provided by FMNH PR 2100 is unavailable for other abelisaurid taxa. Thus, once better quality materials are recovered for other members of this clade, it may turn out that the skull of *Majungasaurus* is not as distinctive as it currently appears.

DESCRIPTION AND COMPARISONS

General Features

The skull of *Majungasaurus crenatissimus* is relatively tall, rostrocaudally abbreviated, and transversely broad, with a rounded snout (Fig. 1). These features are shared with other members of Abelisauridae and contrast with those of other basal theropods, the latter tending toward more elongate and transversely compressed skulls with narrower snouts (Fig. 2). However, even relative to other abelisaurids, the broad and rounded snout morphology appears to be more extreme in *Majungasaurus* (Fig. 2). The laterotemporal and external mandibular fenestrae are relatively large in *Majungasaurus*, whereas the antorbital fenestra and bony naris are small. The relative shortening of the skull in abelisaurids appears to be associated with telescoping of certain aspects of the skull, as evidenced by the strongly inclined jugal and its elongate contact with the maxilla.

As in other abelisaurids, rugose texturing covers most of the external surface of the skull. The rugosity largely results from mineralization of the overlying periosteum and dermis (Hieronymus and Witmer, 2003, 2004, unpubl. data). Mineralization of integumentary components has the effect of apomorphically reducing the size of some of the bony apertures in the skull, such as the narial region, external antorbital fenestra, and orbit. Moreover, this rugosity provides robust osteological correlates for bony regions covered with skin, and thus those bony areas not directly adjacent to skin, such as muscular fossae and pneumatic recesses, stand out clearly. Further examples are provided in the descriptions below, and the general phenomenon is taken up in the Discussion.

Dermal Skull Roof

Premaxilla—The paired premaxillae of *Majungasaurus* form the relatively blunt tip of the snout (Figs. 1, 3). In addition to the right premaxilla preserved with FMNH PR 2100 (Fig. 3A-C), five additional premaxillae of *Majungasaurus* were recovered from the same field area, including: FMNH PR 2008, a right premaxilla described by Sampson and colleagues (1996b); UA 8716, a right premaxilla; UA 8717, including both right and left premaxillae; and FMNH PR 2278, including the partially fused left and right premaxillae (Fig. 3D). The premaxilla contacts the nasal dorsally, the maxilla caudally, and presumably the vomer medially, although this last bone is not known for *Majungasaurus*. For descriptive purposes, the premaxilla can be subdivided into a body and a nasal process (ascending or supranarial process of some authors). The maxillary process (subnarial posterior process of some authors) is greatly reduced (see below) and does not make a substantial contribution to this element. The premaxillary body has internal (medial) and external (lateral) surfaces as well as articular surfaces rostrally for the contralateral premaxilla and caudally for the body of the maxilla; the palatal process varies from being a low ridge to tab-like process (see below). The premaxilla bears four teeth, as in most theropods and all other abelisaurids, where known. Variation in premaxillary tooth count ranges from three in *Ceratosaurus* and *Torvosaurus*, to five in *Allosaurus* and *Neovenator*, to seven in *Baryonyx*. However, the basal theropods or basal saurischians *Eoraptor* and *Herrerasaurus* possess four teeth in the premaxilla, and this is likely the plesiomorphic condition for theropods.

The premaxillary body is quadrangular, with a blocky conformation that is typical of all abelisaurids for which this element is known (Novas, 1997; Sampson et al., 1996b, 1998). *Ceratosaurus* and some allosauroids (e.g., *Allosaurus*) have premaxillae with similarly blocky shapes. The body of the premaxilla is higher than long, as in other abelisaurids and various other basal theropods (e.g., *Ceratosaurus*, *Yangchuanosaurus*, and *Torvosaurus*). A nearly vertical rostral margin of the premaxilla is also found in several basal tetanurans (e.g., *Sinraptor*, *Allosaurus*), but the caudal margin tends to be more inclined, particularly in its dorsal portion, reflecting the more elongate nature of the skulls in these taxa relative to those of abelisaurids.

The external surface of the premaxillary body in *Majungasaurus* is gently convex and highly sculptured (Fig. 3A). The only exception to the roughened surface is a smooth region located dorsally in association with the narial fossa. The demarcation between the smooth narial fossa and the surrounding roughened surface marked the juncture in life between the mucous membrane of the nasal vestibule and the skin, respectively. This demarcation is sharper and more ventrally placed in *Carnotaurus*, whereas some specimens within the Lameta abelisaurid collection (e.g., AMNH 1733; GSI-IM K20/619) are more similar to *Majungasaurus* in this regard. Numerous (>60) small foramina pierce the sculptured external surface. These foramina are more-or-less evenly distributed, with the exception of the ventral margin, where the concentration of foramina increases. A similarly large number of small foramina occur externally on a premaxilla from the Lameta abelisaurid collection (AMNH 1733; Sampson et al., 1996b; Novas et al., 2004) as well as in *Carnotaurus*. The tetanuran *Allosaurus* shows the more typical theropod conformation, with fewer and larger foramina, whereas the abelisaurid *Abelisaurus* exhibits an intermediate condition, with fewer than 10 relatively large foramina along with numerous smaller foramina. In all instances, these foramina transmitted sensory branches of the ophthalmic nerve (cranial nerve V_1; specifically, premaxillary branches of its medial nasal ramus; Wettstein, 1954; Bubien-Waluszewska, 1981; Witmer, 1995), as well as premaxillary branches of the dorsal alveolar, medial nasal, and subnarial vessels (Currie and Zhao, 1994a; Sedlmayr, 2002).

The interpremaxillary contact forms a robust, flat surface, approximately 25 mm at its greatest rostrocaudal dimension in FMNH PR 2100 (Fig. 3B). Several small foramina pierce this surface. The articular surface is much more rugose in the larger FMNH PR 2100 than it is in FMNH PR 2008, UA 8716, and UA 8717, where the surface bears finer striae that trend roughly parallel to the bone's rostral margin (this surface is not visible in FMNH PR 2278; Fig. 3D). The rugosity of the surface in FMNH PR 2100 is likely related to its relatively advanced ontogenetic stage. In all instances, however, the ventral portion of the articular surface possesses several parallel, obliquely directed ridges. A more pronounced bony ridge separates the interpremaxillary articular surface from the caudal portion of the body. This ridge is near vertical ventrally whereas the more dorsal portion arches caudally, ultimately becoming confluent with the maxillary pro-

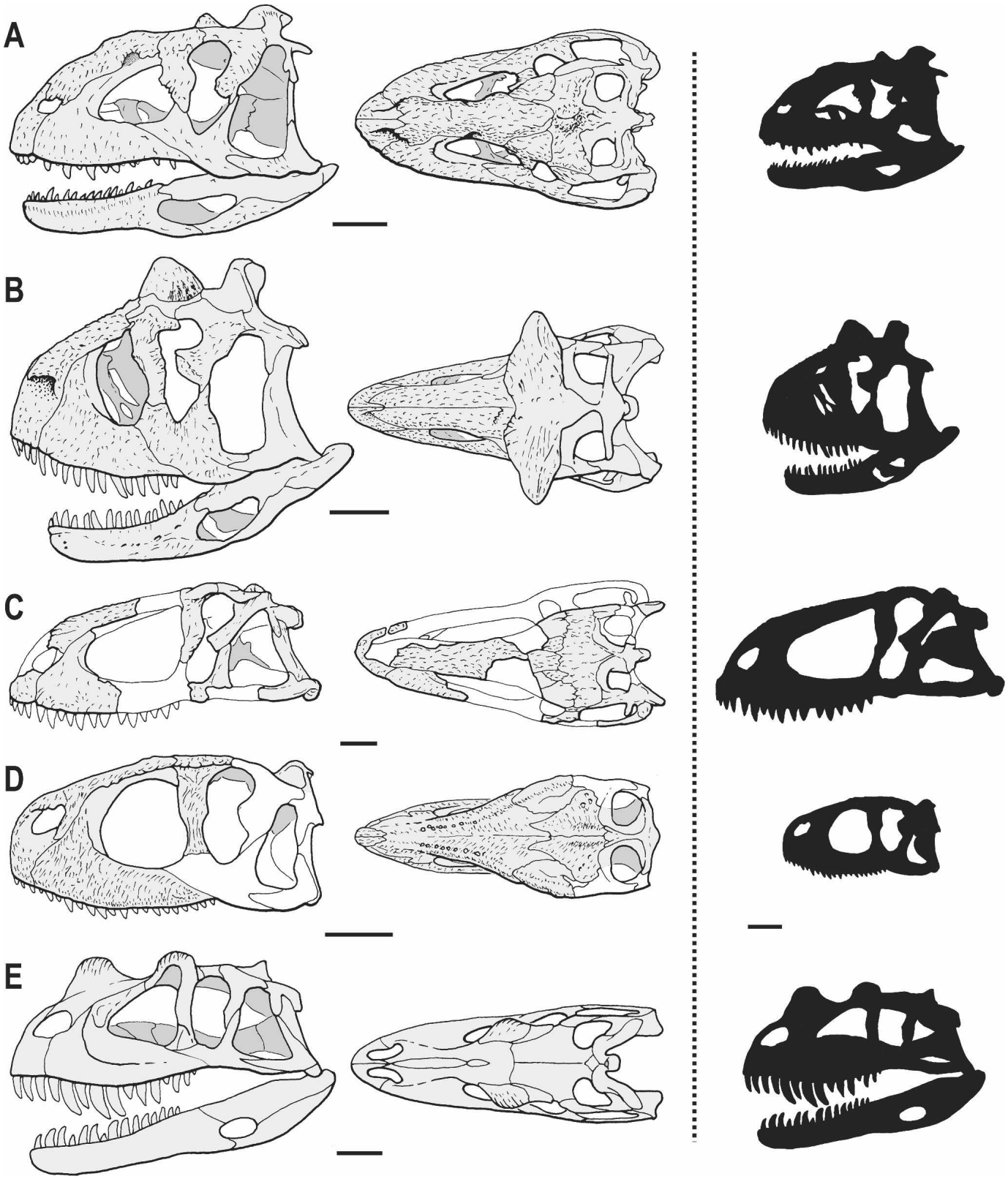

FIGURE 2. Skulls of ceratosaur theropods in lateral (left) and dorsal (middle) views. Skulls to the left of the dotted line are scaled to unit length, whereas the silhouettes to the right are all to the same scale. **A**, *Majungasaurus crenatissimus* (FMNH PR 2100); **B**, *Carnotaurus sastrei* (MACN-CH 894); **C**, *Abelisaurus comahuensis* (MC 11098); **D**, *Rugops primus* (MNN IGU1); and **E**, *Ceratosaurus* sp. (based on several specimens). **B**, **C**, **D**, and **E** modified from Bonaparte et al. (1990), Bonaparte and Novas (1985), Sereno et al. (2004), and Rauhut (2003), respectively. Scale bars equal 10 cm.

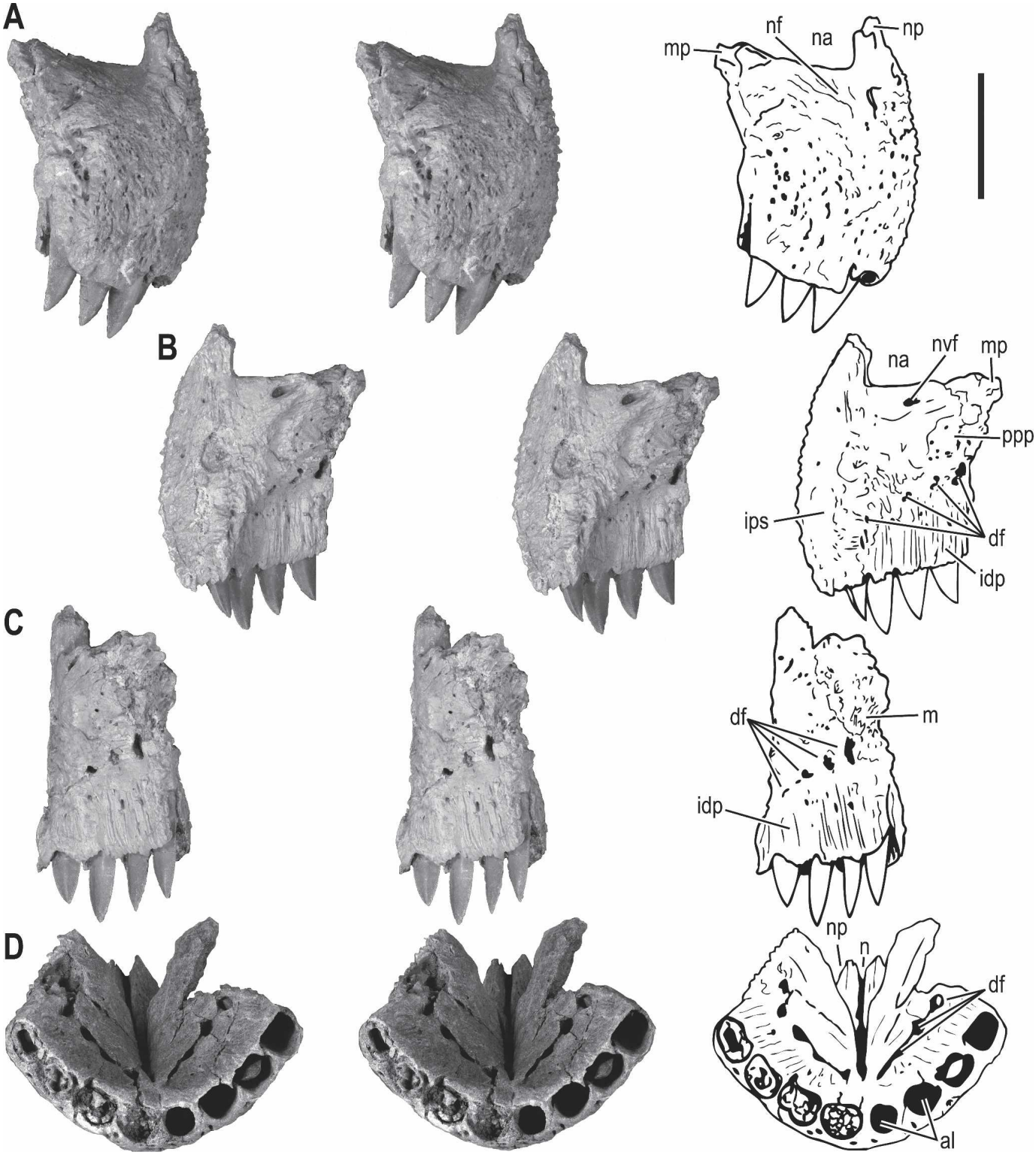

FIGURE 3. Premaxillae of *Majungasaurus crenatissimus*. **A**–**C**, Stereopairs of right premaxilla of FMNH PR 2100 in **A**, lateral; **B**, medial; and **C**, caudal views. Only the base of the nasal process (**np**) is preserved in this specimen. **D**, Fused right and left premaxilla of FMNH PR 2278 in ventral view, demonstrating blunt, rounded snout. Scale bar equals 5 cm. See Appendix 1 for abbreviations.

cess (subnarial process of some authors). The angle between the interpremaxillary articular surface and the premaxillary body (Fig. 3D) is much greater in *Majungasaurus* than in most theropods. For example, the angle (as measured between the articular surface and a line drawn between the centers of the most mesial and most distal alveoli) in *Majungasaurus* (FMNH PR 2100) is about twice that (55–60º) of *Allosaurus* (25–30º; UMNH VP 18046). The consequence of this greater angle is a much broader

snout than in most other theropods. Although equivalent angles cannot be precisely measured in *Carnotaurus* and *Abelisaurus*, their snouts seem to resemble that of *Majungasaurus* in being relatively broad and blunt (Fig. 2). Nonetheless, as indicated in Figure 2, the relative breadth of the snout is extreme in *Majungasaurus*, perhaps more than in any other basal theropod.

Dorsally, the maxillary process is greatly abbreviated and extends caudodorsally to a point just behind the maxillary contact surface (Fig. 3B). The length of this process varies considerably among theropods, apparently associated (at least in certain taxa) with relative skull length. Thus, some taxa with relatively long skulls (e.g., *Marshosaurus*, *Eustreptospondylus*) have elongate maxillary processes, sometimes even exceeding the length of the premaxillary body (e.g., *Marshosaurus*, DINO 343). However, this process can be extremely gracile, and may frequently be missing due to postmortem breakage. In *Majungasaurus*, however, its abbreviated form in all specimens can be regarded as essentially vestigial. The same appears to be true for *Carnotaurus* and *Ceratosaurus*. Thus, in these taxa the premaxilla and nasal lack any contact below the bony naris (Figs. 2, 3).

The slightly convex contact with the maxilla is partially preserved in FMNH PR 2008, present but somewhat eroded in FMNH PR 2100 (Fig. 3C) and FMNH PR 2278, and largely intact in UA 8716 and UA 8717. In all specimens, the maxillary articular surface is broad, with a medially deflected dorsal portion such that the entire caudal margin is notably curved. This feature, more exaggerated in abelisaurids than in most other theropods, reflects the rounding of the snout. The contact surface for the maxilla is highly rugose, with each side bearing a congruent array of pegs and sockets with ridges and grooves, suggesting a firm union between these bones. This feature is not observed in non-abelisaurid theropods, in which the premaxillomaxillary contact is much simpler (generally with a premaxillary convexity fitting into a maxillary concavity). As in other theropods, there are one or more foramina within the articular surfaces of both premaxilla and maxilla that together form a passage between the bones for the dorsal alveolar neurovascular bundle (Witmer, 1995; Sedlmayr, 2002). Ventrally, there is no indication of the premaxillary-maxillary incisure, or subnarial gap, characteristic of coelophysoids (Rowe and Gauthier, 1990; Holtz, 1994). Likewise, the subnarial foramen that is so typical of saurischians generally (Gauthier, 1986) is apparently absent in *Majungasaurus* and other abelisaurids. In those theropods retaining it (e.g., *Ceratosaurus*, *Allosaurus*, *Tyrannosaurus*), the subnarial foramen lies between the maxilla and the maxillary (subnarial) process of the premaxilla.

An oblique line directly above the row of dental foramina divides the internal premaxillary surface into a ventral alveolar portion and a dorsal nonalveolar portion. The dorsal portion includes a low swelling and associated, fingerprint-like fossa. Surrounding this fossa rostrally and ventrally is a structure that appears to correspond to the palatal process (maxillary process of some authors). In FMNH PR 2008 (Sampson et al., 1996b), FMNH PR 2100, and UA 8716, the palatal process is vestigial, forming a low ridge, whereas in both premaxillae of UA 8717, the process is larger, more tab-like, and projects ventromedially. In this regard, UA 8717 is closer to the primitive condition found in many basal theropod taxa, although the process is still by comparison more reduced in this individual of *Majungasaurus*. The palatal process is also vestigial in the known Indian abelisaurid material (AMNH 1733, GSI-IM K27/710; Sampson et al., 1996b). The condition of this feature is thus far unknown in Argentine abelisaurid taxa. We regard the vestigial condition in the specimens noted above as being natural (i.e., not an artifact of preservation), and suggest that the somewhat more projecting process of UA 8717 is simply a variant.

As in other theropods, a well-developed, rostrally-directed neurovascular foramen is present just ventral to the narial margin in *Majungasaurus*, located midway along the length of the premaxillary body and immediately caudal to the interpremaxillary articular surface. This foramen almost certainly communicates with the numerous external foramina. When the premaxillae are placed in articulation, the contralateral foramina are very close to each other and in life would have flanked the cartilaginous internasal septum (the presence of which is confirmed by the structure of the co-ossified nasal bones). These foramina almost certainly conducted branches of the medial nasal nerve (cranial nerve [CN] V_1) and vessels, which in modern sauropsids travel within the septal mucosa on their way to the premaxillary bone (Witmer, 1995).

At the dorsal limit of the alveolar region is an arching series of four unusually large (5–7 mm) dental foramina, one per alveolus (Fig. 3B-D). The fully fused interdental plates possess prominent, vertically oriented ridges concentrated directly medial to each of the four alveoli. This same condition, as well as the enlarged dental foramina, also occurs in the Lameta abelisaurid material (Sampson et al., 1996b). The interdental plates increase in height caudally, reaching approximately the mid-height of the premaxillary body. In contrast, the alveolar/oral region of the premaxilla is restricted to the lower one third of the body in most other theropods (e.g., *Ceratosaurus*, *Allosaurus*, and *Sinraptor*).

The nasal process is preserved in UA 8716, UA 8717, and FMNH PR 2278, where it is a robust, wedge-shaped prong approximately equal in length to that of the premaxillary body (Fig. 1). It is angled about 55º relative to the long axis of the skull. The ventral half contributes to the interpremaxillary symphysis and forms the rostral margin of the bony naris. The dorsal half rests firmly within a deep fossa of the nasal and was separated from its counterpart by a thin bony septum. This same conformation occurs in two abelisaurid premaxillae from the Indian abelisaurid collection (AMNH 1733, GSI-IM K20/619). A notable difference, however, between the Lameta abelisaurid material and *Majungasaurus* is that the base of the nasal process is relatively slender in the Malagasy taxon whereas the base is much more swollen in the Indian material, which then tapers rapidly as it approaches the nasal.

Maxilla—The maxilla (Figs. 1, 4) contacts the premaxilla rostrally, the nasal rostrodorsally, the jugal caudally, and the palatine medially. Although the caudal tips of the maxillary ascending rami are not fully preserved on either side of FMNH PR 2100 or UA 8709, a well defined groove on the ventral surface of the nasal, as well as an articular facet preserved on the left lacrimal of FMNH PR 2100, indicates that the maxilla also contacted the rostral ramus of the lacrimal, reaching as far caudally as the middle of the nasal pneumatic foramen. As in several other basal theropod taxa, there is no contact between the ventral ramus of the lacrimal and the maxilla in that the jugal intervenes between the two.

The maxilla forms the caudal margin of the narial fossa, as well as the rostral half of the external antorbital fenestra. In FMNH PR 2100 there are 17 alveoli that extend the entire length of the maxilla, with the largest alveolus (tooth position 5) being more than twice as long as the caudalmost alveolus. Each alveolus is subrectangular as viewed ventrally, and virtually all are occupied by erupted and/or unerupted teeth. Another specimen of *Majungasaurus* (FMNH PR 2278) also possesses 17 maxillary alveoli, but neither maxilla of UA 8709 is sufficiently well preserved to provide a reliable tooth count. Maxillary tooth counts vary considerably among theropods; for example, there are 12 maxillary tooth positions in *Tyrannosaurus*, 14 to 16 in *Allosaurus*, 15 in *Ceratosaurus* and *Sinraptor*, 17 or 18 in *Herrerasaurus*, up to 20 in *Syntarsus*, 22 in *Suchomimus*, and up to 26 in *Coelophysis*. Among abelisaurids, there are 14 in *Carnotaurus*, 14–15 in the Bajo Barreal abelisaurid (Lamanna et al., 2002), and 14 in the Lameta abelisaurid material (AMNH 1955; Huene and Matley [1933] also reported 14 tooth positions for GSI-IM K27/548, but

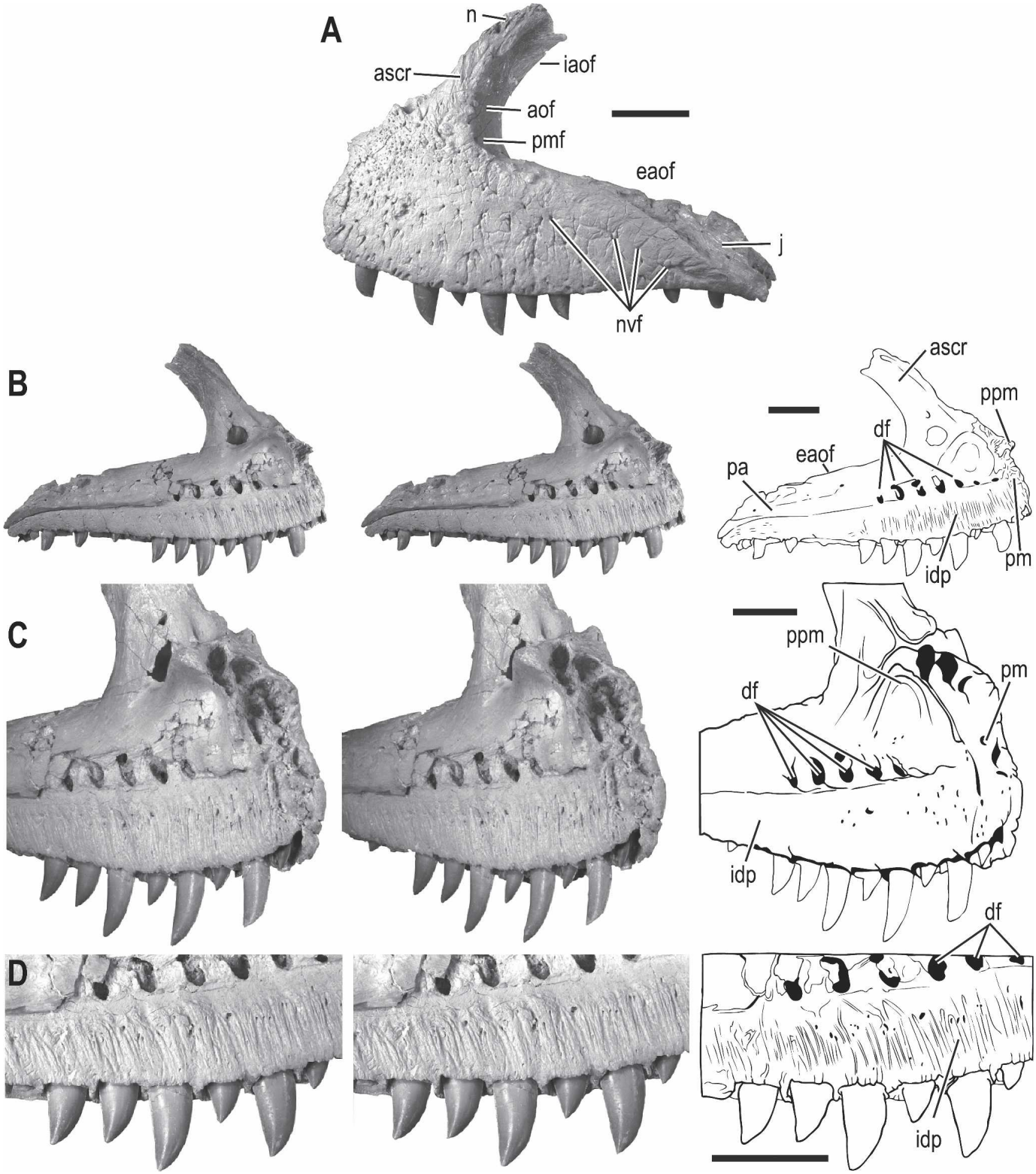

FIGURE 4. Left maxilla of *Majungasaurus crenatissimus* (FMNH PR 2100) in **A**, lateral; **B**, medial; **C**, rostromedial (highlighting the premaxillary contact surface [**pm**]); and **D**, medial (close-up, highlighting the dentition and fused interdental plates [**idp**]) views. **B**–**D** are stereopairs. Dental foramina (**df**) artificially exposed in medial view due to specimen damage. Palatal process only partially preserved in this specimen (see text). Scale bars equal 5 cm. See Appendix 1 for abbreviations.

we could confirm only 11). Thus, the 17 tooth positions in *Majungasaurus* are considerably more than in other published abelisaurids, with the exception of *Rugops* (MNN IGU 1; Sereno et al., 2004), which has 18.

The external surface is covered with the same sculptured bone as the premaxilla and most other craniofacial elements (Fig. 1A). This roughened surface forms pronounced, raised nodules up to one cm in length along the rim of the external antorbital fenestra. Greater than 100 foramina pierce the external surface. Most of these are confluent with ventrally directed neurovascular sulci, some of which branch several times. Caudally, at the level of the 12th tooth position, there is a pronounced external neurovascular feature consisting of a large foramen leading to broad sulci. It is symmetrical in FMNH PR 2100, and a similar feature is present in *Carnotaurus* and apparently the Bajo Barreal abelisaurid (Lamanna et al., 2002) and *Rugops* (the "posterior groove" of Sereno et al., 2004:1328). The maxillae of *Majungasaurus* differ from those of the Bajo Barreal abelisaurid and *Rugops* in lacking the "curved [neurovascular] grooves" issuing from the antorbital cavity (Sereno et al., 2004:1327). The pattern of external sculpturing is generally symmetrical on the maxillae but is not uniform across the bone. For example, there is a field of smaller foramina at the base of the ascending ramus that spreads rostrally onto the premaxilla, whereas the rest of the maxilla has the pattern of foramina with branching grooves noted above. These differences in sculpturing no doubt reflect variation in the structure of the overlying integument (see Discussion). As with other theropods, there is the typical row of external neurovascular foramina at the ventral margin of the maxilla that carried vessels and nerves supplying the oral margin.

The ascending ramus of the maxilla is short rostrocaudally relative to other basal theropods, probably reflecting the general shortening of the snout. The antorbital fossa is limited to a narrow band extending along the rostral and dorsal borders of the internal antorbital fenestra from the lacrimal to the base of the maxillary ascending ramus (Fig. 1). In most basal theropods, including coelophysoids, *Ceratosaurus*, and allosauroids, the antorbital fossa is more extensive, lapping laterally onto the body of the maxilla below the internal antorbital fenestra, and, in some taxa, onto the jugal and lacrimal as well. The *Majungasaurus* condition, with a more restricted antorbital fossa, occurs in *Rugops*, *Carnotaurus*, and several Lameta specimens among abelisaurids, but the Bajo Barreal abelisaurid (Lamanna et al., 2002) shows exposure of antorbital fossa on the body of the maxilla, as do the noasaurid abelisauroids *Masiakasaurus* and *Noasaurus* (Sampson et al., 2001; Carrano et al., 2002). Although there clearly is some homoplasy in this attribute within Theropoda, it would appear that *Majungasaurus* has the derived condition and shares it with some but not all (e.g., the Bajo Barreal taxon) abelisaurids.

The maxilla of *Majungasaurus* possesses a well-developed pneumatic sinus within the ascending ramus. This sinus and the aperture leading into it probably correspond to the promaxillary recess and fenestra, respectively, of neotetanuran theropods but the homology is not certain. That is, it is not certain which of the two openings (i.e., promaxillary fenestra or maxillary fenestra) of most neotetanurans is homologous with the single sinus aperture of basal theropods (see Witmer, 1997a, for discussion). Nevertheless, most researchers (e.g., Sereno, 1999; Holtz, 2000; Lamanna et al., 2002; Carrano et al., 2002; Sereno et al., 2004) have been comfortable regarding this aperture as the promaxillary fenestra, and we follow that here. The promaxillary fenestra is not visible in lateral view, as it is concealed by the lateral lamina of the ascending ramus. The recess is triangular in cross-section, with several associated neurovascular foramina. Some foramina exit the promaxillary recess ventrolaterally, where they enter the body of the maxilla and likely communicate with the numerous external maxillary foramina as well as the rostralmost maxillary alveoli. Others exit rostrally and likely transmitted nerves and/or vessels into the premaxilla. The promaxillary recess of UA 8709 bears a broken transverse strut projecting dorsally from the floor, suggesting some internal compartmentalization of the chamber. Nevertheless, there is no evidence of either a maxillary fenestra or antrum, which occur as a more-or-less round opening and cavity, respectively, in the medial lamina of the maxillary ascending ramus of most neotetanurans (Witmer, 1997a). Although the thin bone in this region is broken on the left maxilla of FMNH PR 2100, it is complete on the right side, showing that the medial lamina is unfenestrated. Unlike the condition in many neotetanurans, the promaxillary recess in *Majungasaurus* does not extend into the floor of the nasal vestibule as an inflated, thin-walled bony bubble (vestibular bulla; Witmer, 1997a), but rather remains well caudal to it. Similar morphology of the promaxillary recess and sinus is found in other abelisauroids, as well as *Ceratosaurus*. *Carnotaurus* is notable here in that, while retaining a typically abelisaurid promaxillary recess, it apomorphically has an additional pneumatic aperture in the maxillary ascending ramus dorsal to the promaxillary fenestra (Fig. 2); there is no reason, either phylogenetically or morphologically, to regard this second opening as being homologous to the maxillary fenestra of neotetanurans, and we regard it as an autapomorphy of *Carnotaurus sastrei*.

The ascending ramus of the maxilla contacts the nasal bone along an uneven, porous articular surface that forms a firm and highly congruent contact with a correspondingly sculptured margin on the nasal. A prominent notch or socket just rostral to the base of the ascending ramus receives a prong from the nasal and marks the ventral limit of this element (Fig. 4A, C). A similar notch is present in the basal abelisaurid *Rugops* (MNN IGU 1), and a socketed nasal articulation is faintly visible in *Carnotaurus*, *Abelisaurus*, and *Masiakasaurus*, as well as in *Noasaurus*. Thus, this peg-and-socket conformation of the nasomaxillary contact likely represents the derived abelisauroid condition.

The contact surface for the premaxilla is distinctive, formed by a broad, rugose concavity with several deep recesses separated by thin struts, especially in the dorsal portion (Fig. 4C). Dorsally, the premaxilla contact is deflected medially, reflecting the rounded, blunt shape of the snout. Although the short maxillary (subnarial) process of the premaxilla extends dorsally to the level of the ventral limit of the nasal, these two bones do not contact in this region because of the medial deflection of the premaxilla. Consequently, the maxilla makes a small, triangular contribution to the bony naris and narial fossa. In contrast to the notched and somewhat less robust contact between premaxilla and maxilla in coelophysoids, in *Majungasaurus* the contact between these elements is strong and immobile, buttressed by lateral and medial laminae of the maxilla, particularly in the dorsal one half. A similarly extensive, strong, and reinforced premaxilla-maxilla contact is also present in *Rugops*, the Bajo Barreal abelisaurid (Lamanna et al., 2002), and is indicated on isolated Lameta abelisaurid premaxillary and maxillary specimens from India (e.g., AMNH 1733, 1755); however, none of these reach the level of joint complexity and interdigitation observed in *Majungasaurus*. Although both the maxilla and premaxilla are preserved in the holotype specimen of *Carnotaurus* (MACN-CH 894), the contact between these elements is obscured by postmortem distortion, preventing detailed comparisons with this region in *Majungasaurus*.

Internally, a well-developed palatal process (anteromedial process of some authors) projects rostromedially to contact the premaxilla laterally and presumably the vomer medially. Although only partially preserved on the maxillae of FMNH PR 2100 (Fig. 4B, C), relatively complete palatal processes are preserved on the left and right sides of UA 8709. The latter shows that the contralateral palatal processes did not contact each other on the midline, contrasting the condition in most other

theropods (e.g., *Dilophosaurus*, *Allosaurus* – Madsen, 1976a; *Sinraptor* – Currie and Zhao, 1994a; *Poekilopleuron*? – Allain, 2002; Tyrannosauridae – Hurum and Sabath, 2003) and probably resulting from the relatively great breadth of the snout. The base of the palatal process is relatively robust dorsally and thins ventrally. This laminar-like process hooks forward, tapering rostrally almost to a point. It is unclear whether this process contacted the cartilaginous internasal septum, but it is reasonable to assume that it did. The palatal process effectively buttresses the premaxilla along the dorsal portion of the premaxillary contact. Ventral to the base of the palatal process on all specimens is a deep fossa that was topologically within the oral cavity (Fig. 4C). Immediately dorsal to the palatal process, at the base of the ascending process, is a nearly vertical fossa that housed a recess of the main nasal cavity behind the nasal vestibule (Figs. 1B, I, 4B). Rostral to this nasal recess, dorsal to the premaxillary contact, and just medial to the nasal contact, is a distinct oval fossa that leads into a groove extending caudodorsally along the rostral margin of the medial surface of the ascending ramus. This fossa and groove are best interpreted as housing the nasal gland in that these are the osteological correlates identified in extant archosaurs and several non-avian dinosaurs (Witmer, 1997a). Given that in extant sauropsids the nasal gland system opens into the nasal cavity at the caudal extremity of the nasal vestibule (Witmer, 1995), this fossa and groove in FMNH PR 2100 effectively demarcate the boundaries between vestibule and main nasal cavity.

As with the premaxilla, maxillary interdental plates are fully fused and extensive, extending the length of the maxillary body and occupying almost half of its height. Similarly, vertical series of ridges are concentrated in association with each alveolus, though they become less distinct and ultimately disappear over the caudal one-third of the interdental plates. A portion of the interdental plates was broken away postmortem on the left maxilla of FMNH PR 2100 (Figs. 4B-D), revealing large dental foramina that otherwise are not visible in medial view. Interdental plates are fused in a number of theropod taxa—including *Rugops* (MNN IGU 1), *Carnotaurus,* Lameta abelisaurid material, the Bajo Barreal abelisaurid [Lamanna et al., 2002], *Masiakasaurus* [Carrano et al., 2002]), *Ceratosaurus*, *Allosaurus*, and *Torvosaurus*—yet are unfused in *Sinraptor*, *Monolophosaurus*, *Megalosaurus*, *Torvosaurus*, and tyrannosaurids. The elongate contact surface for the palatine is visible as a roughened, shallow depression extending from approximately the rostral margin of the eighth alveolus to the caudal margin of the fourteenth alveolus immediately dorsal to the interdental plates. The palatine articular surface is basically identical to that in the Bajo Barreal abelisaurid (Lamanna et al., 2002) but is less deeply etched into the bone than in the Lameta abelisaurid material (AMNH 1955, GSI-IM K27/538).

The extensive jugal contact, fully exposed in lateral view, occupies almost one half of the total maxillary length (Fig. 4A), and the rostral ramus of the jugal is thus entirely exposed laterally (Fig. 1). Moreover, the angulation of the contact is relatively high, which has the effect of making the long axis of the jugal more oblique than in most other theropods. This morphology is also present in most other abelisaurids, and contrasts with that seen in various other basal theropods. In *Ceratosaurus* (MWC 1.1), *Allosaurus* (UMNH VP 18047), and *Sinraptor*, for example, the caudal portion of the maxilla wraps around laterally to form a deep slot that houses the jugal and (in the former two taxa) the lacrimal as well. Interestingly, both the Bajo Barreal abelisaurid (Lamanna et al., 2002) and *Rugops* (MNN IGU 1) appear to have relatively slight overlap of the jugal on the maxilla, suggesting a rather different shape for the jugal.

Nasal—As in other theropods, the nasals (Figs. 1, 5–7) are juxtaposed between the premaxillae rostrally and the frontals caudally, sharing additional contacts with the maxilla ventrally and lacrimal caudolaterally. However, the nasals of *Majungasaurus* are highly derived and autapomorphic in several respects. In most theropods, the nasal is relatively thin and gracile, tapering rostrally, bifurcating caudally, and unfused to its counterpart. In *Majungasaurus*, however, they are fully fused into a single unit, with no indication of a median suture, even when subjected to the scrutiny of CT scanning. The nasals are also remarkably deep, particularly in the dorsoventral plane. The rostral margin is gently concave as viewed laterally (Fig. 5A), resulting in a shallow curvature for the dorsal margin of the bony nostril. As in other abelisaurids, however, the dorsal surface is transversely convex and highly rugose (Figs. 1, 5A). The latter character also occurs in carcharodontosaurids, *Monolophosaurus*, and tyrannosaurids (e.g., Molnar, 1991; Zhao and Currie, 1994). *Rugops* (Sereno et al., 2004) is an exception among known abelisaurids in having transversely concave nasals, almost certainly an apomorphy linked to its peculiar lateral nasal crest and associated dorsal pits or foramina (Fig. 2D).

The fused nasals can be divided into two general regions: a larger, dorsally convex rostral portion, and a smaller, saddle-shaped caudal portion. The rostral two-thirds of the element—including a large, pneumatic foramen on each side—is convex dorsally and concave ventrally, with a low, median, dorsal ridge. The rugose external morphology is interrupted rostrally by a pair of elongate (about 63 mm long in FMNH PR 2100), deep and smooth facets for the nasal processes of the premaxillae (Figs. 5B, 6A). These facets are separated by a median lamina that is thickest ventrally and tapers dorsally. The saddle-shaped caudal one-third of the nasals is the broadest portion of the fused unit. This portion forms a broad contact surface ventrally that overlaps the frontals. Laterally and rostrally, the saddle possesses auricular-like outgrowths and, more caudally, broad and nearly vertical contact surfaces for the lacrimals. Each auricular process includes a caudal extension that slots into a deep notch within the lacrimal. A gracile rostral process of the lacrimal is received by a groove on the ventral surface of the nasal.

In FMNH PR 2100, the rostral and caudal portions are at an angle to each other, such that in anatomical position the caudal portion is more-or-less horizontal, and the rostral portion angles ventrally at about 145º. There is a distinct 'hump' at the inflection point, directly above the pneumatic foramen (Fig. 1). In UA 8709, by comparison (Fig. 7), the rostral and caudal portions are oriented at a more acute angle (about 135º) such that the hump is more pronounced and projecting, which might have given this individual a more marked 'Roman nose.'

Viewed ventrally (Fig. 5C), the nasals are relatively broad and transversely concave rostrally in association with the ventrolaterally projecting maxillary processes, giving a vaulted appearance to the rostral part of the nasal cavity. They become narrower in the mid-region below the large pneumatic foramina, and broaden again caudally in association with the auricular processes and the frontal and lacrimal contacts. A low median ridge runs the length of the ventral surface. This ridge is a reliable osteological correlate for the cartilaginous internasal septum (Witmer, 1995, 1997a), which thus confirms that, in life, the two nasal cavities were separate throughout their length in *Majungasaurus*. The lateral margins of the nasal have grooves that contact the maxillae and lacrimals. Several relatively large neurovascular foramina occur ventrally. One pair is located rostrally below each of the premaxillary facets; CT scans show that each foramen leads into a canal that branches dorsally, with a medial canal opening within the premaxillary articular surface and a lateral canal opening into the substance of the bone. Another pair of small foramina is located just rostral to the large pneumatic foramina, and these pass through only 4 mm of bone to open directly above into the pneumatic chamber. Further caudally, a single foramen pierces the underside of each auricular process, and contributes to the anastomosing network within the rugose mineralized tissue before opening externally dorsolater-

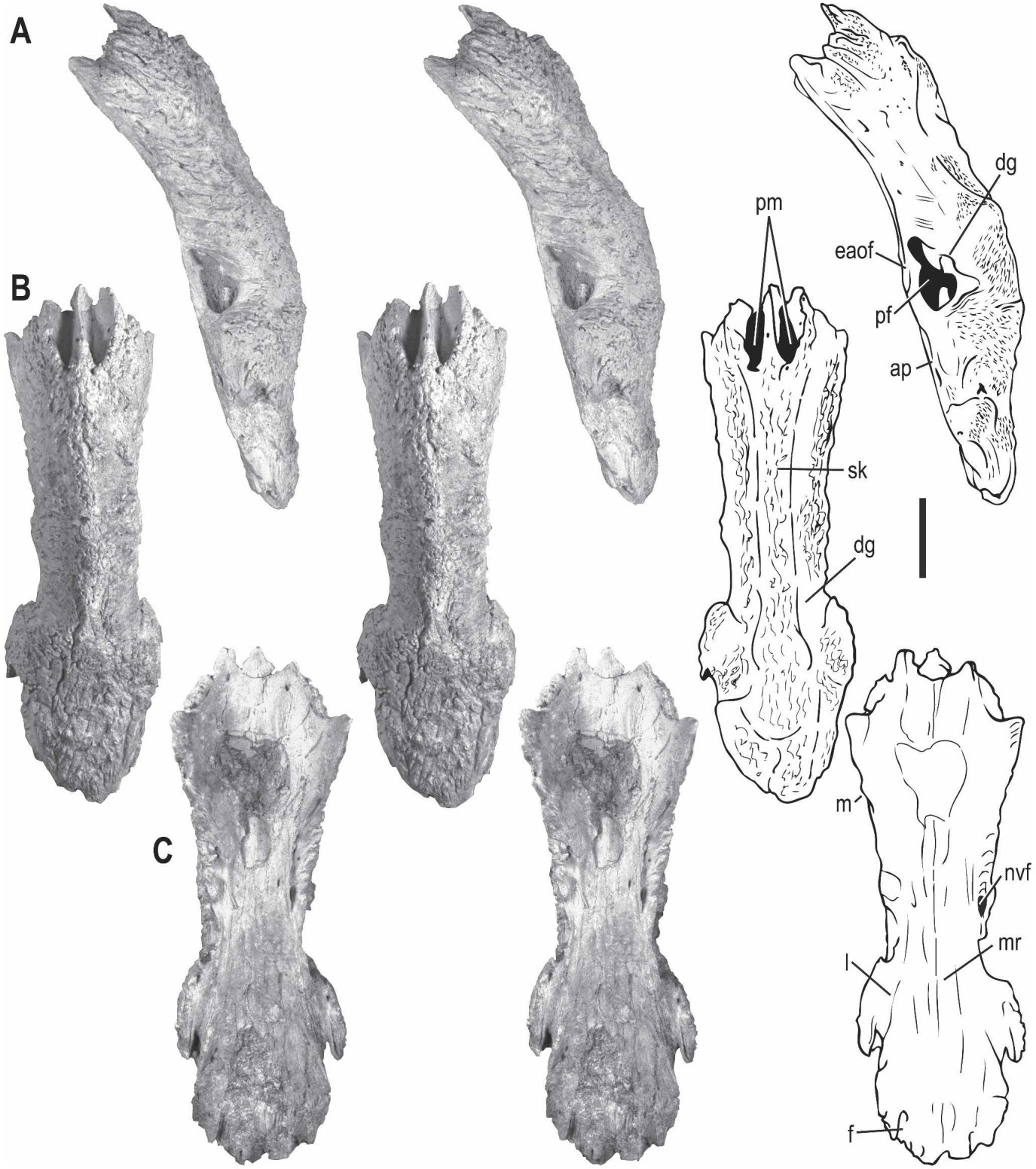

FIGURE 5. Stereopairs of fused nasals of *Majungasaurus crenatissimus* (FMNH PR 2100) in **A**, lateral; **B**, dorsal; and **C**, ventral views. Scale bar equals 5 cm. See Appendix 1 for abbreviations.

ally. Additional, larger foramina occur ventral to the saddle-like caudal portion, leading to canals that enter both the internal pneumatic chamber and the substance of the bone.

The nasal of most basal theropods forks rostrally into premaxillary and maxillary processes, separated by the margin of the bony naris. These processes are only weakly developed in *Majungasaurus*, as well as in *Carnotaurus* and *Abelisaurus*, due to rostral expansion of the intervening bone (Fig. 2). As a result, this web of the nasal present in *Majungasaurus* roofs over the caudodorsal margin of the bony naris. It is as if the narial skin

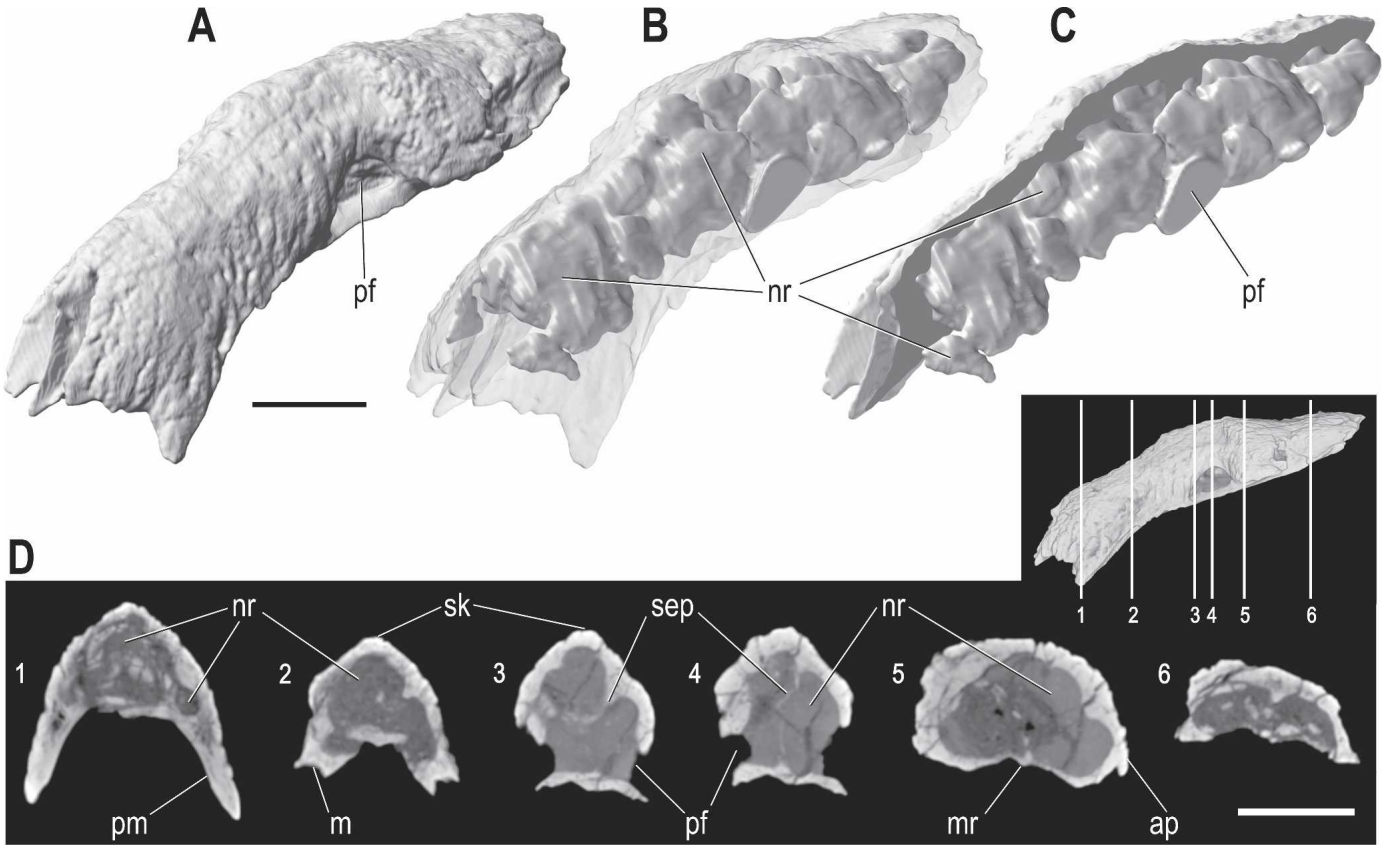

FIGURE 6. Fused nasals of *Majungasaurus crenatissimus* (FMNH PR 2100). **A**–**C**, Oblique left rostrodorsolateral view, derived from reconstructed CT scans. **A**, Solid. **B**, Bone semitransparent, revealing extent of nasal pneumatic recess. **C**, Left half of nasal element removed, revealing nasal recess and showing the thickness of the nasal bone along the midline. **D**, Representative axial CT slices through the nasal element (small lateral view shows slice positions). Scale bars equal 5 cm. See Appendix 1 for abbreviations.

between the premaxillary and maxillary processes had mineralized, and, in fact, such a process may well be the most likely mechanism to explain these findings. This situation stands in contrast to that of the basal abelisaurid *Rugops* (MNN IGU 1; Sereno et al., 2004), in which the nasals retain the primitive rostral fork, yet are apomorphically ornamented, although not to the extent as in the above-cited taxa.

The pattern of dermal sculpturing on the fused nasal element is not uniform, suggesting regional differences in the overlying integument (Figs. 1, 4A, B, 6). The caudal one-third, located between the lacrimals and rostral to the frontal bone, bears an ornamentation pattern consisting of more-or-less longitudinally running grooves and rounded ridges. These features lead rostrally to the nasal hump noted earlier (i.e., the inflection point between rostral and caudal portions). This hump area would seem to be a key point in that different ornamentation regimes intersect here. For example, extending rostrally from this point is a rugose sagittal keel that is completely absent from the caudal one-third. This keel splits caudally into a high, tuberculate field that extends ventrolaterally on each side down the caudal part of the nasal's auricular process. Immediately surrounding the nasal pneumatic foramen and its narrow rim of smooth antorbital fossa (see below) is another identifiable field of dermal ornamentation. Caudally, this field extends onto the rostral portion of the auricular process, where it is separated by a relatively smooth groove from the tuberculate field on the caudal part of the auricular process noted above. This groove seems to be carried caudally onto the lacrimal bone, where it also separates two ornamentation domains, and is carried rostrodorsally onto the nasal, expanding into a relatively broad smooth region over the nasal pneumatic foramen. It seems likely that this smooth groove is just an epiphenomenon of relatively greater dermal ornamentation of adjacent areas. Rostral to the nasal pneumatic foramen, the ornamentation forms a consistent and regular pattern of oblique grooves and ridges that is completely carried over onto the maxillary ascending ramus. The ornamentation patterns described above are quite symmetrical in FMNH PR 2100, with the exception that the right side possesses a very prominent patch of highly rugose bone rostrodorsal to the pneumatic foramen that bears at least three well-defined oblique ridges. The patterns of rugosity on UA 8709 (Fig. 7) are generally similar but seem more subdued, perhaps due to preservational artifact.

In most theropod taxa, contact between the lacrimal and maxilla excludes the nasal from the antorbital fossa. In *Majungasaurus*, the antorbital fossa extends onto the nasal in its mid portion. Other taxa in which the nasal contributes to this fossa include *Monolophosaurus* (Zhao and Currie, 1994); various allosauroids (Madsen, 1976a; Currie and Zhao, 1994a, Sereno et al., 1996), and even some dromaeosaurids (e.g., *Deinonychus*; Witmer, 1997a). The antorbital fossa in *Carnotaurus* may have extended onto the nasal, but postmortem breakage of the maxilla and lacrimal prevent definitive assessment. This region is not adequately preserved in other abelisaurids. Nevertheless, *Majungasaurus* appears to be unique in possessing a large, oval, pneumatic foramen (40 mm long on the left side, 32 mm long on the right side in FMNH PR 2100) near the midpoint of the nasals (Figs. 1, 5A, 6A, 7A). These openings are surrounded by smooth bone continuous with the antorbital fossa, clearly indicating that

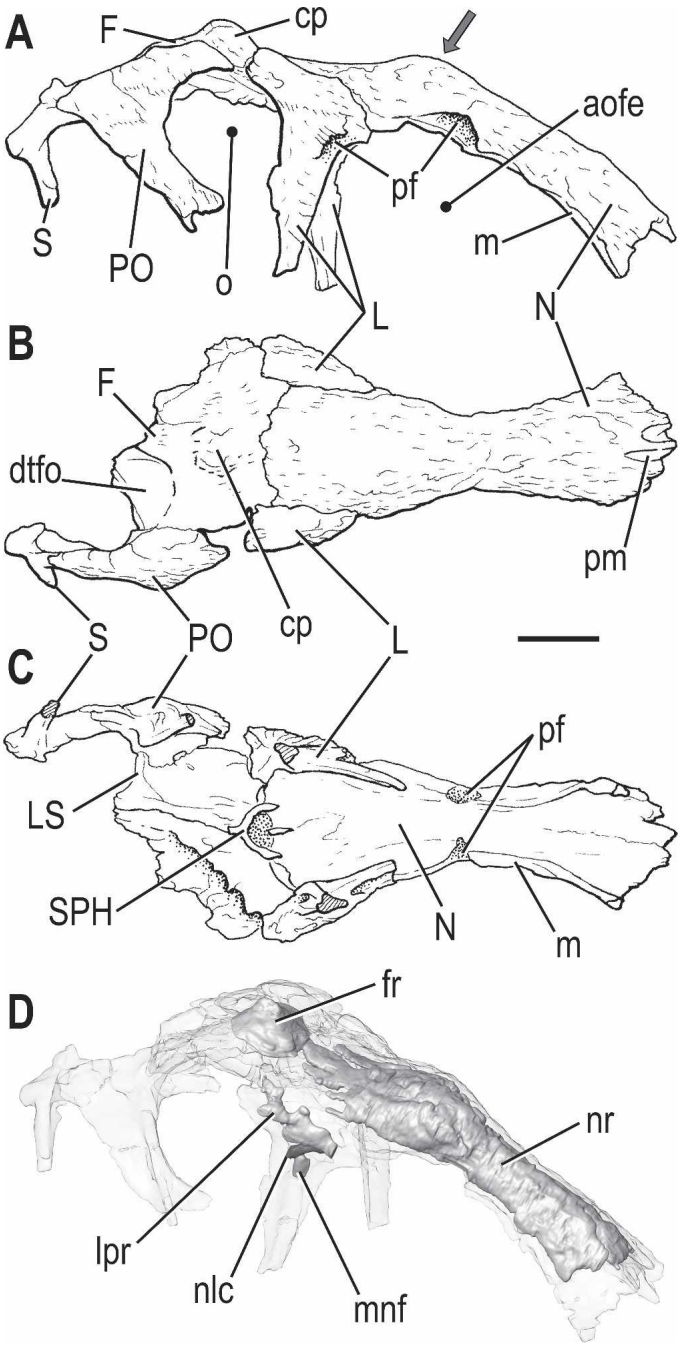

FIGURE 7. Portion of articulated skull (UA 8709) of *Majungasaurus crenatissimus* in **A**, right lateral; **B**, dorsal; **C**, ventral; and **D**, right rostrodorsolateral views. **D** derives from reconstructed CT scans; the bone is semitransparent, revealing the extent of frontal, nasal, and lacrimal pneumatic recesses. Arrow points to the enlarged nasal 'hump' observed in this specimen. Scale bar equals 5 cm. See Appendix 1 for abbreviations.

the antorbital air sac provided the pneumatic source. CT scans reveal that the fused nasals of *Majungasaurus* are thoroughly pneumatized, from the maxillary processes rostrally to the tips of the frontal processes caudally (Figs. 6, 7). Many regions are composed of a thin outer wall only 2–3 mm thick reinforced by thin internal struts (Figs. 1B, I, 6D). In fact, a remarkable finding is how little of the internal chamber is supported by struts. Overall, the internal cavity system resembles a simple hollow tube, with only a vestige of a median septum in one or two places (Fig. 6D). The nasal sinus volume in FMNH PR 2100 is 362.3 cm^3, which accounts for 45.5% of the total volume of the element.

Pneumatization of the nasal via a paranasal air source (the antorbital sinus) occurs in several other theropod taxa (Witmer, 1997a). In all instances, the nasal pneumatic foramina occur within the boundaries of the antorbital fossa. Among allosauroids, *Sinraptor dongi* has two pneumatic foramina piercing each nasal (Currie and Zhao, 1994a), whereas *Allosaurus* has between one and three, depending on the specimen (Gilmore, 1920; Madsen, 1976a; Currie and Zhao, 1994a; Witmer, 1997a). The nasals of *Monolophosaurus* resemble those of *Majungasaurus* in being rugose, highly pneumatic, and fused, though a midline suture remains visible. The Asian taxon is dramatically different, however, in that the nasals are elaborated into a tall, transversely compressed, pneumatized crest that also incorporates the premaxillae and lacrimals (Zhao and Currie, 1994). The carcharodontosaurid *Carcharodontosaurus* also has pneumatic foramina piercing the nasal ventrally in its central portion (Sereno et al., 1996), and a similar structure has been reported for *Acrocanthosaurus* (Currie and Carpenter, 2000). Pneumaticity has been implicated in several other elaborations of the facial skeleton among extant vertebrates (Witmer, 1995, 1997a, b), and provides a means of increasing bone surface area, as implicated here for the nasal of *Majungasaurus*.

Majungasaurus resembles all of the other taxa with nasal pneumaticity (Witmer, 1997a, b) in that the nasal pneumatic foramen is fully within the antorbital fossa, but differs from them strikingly in that the rim of the antorbital fossa does not form a smooth arching curve but rather must take a dorsal excursion to envelop the nasal pneumatic foramen (Figs. 1, 6, 7). Thus, a dorsal diverticulum of the antorbital air sac passed onto the lateral surface of the nasal to enter the bone such that the pneumatic foramen is bordered rostrally, dorsally, and caudally by rugose, subcutaneous bone while still being continuous with the rest of the antorbital cavity ventrally. It is reasonable to suggest that this paranasal pneumaticity is the likely cause of fusion between opposing nasals in *Majungasaurus*, as well as formation of interior cavities, obliteration of the midline suture, and overall expansion, or 'inflation,' of the nasals, because extramural pneumaticity has been implicated in such phenomena in extant birds (Witmer, 1990, 1997a, and references therein).

The nasals of *Majungasaurus* most closely resemble those of *Carnotaurus*. In both taxa this element is remarkably rugose and broad rostrally as well as caudally. However, the nasals of *Carnotaurus* are less derived in having a thinner profile, a bifurcate contact with the frontals, and no evidence of either nasal-nasal fusion or pneumaticity. The nasals of *Abelisaurus* appear to be fused into a single element and are rugose, but pneumaticity cannot be confirmed. The nasals of the basal abelisaurid *Rugops* are neither completely fused nor apparently pneumatic, but they are rugose (Fig. 2D).

Lacrimal—As in other abelisaurids, the lacrimal (Figs. 1, 7–9) is a relatively massive element that contacts the maxilla and nasal rostrodorsally, the nasal dorsomedially, the postorbital caudodorsally, the frontal caudally and dorsomedially, and the jugal ventrally. Five examples are known: both right and left in FMNH PR 2100 (Figs. 1, 8, 9) and UA 8709 (Fig. 7), and an isolated left lacrimal (UA 8718). In most theropods, the lacrimal is L-shaped, with well-developed rostral and ventral rami. In *Majungasaurus*, the ventral ramus of the lacrimal is hypertrophied due to dermal sculpturing, whereas the rostral ramus is relatively diminutive. More unusually, it seems likely that the prefrontal bone is fused onto the lacrimal, such that the prefrontal would project caudomedially from the body of the lacrimal as a thin prong (Fig. 8B; see prefrontal discussion below). Sereno and colleagues (2004) likewise regarded the prefrontal of *Rugops* as being fused onto the lacrimal, although in *Rugops* the prefrontal is not styloid.

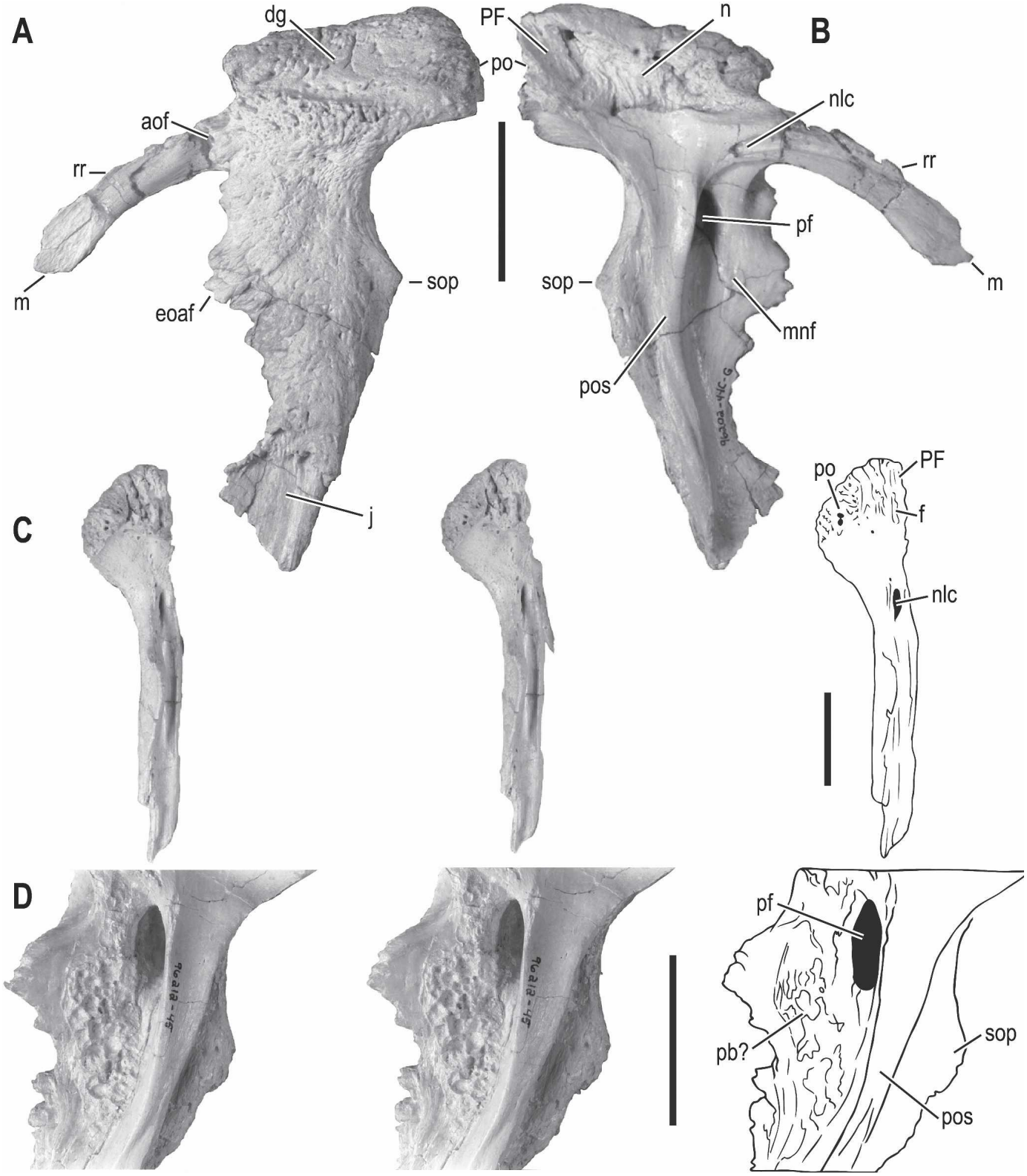

FIGURE 8. Left lacrimal of *Majungasaurus crenatissimus* (FMNH PR 2100) in **A**, lateral; **B**, medial; and **C**, caudal views. **D**, Medial view of right lacrimal showing patch of putatively pathological bone. **C** & **D** are stereopairs. The prefrontal (**PF**) is assumed to be fused to the caudomedial portion of the lacrimal (see text). Scale bars equal 5 cm. See Appendix 1 for abbreviations.

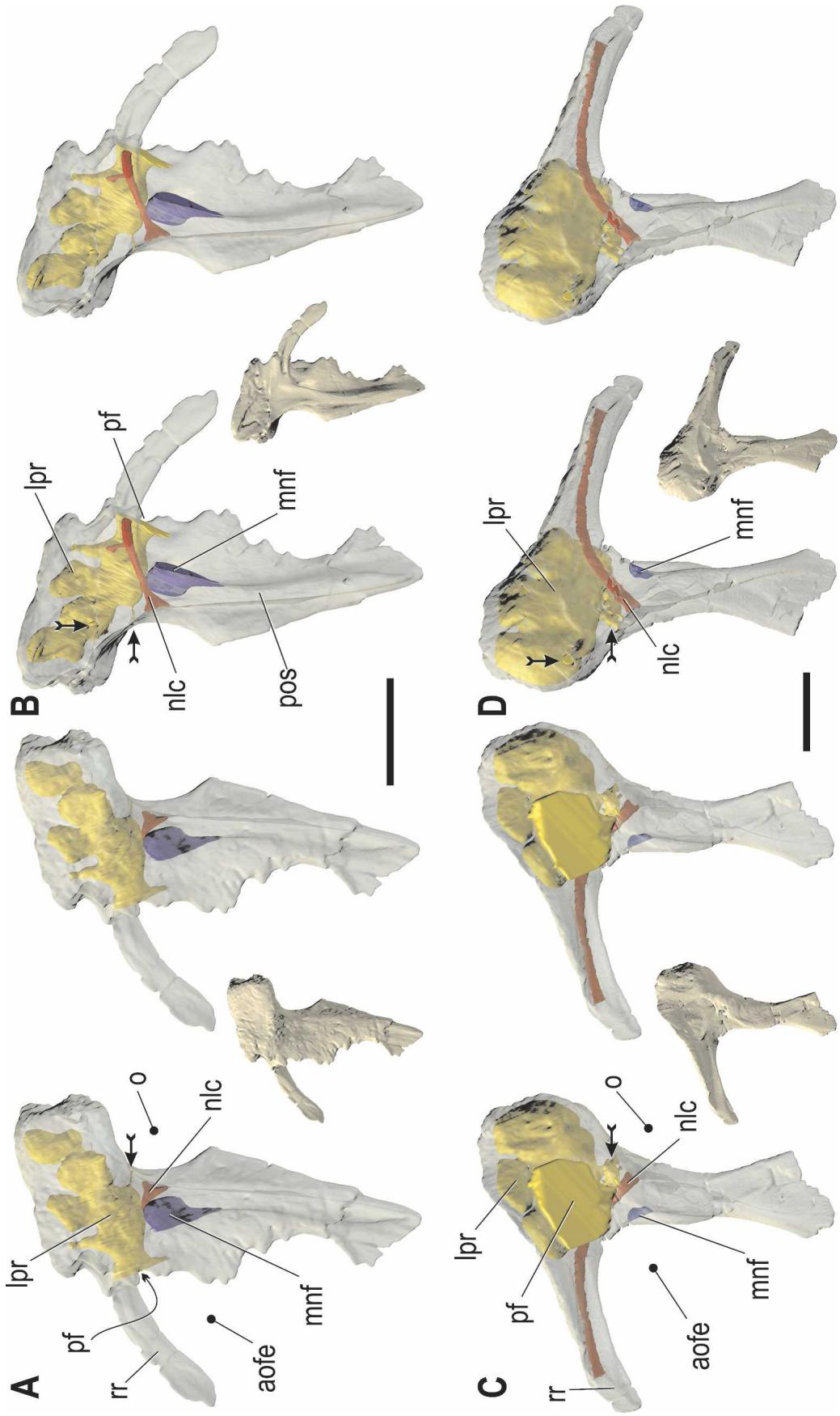

FIGURE 9. Left lacrimals of *Majungasaurus crenatissimus* (FMNH PR 2100) (**A**, **B**) and *Allosaurus fragilis* (UMNH VP 18048) (**C**, **D**) in lateral (**A**, **C**) and medial (**B**, **D**) views. Images derived from reconstructed CT scans. Large images are stereopairs in which the bone has been made somewhat transparent to reveal internal structures (lacrimal pneumatic sinuses [in yellow and blue]; nasolacrimal canals [in red]); small images are solid versions of the bone for orientation. Vertical arrows are potential diverticula from the lacrimal sinus; horizontal arrows are communications between the lacrimal sinus and a putative air sac within the orbit. Scale bars equal 5 cm. See Appendix 1 for abbreviations.

The line of fusion cannot be discerned in any specimen of *Majungasaurus*, and the only specimen that might preserve the lacrimal-prefrontal juncture (UA 8709) is too fractured to be definitive. In *Majungasaurus*, the rostral ramus is reduced to a thin lamina not visible in dorsal view of the skull. The rostral ramus is virtually complete on the left side of FMNH PR 2100 and, although slightly distorted (deflected ventrally), clearly forms only the dorsal part of the internal antorbital fenestra and fossa and does not contribute at all to the external antorbital fenestra. This condition is found in other abelisaurids, such as *Carnotaurus* and *Rugops*; in contrast, the rostral ramus of the lacrimal in other mid- to large-sized theropods (e.g., *Ceratosaurus*, *Allosaurus*, *Tyrannosaurus*) is typically robust, forming much of the subcutaneous dorsal and caudodorsal margin of the external antorbital fenestra (Fig. 2). The rostralmost portion of this ramus in *Majungasaurus* includes a roughened fossa on the external surface for contact with the terminal end of the maxillary ascending process.

A large pneumatic foramen leading from the antorbital cavity enters the body of the lacrimal at the juncture of the rostral and ventral rami. This position is fairly typical for other theropods (Witmer, 1997a), but differs in that, whereas the aperture is visible in lateral view in most other theropods, in *Majungasaurus* the aperture is obscured laterally by overgrowth of dermal ornamentation. Thus, the pneumatic aperture faces directly rostrally rather than rostrolaterally. CT scanning allows the details of the lacrimal recess to be discerned (Figs. 7, 9). As is typical for pneumaticity, there is considerable variation in the precise form and size of the enclosed sinuses. In all cases, the sinus expands within the body of the bone immediately behind the initial constriction of the pneumatic foramen. Within the body, the sinus forms a series of communicating chambers partially separated by septa. From the main portion of the sinus, there are 3–4 balloon-shaped diverticula that expand dorsally and caudally. The caudalmost sac is always quite distinct and is situated caudodorsomedially. In FMNH PR 2100, there appears to be a communication between the lacrimal pneumatic recess and nasolacrimal canal, but such a communication is demonstrably absent in UA 8718 as well as in *Allosaurus*. In *Allosaurus* (Fig. 9C, D), the lacrimal recess communicates with the orbit via short canals, and Witmer (1997a) regarded this as evidence for a suborbital diverticulum of the antorbital air sinus. In *Majungasaurus*, there also is evidence for such a communication (Fig. 9A, B, horizontal arrows), but it cannot be ruled out that the observed canal between recess and orbit is vascular in origin. Another potential pneumatic conduit is located dorsomedially within the roughened articular surface for the frontal in that there are openings within this surface that communicate with the lacrimal pneumatic recess (Fig. 9, vertical arrows). These openings are discussed below in the section on the frontal bone in the context of providing the source of a diverticulum pneumatizing the frontal.

The lacrimal bone is located at the intersection of different soft-tissue domains, principally the antorbital cavity rostrally, the orbital cavity caudally, and the nasal cavity medially. As noted above, the pneumatic aperture and cavity were made by a diverticulum of the antorbital sinus (Witmer, 1995, 1997a), but a number of other morphological features were shaped by the main antorbital sinus itself. For example, the smooth lateral surface of the rostral ramus noted above was adjacent to the main sinus, as was the broad smooth surface located medially on the ventral ramus, rostral to the vertical pillar of bone separating the orbital and antorbital cavities (termed here the preorbital strut; Figs. 8B, 9). This medial antorbital surface is delimited by an arching crest formed by the preorbital strut caudally and the ventral edge of the rostral ramus dorsally (Figs. 8B, 9). At the caudodorsal depth of the medial antorbital surface is a fairly deep fossa, referred to as "medial vacuity" by Currie and Zhao (1994a) for *Sinraptor*. Given its relationship to the antorbital sinus, it clearly is a pneumatic fossa. In some theropod taxa (e.g., *Allosaurus*, UMNH VP 18048, 5814; Fig. 9C, D), the medial pneumatic fossa is quite small, whereas in others (e.g., *Ceratosaurus*, MWC 1.1), it is larger and even subdivided by internal septa. The medial pneumatic fossa in all known lacrimals of *Majungasaurus* (FMNH PR 2100, UA 8709, UA 8718) is intermediate between these two conditions. As confirmed by CT, the medial pneumatic fossa does not communicate with the main lacrimal recess in any of the *Majungasaurus* lacrimals. In many, if not most, theropods, the medial antorbital surface wraps around the rostral edge of the ventral ramus and is visible laterally as the lacrimal antorbital fossa passes onto the adjacent jugal bone (Currie, 2003). However, in *Majungasaurus* (and apparently also *Carnotaurus*), there is no lateral exposure of the antorbital fossa on the ventral ramus of the lacrimal (or adjacent jugal; see below).

The right lacrimal of FMNH PR 2100 has an apparent pathological condition in which the medial pneumatic fossa is covered by a patch of mineralized tissue that takes the form of a series of deep, rounded pits of variable size (Fig. 8D). The patch resembles the impression of raindrops in mud. It does not seem that the patch was the result of some process (pathological or otherwise) that occurred *within* the bone, but rather something *adjacent* to the bone that then adhered to the bone surface. Such morphology has not been observed by either of us in any extant taxon, despite one of us (LMW) having looked at the bony pneumatic sinuses of numerous living and extinct animals from throughout Amniota. The closest match is perhaps in the basal dromaeosaurid *Sinornithosaurus*, which has a very similar pattern of bone surface structure in the maxillary antorbital fossa (Xu and Wu, 2001). Xu and Wu (2001) did not regard the condition in *Sinornithosaurus* as pathological but certainly in *Majungasaurus* it is pathological, or at least atypical, being positively absent from the four other known examples. Perhaps significantly, in both taxa, the unusual texture is found on bone surfaces that were directly in contact with the antorbital sinus, perhaps suggesting that the pathological process was associated with the pneumatic epithelium.

In lateral aspect, most of the external surface of the lacrimal (exclusive of the rostral ramus and jugal contact) is sculptured (Figs. 1, 8A). A raised and highly ornamented longitudinal ridge separates the robust and blocky body of the lacrimal from the thinner ventral ramus. This ridge is confluent rostrally with the patch of rugose bone mentioned above, on the nasal bone just caudal to the nasal pneumatic foramen, and caudally with a similar ridge on the postorbital. *Carnotaurus* and *Abelisaurus* (and perhaps also *Rugops* [Sereno et al., 2004]) also bear a continuous rugose ridge from lacrimal to postorbital, but in these the ridge is thicker and fully dorsal to the orbit, whereas in *Majungasaurus* the ridge is thinner and discontinuous across the dorsal part of the orbit. Dorsal to the lacrimal ridge is a groove that is continuous with the sinusoidal sulcus on the nasal. There is a relatively smooth, less ornamented region immediately dorsomedial to this sulcus, but then the surface sculpture becomes more rugose as it approaches the contact with the nasal medially. A very similar ornamentation pattern occurs on the adjacent dorsal portion of the postorbital bone, no doubt reflecting integumentary features that span these bones. A large neurovascular foramen pierces the lacrimal just below the longitudinal ridge on the right side in FMNH PR 2100 but not in the other known lacrimals.

The ventral ramus is relatively expanded in its proximal half, due largely to the occurrence of processes on both the rostral and caudal margins. Dermal sculpturing on the lateral surface produces a ragged rostral margin, with several rugosities projecting into the antorbital cavity. Significantly, the internal surfaces of these rugosities are smooth, reflecting that here the mineralized tissues were shaped by the epithelium of the antorbital paranasal air sinus (see above). Most of the dermal sculpturing on the ventral ramus of the lacrimal consists of vascular (or perhaps

neurovascular) sulci emanating from foramina. Most of these features are directed rostrally or rostroventrally toward the antorbital cavity, and only the caudalmost sulci enter the orbital margin. The caudal margin of the ventral ramus is relatively smooth, with a large suborbital process that projects caudally into the orbit. This process, which also bulges medially and is somewhat concave laterally, was almost certainly an attachment site for the suborbital ligament. In extant birds this ligament runs between the lacrimal bone and postorbital process (Baumel and Raikow, 1993). It has been inferred for some extinct theropods, such that the suborbital process can be interpreted as demarcating the ventral limit of the eyeball (Currie and Zhao, 1994a; Chure, 2000a). A well-developed suborbital process also occurs in *Abelisaurus* and *Rugops*, whereas it is more weakly developed in *Carnotaurus* and many other theropods (Fig. 2; see Chure, 2000a, for a review). The ventral ramus narrows below the rostral and suborbital processes, and then broadens slightly at the distal end, particularly along the rostral margin.

Caudally, the dorsal portion of the lacrimal forms an interdigitating contact that is thickest medially and thinnest laterally (Fig. 8C). The thinner lateral region contacts the postorbital, whereas the broader medial portion slots into a deep notch of the frontal, forming a broad, interlocking suture. Theropods typically lack contact between the lacrimal and postorbital, resulting in a characteristic emargination of the dorsal orbital margin, allowing the frontal and prefrontal to contribute to the orbital margin. Lacrimal-postorbital contact is characteristic of abelisaurids, and appears to have evolved independently within Allosauroidea (reaching its culmination in Carcharodontosauridae) and Tyrannosauridae.

The articulation with the nasal bone is complicated. As mentioned above, the thin rostral ramus fits within a shallow ventral groove on the nasal. More caudally, the lacrimal has a rostrally-facing fossa that interlocks with a large lateral prong of the auricular process of the nasal. Dorsomedially is another articular surface for the nasal that runs the length of the body of the lacrimal. Mazzetta and colleagues (2000) regarded the nasolacrimal contact as a potentially kinetic joint in *Carnotaurus*, but the contact was clearly immobile in *Majungasaurus* (and we suspect in *Carnotaurus* as well). The dermal sculpturing of both the lacrimal and nasal seems to pass directly into the articular areas (Fig. 1C), suggesting that a sutural furrow may have been apparent in the overlying skin.

Medially, the preorbital strut forms a pronounced vertical ridge running the height of the ventral ramus, separating the orbital cavity from the antorbital cavity (Figs. 8B, 9B). The strut is broadest dorsally and thins ventrally. Moreover, the strut is smoothly concave dorsally, presenting sharp crests caudally to the orbit and rostrally to the antorbital cavity. The medial surface of the preorbital strut, including the dorsal concavity, is clearly associated with the nasal cavity and, in particular, the nasal cartilages. In extant archosaurs, the olfactory concha attaches partly to the lacrimal (Witmer, 1995), and it is reasonable to assume the same for *Majungasaurus* given proximity of this region to the opening in the sphenethmoid for the olfactory bulb. In fact, there is a low vertical ridge that may well indicate the attachment site of the concha. Rostral to this putative conchal ridge is the base of the lacrimal's rostral ramus, which bears a foramen leading into a groove that courses rostrally along the medial surface of the rostral ramus. This foramen and groove represent the nasal opening of the nasolacrimal canal. Thus, the nasolacrimal canal passes from the bulbar region of the orbit through the body of the lacrimal bone to open medially into the antorbital cavity in association with the lacrimal's rostral ramus (Figs. 7–9). Along the way, the nasolacrimal canal passes dorsal to the medial pneumatic cavity and medial to the main lacrimal recess. Witmer (1997a) discussed the course of the nasolacrimal duct in archosaurs, and the pattern suggested here for *Majungasaurus* is characteristic of a number of dinosaurs in general and theropods in particular.

Majungasaurus is unusual in one respect, however; whereas in most theropods the nasolacrimal canal passes through essentially the full length of the lacrimal's rostral ramus, in *Majungasaurus*, the bony canal opens at the very base of the rostral ramus and the duct would have been conveyed forward within the groove. We will take this opportunity to correct an error in Witmer (1997a, fig. 29A) in which the nasolacrimal canal of *Allosaurus* is reconstructed as passing through the lacrimal recess. CT scans of *Allosaurus* lacrimals (UMNH VP 18048, 18049) confirm that the labeled passage is a pneumatic conduit between the orbit and lacrimal recess, and the nasolacrimal canal takes the typical course through the lacrimal's rostral ramus, opening medially near its rostral tip (Fig. 9C, D).

Directly behind the preorbital strut is the orbital surface of the lacrimal (Fig. 8C). This is a relatively narrow space that expands dorsally. Most of the orbital surface is smooth, although dorsally the relatively sharp juncture between orbital and integumentary domains is apparent. Also, the roughness associated with the suborbital process extends somewhat onto the medial surface, confirming the presence in life of a relatively broad sheet of dense connective tissue—that is, the suborbital ligament noted above. The orbital opening of the bony nasolacrimal canal is located roughly mid-height within the dorsal, bulbar (eyeball) region of the orbit, forming an oval foramen within the groove between the external and internal margins of the bone (Fig. 8C), the latter being the caudal edge of the preorbital strut. Dorsal to the nasolacrimal foramen is a series of smaller foramina that probably transmitted neurovascular bundles from the orbit into the substance of the bone. This series continues caudally in that portion of the roof of the orbit formed by the frontal bone.

Prefrontal—The status of a separate prefrontal in *Majungasaurus* is not entirely clear. Certainly, no separate prefrontal element is visible externally on the skull. Likewise, Bonaparte and colleagues (1990) did not describe or figure this element for *Carnotaurus*. In most theropods, the prefrontal is interposed between the lacrimal, frontal, and nasal, forming either a substantial portion (*Herrerasaurus*) or a small dorsal portion (e.g., *Allosaurus*, *Sinraptor*, *Ceratosaurus*, *Tyrannosaurus*) of the orbital margin. In *Majungasaurus* (Fig. 8), the prefrontal could be absent or present but fused completely into the lacrimal. The apparent tendency toward hypermineralization in the skeleton of *Majungasaurus* and other neoceratosaurs might tend to corroborate the latter hypothesis. In support of this view, the prefrontal can be seen partially fused onto the lacrimal in a specimen of *Ceratosaurus* (MWC 1.1). Moreover, Sereno and colleagues (2004) reported an apparent line of fusion between the lacrimal and prefrontal in the African abelisaurid *Rugops*. Thus it seems likely that the long, caudal prong that slots deeply into the frontal in all known specimens of *Majungasaurus* is actually a portion of the prefrontal. Nevertheless, pneumatization and hypermineralization of the conjoined lacrimal/prefrontal element obliterated all evidence of their junction.

Postorbital—A complete left postorbital was preserved with FMNH PR 2100 as an associated but isolated element (Fig. 10); the right postorbital was fused into the skull roof such that a small dorsal portion remained attached to the frontal and the remainder broke away postmortem to be preserved as a separate element (Fig. 1). The right postorbital is preserved in articulation in UA 8709 (Fig. 7), and in UA 8719 both postorbitals are essentially fused to the frontals, the line of fusion being marked by a series of foramina within the orbital (ventral) surface. In all cases, the robust postorbital contacts the lacrimal rostrodorsally, the frontal and laterosphenoid dorsomedially, the squamosal caudodorsally, and the jugal ventrally. It forms the caudodorsal margin of the orbit, the rostrodorsal portion of the laterotempo-

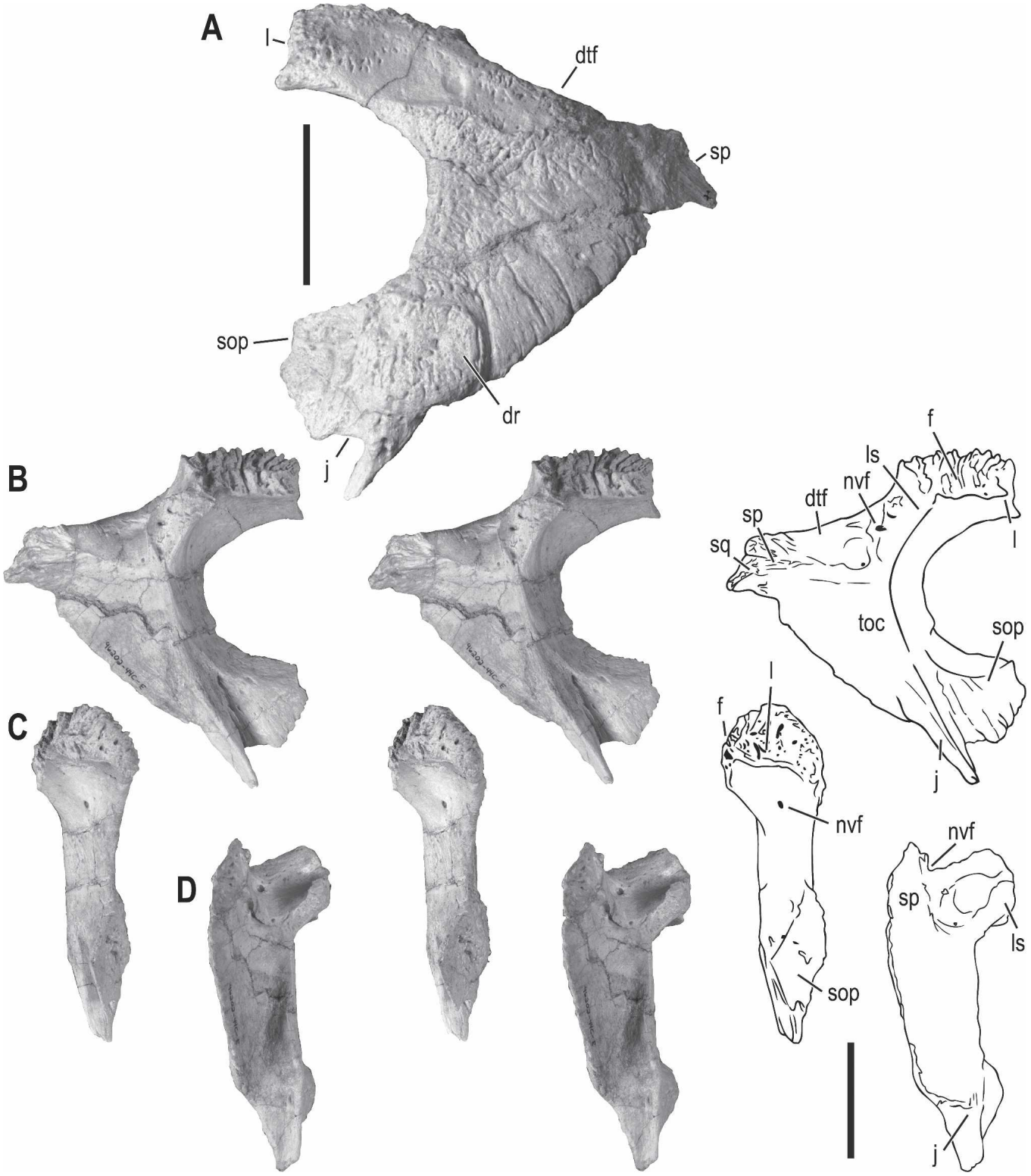

FIGURE 10. Left postorbital of *Majungasaurus crenatissimus* (FMNH PR 2100) in **A**, lateral; **B**, medial; **C**, rostral; and **D**, caudal views. **B**–**D** are stereopairs. Scale bars equal 5 cm. See Appendix 1 for abbreviations.

ral fenestra, and the lateral portion of the dorsotemporal fenestra.

The postorbital of *Majungasaurus* is distinctive among abelisaurids, and comparable in several details only to *Carnotaurus* (Bonaparte et al., 1990). Whereas the postorbital of most theropods is distinctly triradiate, with rostral (frontal), caudal (squamosal), and ventral (jugal) rami (e.g., *Herrerasaurus*, *Allosaurus*, tyrannosaurids; Fig. 2), that of *Majungasaurus* is more L-shaped, or even C-shaped (Fig. 10). The difference is due largely to a rearward expansion of the ventral ramus, resulting in a more

robust element with a nearly straight caudal margin and a more extensive external wall of the adductor chamber. This conformation also occurs in *Carnotaurus*. A very large suborbital process, together with the suborbital process of the lacrimal, effectively rounds out much of the ventral portion of the orbit, indicating the position of the eyeball, as well as the attachment sites of the suborbital ligament. Like its counterpart on the lacrimal, the suborbital process of the postorbital is deflected somewhat medially. A well-developed suborbital process occurs in *Carnotaurus*, *Ilokelesia*, and, to a lesser extent, *Abelisaurus* (Fig. 2), and appears to have evolved convergently in carcharodontosaurids, as well as in tyrannosaurids.

Externally, the postorbital is characterized by dermal sculpturing similar to that seen on many other skull elements (Figs. 1, 10A). A low, longitudinal ridge reaches the dorsal margin of the orbit and then reappears as a similar ridge on the lacrimal and extending onto the nasals (see above; Fig. 1). Again, in *Carnotaurus* and *Abelisaurus*, this ridge is thicker and fully continuous above the orbit. Ventral to this ridge, there is a fore-aft partitioning of the surface ornamentation, with a more rugose and punctate texture rostrally and a smoother texture caudally interrupted by long vascular grooves on their way to the laterotemporal fenestra. In FMNH PR 2100, there is a large, ovoid, rugosity on the lateral side slightly above and caudal to the suborbital process (Figs. 1, 10A). This rugosity is elevated relative to the surrounding ornamentation and has distinct margins, as if the rugosity were a separate dermal element secondarily attached to the postorbital bone. In UA 8709, the rugosity is less distinct. A similar rugosity may also be present in *Carnotaurus.*

In medial aspect (Fig. 10B), a pronounced vertical crest separates the adductor chamber from the orbital cavity, and no doubt served as the caudal attachment site for the circumorbital membrane (Elzanowski, 1987; Baumel and Raikow, 1993; Sedlmayr, 2002). Ventrally, an extension of this crest contacts the jugal caudally and projects slightly ventral to the suborbital process. This jugal articular surface twists as it passes ventrally, facing progressively more medially and matching a congruent twist on the jugal's postorbital ramus. Dorsally, the crest terminates at a cup-shaped facet for the capitate process (= laterosphenoid buttress, dorsolateral boss of Madsen and Welles, 2000), which is pierced on each side by two foramina, presumably supplying the soft tissues of the putative synovial postorbital-laterosphenoid joint (see below).

The rostral ramus of the postorbital is thickened and bordered medially by a deeply interdigitating contact surface for the frontal. The abbreviated caudal ramus terminates in a relatively thin, squamous-type facet for the squamosal (Fig. 10B, D). This facet is divided into dorsal and ventral portions by a medially projecting ridge that is received by a complementary fossa on the squamosal. Between the rostral and caudal rami, the postorbital forms the smooth-walled rostrolateral portion of the dorsotemporal fenestra. A large foramen pierces the postorbital just below the rim of the fenestra, transmitting the temporo-orbital vessels (Fig. 10D; Sedlmayr, 2002). The bone surface within the adductor chamber ventral to the squamosal articular surface is generally smooth and featureless.

Rostral to the vertical crest on the internal surface is the orbital cavity, best viewed medially. The bone surface here is generally smooth to finely striate. The crest bifurcates ventrally as the suborbital process projects into the orbit. The medial aspect of the suborbital process has two surfaces: a dorsal surface that continues the rounded margin of the bulbar region of the orbital cavity, and a triangular ventral surface that is more striate and probably relates to the connective tissues of the suborbital ligament (Fig. 10B, C). The boundary between these two surfaces most likely represents the ventral attachment of the circumorbital membrane.

Although the rostral ramus of the postorbital of FMNH PR 2100 is thickened, there is no distinct postorbital rugosity or cornual process as occurs in many other theropods (e.g., *Ceratosaurus*, *Allosaurus*, *Sinraptor*, various tyrannosaurids). Whereas the squamosal process of the postorbital is generally narrow and gracile in basal theropods, it is dorsoventrally expanded in *Majungasaurus* and *Carnotaurus* (Fig. 2), reflecting the dorsal enlargement of the caudal skull roof in abelisaurids.

Jugal—In general conformation, the jugal resembles that of most other theropods (Figs. 1, 11). It is thin transversely with two dorsal processes (for the lacrimal and the postorbital), a rostral process for the maxilla, and a bifurcate caudal process for the quadratojugal (Fig. 1). There is also a distinct contact surface medially for the ectopterygoid. The ventral margin is relatively thin and straight throughout most of its length, except caudally where it forms a thickened, rounded process or rugosity just ventral to the ectopterygoid contact. In contrast to nonabelisaurid theropods, telescoping of the facial elements has resulted in a more extensive jugal-maxillary contact as well as a

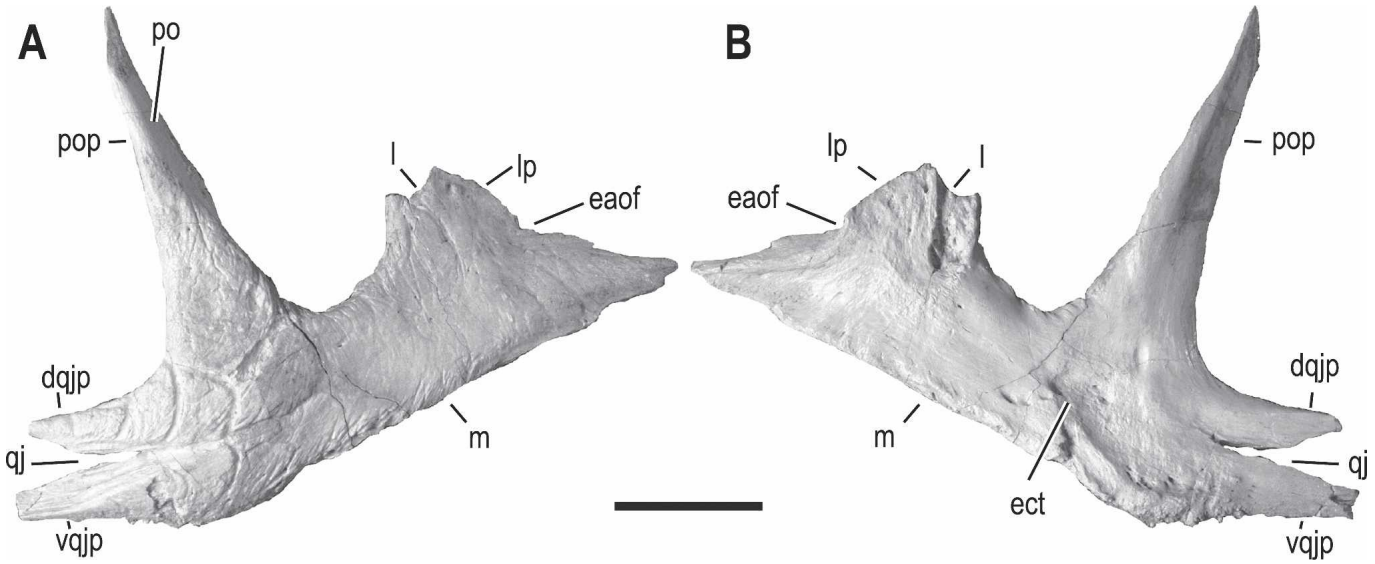

FIGURE 11. Right jugal of *Majungasaurus crenatissimus* (FMNH PR 2100) in **A**, lateral; and **B**, medial views. Scale bar equals 5 cm. See Appendix 1 for abbreviations.

more steeply angled orientation of the jugal. These features appear to be further exaggerated in the abelisaurid *Carnotaurus*, in which the jugal is considerably deeper and more compact than in *Majungasaurus*, almost lacking the rostral portion present in other theropods (Fig. 2).

Rostrally, the jugal separates the maxilla from the lacrimal and thereby contributes to the border of the external antorbital fenestra. The lack of contact between maxilla and lacrimal is prevented by expansion of a laminar flange of the jugal that is absent from the less derived forms. Separation of maxilla and lacrimal by the jugal occurs in many mid- to large-sized theropods, including other abelisaurids (*Carnotaurus*, *Aucasaurus*), as well as carcharodontosaurids, *Herrerasaurus* and *Sinraptor*. Lacrimal-maxillary contact is present in several taxa, however, including *Allosaurus* and the neoceratosaur *Ceratosaurus* (Fig. 2). The antorbital margin of the jugal is similar to that of the lacrimal and maxilla in being sculptured, and lacking any external antorbital fossa. There is a slight external depression just behind the antorbital margin, but it bears the texture of subcutaneous bone rather than the smooth texture characteristic of the pneumatic fossa typical of many other theropods (Witmer, 1997a).

The jugal-maxillary contact of *Majungasaurus* is derived in its relative simplicity. The straight edged ventral margin of the jugal, which extends over half of the length of this element, sits in a shallow groove on the maxilla, reinforced medially by an elongate, tall, and steeply angled maxillary contact. The maxillary articular surface is bordered rostrally by a medial thickening of the antorbital margin, which bears the smooth surface texture of the antorbital cavity. The rostral ramus of the jugal lacks any of the complex features noted for other basal theropods such as *Edmarka* (Bakker et al., 1992), *Sinraptor* (Currie and Zhao, 1994a), *Allosaurus* (Madsen, 1976a), and *Ceratosaurus* (Gilmore, 1920). Also in contrast to these taxa, the rostroventral portion of the jugal is not overlapped laterally by the maxilla.

The postorbital ramus is relatively slender and tall, approximately one half the total length of the jugal, reflecting the relatively tall orbit and large laterotemporal fenestra. Along its rostral margin, this ramus shares a loose fitting contact with the ventral (jugal) ramus of the postorbital, with both elements making a reciprocal twist, as noted above. The dorsalmost portion of the postorbital ramus of the jugal is not visible in lateral view as it is covered by the caudally expanded postorbital. An elongate, slender postorbital ramus is present in many other basal theropods (e.g., *Ceratosaurus*, *Allosaurus*, *Syntarsus*, *Coelophysis* and *Dilophosaurus*, *Sinraptor*), whereas a number of tetanuran taxa (*Edmarka*, *Torvosaurus*, *Tyrannosaurus*) possess short and broad postorbital rami. The basal theropods *Herrerasaurus* and *Eoraptor* also appear to have relatively short postorbital processes, however, and thus the elongate condition may not be primitive for Theropoda. In contrast to *Majungasaurus*, *Carnotaurus* possesses a relatively broad, triangular postorbital ramus, broadest at the base and more convex along the caudal margin. Likewise, a fragmentary element in the Lameta abelisaurid collection interpreted to be a jugal (GSI-IM K27/577) has a relatively broader base than does *Majungasaurus*. The ventral ramus of the postorbital terminates well above the ventral limit of the orbit in *Majungasaurus*, articulating with the upper two-thirds of the jugal postorbital process. This is the standard condition among theropods, although this ramus does reach the ventral orbit in some taxa, including *Afrovenator* and *Marshosaurus*.

The quadratojugal processes are similar in length, the ventral process being slightly longer than its dorsal counterpart. This morphology is comparable to *Ceratosaurus* and distinct from *Allosaurus*, *Sinraptor*, and *Torvosaurus*, for which the dorsal process is markedly shorter than the ventral process (Bakker et al., 1992; Fig. 2). Both dorsal and ventral quadratojugal processes are relatively robust in FMNH PR 2100, and bear ridges and grooves within the external articular surface such that the contact with the quadratojugal is tight. The articulation is further reinforced by a medial lamina of the quadratojugal that wraps around and firmly clasps the dorsal quadratojugal process of the jugal. As a result, it seems unlikely that there was any lateral movement of the dorsal (postorbital) process, such as that suggested by Bakker and colleagues (1992) for *Edmarka*. Moreover, the occurrence and functional importance of kinesis at this joint is brought into question by the fact that this suture is at least partially fused in some ceratosaur individuals (e.g., MACN-CH 894, *Carnotaurus*; MWC 1.1, *Ceratosaurus*).

From the medial aspect (Fig. 11B), contact surfaces for the maxilla (see above), lacrimal, and ectopterygoid are clearly visible. The palatine bone also has a small area of contact above the maxillary articular surface and rostroventral to the lacrimal contact. The lacrimal articular surface occupies the entire lacrimal process. The lacrimal articular surface is complicated such that the rostral portion is broad, flat, and faintly striate, whereas the caudal portion (shown well on both sides of FMNH PR 2100) is excavated by a broad sulcus that leads ventrally to several small foramina entering the body of the jugal. The reciprocal surface of the lacrimal shows the same bipartite articular structure, but the caudal part (again, well shown on FMNH PR 2100) does not seem stout enough to account for the broad sulcus in the jugal. Nevertheless, the left lacrimal and jugal of UA 8709 are preserved in natural articulation and clearly show the articulation to be very tight and congruent.

The contact surface for the ectopterygoid is marked partially by a large, crescentic roughened region ventral to the postorbital ramus (Fig. 11B). This surface accommodates the caudal facet of the ectopterygoid's jugal process, whereas its rostral facet is not associated with much of a discernible articular surface on the jugal. In fact, the rostral contact on the jugal might have been missed had it not been possible to manually fit together the well preserved elements of FMNH PR 2100. The two surfaces are separated by a vascular groove on the jugal that begins caudally at the ventral apex of the laterotemporal fenestra, and then courses rostrally between the two facets of the ectopterygoid-jugal joint to reach the region in which the jugal articulates with the maxilla and lacrimal. This groove presumably conducted the jugal branch of the maxillary vessels (Sedlmayr, 2002).

The dermal ornamentation of the external surface is not as strongly rugose as on the more dorsal elements, and is dominated by vascular or neurovascular grooves. The following description is based largely on FMNH PR 2100 (UA 8709 has the same general features but they are not as well developed). The postorbital ramus is sculptured on only its ventral half because the dorsal portion is covered laterally by the postorbital bone, as noted above. The sculptured portion is characterized by a series of oblique vascular grooves that open rostrodorsally into the articular region but are not carried across the joint onto the postorbital. The vascular groove on the medial surface noted above (i.e., separating the ectopterygoid facets) is exactly matched by a large vascular groove on the lateral surface, demonstrating that a large vessel passed through the laterotemporal fossa superficially and then split into lateral and medial branches as it reached the rostroventral corner of the fenestra. The lateral vascular groove sweeps ventrally and then dorsally before passing into the orbit. On its way, it sends several large branches caudoventrally to the region of the quadratojugal articular surface. In fact, a vascular groove passes rostrally from the apex of the quadratojugal contact and ramifies on the body of the jugal. More rostrally, the external surface of the jugal bears a series of curving grooves that are more pronounced dorsally at the orbital and antorbital margins and ventrally at the edge of the bone. As noted earlier, the ventral margin of the jugal below the ectopterygoid contact has a marked rugosity characterized by grooves and foramina.

Quadratojugal—The L-shaped quadratojugal (Figs. 1, 12) possesses a relatively long rostral (jugal) ramus and a shorter dorsal (squamosal) ramus. A third, smaller process for contact with the quadrate occurs caudoventrally, and a low, horizontal ridge occurs externally at the junction of these three processes (Fig. 1). The thick rostral ramus (maximal thickness 16 mm in FMNH PR 2100) is deepest caudally and tapers rostrally. The jugal contact consists of a well-developed slot on the dorsal surface, which receives the dorsal quadratojugal process of the jugal, and a sloping contact ventromedially for the ventral quadratojugal process. The more gracile dorsal ramus (maximal thickness 9 mm in FMNH PR 2100) has a nearly straight caudal border and a convex rostral border. The rostral ramus is much more ornamented on its external surface than is the dorsal ramus, and the former bears a well marked rugosity that continues caudally as the horizontal ridge noted above. Distally, the dorsal ramus tapers to a blunt end that does not contact the squamosal; thus the quadrate forms a small caudal portion of the laterotemporal fenestra (Fig. 1). Caudomedially, a highly rugose and convoluted surface on the quadrate process continues upward along the caudal margin of the dorsal ramus, clearly showing the quadrate contact. This contact is broadest ventrally and narrows dorsally, ultimately forming a slot that clasps the lateral wing of the quadrate. The articular surface extends almost two-thirds the height of the quadrate, and forms a tight, immobile joint. A small platform on the outer surface of the quadrate process combines with the lateral wing of the quadrate to form a smooth, caudally directed fossa. As in other theropods, the caudoventral corner of the quadrate process closely approaches, but does not contribute to, the lower jaw articulation.

The quadratojugal of *Majungasaurus* compares closely to that of other basal theropods in most of the above features (Fig. 2). Taxonomic variation is largely associated with the relative size and shape of the rostral and dorsal rami. Contact between the squamosal and quadratojugal is extremely variable, even within basal theropods. In *Herrerasaurus*, the dorsal ramus is almost twice the width of the rostral ramus, but does not appear to contact the squamosal (Sereno and Novas, 1993). In contrast, both dorsal and ventral rami are relatively slender in some taxa, with at least a narrow quadratojugal-squamosal contact (e.g., *Eoraptor*, *Ceratosaurus*). Quadratojugal-squamosal contact also occurs in *Allosaurus*, but the dorsal ramus is considerably broader (Madsen, 1976a). The latter trend reaches its extreme among tyrannosaurs (e.g., *Tyrannosaurus*, *Daspletosaurus*), in which the dorsal ramus is dramatically expanded, shares a broad, rostrally projecting contact with the squamosal, and effectively divides the laterotemporal fenestra into dorsal and ventral portions. In overall conformation, the quadratojugal of *Majungasaurus* is most closely similar to that of other abelisaurids (e.g., *Carnotaurus*, *Abelisaurus*), which also possess a thickened, relatively elongate rostral ramus and a more gracile, abbreviated dorsal ramus.

Squamosal—The squamosal (Figs 1, 7, 13) is a complex element contacting the postorbital rostrally, the parietal medially, the quadrate ventrally, and the paroccipital process caudally (Fig. 1). In contrast to the condition typical of non-abelisaurid theropods, there is no ventral contact with the quadratojugal. The triradiate squamosal can be subdivided into a broad, curved rostrodorsal portion (parietal process), and two robust projections or rami, one ventral (the quadratojugal process) and the other caudoventral (the postquadratic process). In most theropods, the squamosal is tetraradiate, with an additional projection—the postorbital process. This process appears to have become incorporated with the parietal process in *Majungasaurus* and perhaps other abelisaurids. The flattened parietal process flares upward medially to abut the parietal in an elongate, vertical suture. As a result, the squamosals comprise the lateral portions of a tall and broad transverse nuchal crest, with the attachment surface for nuchal musculature visible as a smooth region covering most of the caudal surface. The greatly expanded transverse nuchal crest is a synapomorphy of Abelisauridae (Bonaparte et al., 1990). In non-abelisaurid theropods, it is composed primarily of the parietals, with a median contribution from the supraoccipital, and little or no contribution from the squamosals. In *Majungasaurus*, the peripheral rugosity on the crest for muscle attachment (principally M. complexus, see below) is concentrated on the parietal but does extend somewhat onto the squamosal, suggesting that muscular expansion may have played a role in elaboration of the crest.

One consequence of the dorsomedial expansion of the squamosal is that, whereas the squamosal tends to roof the adductor chamber in most other theropods, the same surface is almost vertical in *Majungasaurus* and so contributes (with the parietal) to the caudal wall of the adductor chamber (Fig. 1). Another consequence is that the parietal process is much less distinct than that of most other large theropods in which the squamosal contacts the parietal via a more pointed process. The parietal contact in *Majungasaurus* is extremely thin in its mid portion (minimal thickness 1 mm in FMNH PR 2100), but broadens dorsally, where it contributes to a thick, rugose border of the nuchal crest.

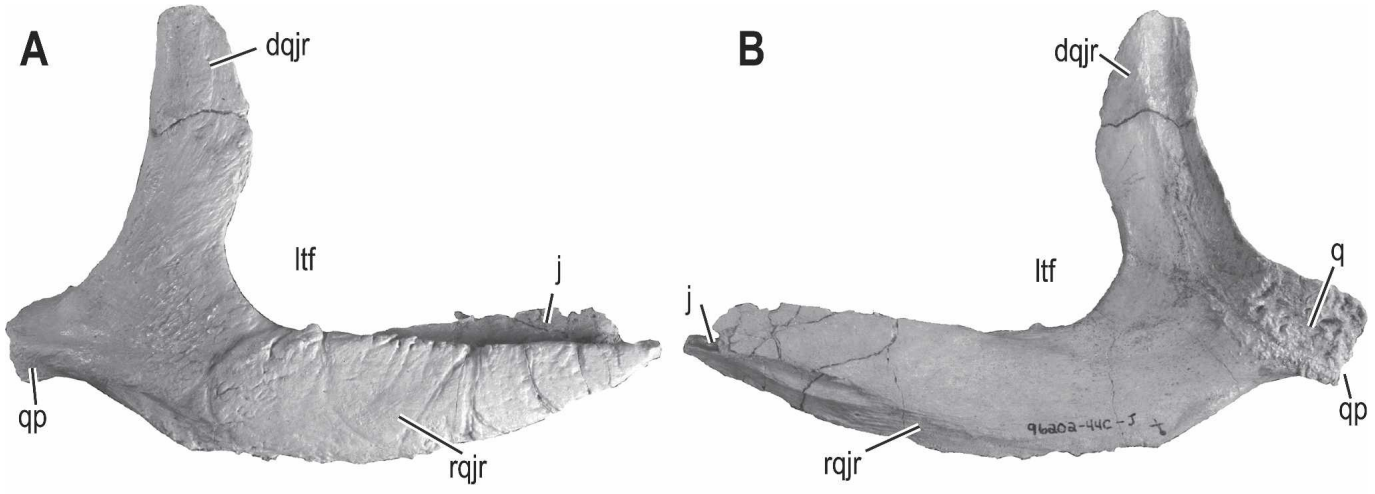

FIGURE 12. Right quadratojugal of *Majungasaurus crenatissimus* (FMNH PR 2100) in **A**, lateral; and **B**, medial views. Scale bar equals 5 cm. See Appendix 1 for abbreviations.

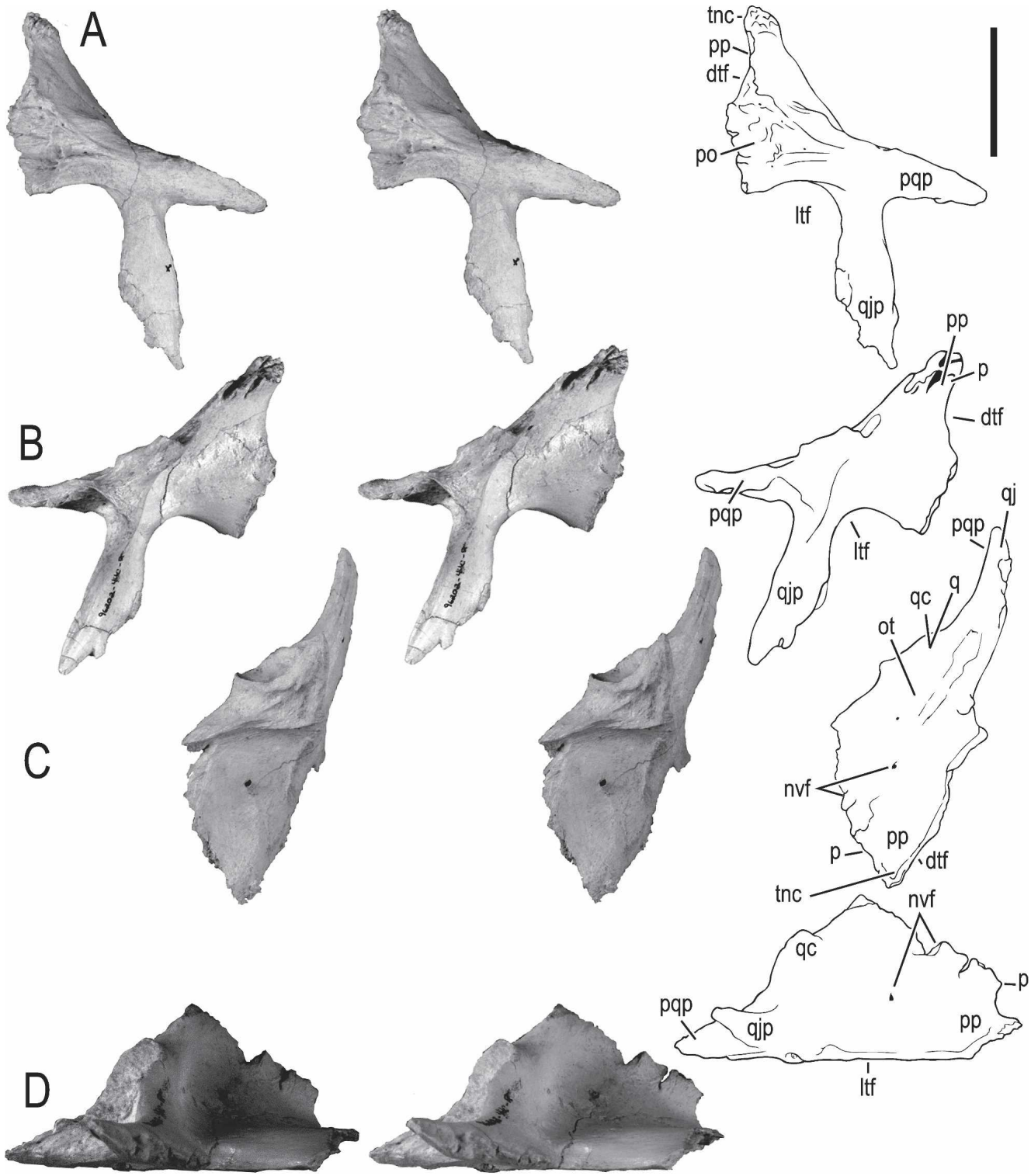

FIGURE 13. Stereopairs of left squamosal of *Majungasaurus crenatissimus* (FMNH PR 2100) in **A**, lateral; **B**, medial; **C**, dorsal; and **D**, ventral views. Scale bar equals 5 cm. See Appendix 1 for abbreviations.

It is also relatively broad ventrally, where it buttresses the paroccipital process. A foramen occurs along the parietal-squamosal contact ventrally, just above the paroccipital process. The foramen is confluent with a dorsomedially directed sulcus on the parietal (see below), and most likely represents the remnants of the posttemporal fenestra of other sauropsids, which in most archosaurs is lost or reduced to a foramen, as seen here and in other theropods. It probably served as a conduit for vasculature (e.g., the dorsal head vein) passing between the adductor chamber and the occipital region (Walker, 1990; see below).

In lateral aspect, there is a rugose, triangular facet for the postorbital (Fig. 13A). Although the rostralmost portion of the postorbital facet has been lost on both sides of FMNH PR 2100, the reciprocal facets for the squamosal are preserved on both postorbitals and show that the squamosal forms much of the lateral bony wall of the dorsal part of the adductor chamber. Viewed rostrally, the squamosal is sigmoidal, due in part to a ventral concavity within the above facet for reception of a corresponding ridge on the postorbital. Dorsal to the postorbital facet, the rostral margin of the squamosal forms a small caudolateral portion of the dorsotemporal fenestra.

The nearly vertical ventral ramus is narrow proximally, where it forms the caudodorsal corner of the laterotemporal fenestra, expands somewhat in its mid portion, and then narrows distally to a blunt tip. A relatively short, tapering ventral ramus of the squamosal is characteristic of abelisaurids. Bonaparte and Novas (1985) reported a contact between the squamosal and quadratojugal in *Abelisaurus*, but the dorsal portion of the quadratojugal is absent in the one known specimen, and the ventral ramus of the squamosal shows no indication of a distal contact (Fig. 2). The corresponding process in *Ceratosaurus* is also relatively short, but differs in being narrow throughout its length and sharing a contact with the quadratojugal. In many large theropods (e.g., *Allosaurus*), the ventral ramus shows a marked rostral expansion that invades the laterotemporal fenestra. The most exaggerated condition is present in tyrannosaurids, where the laterotemporal fenestra is effectively divided into dorsal and ventral portions by rostral projections of the squamosal and quadratojugal. In *Majungasaurus*, a well-developed sulcus between two sharp crests traverses the length of the ventral ramus caudally, extending from the quadrate cotyle to the ventral tip.

The postquadratic process is straight and projects only a short distance (26 mm on the right squamosal of FMNH PR 2100) behind the quadrate cotyle. The same conformation occurs in *Carnotaurus* and *Abelisaurus*, while differing from that of other basal theropods (e.g., *Dilophosaurus*, *Allosaurus*, *Ceratosaurus*), in which the postquadratic process typically curves ventrally to wrap around the head of the quadrate (Fig. 2). The basal theropod *Herrerasaurus* (e.g., PVSJ 407) lacks this process altogether. On both left and right squamosals of FMNH PR 2100, a small ridge projects ventromedially from the postquadratic process (Fig. 13B), forming a shallow sulcus along the ventral surface. This ridge, along with the rest of the postquadratic process, buttresses the paroccipital process, and a broad contact surface for the rostral surface of the latter is clearly visible as a roughened area separated from the remainder of the squamosal by a raised rim. This articular surface extends to the lateral margin of the squamosal and caps the postquadratic process throughout its length. Although the distal portions of the paroccipital processes are absent in FMNH PR 2100, the facets on both left and right squamosals demonstrate the full extent of the paroccipital processes (see below). Rostroventromedial to the postquadratic process is the relatively shallow quadrate cotyle, which forms a loose, presumably synovial, articulation with the head of the quadrate. A shallow quadrate cotyle also occurs in *Ceratosaurus* whereas it is significantly deeper in *Allosaurus*.

Frontal—With the possible exception of the nasal, the single most distinctive element in the skull of *Majungasaurus* is the greatly thickened frontal that, together with its opposite, forms a rounded, median dorsal projection, unknown in any other theropod (Figs. 1, 14–17). The frontal tends to show considerable taxonomic variation within Abelisauridae. However, the great majority of this variation is autapomorphic, which means that the frontal can be very useful for identifying taxa, but has minimal phylogenetic utility. Not surprisingly, the greatly thickened, coossified frontals are the most commonly found skull elements of *Majungasaurus*. Five frontal specimens are currently available for study (Fig. 16): a skull roof largely composed of partially fused frontals (MNHN.MAJ 4); a second pair of isolated frontals (FMNH PR 2099); a third pair of fused frontals (UA 8719); and two additional examples in skulls (FMNH PR 2100 and UA 8709; Figs. 1, 7). Other examples have been collected from the Berivotra field area, but have not been prepared. There is considerable variation among the prepared specimens, both in terms of absolute size and morphology of the cornual process. Nonetheless, it is postulated here that all five specimens pertain to a single species, *M. crenatissimus*. If so, the observed differences are likely due to individual, sexually dimorphic, and/or ontogenetic variation. The frontals can be grouped according to patterns of size and morphology (and presumably ontogeny; see below).

The frontals contact the nasals rostrally, the lacrimals rostrolaterally, the postorbitals laterally, the parietals caudally, the sphenethmoid ventrally, and the laterosphenoid caudoventrally. The frontal bones of MNHN.MAJ 4 were described as fused (Sues and Taquet, 1979; Sues 1980; Sampson et al., 1998), but CT scans show that a suture is visible internally despite being obliterated by the proliferation of highly vascular bone dorsally. Likewise, evidence of an interfrontal suture is present in all other known specimens, as confirmed by CT, with the exception of UA 8709, which is too poorly preserved in this region to reveal internal bony architecture. In addition to the median cornual process, which varies considerably in overall size and extent, the frontals are greatly thickened, and, in some cases, penetrated by sinus cavities (see below).

Rostrally, the frontals form a broad, sloping platform for contacting the nasals (Fig. 14B, E, H). This nasal process is much steeper in MNHN.MAJ 4 (Fig. 16A) than in the other specimens (angled about 50 degrees to the horizontal relative to about 30 degrees in FMNH PR 2100 and 20 degrees in FMNH PR 2099), presumably resulting from the strongly developed cornual process in this individual. The nasal process extends caudally only up to the base of the cornual process, confirming that the nasal does not significantly contribute to the cornual process, in contrast to *Rajasaurus*, in which the nasal and frontal together comprise the median protuberance (Wilson et al., 2003). The nasal articular surface of all specimens is characterized by a series of longitudinal grooves with scattered foramina and flanked laterally by an elongate socket that received a peg from the nasal, forming a tight, immobile union (Figs. 14E, H, 16). In contrast, Mazzetta and colleagues (2000, p.188) described the frontonasal contact in *Carnotaurus* as forming "a conspicuous hinge joint" that they regarded as "prokinetic," and part of a highly kinetic skull apparatus. As detailed below, our findings for *Majungasaurus* restrict any kinesis to the intramandibular joint. In fact, many of the sutural attributes of *Majungasaurus* reflect a trend to decrease the amount of any movement within the craniofacial skeleton (see Discussion), and we suggest that *Carnotaurus* shares many of these same attributes. CT shows that the foramina within the nasal articular surface open into relatively simple neurovascular canals that no doubt served primarily a nutritive function. The nasal articular surface also has a rostrolateral tongue (largely missing on MNHN.MAJ 4, FMNH PR 2100, and FMNH PR 2099 but present on UA 8709 and UA 8719) that projects internally under the nasals and covers the roughened medial surface of the lacrimal noted above.

A thick, deeply striate lateral projection of the frontal bears firm, interdigitating contacts for the lacrimal and most likely the prefrontal rostrally (Fig. 14E). Between the nasal platform and the lacrimal contact, the frontal has a deep slot for a long caudal prong of the prefrontal (again, which is fused to the lacrimal). Such a deep slot may well be unique. Whereas a variety of theropods (e.g., *Allosaurus*) have a moderately deep, more-or-less conical recess in the frontal bone for the prefrontal, *Majungasaurus* has a very deep, narrow canal that extends as far caudally as just beyond the rostrocaudal level of the apex of the cornual

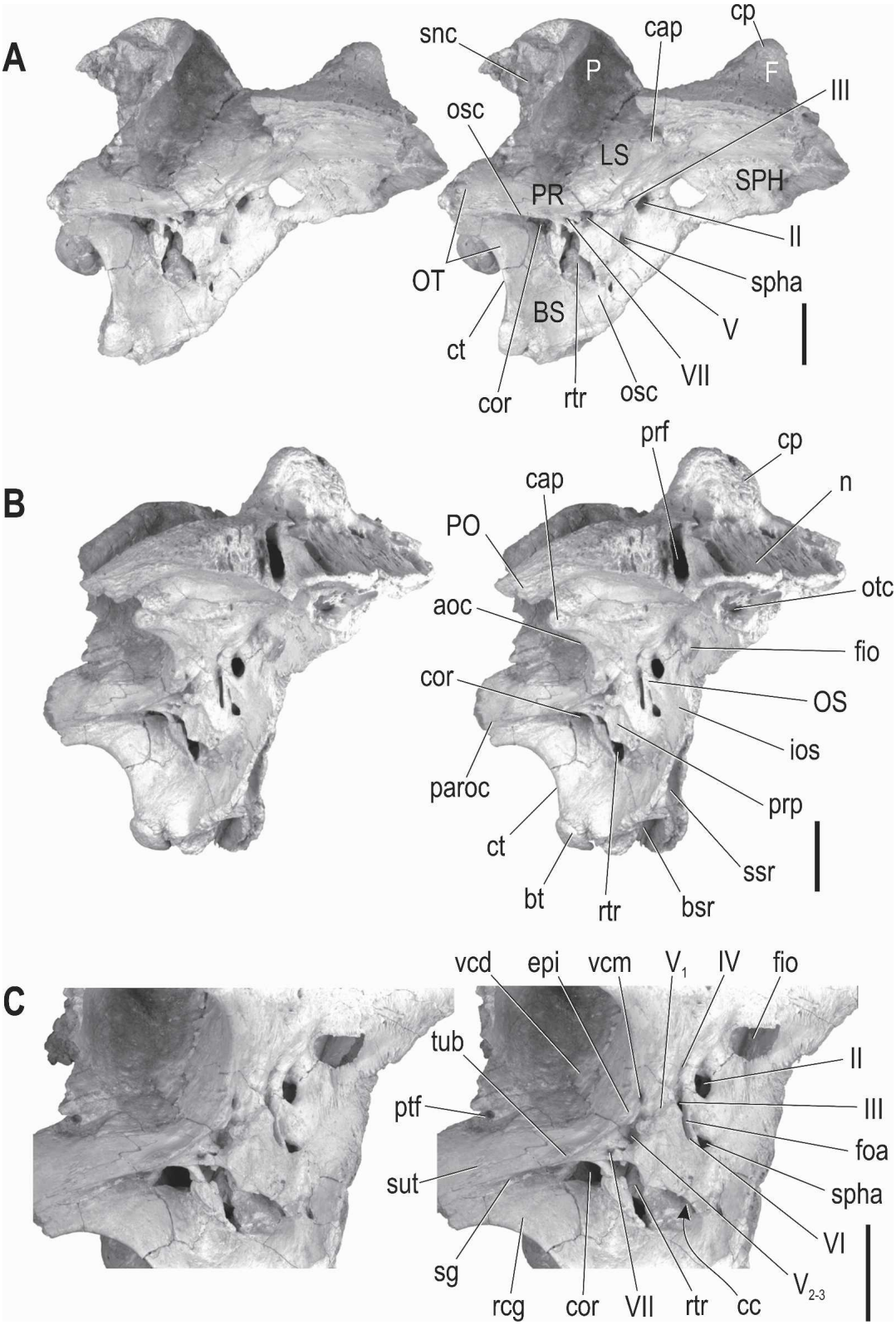

FIGURE 14. Stereopairs of articulated braincase of *Majungasaurus crenatissimus* (FMNH PR 2100) in the following views: **A**, right lateral; **B**, right rostrolateral; **C**, close-up of right rostrolateral; **D**, left lateral; **E**, rostral; **F**, ventral; **G**, caudal; **H**, dorsal. Scale bars equal 4 cm. See Appendix 1 for abbreviations.

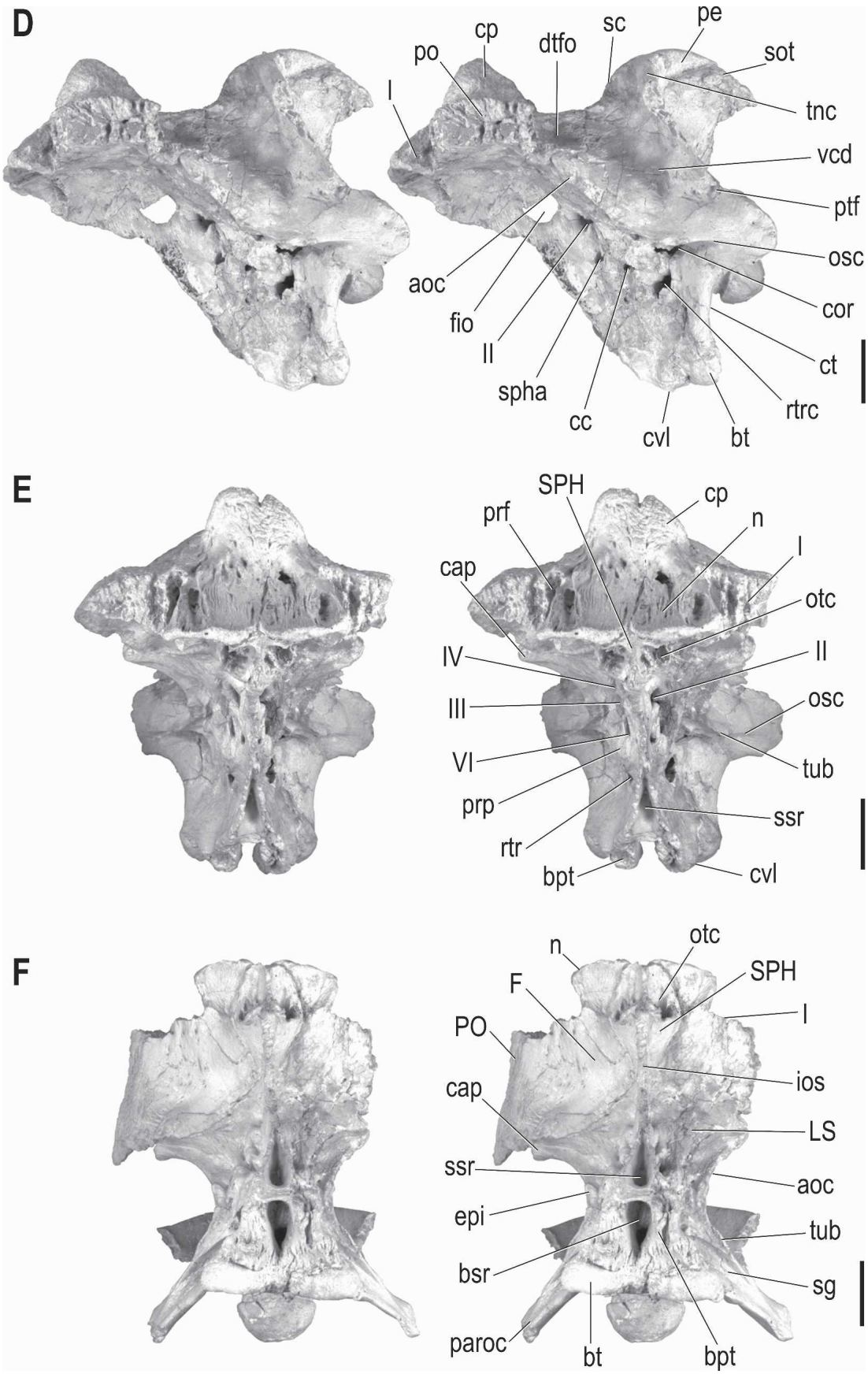
D
pe
cp
sc
dtfo
po
sot
l
tnc
vcd
ptf
osc
aoc
cor
fio
ct
ll
spha
rtrc
cc
cvl
bt
E
SPH
cp
prf
n
l
cap
otc
IV
ll
III
osc
VI
tub
prp
ssr
rtr
bpt
cvl
F
otc
n
SPH
F
l
PO
ios
cap
LS
ssr
aoc
epi
tub
bsr
sg
paroc
bt
bpt

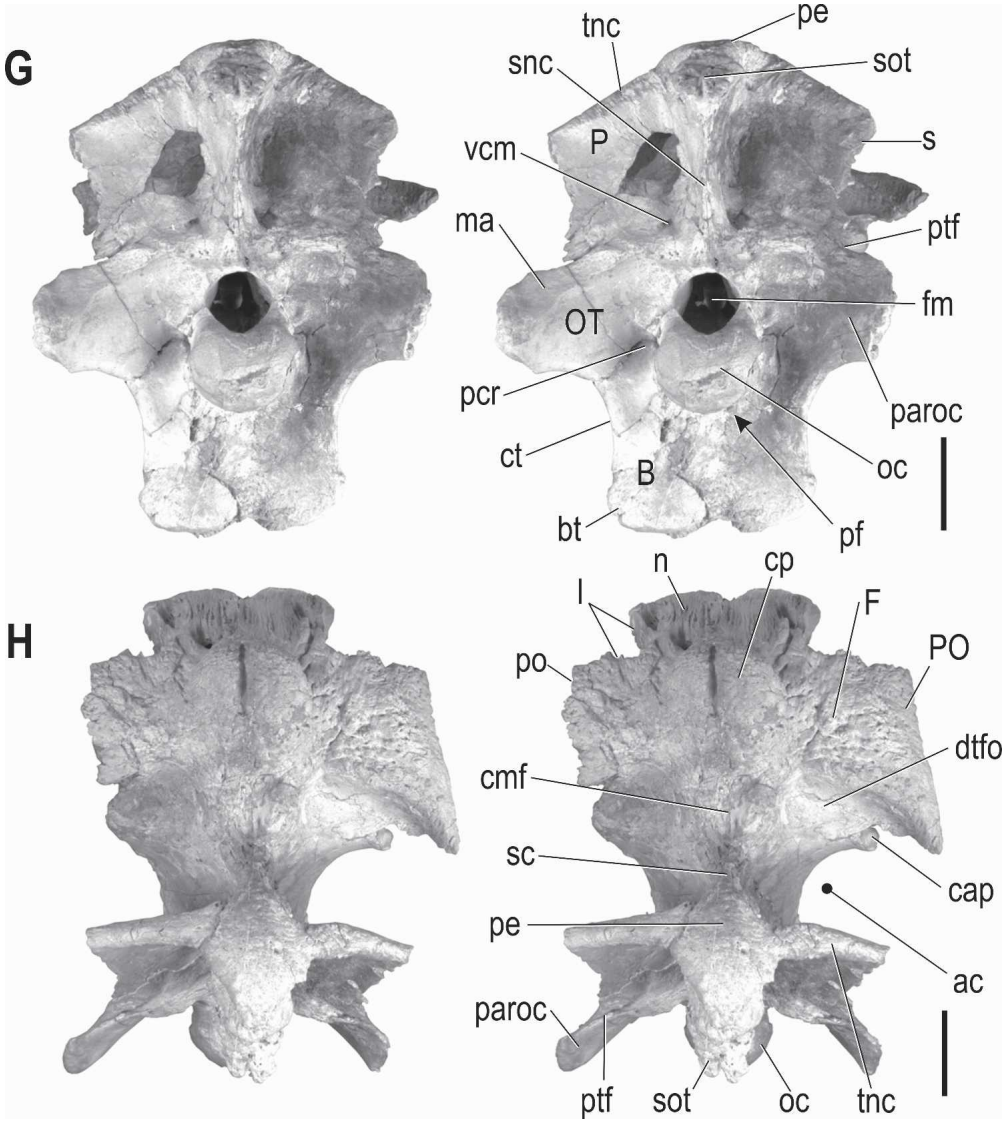

process (Fig. 14B, E). In some specimens, this prefrontal slot communicates with the frontal sinuses (see below; Fig. 2, arrows in B and C). Laterally, the frontal also interdigitates deeply with the postorbital. In fact, this contact is so firm that it was basically fused on the right side of FMNH PR 2100 and both sides of UA 8719 (Fig. 16E). The frontal-postorbital suture is marked by textural differences dorsally and a row of foramina ventrally within the orbital roof.

The frontoparietal suture is difficult to trace even on CT scans, but, where visible, it is strongly interdigitating. As is typical of theropods, the frontals also contribute to a deep fossa at the rostromedial corner of each dorsotemporal fenestra, which in life housed jaw adductor musculature, fat, and blood vessels (Holliday, 2006). In the larger specimens (e.g., MNHN.MAJ 4, FMNH PR 2100), this dorsotemporal fossa is more deeply etched into the frontal bone, whereas in smaller specimens (FMNH PR 2099, UA 8709), the fossa is shallower. A pronounced median fossa of significant breadth occurs caudally at the base of the cornual process in association with the frontoparietal suture. Consequently, the sagittal crest (frontoparietal or intertemporal crest of some authors) is relatively broad rostrally and tapers in the mid-section before broadening again in association with the parietal eminence. This conformation of the sagittal crest is present in other ceratosaurs, and may be apomorphic for the clade. The median fossa behind the cornual process bears the sculpturing of subcutaneous bone, although it is much less rugose than the cornual process itself (Fig. 14H). The fossa is almost round in MNHN.MAJ 4 and somewhat undercuts the cornual process (Fig. 16A), whereas the fossa is more elongate and shallower in other specimens.

Although highly derived, the frontals of *Majungasaurus* do share some similarities with those of other abelisaurid theropods. Indeed, skull roof thickening and elaboration has often been cited as a feature common to many abelisaurid taxa. These features are highly variable and, in many cases, taxon specific, each species bearing a unique conformation. *Carnotaurus*, *Indosaurus*, and *Rajasaurus* also possess a thickened skull roof, including dorsoventrally thickened frontals. Of these, the Indian form *Rajasaurus* most closely resembles *Majungasaurus*, possessing a median eminence or 'horn;' however, whereas this structure is composed almost entirely of the frontals in the Malagasy taxon, in *Rajasaurus* it was apparently formed primarily by the nasals, with some frontal contribution (Wilson et al., 2003). *Carnotaurus* possesses paired frontal horncores rather than a median eminence (Fig. 2), whereas *Aucasaurus* is reported to have "frontal swells instead of horns" (Coria et al., 2002:461). Although clearly thickened, the detailed nature of the skull roof is difficult to ascertain in the holotype of *Indosaurus.* In contrast, the basal

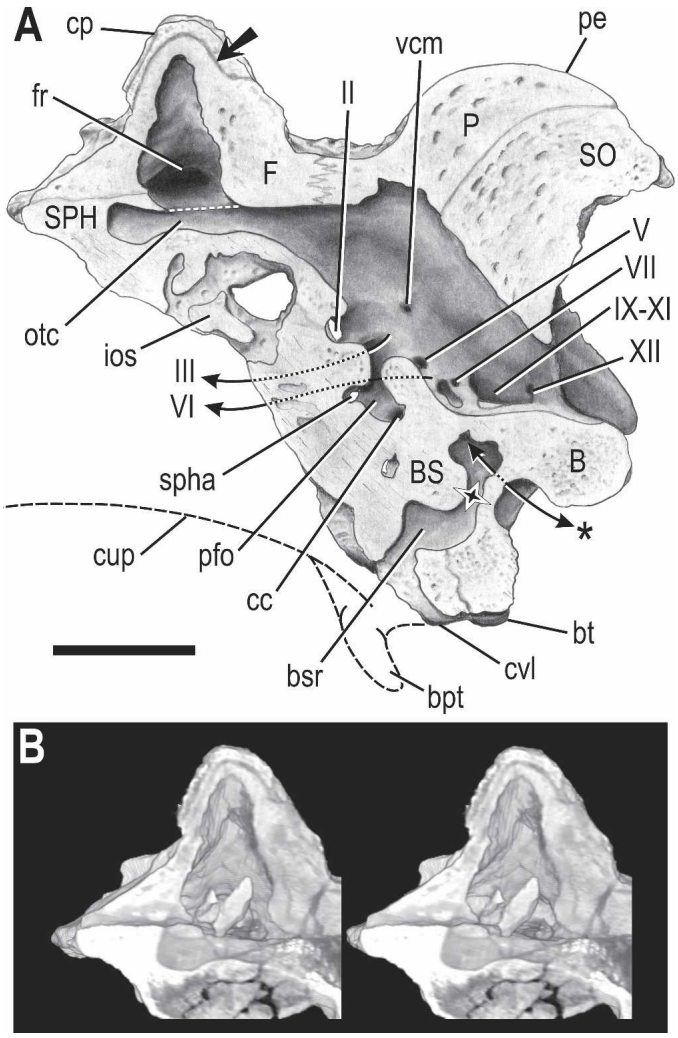

FIGURE 15. Sagittal section of braincase of *Majungasaurus crenatissimus* (FMNH PR 2100) derived from CT scan data. **A**, Drawing of right half of braincase in medial view, with cultriform (**cup**) and basipterygoid (**bpt**) processes (dashed line at bottom) reconstructed from UA 8709. Arrow within cornual process (**cp**) points to radiolucent line between 'normal' bone of the frontal (**F**) and the more superficial, ornamented layer. White dashed line above the olfactory tract cavity (**otc**) marks the roof of the cavity, which is missing in this specimen due to damage, but present in all other specimens. Arrow marked by an asterisk (*) indicates a communication between the occipital surface of the basioccipital bone and a caudal, basicranial diverticulum of the rostral tympanic recess. Four-pointed star indicates an artificial communication between the latter space and the basisphenoid recess (**bsr**). The spaces below and behind the facial nerve foramen (**VII**) are artificially enlarged due to damage. **B**, Stereopairs of right half of sphenethmoid (**SPH**) and frontal (**F**) bones in medial view, showing the pneumatic frontal recess (**fr**) within the cornual process (**cp**). Objects visible medially within the floor of the recess are loose fragments of the frontal bone. Scale bar equal 5 cm. See Appendix 1 for abbreviations.

abelisaurid *Rugops* lacks both thickened frontals and any development of frontal cornual processes (Sereno et al., 2004), as does the holotype of *Indosuchus*. The holotype (and only) specimen of *Abelisaurus* (MC 11098) appears to have frontals that are somewhat thickened relative to *Rugops* and non-abelisaurid basal theropods, yet this feature does not approach the condition seen in *Majungasaurus*.

The frontal is perhaps the most variable skull element in *Majungasaurus* (Fig. 16). The salient features of each specimen are addressed in succession. They will be taken roughly in order of size. Relative size, despite being perhaps the single most important biological parameter, is difficult to assess in these five specimens because of two factors: (1) each is incomplete and equivalent measurements cannot be made on all specimens, and (2) perception of general size is clouded by the variable development of the cornual process. After considerable effort, only a single 'size' metric could be identified: the breadth across the olfactory bulb cavity, as measured on 3D surface models of the cranial endocasts of each specimen derived from CT data (see below). This is the only available metric present on all specimens, other than any pertaining to the cornual process itself. Although certainly unconventional, olfactory bulb breadth may be an acceptable size proxy in that it may be less subject to many of the causes of individual variation (e.g., health status and history, conditioning, pathological remodeling). Although it is tempting to attribute these size differences to ontogeny, the size range of the available sample is not great and, more significantly, there is evidence that some of the 'smaller' specimens may pertain to more mature individuals (see below).

The largest example is MNHN.MAJ 4, which possesses greatly thickened frontals topped by a broad, dome-like projection (Fig. 16A). As preserved, the highly rugose and convoluted cornual process is approximately 91 mm long and 96 mm wide. The lateral postorbital rami are not preserved on this specimen, and it is likely that the horncore extended somewhat farther to the sides, forming a roughly circular base on the frontals. The greatest height of the cornual process, as measured in CT slices from dorsal apex to the roof of the endocranial surface, is about 66.2 mm. This value is actually slightly less than the equivalent measure in FMNH PR 2100 (67.3 mm), but the cornual process in MNHN.MAJ 4 is much more impressive because of its greater rugosity and greater mediolateral and rostrocaudal extent. The texture of the cornual process is generally characterized by a seemingly random pattern of tubercles and ridges separated by grooves and foramina. CT shows that these grooves and foramina open internally into a complex series of vascular canals. The canals are best developed peripherally, and it is again reasonable to regard the surface rugosity as representing entrapped vessels within a mineralized periosteum or dermis (Hieronymus and Witmer, 2004). Unlike the other specimens, in which the horncore represents a single, predominant structure, in MNHN.MAJ 4 there is evidence that the regions lateral to the central eminence also bore perhaps somewhat separate structures. Although these lateralmost portions are not fully preserved, on each side there is a raised, highly rugose region partially separated by a groove from the central main cornual process. Just what these lateral portions may represent await the discovery of more complete specimens.

FMNH PR 2100 is a somewhat smaller specimen than MNHN.MAJ 4 (Figs. 1, 14, 15, 16B). The median cornual process is both relatively and absolutely smaller in length (56 mm) and breadth (59 mm) but is actually somewhat taller than MNHN.MAJ 4 (see previous paragraph). This structure is somewhat asymmetrical, being higher on the right side than the left, and lacks the extreme development of surface convolutions of MNHN.MAJ 4. A longitudinal dorsal sulcus approximately on the midline of the cornual process is apparently the result of incomplete fusion of opposing sides, perhaps suggesting immaturity, although none of the other specimens have such a sulcus. CT confirms the presence of an interfrontal suture internally. The horncore itself is more restricted than in MNHN.MAJ 4, occupying a smaller 'footprint' on the frontal. The caudal margin is at approximately the same position, adjacent to the rostral margin of the dorsotemporal fenestrae, but it does not extend rostrally or laterally to the same degree as in MNHN.MAJ 4. As a result, it occurs fully caudal to the prefrontal slots, and its breadth is significantly less than that of the nasal articular sur-

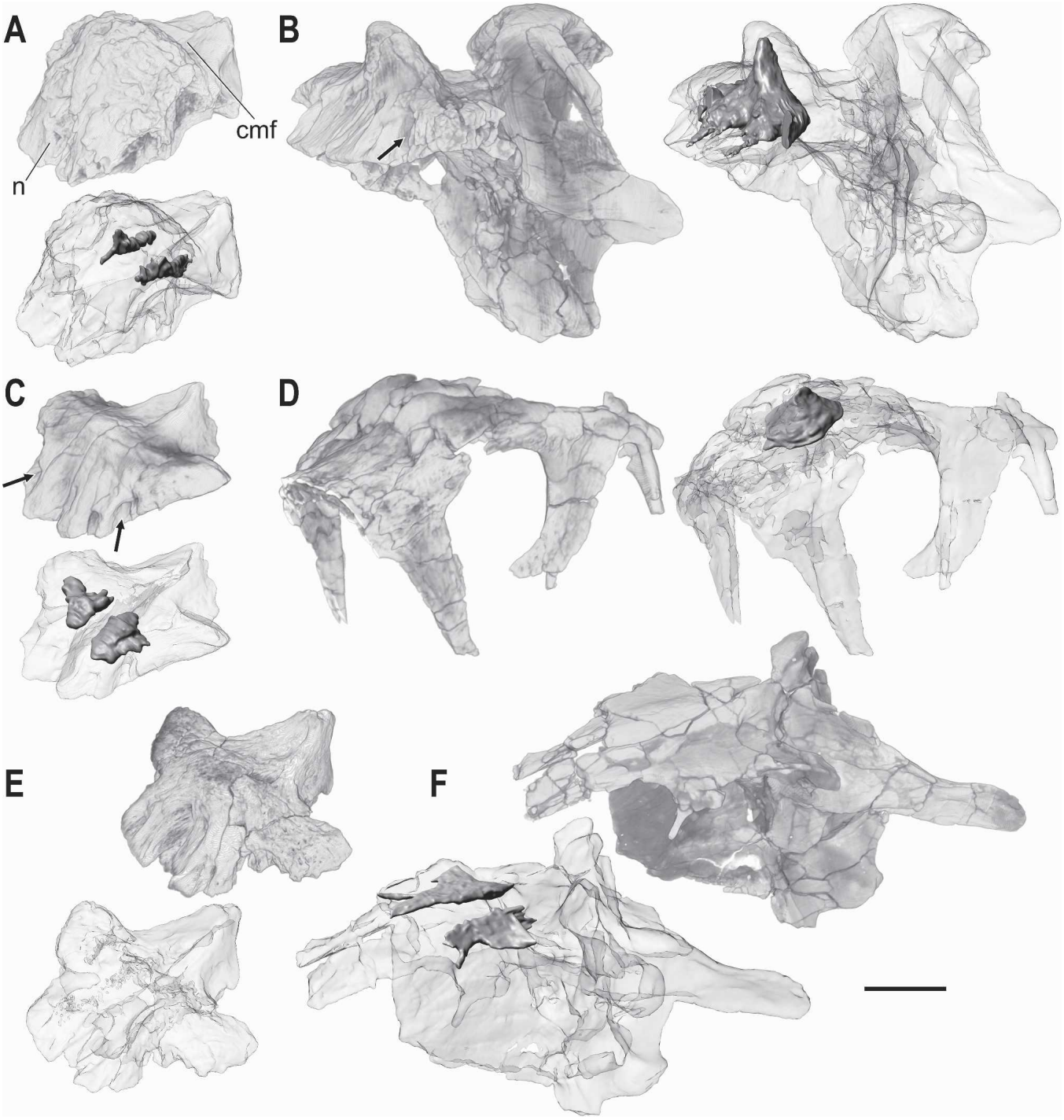

FIGURE 16. Variation in morphology of the frontal bones in *Majungasaurus crenatissimus* (**A**–**E**) and *Ceratosaurus magnicornis* (**F**, MWC 1.1; c.f. *C. nasicornis*). *Majungasaurus* specimens are **A**, MNHN.MAJ 4; **B**, FMNH PR 2100; **C**, FMNH PR 2099; **D**, UA 8709 (nasal truncated and specimen reversed for easier comparison); and **E**, UA 8719. In all cases, the elements are in left rostrodorsolateral view, derived from reconstructed CT scans; each specimen is illustrated with a volume rendering showing overall form and with a semitransparent surface rendering revealing the frontal recess(es) within (absent in UA 8719). Arrows in **B** and **C** show the putative entrance of the diverticulum via the articular slot for the lacrimoprefrontal prong. Scale bar equals 5 cm. See Appendix 1 for abbreviations.

face. The pattern of surface sculpture, as noted, is much finer than in MNHN.MAJ 4, but still consists of grooves, ridges, tubercles, and foramina. CT shows that the vascular canals within the bone are much finer than in MNHN.MAJ 4 and, instead, the periphery of the process has a more laminar appearance (Fig. 15).

UA 8709 has a relatively low cornual process (approximately 35.8 mm) occupying a relatively small footprint on the frontal (Figs. 7, 16D). It ends well forward of the dorsotemporal fenestrae rather than caudally reaching the level of the fenestrae as in MNHN.MAJ 4 and FMNH PR 2100. The fragmented and weathered specimen is not well enough preserved to determine if an

interfrontal suture is present or if the apparently smooth cornual process is natural or an artifact.

UA 8719 also has a low cornual process; in fact, at 33.5 mm in height (again, as measured in CT from apex to endocranial cavity), it is the lowest of the five known frontals (Fig. 16E). Its footprint on the frontal is a little more extensive than that of UA 8709. Interestingly, it is among the most completely co-ossified of all the specimens, in that, in addition to the near obliteration of the frontal-postorbital sutures noted above, the interfrontal suture also is barely discernible on CT and is obliterated externally. Thus, despite its small size and low cornual process, it would seem to have come from a mature individual. The surface texture of the cornual process is the best preserved of the three 'low-horned' individuals. The center region of the cornual process is relatively smooth and is penetrated by more-or-less vertical vascular canals (confirmed by CT), whereas the periphery has a more rugose texture characterized by the typical pattern of grooves, ridges, and tubercles.

The final and (by our measure) smallest specimen is FMNH PR 2099, consisting of frontals separated approximately along the midline (Fig. 16C). The cornual process occurs as a low median projection, which, with a height of 34.5 mm, is intermediate between UA 8719 and UA 8709. As preserved, opposing frontals are divided at least partially along the midline, but it is difficult to determine whether the two sides were fully fused and subsequently broken, or only partially fused. CT scans show very little evidence of a suture, certainly less than in MNHN.MAJ 4 and FMNH PR 2100, and so, as with UA 8719, it is possible that, despite its small size, FMNH PR 2099 may pertain to a mature individual. Although not as well preserved as UA 8719, the pattern of surface ornamentation seems to be much the same, with a central smoother area surrounded by a more rugose periphery.

The frontal sinus is largest in FMNH PR 2100, where it is an expansive space with relatively smooth walls and, as preserved, few internal struts (Figs. 15, 16B, 17). The sinus is confluent across the midline but is not particularly symmetrical, reaching farther caudally and laterally on the right side. The sinus extends dorsally well up into the cornual process, with lateral tongues into the postorbital rami and rostral tongues into the nasal processes. The sinus overlies those portions of the endocranial cavity that housed the olfactory tract and bulb. In fact, as preserved, the sinus is confluent with the endocranial cavity in this region of FMNH PR 2100, but this must be an artifact of preservation in this specimen because all of the other specimens show a complete bony endocranial roof.

Indeed, consideration of the other specimens (Fig. 16) shows FMNH PR 2100 to be exceptional in a number of regards. Frontal sinuses are present in all of the other specimens except for UA 8719, in which they seem to be completely absent. The frontal sinus of UA 8709 resembles that of FMNH PR 2100 in being confluent across the midline and extending up into the cornual process, but the specimen is not well enough preserved to say much more. MNHN.MAJ 4 and FMNH PR 2099 resemble each other and differ from FMNH PR 2100 in having much smaller and separate, paired frontal sinuses that are not confluent across the midline and do not reach up into the cornual process. In both cases, the sinuses are generally smooth walled, although there also are areas where the sinuses seem to grade into the surrounding trabecular bone. It may be noted that, armed with the CT search image provided by *Majungasaurus*, we discovered that *Ceratosaurus* (MWC 1.1) also has paired smooth-walled sinuses within its frontal bones (Fig. 16F), resembling MNHN.MAJ 4 and FMNH PR 2099 in not crossing the midline. The unexpected similarity to *Majungasaurus* is striking and raises the question of just how many other theropods may be found to have such cavities within their frontal bones. The latter issue is addressed in the Discussion.

Parietal—The parietal (Figs. 1, 14–17) contacts its opposite medially, the frontal rostrally, the supraoccipital caudally and ventromedially, the laterosphenoid and probably also the prootic ventrolaterally, the squamosal caudolaterally, and the paroccipital process caudoventrally (Figs. 1, 14). The frontoparietal suture is visible in FMNH PR 2100, passing through the rear portion of the median fossa (described above; Fig. 15A). Farther from the midline, within the adductor chamber, the suture turns ventrally to contact the laterosphenoid. Although the suture is difficult to make out, even on CT, it presumably reaches the foramen within the adductor chamber for the dorsal head vein (v. capitis dorsalis), because it does so in other theropods (e.g., *Ceratosaurus*, MWC 1.1; *Allosaurus*, UMNH VP 18050, 18055; *Tyrannosaurus*, AMNH 5117) and indeed many other archosaurs. The parietal may have a glancing contact with the prootic in the vicinity of the dorsal head vein foramen, but it broadly contacts the otoccipital (exoccipital + opisthotic) dorsally along the base of the paroccipital process. The suture between the parietal and otoccipital is almost obliterated, which is unusual in theropods, but the parietal retains the free caudoventral prong that projects laterally above the posttemporal foramen.

As mentioned above in the squamosal description, the posttemporal foramen (a large fenestra in extant lepidosaurs) is bordered by the squamosal, parietal, and otoccipital (Fig. 14G), and presumably transmits the dorsal head vein from the occipital region to the adductor chamber. Within the adductor chamber (i.e., rostral to the parietal's transverse nuchal crest), the posttemporal foramen leads to a groove, which is relatively faint in *Majungasaurus* but deeper in some other theropods (e.g., *Allosaurus*), running between the parietal, otoccipital, and prootic and terminating in the dorsal head vein foramen noted above (Fig. 14C, D). CT shows that this latter foramen communicates internally with the middle cerebral vein canal, which is in accord with the descriptions of the cephalic veins in lizards (Bruner, 1908) and *Sphenodon* (O'Donoghue, 1920). The dorsal head vein foramen is a typical feature of theropods (and many other extinct archosaurs) but is seldom described. Chure (2000b) regarded this foramen in *Allosaurus* and a second, as yet unnamed allosauroid as being pneumatic in origin (viz. the dorsal tympanic recess). Pneumaticity could certainly be a possible interpretation in some cases (e.g., an undescribed basal theropod taxon, for which the opening is quite large; Chure, 2000b), because pneumaticity often tracks along heterogeneities provided by vasculature (Witmer, 1997a, b). Nevertheless, a venous rather than pneumatic interpretation is indicated in *Majungasaurus* (and also *Allosaurus*).

The parietal of *Majungasaurus* has an additional vascular groove emanating from the posttemporal fenestra, in this case a groove on the bone's caudal surface that courses dorsomedially (Fig. 14G). In a variety of theropods (e.g., *Allosaurus*) this groove anastomoses with a more medial foramen located at or near the juncture of the parietal, otoccipital, and supraoccipital (or the epiotic portion of the supraoccipital). This foramen marks the point where the middle cerebral vein (caudal petrosal sinus of the avian literature) exits the skull to become the external occipital vein and has been labeled according to either vein (e.g., Kurzanov, 1976; Currie and Zhao, 1994b). We will regard this opening as the middle cerebral vein foramen (Fig. 14G). *Majungasaurus* has a well-developed middle cerebral vein foramen that, based on CT, indeed leads to the middle cerebral vein canal (Figs. 16, 17). Yet, unlike *Allosaurus*, it does not obviously anastomose with the parietal groove leading to the posttemporal foramen, although it seems reasonable to assume that, in life, such an anastomosis did exist but was simply not sufficiently appressed against the bone to leave a groove.

Dorsally, the parietal is pinched immediately caudal to the median fossa, resulting in a narrow sagittal crest separating the two jaw adductor chambers (Fig. 14H). The caudal, thin portion

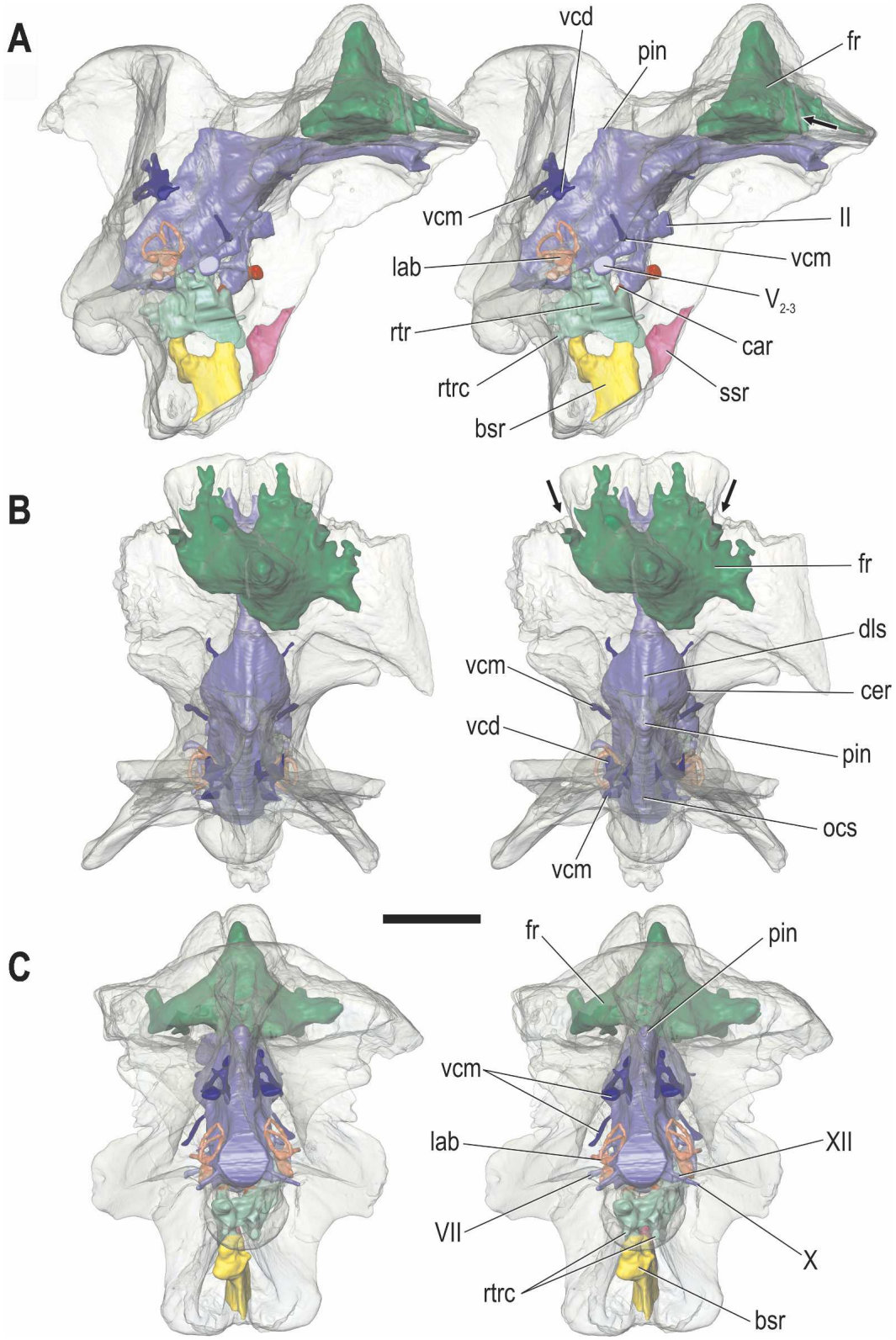

FIGURE 17. Stereopairs of articulated braincase of *Majungasaurus crenatissimus* (FMNH PR 2100) derived from reconstructed CT scans and in the following views: **A**, right lateral; **B**, dorsal; **C**, caudal; **D**, left lateral; **E**, ventral; **F**, rostral. Bone is rendered semitransparent, revealing pneumatic recesses (green, yellow, magenta, cyan), cranial endocast (blue), vascular elements (red, purple), and the osseous labyrinth (pink). For detailed labeling of the bony braincase, cranial endocast, and osseous labyrinth, see Figures 14, 18, and 19, respectively. Arrows show the putative entrance of the frontal sinus diverticulum via the articular slot for the lacrimoprefrontal prong. Scale bars equal 5 cm. See Appendix 1 for abbreviations.

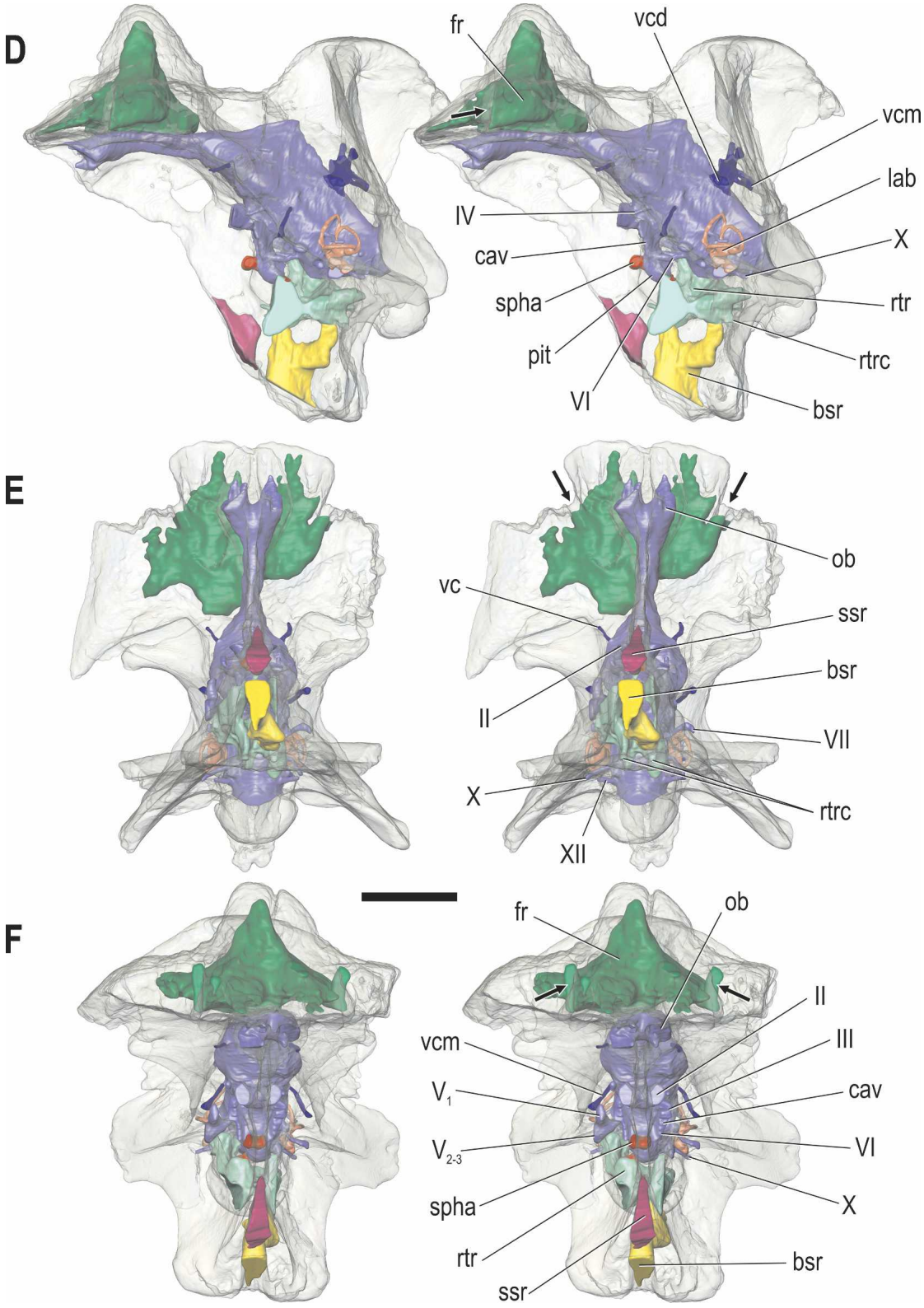

of the crest turns abruptly upward to form a well-developed eminence, diamond-shaped in dorsal view, extending rearward to cap the supraoccipital. Although most basal theropods have a significant dorsal projection of the parietal in association with the nuchal crest, this feature is greatly elaborated in *Majungasaurus*. The parietal portion of this eminence is relatively long and broad (65 mm × 45 mm) in FMNH PR 2100, approaching the height of the frontal cornual process. Between the frontal and parietal eminences is a distinct concavity floored by the sagittal crest. Caudal expansion of the eminence is achieved by a thickened contribution from the supraoccipital, and forms the dorsal portion of the sagittal nuchal crest (Fig. 14H). The parietal has a clear suture with the supraoccipital bone dorsally and internally, as revealed by CT (Figs. 14H, 15A); externally on the occiput,

the suture can be traced at the juncture of the transverse and sagittal nuchal crests.

The parietal eminence contributes to the tall, laterally extensive transverse nuchal crest, with the squamosals forming the lateral portions. The parietal portion of the transverse nuchal crest has a thickened dorsal margin but tapers ventrally, becoming relatively thin and platelike. As in other regions of the skull, there is an evident demarcation between subcutaneous bone and regions bearing other soft tissues. Thus, the rim of the adductor chamber, including the transverse nuchal and sagittal crests, is roughened for attachment of skin and muscular aponeuroses, whereas the interior of this chamber is smooth for more fleshy attachments of jaw adductor musculature (Fig. 14G, H). It is worth noting that most of the rugosity on the edge of the transverse nuchal crest extends onto its caudal (occipital) surface rather than its rostral (adductor chamber) surface. This would suggest that the muscular rugosity of the transverse crest results more from cervical than jaw musculature, and in this case the best candidates would be portions of M. transversospinalis capitis (e.g., M. complexus, M. biventer cervicis) and perhaps M. splenius capitis (Tsuihiji, 2005). Expansion of the transverse nuchal crest and the muscle rugosity onto the squamosal in abelisaurids suggests greater importance of these muscles, which, based on its attachments, would elevate (extend, dorsiflex) the head when contracting bilaterally and flex the head ipsilaterally when contracting unilaterally.

The parietal of *Majungasaurus* is derived in a number of features. In most basal theropods, including the ceratosaur *Ceratosaurus*, the dorsum of the skull roof is relatively flat except for a modest caudodorsal expansion associated with the transverse nuchal crest. In *Majungasaurus*, the skull roof is interrupted not only by the frontal cornual process but also by the massive parietal eminence. Within Abelisauridae, a similarly elaborate median projection of the parietal is also present in *Carnotaurus* and *Rajasaurus*, whereas this feature is much more poorly developed in *Rugops* and *Abelisaurus* and apparently in *Aucasaurus* as well (Coria et al., 2002; Fig. 2). The condition of this character is currently unknown in other abelisaurids, including the Indian holotype specimens of *Indosaurus* and *Indosuchus*. The nature of the sagittal crest of the Malagasy taxon is also closely similar to *Ceratosaurus*, *Carnotaurus*, *Rajasaurus*, and *Abelisaurus*, being relatively broad and wedge-shaped rostrally—although somewhat broader than in *Majungasaurus*—and narrowing caudally to a transversely thin crest. Both of the Argentine taxa lack a distinctive median fossa in this region, as do apparently *Rajasaurus* (Wilson et al., 2003) and *Rugops*. The capping of the supraoccipital by the parietal is a feature present in several theropod taxa, including abelisaurids, *Ceratosaurus*, and carcharodontosaurids (Coria and Currie, 2002). However, the relative size (length and width) of the parietal eminence, together with a substantial caudal contribution from the supraoccipital, is characteristic of abelisaurids (*Majungasaurus*, *Carnotaurus*, *Abelisaurus*; Fig. 15A). The caudal portion of the sagittal crest is broader and more rounded in non-abelisaurid basal theropods, including *Herrerasaurus*, coelophysoids, *Ceratosaurus*, allosaurids, and carcharodontosaurids. The dorsotemporal fenestra of *Majungasaurus*, *Abelisaurus*, *Carnotaurus*, and apparently *Rugops* (Sereno et al., 2004) is also distinctive in that, as viewed dorsally, its rostralmost extent occurs medially (Fig. 2).

Braincase

Supraoccipital—The supraoccipital bone is currently known only from FMNH PR 2100 (Figs. 1, 14, 15). It contacts the parietal dorsally and laterally, and these sutures are described above. Although they are difficult to make out externally, the sutures between the supraoccipital and otoccipital are visible on CT, and reveal that the supraoccipital contributed to the dorsal margin of the foramen magnum (Fig. 15A). The supraoccipital-otoccipital suture probably corresponds roughly to the region of the proatlantal tuberosity on the occiput. As noted above in the parietal discussion, the supraoccipital bone is most notable for its role in forming a pronounced, rostrocaudally elongate sagittal nuchal crest (Fig. 14G). This crest begins ventrally at about the level of the middle cerebral vein foramina and expands dorsally in its rostrocaudal dimension such that the supraoccipital tuberosity projects caudally beyond the level of the occipital condyle and overhangs the occiput (Fig. 15A). The sagittal nuchal crest is sharp ventral to the tuberosity, which is transversely expanded behind the parietal eminence. The tuberosity is equivalent to the "supraoccipital knob" identified in *Giganotosaurus* by Coria and Currie (2002:803).

The sagittal nuchal crest may represent the attachment of a nuchal ligament (lig. supraspinale) similar to that present in mammals. However, in extant birds the ligament does not reach as far forward as the occiput; likewise, a nuchal ligament attaching to the skull has been generally regarded as absent in crocodilians, although, significantly, Tsuihiji (2004) identified it in *Alligator*, as well as in *Iguana*. An alternative hypothesis is that the sagittal nuchal crest is largely an epiphenomenon of the apparently powerful craniocervical muscles attaching to the transverse nuchal crest, such that the medialmost portions of these muscles may have merged in the midline, generating the supraoccipital tuberosity, with the sharp crest below simply representing a structural web buttressing the tuberosity. The area in the vicinity of the contact between the supraoccipital tuberosity and parietal eminence is roughened in such a way as to suggest the presence of persistent cartilage, as is often seen in extant crocodilians.

The supraoccipital has often been associated with an otic ossification termed the epiotic bone, an element that forms in extant birds and crocodilians (Parker 1866, 1883) in the midportion of the rostral semicircular canal and subsequently fuses to the supraoccipital. Although a separate epiotic has sometimes been identified interposed between the supraoccipital and parietal in extinct theropods (e.g., *Dilophosaurus*, Welles, 1984; *Ceratosaurus*, Madsen and Welles, 2000), there is no evidence for a separate epiotic in *Majungasaurus*.

Otoccipital (Exoccipital + Opisthotic)—As in almost all posthatching archosaurs, the exoccipital and opisthotic bones of *Majungasaurus* are indistinguishably fused into a single element (Figs. 1, 14, 15, 17). With the exception of a small fragment on UA 8709, the only known examples of the otoccipital in *Majungasaurus* are the two preserved in FMNH PR 2100, which are fairly complete although missing their distal tips and some portions of the otic region (Figs. 1, 14). As in most other dinosaurs, the otoccipital contacts the supraoccipital (including the epiotic, if identifiable as such) dorsomedially, the prootic rostrally, the basioccipital and basisphenoid ventrally, the parietal dorsomedially, and the squamosal dorsolaterally. The articulations between the otoccipital (including its paroccipital process) and the parietal, squamosal, and supraoccipital bones have been described above (Fig. 14); again, perhaps the most significant aspects of these latter articulations relate to the form of the posttemporal foramen and the anastomoses of the dorsal head vein and middle cerebral vein (Fig. 17). The most conspicuous aspects of the otoccipital are the paroccipital process and the crista tuberalis, which will be described in turn along with the other articulations of the otoccipital.

The paroccipital processes project caudolaterally from either side of the foramen magnum (Figs. 1E, 14G). They are not strongly angled backward as is seen in some other theropods, such as *Ceratosaurus* (MWC 1.1), *Allosaurus* (UMNH VP 18050, 18055; but see CM 21703, in which the paroccipital processes are much less caudally angled), and *Giganotosaurus* (Coria and Currie, 2002), but are comparable to the abelisaurids *Abelisaurus* and *Carnotaurus* (Fig. 2). As noted above, although the lateral

extremities of the processes have been lost in FMNH PR 2100, their full extent and much of their general form is preserved by the extensive contact they have with the caudoventral margins of the squamosal (Fig. 1E, M). Based on this articular surface, it is clear that the paroccipital processes have a slightly concave dorsal margin; that is, they curve dorsally in their distal portions. The distal ends of the paroccipital processes are also rotated so as to face caudodorsally rather than caudally. This morphology, including the dorsally upturned distal ends of the paroccipital process, is shared by other abelisaurids (*Carnotaurus*, *Abelisaurus*), although the overlap between elements is less developed in *Abelisaurus*. The distal portions of the paroccipital processes of dromaeosaurids are also twisted dorsally somewhat. In contrast, the paroccipital processes of most theropods (e.g., *Herrerasaurus*, *Sinraptor*, and *Allosaurus*) are horizontal or angled ventrally.

The caudal surface of the paroccipital process has a roughened, raised area located dorsally and demarcated from the smoother area below by a sharp crest. The roughened area is not common among theropods (absent in *Ceratosaurus*, *Allosaurus*, *Tyrannosaurus*, among others) and may well indicate the tendinous attachment of a particularly well developed craniocervical muscle, perhaps a portion of M. rectus capitis lateralis.

The rostral surface of the paroccipital process is covered largely by the prootic bone (Fig. 14). As in most theropods (indeed most dinosaurs), the articulation between the prootic and the paroccipital process of the otoccipital remains open and obvious, forming a strongly interdigitating suture on the rostrolateral surface of the paroccipital process. Enough of the paroccipital processes are preserved distally to show that, as in most other theropods, the otosphenoidal crest (= crista prootica of some authors) extended onto the otoccipital. The otosphenoidal crest continues rostrally and then ventrally as it traverses the prootic and basisphenoid bones (see below; Fig. 14A). The otosphenoidal crest on the paroccipital process leads forward to the columellar (stapedial) recess, the area associated with the fenestra vestibuli (f. ovalis), into which the footplate of the columella auris (stapes) attaches (Fig. 14C). The fenestra vestibuli is situated between the prootic and otoccipital (specifically its opisthotic portion). The full caudal margin of the fenestra vestibuli cannot be assessed, because the process of the otoccipital forming the caudal margin of the fenestra is broken on both sides. This otoccipital process derives from the opisthotic, and it has been variably termed the crista interfenestralis (Save-Soderbergh, 1947), the ventral process of the opisthotic (Walker, 1990; Gower and Weber, 1998), and opisthotic bar (Chatterjee, 1991). Because this bony bar is broken, the fenestra vestibuli is now open to the aperture in the braincase directly behind it, which itself has had a variety of names: e.g., jugular foramen (Walker, 1961; Wilson et al., 2003), metotic foramen (Chatterjee, 1991; Gower and Weber, 1998).

The primitive condition for archosaurs (Gower and Weber, 1998) and apparently theropods (see Raath, 1985 for *Syntarsus*), if not all diapsids, is to have a metotic (jugular) foramen situated directly behind the fenestra vestibuli and transmitting the jugular (posterior cerebral) vein and cranial nerves IX–XI; the metotic foramen is fully within the otoccipital, and in fact is positioned between its two embryonic components (exoccipital caudally and opisthotic rostrally). In some clades of archosaurs, the situation becomes more complicated (see Gower and Weber, 1998, for discussion) in that the metotic foramen becomes subdivided in association with the formation of a secondary tympanic membrane covering the fenestra cochleae (f. 'pseudorotunda') and diversion of the vagal canal (minimally for cranial nerves X and XI) caudally such that it opens at the occiput (Walker, 1990; Witmer, 1990; Chatterjee, 1991; Currie and Zhao, 1994b). These changes apparently took place independently in the clades leading to extant crocodilians and birds (Gower and Weber, 1998), but it has not been clear precisely where the phylogenetic transition occurred. Chatterjee (1993) regarded the caudal diversion of the vagal canal as being a tetanuran character, whereas Rauhut (2003) placed its origin more basally, just above the Neotheropoda node. Interestingly, Rauhut (2003) reported the *primitive* condition for this character (i.e., presence of a metotic foramen with no vagal diversion) for Abelisauridae based on *Majungasaurus* and his study of FMNH PR 2100.

However, CT scanning of this specimen (and of an *Allosaurus* specimen, UMNH VP 18055) reveals that *Majungasaurus* in fact has the derived state of the vagal canal being caudally diverted to the occiput (Fig. 17). Just lateral to the occipital condyle, within the shallow paracondylar recess (Chure, 2000b; paracondylar pocket of Welles, 1984), is a somewhat ragged opening within a shallow fossa that Rauhut (2003) presumably interpreted to be solely for the hypoglossal nerve (CN XII). CT indeed confirms that, on each side, a single unbranching hypoglossal canal begins medially in the endocranial cavity as a foramen within the endocranial floor (Fig. 15) and then passes directly laterally through the otoccipital to open within the medial wall of the ragged occipital opening. However, enough of this opening is adequately preserved to show that there is another foramen in addition to the hypoglossal foramen. In fact, CT reveals a canal leading rostromedially from this foramen, opening in the region of the 'metotic/jugular' foramen (Fig. 17). This canal must be a vagal canal, demonstrating that *Majungasaurus*, and probably other abelisaurids, display the derived state. Given these findings, it seems possible that the "pair of foramina in a common oval fossa" on the occiput of *Rajasaurus* attributed by Wilson and colleagues (2003:11) to the hypoglossal nerve may actually represent, as in *Majungasaurus*, the openings of both the hypoglossal and vagal canals.

Typically, the identification of caudal diversion of the vagus nerve is sufficient to allow inference of subdivision of the embryonic metotic fissure (sensu Gower and Weber, 1998) such that the opening within the otoccipital behind the fenestra vestibuli becomes the fenestra cochleae (f. 'pseudorotunda'), implying a shift of the perilymphatic sac and the presence of a secondary tympanic membrane (Walker, 1990; Chatterjee, 1991).

The crista tuberalis is fully continuous with the paroccipital process, but it is a large enough structure that it merits its own discussion. The crista tuberalis is the web of otoccipital that connects the paroccipital process above with the basal tuber below, contacting the basioccipital and basisphenoid along the way (Fig. 14). The term 'crista tuberalis' is one that has been used by dinosaur workers (e.g., Kurzanov, 1976; Madsen and Welles, 2000) and is widely used by lepidosaur workers (e.g., Save-Soderbergh, 1947; Oelrich, 1956). Bakker and colleagues (1988: 10) used the term "descending ventral root of the paroccipital process." More recently, Currie (1995, 2003; see also Currie and Zhao, 1994b; Coria and Currie, 2002) and Makovicky and Norell (1998) used the term 'metotic strut' for this web in various theropods, presumably following Witmer (1990), who coined and later codified the term for avian braincases (Baumel and Witmer, 1993). However, given the confusion surrounding all the structures bearing the name 'metotic,' Gower and Weber (1998:397) were probably justified in suggesting that the "term 'metotic' should perhaps be avoided when referring to structures of the osteocranium." Certainly, many diapsids have a crista tuberalis of unquestioned homology to that of, say, *Majungasaurus* but lack any chondrification, let alone ossification, of the embryonic metotic cartilage (the basis for the term in birds; e.g., de Beer, 1937).

Terminology aside, the crista tuberalis of *Majungasaurus* is generally a smooth, triangular sheet of bone with a curved, concave lateral margin. It separates the middle ear domain rostrally from the occipital domain (which is largely muscular) caudally. The margin of the crista is basically in line with the basal tubera

on the basioccipital. The suture with the basioccipital starts from just above the lateral corner of the basal tuber and extends dorsomedially to the neck of the occipital condyle. In contrast to the general theropod condition, the otoccipital does not contribute to the articular surface of the condyle, although it does contribute to the condylar neck. The basisphenoid overlaps the crista tuberalis rostrally, and the suture extends from the basal tuber dorsally up to the region of the fenestra vestibuli. The rostrolateral (tympanic) surface of the crista tuberalis is smooth but bears a couple of features of interest. The first is the ridge demarcating the ventral edge of the stapedial groove, which, again, is roofed by the prootic (Fig. 14C). The lateral head vein and stapedial artery should be near, if not within, this sulcus. The lateral head vein occupies this groove in extant lepidosaurs (Save-Soderbergh, 1947; Oelrich, 1956; extant archosaurs have divergent apomorphies in this region, see Sedlmayr, 2002), and the same has been inferred for various basal archosauromorphs (Benton, 1983; Walker, 1990) and even some theropod dinosaurs (*Dromaeosaurus*, Colbert and Russell, 1969). The second feature is just below the stapedial groove and represents another groove. This groove passes caudoventrally from the region of the columellar recess (fenestra vestibuli + jugular/metotic foramen) and extends to the edge of the bone (Fig. 14C). This groove is matched by another groove on the opposite side (the caudomedial or occipital) surface of the crista tuberalis. This caudal groove passes from the vagal foramen to the edge of the crista.

The rostral cristal groove is found in other theropods, such as *Allosaurus* (UMNH VP 18050, 18055), *Tyrannosaurus* (AMNH 5117), *Itemirus* (Kurzanov, 1976), and *Dromaeosaurus* (AMNH 5356), but the caudal cristal groove is not present on these specimens. Both grooves, although clear enough, are seldom (if ever) described in the literature. The function of these grooves is not entirely clear. The caudal groove most likely transmitted the vagus nerve (CN X) and accompanying vessels (which are present in extant archosaurs; Sedlmayr, 2002), or even the jugular (posterior cerebral) vein if the vein passed through the vagal canal. Likewise, the rostral cristal groove could have conveyed the glossopharyngeal nerve (as suggested for *Itemirus* by Kurzanov, 1976) or the columella itself.

Prootic—The prootic of *Majungasaurus* (Figs. 14, 17) is a relatively complex element, but is comparable to those of other theropods. The prootic is known from both sides of FMNH PR 2100 and UA 8709, but it is most complete on the right side of the former specimen. The bone has the typical contacts observed in most dinosaurs: the otoccipital caudally, the supraoccipital dorsomedially, the parietal dorsolaterally, the laterosphenoid rostrally, and basisphenoid ventrally; there may also be a contact with the basioccipital, but that could not be reliably confirmed (Fig. 14A). As noted above, the prootic laps onto the base of the rostrolateral surface of the paroccipital process of the otoccipital, forming an interdigitating suture (Fig. 14C). Although it is a little difficult to make out in its entirety, this suture passes rostrodorsomedially, contacting the parietal just rostral to the posttemporal foramen, and then the two form a triple junction with the addition of the laterosphenoid at the foramen for the dorsal head vein (see above; Figs. 14A, C, D, 17A, D). From the dorsal head vein foramen, the suture of the prootic with the laterosphenoid is very difficult to trace in detail, even on CT. It is safe to assume that *Majungasaurus* is like other archosaurs in having the prootic-laterosphenoid suture intersect the trigeminal foramen. As with the laterosphenoid, the suture of the prootic with the basisphenoid has been largely obliterated.

The prootic bone is intimately involved with several functional systems, including the auditory apparatus, the tympanic pneumatic system, the jaw adductor musculature, and the brain and its meninges. With regard to the auditory system, it was mentioned above that the prootic forms the rostral margin of the fenestra vestibuli (f. ovalis) into which the footplate of the columella auris (stapes) inserts. Not enough of the fenestra is intact to know its size or shape in detail. What can be observed, however, is that the fenestra vestibuli is located within a relatively deep and broad columellar recess (Fig. 14C), whereas the columellar recess of *Ceratosaurus* and *Allosaurus* is shallower and smaller. Most of the stapedial groove, including all of its roof, is formed by the prootic. The lateral margin of the groove is formed by the otosphenoidal crest. There is a bar of bone separating the fenestra vestibuli behind from the rostral tympanic recess in front. This bar is at least partly prootic but also may be formed by basisphenoid ventrally. The bar has a prominent vertical ridge on its caudal surface that, together with the base of the crista tuberalis of the otoccipital, demarcates a vertical sulcus emanating from the columellar recess. This sulcus may be continuous ventrally with a shallow sulcus on the lateral surface of the basisphenoid between the basal tuber and basipterygoid process. The function of the ridge and sulcus is not certain and has not been described previously in theropods to our knowledge. The ridge is strong enough that it suggests some kind of attachment. The sulcus is not positioned appropriately for the major vessels in this region (e.g., stapedial artery, lateral head vein), and perhaps the best candidate is some portion of the Eustachian (pharyngotympanic, auditory) tube, but the identification remains open.

The otosphenoidal crest is discontinuous on the prootic, which is ironic because the crest is commonly called the crista prootica. We prefer to use the term 'otosphenoidal crest' because it is an existing name (e.g., Colbert and Russell, 1969; Norell et al., 2004) and is more apt. The crest in virtually all archosaurs (if not all diapsids) extends from the otic region to the sphenoid region (hence 'otosphenoidal'), and is built not only from the prootic but also from the opisthotic portion of the otoccipital and the basisphenoid (and sometimes the parasphenoid, if present). The otosphenoidal crest separates the middle ear domain from the temporal domain above and orbital domain in front. In *Majungasaurus*, the crest extends in a sweeping arc from the paroccipital process to the ventral tip of the basipterygoid process (the latter shown on UA 8709), with the only hiatus being on the prootic in the area of the foramen for the facial nerve (CN VII; Fig. 14A). Normally in diapsids, the facial nerve foramen is fully within the middle ear, being tucked below the otosphenoidal crest. The same would generally seem to be true even for *Majungasaurus* in that the two grooves that issue from the facial nerve foramen and conducted branches of the nerve (see below) are fully within the confines of the otosphenoidal crest and middle ear. The reason for the discontinuity in the crest probably relates to the disposition of the trigeminal foramen, which is just rostral to the facial foramen, and bears a caudally directed fossa or groove.

As noted above, the facial nerve foramen is fully within the prootic bone, as in diapsids generally. The facial foramen itself opens into an elliptical fossa (almost certainly for the geniculate ganglion), and grooves emerge at each of its major axes (Fig. 14C). The caudal groove is for the hyomandibular branch of the facial nerve (which innervated the depressor mandibulae muscle and probably various hyolingual muscles before giving off its chorda tympani branch); the groove curves caudodorsally below the otosphenoidal crest, but does not enter the columellar recess. The rostral groove is for the palatine ramus of the facial nerve. This groove passes rostroventrally in the region of the hiatus in the otosphenoidal crest. Nevertheless, it seems certain that the palatine ramus passed ventrally within the middle ear under cover of the otosphenoidal crest in that the groove is directed toward the right area (behind the crest) and, moreover, such a relationship is highly conserved in diapsids, let alone theropods.

Although the prootic bone shares the margin of the trigeminal foramen, the trigeminal nerve and its osteological correlates will be presented in the section on the laterosphenoid below.

The prootic is clearly pneumatic, bearing a prootic recess within a larger rostral tympanic recess (see Witmer, 1997b, for classification of paratympanic pneumatic spaces). Directly ventral to the facial nerve foramen is a triangular opening in the prootic, separated from the rostral margin of the fenestra vestibuli by a strong bar of bone (Fig. 14A–C). This foramen leads into a cavity, the prootic recess, which extends dorsally and rostrally into the bone, undercutting the bony canals for the facial and trigeminal nerves (Fig. 17A). This recess also extends caudally into the cranial base, although breakage makes definitive interpretation difficult. The prootic recess is fully confluent ventrally with the main rostral tympanic recess, which is housed largely in the prootic and basisphenoid bones. The rostral tympanic recess clearly extends caudally into the prootic and cranial base, and also rostrally under the otosphenoidal crest and preotic pendant (ala basisphenoidalis, see below) in the region of the cerebral carotid artery foramen (Figs. 14A–C, 17). The medial wall of the recess is composed of both prootic and basisphenoid, but it is not clear where their suture is. Wilson and colleagues (2003:12) identified a pneumatic opening and "lateral fossa" in *Rajasaurus*, which suggests that a broadly similar pattern of pneumaticity was present in this abelisaurid.

The prootic bone has a broad exposure in the dorsotemporal fossa, which is typical for theropods and archosaurs generally. Due to the hiatus in the region of the facial nerve, the otosphenoidal crest is basically continuous with the crista antotica (the crest on the laterosphenoid leading to the capitate process; see below). The otosphenoidal crest bears a curious tuberosity on its margin that is present on both sides of FMNH PR 2100, but has not been observed elsewhere (Fig. 14C, E, F). The function of this tuberosity is unclear, but Oelrich (1956) described in the iguanid lizard *Ctenosaura* a stabilizing ligament running from the quadrate to a similar spot on the prootic, and perhaps *Majungasaurus* had a similar ligament. The temporal surface of the prootic is smooth and relatively featureless, reflecting a fleshy attachment for M. pseudotemporalis superificalis (Fig. 14A–D; Holliday, 2006). This is similar to the situation in *Ceratosaurus* (MWC 1.1) but different from that in *Allosaurus*, which has a depression on the temporal surface of the prootic. Chure (2000b) regarded the depression in *Allosaurus* as being pneumatic in nature (specifically, the dorsal tympanic recess), which is possible but not certain; pneumatic depressions on the prootic for the dorsal tympanic recess exhibit fairly extensive homoplasy in Coelurosauria (Witmer, 1997b). What is clear with regard to *Majungasaurus* is that there is no evidence at all for any pneumatic diverticula in this region, and there is no dorsal tympanic recess.

Basioccipital—The basioccipital bone of *Majungasaurus* (Figs. 1, 14, 15, 17) is known from an almost complete example in FMNH PR 2100 and a partial element in UA 8709. It is generally a typical theropod basioccipital, contacting the otoccipital dorsally and laterally, the basisphenoid rostrally, and the atlas caudally (Fig. 14A, D, F–H). It is 'verticalized' in the sense of Tarsitano (1985) in that the bone's main axis from condylar neck to basal tubera is essentially vertical rather than being more horizontal as in many ornithischians and most neornithine birds. The occipital condyle is rounded and somewhat wider than tall in caudal view. The articular portion is apparently exclusively basioccipital but the otoccipital contributes to the dorsal and lateral sides of the condylar neck. The condylar neck itself is long and slender in comparison to *Ceratosaurus* and *Allosaurus*, and undercuts the condyle ventrally and laterally. The neck and condyle project caudoventrally, as noted also for *Rajasaurus* by Wilson and colleagues (2003).

The basal tubera of *Majungasaurus* are built almost exclusively from the basioccipital, with the basisphenoid contacting the bases of the tubera rostrally with coarsely striate bone (the basisphenoid 'scar' of Bakker et al., 1988). The otoccipital also does not contribute to the tuber, and its contact with the basioccipital ends just dorsal to the tuber. The basal tubera together are wider than the occipital condyle (Fig. 14G), as in *Ceratosaurus* (MWC 1.1) and other abelisaurids but not *Allosaurus*. The tubera form a pair of smooth and rounded surfaces that resemble articular surfaces, although they clearly are nonarticular, serving instead as attachment for craniocervical musculature (probably rectus capitis dorsalis and/or r. c. ventralis). The caudal edges of the tubera are slightly everted for muscle attachment. There is a low median keel on the caudal surface of the basioccipital that extends dorsally onto the ventral surface of the condylar neck. On either side of this keel is a shallow fossa, at the dorsal extremity of which is a foramen (Figs. 14G, 15). The nature of these fossae and foramina are analyzed further in the Discussion in the context of inferences pertaining to braincase pneumaticity.

Basisphenoid-Parasphenoid—The status of the parasphenoid of extinct theropods is problematic because of extensive fusion of any parasphenoid ossifications to the basisphenoid. In extant sauropsids, the parasphenoid ossifies intramembranously (dermally), whereas the basisphenoid is an endochondral ossification. Among extant archosaurs, crocodilians have almost no parasphenoid (just a single, small median center; de Beer, 1937), whereas birds may have as many as seven centers of ossification (Jollie, 1957). Given that in *Majungasaurus* there is no clear way to discriminate between the two bones, we will regard the elements as fused and refer to them both as the basisphenoid, following convention among theropod workers.

The basisphenoid of *Majungasaurus* (Figs. 1, 14, 15, 17) is known from FMNH PR 2100 and UA 8709, and, although the former is more complete, the latter preserves the basipterygoid processes and the ventral margin of the cultriform process, which are missing in the former specimen (Figs. 14, 15A). The basisphenoid, as in most other theropods, contacts the basioccipital caudally, the otoccipital caudodorsally, the prootic dorsally, and the laterosphenoid rostrodorsally. It may contact the orbitosphenoid in the vicinity of the pituitary fossa, but sutures are not visible. In fact, the only sutures visible, even on CT, are those caudally with the basioccipital, just rostral to the basal tubera, and with the base of the crista tuberalis of the otoccipital. With regard to the latter, the basisphenoid-otoccipital suture ascends in the putative Eustachian sulcus perhaps as far dorsally as the columellar recess, but the suture fades out dorsally.

The basipterygoid processes of *Majungasaurus* are relatively long and do not project at all forward, but rather are swept back in lateral view such that the distal tip projects caudally beyond the caudal margin of the base (Fig. 15A). In this regard they resemble the basipterygoid processes of *Carnotaurus* and *Ceratosaurus* (MWC 1.1) but differ from those of *Allosaurus* in which they project more forward. Each basipterygoid process of *Majungasaurus* is angled about 45 degrees from the sagittal plane to reach the articular surface on the dorsal surface of the pterygoid. There is an articular pad on the rostroventral aspect of the process. The lateral surface of the basipterygoid process bears a well defined ridge that extends from the distal tip and arcs rostrodorsally. When UA 8709 and FMNH PR 2100 are compared, it is clear that this ridge is nothing more than the ventral limit of the otosphenoidal crest, which thus can be reconstructed as running from the paroccipital process of the otoccipital to the tip of the basipterygoid process of the basisphenoid, subtending an arc of a circle with a magnitude of 200 degrees or more. This situation again resembles that in *Carnotaurus* and *Ceratosaurus* more so than in *Allosaurus*.

As noted above, the otosphenoidal crest separates the middle ear sac (tympanic domain) from the orbital and temporal regions. In support of this assessment, the otosphenoidal crest of

Allosaurus (e.g., UMNH VP 18055) extends rostrally on the basisphenoid past the level of the pituitary fossa before passing ventrally, ultimately onto the basipterygoid process. The significance here is that the pneumatic fossae that Chure and Madsen (1996) identified on the lateral surface of the basipterygoid processes are fully within the otosphenoidal crest, as identified here, and thus their pneumatic hypothesis is corroborated. By way of correction, Witmer (1997b, fig. 3) erroneously regarded this "basipterygoid recess" as being within the orbit and hence outside the bounds of the otosphenoidal crest and middle ear.

On the ventral surface of the basisphenoid there is a web of bone running between the basipterygoid process and basal tuber. This web is seldom named by dinosaur workers, although Bakker and colleagues (1988:9) referred to it as a "boxwork wall." Lepidosaur workers routinely refer to this web as the 'crista ventrolateralis,' and we will follow Kurzanov (1976) in using this term for theropods. In *Majungasaurus*, the crista ventrolateralis is relatively short rostrocaudally and thick transversely, where it forms the lateral wall to the basisphenoid recess (Figs. 14D–F, 15), a pneumatic sinus associated with the median pharyngeal system (Witmer, 1997b). The crista ventrolateralis expands caudally into a striate pad (the basisphenoid 'scar' of Bakker et al., 1988) just rostral to the basal tuber, to which a craniocervical flexor muscle tendon attached. The paired cristae are connected by a transverse web of bone (the 'basipterygoid web' of Bakker et al., 1988) that forms the rostral wall of the basisphenoid recess and the caudal wall of the subsellar recess, potentially another component of the median pharyngeal system (Witmer, 1997b).

The cultriform process (para-, basi-, parabasi-, or basiparasphenoid rostrum) extends rostrally from the body of the basisphenoid. It is missing from FMNH PR 2100, but is fairly well preserved in UA 8709 (reconstructed in Fig. 15A). The latter specimen shows that the cultriform process rapidly ascends immediately in front of the basipterygoid processes and is almost horizontal for most of its length. This is fairly similar to the situation in *Carnotaurus*, but quite different from that in *Ceratosaurus* and especially *Allosaurus*, in which the cultriform process ascends steeply and continuously. This may reflect a less vaulted palate in *Majungasaurus*. In *Majungasaurus*, the term cultriform 'process' is not particularly apt because the rostral projection takes the form of paired parasagittal sheets of bone extending forward from the basisphenoid just rostral to the basipterygoid processes. These sheets converge dorsally and rostrally, forming a single lamina continuous with the interorbital septum. Prior to converging, however, the sheets enclose a large space termed the subsellar recess (Witmer, 1997b; Chure and Madsen, 1998; Rauhut, 2004a). The subsellar recess is quite large in *Majungasaurus*, whereas it is much smaller in *Allosaurus* and apparently *Ceratosaurus*, in both cases because the two parasagittal sheets are more closely appressed. It is assumed that the recess is pneumatic in nature in *Majungasaurus* (it almost certainly is in *Tyrannosaurus*, AMNH 5117).

The "preotic pendant" (Madsen and Welles, 2000:9) or "ala basisphenoidalis" (Chure and Madsen, 1996:63) is a commonly observed structure in various dinosaurs, especially theropods. The preotic pendant takes the form of a roughened patch of bone composed mostly of basisphenoid and located rostroventral to the trigeminal foramen (or maxillomandibular foramen in those taxa with a separate aperture for the ophthalmic [profundus] nerve). In many taxa (e.g., *Ceratosaurus*), the pendant looks like an elaboration or process of the otosphenoidal crest, and indeed the two are often contiguous in this section, forming a winglike sheet that overhangs the part of the middle ear that bears the entrance to the carotid canal. In *Majungasaurus*, the preotic pendant is preserved only on the right side of FMNH PR 2100 (Fig. 14B, C). The portion overhanging the rostral tympanic recess is broken off but it probably was present and pointed caudoventrally as a triangular wing, as in many theropods. The more proximal portion of the pendant is roughened with striations that trend obliquely from rostrodorsal to caudoventral. These striations presumably result from attachment of M. levator pterygoideus and M. protractor pterygoideus (Holliday, 2006). There are crests delimiting two surfaces, a dorsally-positioned horizontal crest separating the striate portion from the trigeminal fossa above, and a rostrally located vertical crest separating the broad lateral striate surface from a smaller, rostrally-facing surface. The bone is smooth directly below and rostral to the pendant, probably reflecting the passage of the lateral head vein from the orbit to the tympanic cavity.

A final structure associated with the basisphenoid is an opening, the orbital foramen, located at the base of the orbit rostral to the preotic pendant and the abducens-oculomotor fissure (see orbitosphenoid discussion below; Figs. 14A, C, D, 15). This foramen may well be bounded partially by the orbitosphenoid bone, but all the surrounding sutures are obliterated. It is a relatively large, triangular opening that extends dorsally as a groove. The foramen can be traced caudally into the pituitary fossa, and thus the foramen can be readily identified as transmitting the sphenoidal artery as it branched off the cerebral carotid artery. The term orbital foramen comes from the equivalent feature in birds (Baumel and Witmer, 1993), where it also occurs in the base of the orbit.

Laterosphenoid—The laterosphenoid is a complex bone presenting surfaces to the adductor chamber caudally, orbit rostrally, and endocranial cavity medially (Figs. 7, 14, 15, 17). As in most theropods, the laterosphenoid of *Majungasaurus* contacts the prootic caudally, the parietal caudodorsally, the frontal rostrodorsally, the postorbital laterally, the orbitosphenoid rostrally, and the basisphenoid rostroventrally. The details (where discernible) of the sutures with the parietal, frontal, and prootic in the dorsotemporal fossa were described above, and, as noted, the suture with the basisphenoid is obliterated. The suture of the laterosphenoid with the orbitosphenoid is also more or less obliterated, but the contact is marked by a column of fissures and foramina for cranial nerves and various vessels, which will be described in turn. The laterosphenoid is known from both sides of FMNH PR 2100, although more complete on the right side, UA 8709, in which the rostrodorsal portion of the right side is preserved and in articulation with the frontal and postorbital (Fig. 7), and MNHN.MAJ 4, in which only the rostrodorsomedial contact with the frontal is preserved.

The dominant external feature of the laterosphenoid in *Majungasaurus* is the prominent crest dividing the adductor chamber behind from the orbital cavity in front (Fig. 14). This crest has not received much attention among archosaur workers generally, but sauropod workers (e.g., Madsen et al., 1995:19; Chatterjee and Zheng, 2002) have referred to it as the "crista antotica," and we will apply that term here. The antotic crest is directly opposite the medial vertical crest on the postorbital bone (see above), and it is clear that these two crests pertain to the same soft-tissue system, presumably the circumorbital membrane partitioning the ocular contents from the jaw musculature. As noted above, due to the hiatus in the otosphenoidal crest, the antotic crest and caudal portion of the otosphenoidal crest are essentially continuous. The same is true also for *Carnotaurus* and *Ceratosaurus*. The antotic crest is very sharp and overhanging in *Majungasaurus, Carnotaurus*, and also *Ceratosaurus*, much more so than in allosauroids, with the possible exception of carcharodontosaurids (Coria and Currie, 2002).

The antotic crest leads laterally to the capitate process (= laterosphenoid buttress, postorbital process, dorsolateral boss of Madsen and Welles, 2000). The capitate process is well preserved on the right sides of both FMNH PR 2100 and UA 8709 (Figs. 7, 14). In both cases, the process takes the form of an oval articular 'head' (hence its name). The articular surface is punctate, suggesting that a considerable amount of articular cartilage was pres-

ent in life. In support of this interpretation, there is gap of several millimeters between the capitate process and the cotyle on the postorbital bone in UA 8709. Thus, as in extant crocodilians, it would seem that the laterosphenoid-postorbital contact was a synovial joint, although, again as in crocodilians, there is no evidence for movement at this joint in *Majungasaurus*.

The antotic crest also bears the contact for the epipterygoid bone which is not preserved otherwise (Fig. 14C, F). The epipterygoid is rarely described in theropods, mostly because it is rarely preserved (or recognized). Nevertheless, despite its absence in extant archosaurs, most if not all nonavian theropods probably had an epipterygoid, as evidenced by the epipterygoid facet (Holliday, 2006). In *Majungasaurus*, the epipterygoid facet is located on the ventral portion of the antotic crest, just rostrodorsal to the trigeminal foramen (Fig. 14C, F). In *Ceratosaurus* (Hay, 1908; Madsen and Welles, 2000), *Allosaurus* (UMNH VP 18055), *Tyrannosaurus* (AMNH 5117; see also Brochu, 2003), *Dromaeosaurus* (Colbert and Russell, 1969); and apparently also *Itemirus* (Kurzanov, 1976), the epipterygoid facet is located at the caudal portion of the laterosphenoid, in some cases demonstrably overlapping the suture and extending somewhat onto the prootic. Although the laterosphenoid-prootic suture cannot be traced with confidence in *Majungasaurus*, the preserved morphology is consistent with a similar attachment of the epipterygoid to the caudal portion of the laterosphenoid (Fig. 14C, F). The epipterygoid is preserved in place on the right side of the holotype skull of *Carnotaurus* but its contact with the braincase could not be reliably determined. It resembles the triangular structure observed in *Ceratosaurus* (USNM 4735, MWC 1.1) and other theropods (Colbert and Russell, 1969; Currie, 2003); it may be assumed that the epipterygoid of *Majungasaurus* was no different.

The trigeminal foramen is well preserved on the right side of FMNH PR 2100 (Figs. 14A, C, 15). Again, although the suture is not traceable, it may be safely assumed on phylogenetic grounds that the prootic shared in the margin of the foramen. The foramen leaves the endocranial cavity and then expands into a fossa just rostral to the facial nerve foramen and just dorsal to the preotic pendant. This fossa almost certainly was for the trigeminal (Gasserian) ganglion, confirming that this ganglion was extracranial, as in perhaps all nonavian theropods (if not all nonavian diapsids). The course of the ophthalmic division of the trigeminal nerve (CN V_1, profundus nerve), as well as accompanying vessels (which are present in extant archosaurs; Sedlmayr, 2002), is clearly indicated by a well marked groove extending rostrodorsally from the front margin of the trigeminal fossa, ventromedial to the epipterygoid facet (Fig. 14C, F). The ophthalmic nerve would thus pass medial to the epipterygoid, which is a highly conserved relationship among sauropsids (e.g., Goodrich, 1930; Holliday, 2006). There is the possibility that there could have been a small bar of laterosphenoid lateral to the ophthalmic groove that is now broken. If true, this could be interpreted as providing the justification for regarding *Majungasaurus* as having the advanced character of a separate ophthalmic nerve foramen, as is routinely observed in coelurosaurs and many other tetanurans. However, in the tetanuran condition, the ophthalmic nerve branches off closer to the endocranial cavity (as in birds), whereas in *Majungasaurus* the nerve diverges more laterally, externally within a common trigeminal fossa. There is perhaps a fine line between these conditions, and they indeed may be transformationally linked. The other two branches of the trigeminal nerve, the maxillary and mandibular nerves, would have left the trigeminal foramen and fossa more directly laterally before turning toward their targets, and, as a result, they produced no clear osteological correlates in this area.

Just rostrodorsal to the trigeminal foramen and ventral to the antotic crest is the rostral opening of the middle cerebral vein (Fig. 14C). CT confirms that the foramen leads to a long canal that enters the endocranial cavity (Fig. 15A). In many sauropsids the middle cerebral vein opens in conjunction with the trigeminal nerve at the trigeminal foramen (Bruner, 1908; O'Donoghue, 1920). However, according to Rauhut (2003), in saurischian dinosaurs the middle cerebral vein opened separately from the trigeminal nerve, although in most theropods the foramina are still associated. *Majungasaurus* thus would have the derived condition. It should be noted, however, that the trigeminal foramina of both extant archosaur clades transmit veins between the endocranial cavity and orbitotemporal regions (Sedlmayr, 2002), and Larsson (2001) reported that in *Carcharodontosaurus* the middle cerebral vein exits through the trigeminal foramen (which would have to be a reversal to the primitive condition). Thus, the situation is not as simple as perhaps often presented.

The orbital surface of the laterosphenoid is intimately associated with the orbitosphenoid and the interorbital septum. It is probable that the two laterosphenoids almost contacted each other on either side of the interorbital septum, as seen in extant crocodilians and many theropods (e.g., *Allosaurus*), but the sutures between the laterosphenoid and orbitosphenoid are not clear enough in FMNH PR 2100 to be definitive (Fig. 14B, C, E, F). The rostral surface of the laterosphenoid bears a curved crest that descends ventromedially from the capitate process. The suture between the laterosphenoid and frontal is very clear and is marked by a vascular groove and a series of foramina. CT shows that the foramina pass between the orbital and endocranial cavities and almost certainly transmitted vasculature. Assuming that extant archosaurs are reliable guides (Sedlmayr, 2002), the vessel within the groove anastomosed with vessels passing through the foramina and also anastomosed with the supraorbital branch of the stapedial vessels.

Orbitosphenoid—The orbitosphenoid (Figs. 14, 15) is known from MNHN.MAJ 4 and FMNH PR 2100, but is well preserved only in the latter. The sutures between the orbitosphenoid and adjacent elements are completely obliterated, but its bounds are traceable because of consistent relationships among diapsids. As noted above, the orbitosphenoid contacts the laterosphenoid, perhaps the basisphenoid, the contralateral orbitosphenoid, and the interorbital septum (Fig. 14B, C, E, F). The orbitosphenoid-laterosphenoid boundary is marked by a groove with apertures that transmitted those cranial nerves directed to the extraocular muscles. Within the groove is a long fissure ventrally and a foramen dorsally, both of which can be traced to the endocranial cavity on the CT scans (Figs. 14B, C, E, F, 15). The fissure transmitted the abducens nerve (CN VI) ventrally and the oculomotor nerve (CN III) dorsally. The fissure also communicates with the pituitary fossa and likely transmitted veins from the orbit into a cavernous-sinus-like structure; again, extant archosaurs have veins that pass along with the extraocular muscle nerves into the endocranial sinuses (Sedlmayr, 2002). The foramen situated dorsally within the groove transmitted the trochlear nerve (CN IV), no doubt with accompanying veins. CT confirms that the trochlear canal is separate from the abducens-oculomotor fissure (Fig. 17D). The union of abducens and oculomotor foramina, separate from the trochlear foramen, is fully matched by subdivision of the embryonic fenestra metoptica of the chondrocranium observed in extant crocodilians (Starck, 1979), offering support for our interpretation of *Majungasaurus*.

The optic nerve (CN II) foramina are rostral to the orbitosphenoid and separated from each other by the interorbital septum (Figs. 14, 15). The optic nerve foramina are generally confluent in theropods that combine ossified orbitosphenoids with unmineralized interorbital septa, such as *Allosaurus* (CM 21703, UMNH VP 18055), and thus in *Majungasaurus* it can be assumed that the orbitosphenoid forms only the caudolateral margin of the optic foramen. This interpretation is supported by the fact that the characteristic striate texture of the interorbital septum extends almost to the rostromedial margin of the optic nerve

foramen. The foramen itself is oval and quite large, with grooves extending both dorsally and ventrally from it, suggesting that here again orbital veins were traversing the cranial nerve foramen.

Sphenethmoid-Mesethmoid—The sphenethmoid (Figs. 1, 7, 14, 15) is a median ossification (or calcification) of the cartilages (e.g., parietotectal cartilage, interorbital/internasal septal cartilage) located at the juncture of the orbital and nasal cavities (Bellairs, 1958; Witmer, 1995). These cartilages convey the olfactory tracts and associated neurovasculature through the orbit to the nasal cavity and house the olfactory bulbs in their rostral, cup-shaped expansions (Fig. 17). They generally remain cartilaginous throughout life in most extant nonavian sauropsids, but many birds ossify these same cartilages, and the term 'mesethmoid' has been applied to the avian bone (Baumel and Witmer, 1993). Although some dinosaur workers have applied the avian term to nonavian theropods (Witmer and Maxwell, 1996; Larsson, 2001), a variety of other terms have been used for dinosaurs, with 'sphenethmoid' being most popular among recent workers. Although there is no reason to doubt the homologies of the cartilages, the evolution of their mineralization probably has occurred multiple times independently. We will use the term sphenethmoid here.

The sphenethmoid of *Majungasaurus* is well preserved in FMNH PR 2100, and is present in MNHN.MAJ 4, UA 8709, and UA 8719 (Figs. 1, 7, 14, 15). It is located in the roof of the orbit and extends from the area just in front of the laterosphenoids to the rostral edge of the frontal bone. The rostral portion of the sphenethmoid is suturally distinct from the overlying frontals, but the sutures between the elements become progressively obliterated caudally, as confirmed by CT. Internally, the cavity for the olfactory tracts is single and median, but, at the rostral end, as the sphenethmoid expands laterally, the interorbital septum ascends to the roof of the sphenethmoid, separating the two fossae for the olfactory bulbs (Fig. 15). Within the rostral expansion for the olfactory bulbs, the septum bears a series of grooves, and in FMNH PR 2100 there are several small ossifications/calcifications that convert some of these grooves into canals (Fig. 14E, F).

Although the exact soft-tissue contents of the individual grooves cannot be identified, the soft-tissue candidates are known with confidence, due to strong similarities in neurovascular relationships between extant birds and crocodilians (indeed, probably all sauropsids; Baumel and Witmer, 1993; Witmer, 1995; Sedlmayr, 2002; Evans, 2006). Branches of the olfactory nerve, ophthalmic nerve, and ethmoidal artery passed through the sphenethmoid on their way to the nasal cavity and made the grooves. The vascular elements were certainly involved, because the ethmoidal artery no doubt passed through the median olfactory tract cavity as a single vessel and then branched into medial and lateral branches (as in all other sauropsids). At least the ramus medialis of the ophthalmic nerve also passed through the sphenethmoid, although this requires that at least one of the several foramina on the margin of the sphenethmoid transmitted the nerve. And finally, olfactory nerve bundles traversed the sphenethmoid as they passed from the olfactory epithelium in the nasal cavity to the olfactory bulb (Figs. 17, 18).

The external surface of the sphenethmoid is striate and fibrous, much like the interorbital septum below. In fact, there are no visible sutures between the sphenethmoid and the interorbital septum below, as noted also for *Ceratosaurus* by Madsen and Welles (2000). Absence of sutures makes sense given that, as discussed above, the sphenethmoid and interorbital septum derive from fully continuous cartilaginous elements. Coria and Currie (2002) reported that the sphenethmoid of *Carnotaurus* lacked the striate texture, but all specimens of *Majungasaurus* have it, as does *Tyrannosaurus* (AMNH 5117).

Mineralized Interorbital Septum —The interorbital septum is preserved in FMNH PR 2100, UA 8709, MNHN.MAJ 4, and UA 8719 (Figs. 1, 14, 15). The septum is likewise preserved in a number of other theropods, including *Abelisaurus*, *Carnotaurus*, *Ceratosaurus* (MWC 1.1), and *Giganotosaurus* (Coria and Currie, 2002). This feature is also present on a specimen from the Lameta abelisaurid collection (GSI-IM K27/565). In all cases in which preservation is adequate, the surface texture is coarsely striate and fibrous, as noted above for the sphenethmoid, and is qualitatively different from the 'bone grain' of growing periosteal dermal bone (Bennett, 1993; Sampson et al., 1997; Carr, 1999). However, the texture of adjacent bones, including endochondral bones such as the basisphenoid, is generally smooth. Thus, it seems possible that the interorbital septum and sphenethmoid are not truly ossified, as usually reported, but rather are calcified. As noted above, probably all extinct theropods (indeed all extinct archosaurs) had a fully continuous cartilaginous sheet located in the midline from braincase to the tip of the snout, as in extant birds and crocodilians (Witmer, 1995). This cartilaginous interorbital/internasal septum is rarely mineralized, either via calcification or true ossification (definitions vary, see Francillon-Viellot et al., 1991). Although we lack the requisite histological data to test the hypothesis, it is possible, if not likely, that the preserved interorbital septa and sphenethmoids observed in extinct theropods are calcified cartilage, rather than fully ossified and remodeled bone. This would explain the striate, fibrous textures observed.

With regard to structure of the interorbital septum in *Majungasaurus*, it forms a relatively simple median plate above the cultriform process, with which it also is fused and continuous (Figs. 1, 14, 15). There are variations in the surface texture in that some areas are highly striate and others are smoother, although we have no functional explanation for the differences. A consistent feature observable in both FMNH PR 2100 and MNHN.MAJ 4 is a large fonticulus caudodorsally within the septum in the area just rostral to the braincase. There is no reason to believe that anything passed through this fonticulus; rather it simply represents a gap in the cartilaginous septum. Such gaps are common enough in extant birds that have been given names (Baumel and Witmer, 1993); in life they are closed by a fibrous membrane.

Cranial Endocast and Osseous Labyrinth

The endocranial cavity is the space within the braincase that houses the meninges, brain, cerebral arteries and veins, dural venous sinuses, and cranial nerve roots (Fig. 15). There is a long history of using a cast of this cavity (a so-called 'endocast') more or less as a proxy for the size and morphology of the brain (Edinger, 1975; Jerison, 1973; Hopson, 1979; Buchholtz and Seyfarth, 1999; Wharton, 2002; Franzosa, 2004). Although such endocasts typically have been made from latex or silicon (or were available naturally in the course of fossilization and weathering), we generated 'virtual' cranial endocasts of *Majungasaurus* from the CT scan data (Fig. 18), which has a number of advantages over other methods (Witmer et al., 2003). We follow other researchers in referring to these more formally as 'cranial' endocasts, but it should be remembered that other internal ('endo-') casts of cranial cavities can be visualized, such as casts of the pneumatic sinuses (Figs. 6, 9, 17), osseous labyrinth (Fig. 19), or blood vessels. The most complete cranial endocast derives from FMNH PR 2100, although virtual endocasts of the olfactory tract cavities and/or bulbs were made from MNHN.MAJ 4, FMNH PR 2099, UA 8709, and UA 8719; these last four specimens are very similar to the equivalent region in FMNH PR 2100 and will not receive separate treatment here.

The endocranial morphology and cranial endocast of FMNH PR 2100 have been reported on previously (with our permission)

in two doctoral dissertations. Wharton (2002) was provided by C. A. Forster (Stony Brook University) with hard-copy (film) versions of a preliminary CT scan dataset. Wharton (2002) was not able to generate an endocast from these data, and commented on inferred brain structure based on the slice data. Franzosa (2004) was provided by L. M. Witmer with the same, more recent, medical scan data used here, as well as early drafts of our virtual endocast, but he did not receive a set of the high-resolution scans or the most recent medical scans (which were generated subsequently, see Materials and Methods). He produced a virtual endocast and a partial osseous labyrinth, and provided a brief description. Not surprisingly, his findings broadly agree with ours presented below.

Description of the cranial endocast will start with general features, followed by inferences about brain conformation, cranial nerve roots, and vasculature. The endocast will be oriented such that the lateral semicircular canal is horizontal (Fig. 18), corresponding to the typical vertebrate 'alert' posture (Witmer et al., 2003; see below). The only abelisaurid other than *Majungasaurus* for which a cranial endocast has been published is *Indosaurus* (GSI-IM K27/565), and, although Huene and Matley's (1933) sketch is rough and the endocast is incomplete, it is similar to that of *Majungasaurus*. Likewise, the endocast of *Majungasaurus* is similar in shape to those of *Ceratosaurus* (Franzosa, 2004; Sanders and Smith, 2005), *Allosaurus* (Hopson, 1979; Rogers, 1998, 1999), *Acrocanthosaurus* (Franzosa and Rowe, 2005), and *Carcharodontosaurus* (Larsson, 2001), suggesting general endocranial conservatism among basal (non-coelurosaurian) theropods.

The cranial endocast is relatively long and narrow. The olfactory tract and hindbrain are roughly horizontal, and, between them, the midbrain and cerebrum are angled about 45º. As is typical of sauropsids (other than pterosaurs, birds, and advanced nonavian coelurosaurs), the brain obviously did not fill the endocranial cavity, and the reasonable assumption is that the endocast is essentially a cast of the dura mater (Osborn, 1912; Jerison, 1973; Hopson, 1979). Precisely how much of the endocast was occupied by the brain has been a matter of great interest in the paleoneurology literature (see Jerison, 1973; Hopson, 1979; Hurlburt, 1996; Larsson, 2001), and, in the absence of reliable criteria, remains an open issue for *Majungasaurus*. It is generally agreed that the portion of the endocast corresponding to the telencephalon (e.g., olfactory lobes, cerebrum) fairly faithfully represents the contours of the underlying brain. Otherwise, the brain of *Majungasaurus* was largely enveloped in a dural covering that obscures underlying brain parts.

The most prominent dural feature is a large pyramidal peak that projects dorsally above the midbrain region and extends rostrally over the cerebral region and caudally over the mid- and hindbrain regions. Hopson (1979) regarded similar peaks in *Allosaurus* and *Tyrannosaurus* as being partly occupied by persistent cartilage associated with incomplete ossification of the supraoccipital. Such a cartilage plug is unlikely for *Majungasaurus* because the apex of the peak does not correspond to the supraoccipital-parietal juncture but rather is well rostral to the juncture and fully within the parietal (Fig. 15). The same is true in *Allosaurus* (UMNH VP 18050, 18055), in which the peak is within the parietal just rostral to its suture with the supraoccipital bone. Another possibility is that this dural space housed a well developed pineal apparatus (epiphysis). Pineal glands are present in extant birds (Breazile and Hartwig, 1989), and, although pineal glands had been thought to be completely absent in extant crocodilians (Quay, 1979), Sedlmayr and colleagues (2004) presented evidence for pineal-like tissue in alligators as well. Hopson (1979) and Wharton (2002) objected to a pineal interpretation for extinct archosaurs mostly because of the absence of an external opening (a 'parietal foramen'). Nevertheless, extant theropods (i.e., birds), as well as mammals, retain a functional pineal gland in the absence of an external aperture in the skull. Thus, it is likely that at least some of the dural elevation in *Majungasaurus* (and other nonavian theropods) may be attributed to the presence of the pineal gland, as has been suggested for various other archosaurs (e.g., parasuchians [Camp, 1930; Chatterjee, 1978b], stagonolepidids [Case, 1921], sauropods [Janensch, 1935]).

Despite the looseness of the brain within its dural envelope, its general organization can be reliably inferred. For example, there is no reason to believe that *Majungasaurus* had a brain organized like that of a bird or pterosaur (Witmer et al., 2003), but rather was probably much like that of an extant crocodilian for reasons provided below. The lateral and rostroventral aspects of the cerebral hemispheres are visible, and the distance between the neural tissue and dura was probably relatively small in these regions. Dorsally, the contours of the hemispheres are lost within the dural pyramid. The cerebrum itself was housed most intimately within the laterosphenoid (Fig. 15), and the endocranial portions of the frontal and parietal almost certainly housed primarily dural venous sinuses. The greatest breadth of the entire endocast is across the cerebrum (46 mm), but the extent of cerebral expansion is modest, comparable to that in a CT-generated cranial endocast of a large *Alligator mississipiensis* (OUVC 9761).

The presumably paired olfactory tracts extended through the roof of the orbits within a narrow median bony cavity roofed by the frontal and floored by the orbitosphenoids and sphenethmoid (Figs. 14, 15). The single cavity becomes divided by a median septum at the rostral end of the sphenethmoid as the now paired cavities expand to accommodate the neural swellings comprising the olfactory bulbs (Fig. 18). As noted above in the lacrimal description, the location of the olfactory bulb at the juncture of the orbital and nasal cavities is consistent with the presence of a caudodorsally positioned olfactory region involving an olfactory concha associated with the lacrimal bone, as is typically found in extant archosaurs (Witmer, 1995). Whether the olfactory region of *Majungasaurus* had ossified olfactory turbinates of the sort identified in some tyrannosaurids by Witmer and Ridgely (in press) is not entirely clear from the available material.

The optic tecta (optic lobes) are not directly visible in the endocast, and the brain clearly did not fit tightly against the dura in these regions. Nevertheless, important clues to brain conformation are provided by the relationships of cerebral vasculature (which are visible in endocasts) to the major brain parts. For example, in extant sauropsids, the transverse sinus (a dural venous sinus) and middle cerebral vein (the lateral continuation of the sinus) pass between the optic tectum and cerebellum, and thus the course of these vessels can be used to identify the gross positions of these major brain divisions. In *Majungasaurus*, the general position of the optic tectum is thus fixed by the transverse sinus and the middle cerebral vein, both of which are clear in the endocast (Figs. 17, 18). Because these vascular elements are relatively close behind the cerebral hemispheres, the tecta are constrained to occupy a position directly caudal to the cerebral hemispheres, and the tecta almost certainly contacted each other in the midline. That is, *Majungasaurus* apparently lacked the derived maniraptoran ('avian') condition (Hopson, 1979; Burnham, 2004; Franzosa, 2004) of laterally positioned optic tecta (presumably displaced to the side by the expanded cerebrum and cerebellum), and instead had the plesiomorphic condition of more modestly sized brain parts arranged serially in a parasagittal row. This condition is found also in *Ceratosaurus* (Franzosa, 2004; Sanders and Smith, 2005), *Allosaurus* (Hopson, 1979), *Acrocanthosaurus* (Franzosa and Rowe, 2005), and *Carcharodontosaurus* (Larsson, 2001), and is consistent with the relatively basal phylogenetic position of *Majungasaurus* within theropods.

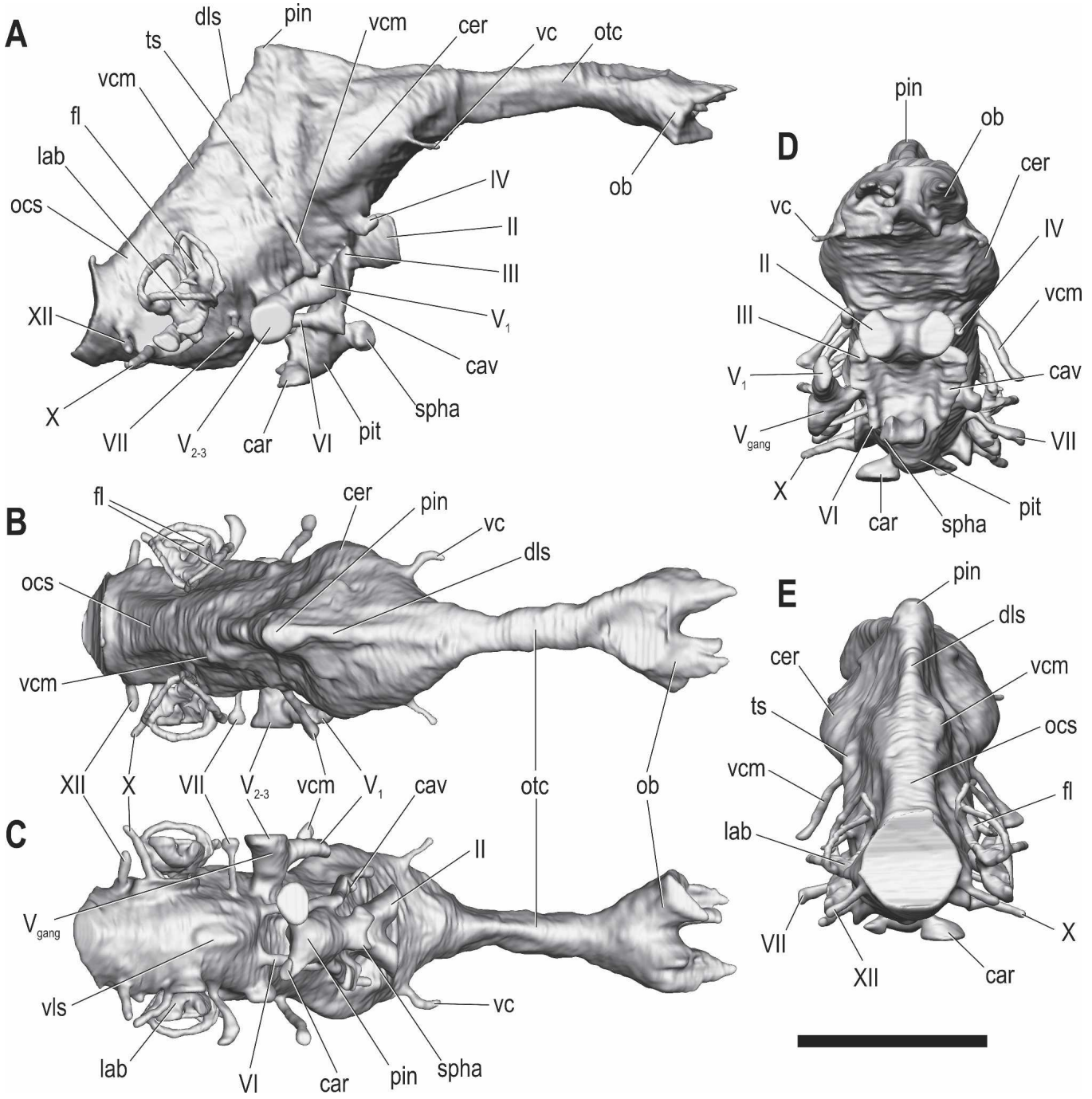

FIGURE 18. Virtual cast of the endocranial cavity (cranial endocast) of *Majungasaurus crenatissimus* (FMNH PR 2100), reconstructed from CT scans. Some vascular elements are depicted, as well as the osseous labyrinth. Labeled illustrations in **A**, right lateral; **B**, dorsal; **C**, ventral; **D**, rostral; and **E**, caudal views. Stereopairs in **F**, left lateral; **G**, right lateral; **H**, dorsal; **I**, ventral; **J**, caudal; and **K**, rostral views. For detailed labeling of the osseous labyrinth, see Figure 19. Scale bars equal 5 cm. See Appendix 1 for abbreviations.

The discrimination of brain divisions in the caudal region is difficult because these divisions (e.g., cerebellum, medulla, pons, etc.) apparently were not large enough to fill the space. Moreover, *Majungasaurus* no doubt resembled its extant archosaur outgroups in having extensive dural venous sinuses (occipital sinuses) covering the caudal portions of the brain (Sedlmayr, 2002). The cerebellum would have been caudal to the transverse sinus and middle cerebral vein, as noted above, and apparently was quite narrow in the region between the paired osseous labyrinths of the inner ears (Fig. 18).

One part of the cerebellum that is visible in the endocast is its floccular lobe (cerebellar auricle), which forms a small tabular swelling that barely projects into the ring formed by the rostral semicircular canal and common crus of the osseous labyrinth (Fig. 18). The flocculus is remarkably small in *Majungasaurus* (and is only a little larger in the abelisaurids *Indosaurus* [GSI-IM K27/565] and *Rugops* [MNN IGU 1]). In comparison, the flocculi of *Dilophosaurus* (UCMP 77270), *Ceratosaurus* (MWC 1.1), *Allosaurus* (UMNH VP 18055; Hopson, 1979), *Acrocanthosaurus* (Franzosa and Rowe, 2005), *Baryonyx* (BMNH R9951), and

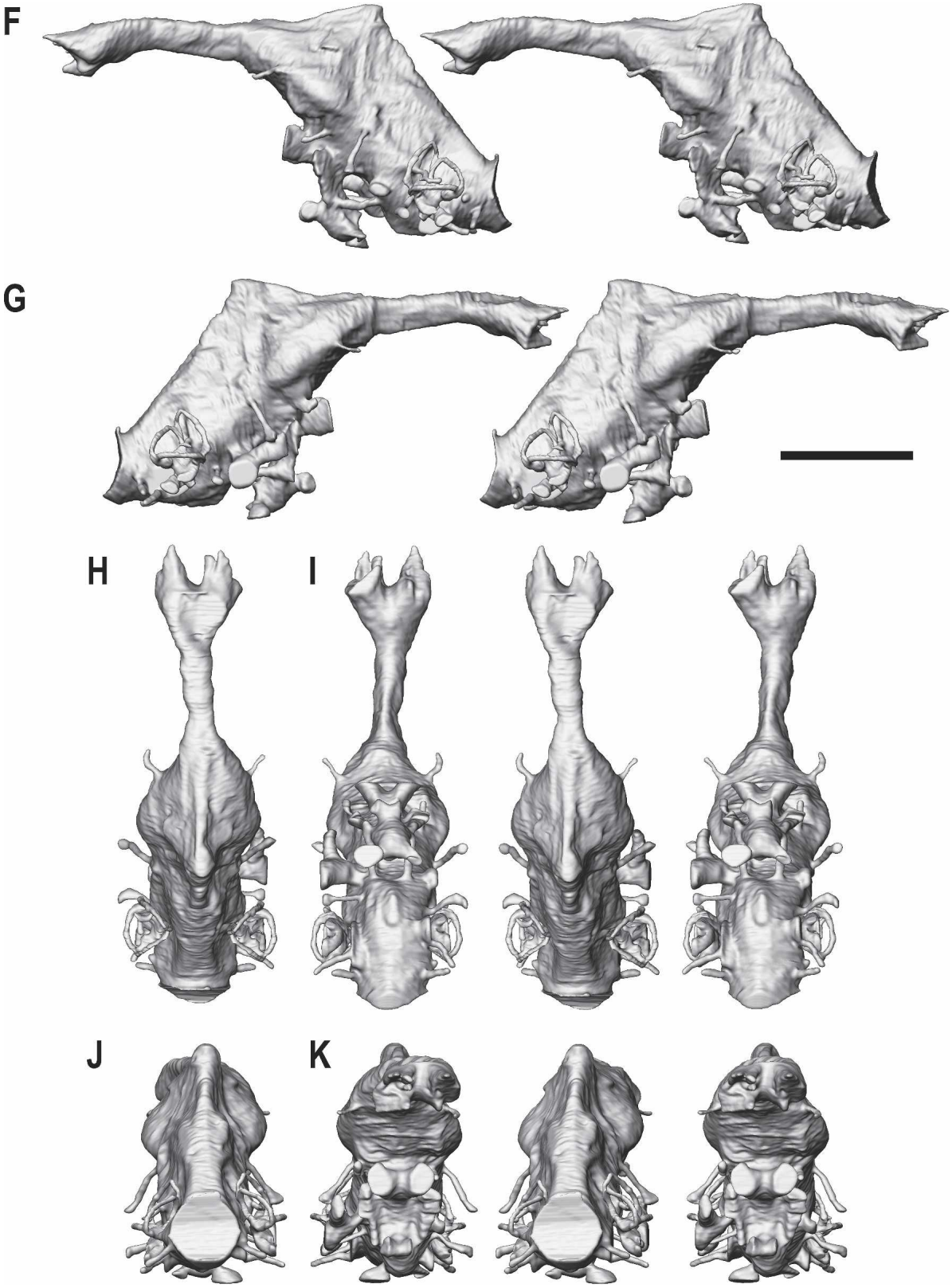

many other theropods are much larger than those observed in *Majungasaurus* and perhaps other abelisaurids. Given the phylogenetic distribution of these attributes, the small flocculus of *Majungasaurus* (and perhaps abelisaurids as a group) must be regarded as an apomorphy. The flocculus plays a role in coordinating eye movements (i.e., gaze) with movements of the head, neck, and body, and tends to be enlarged in taxa that rely on quick movements of the head and/or body (see Witmer et al., 2003, and references therein). Thus, apparent reduction of the flocculus in *Majungasaurus* can be interpreted as correlated with a decrease in reliance on quick movements and sophisticated gaze-stabilization mechanisms.

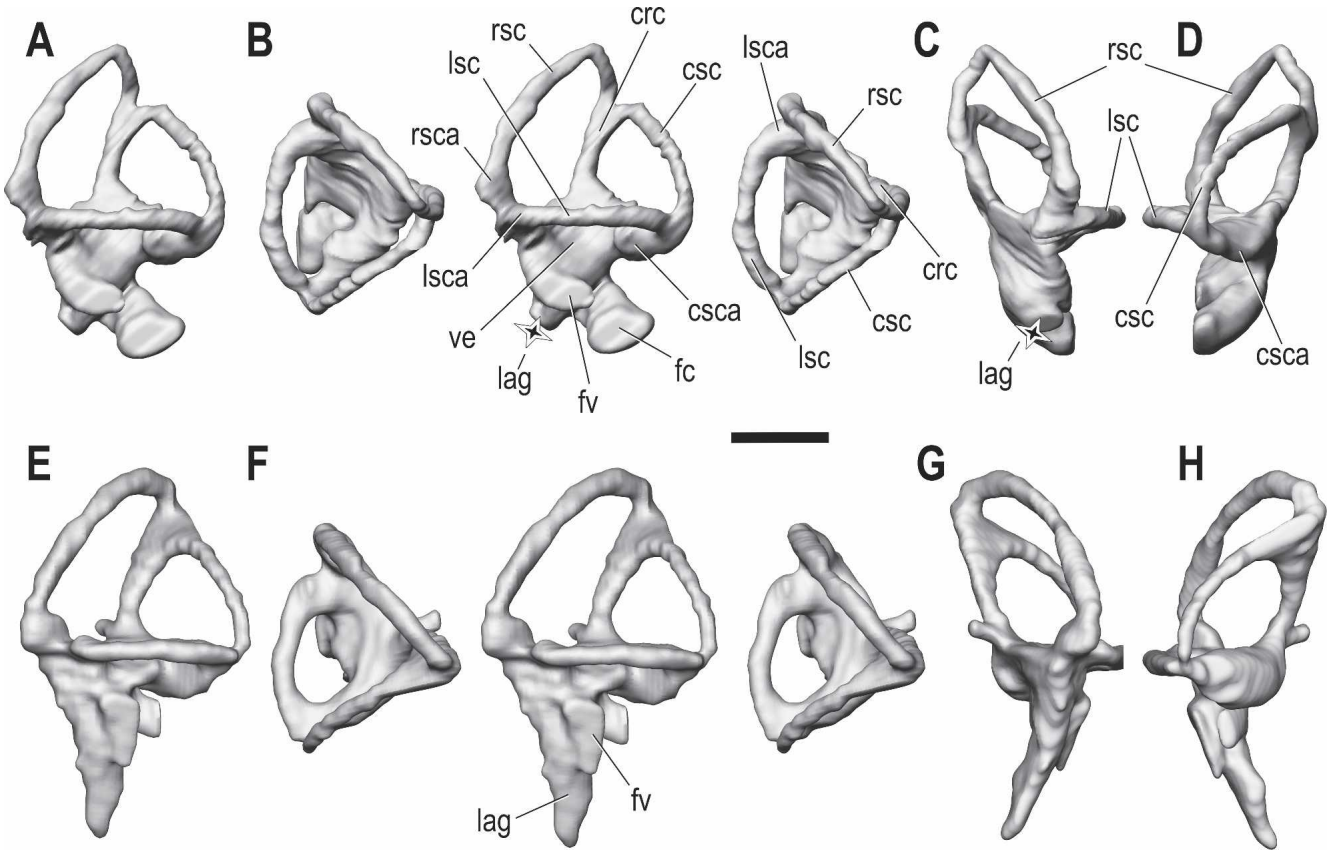

FIGURE 19. Virtual cast of the left osseous labyrinth of *Majungasaurus crenatissimus* (FMNH PR 2100), derived from reconstructed CT scans. Labeled illustrations in **A**, lateral (stereopairs); **B**, dorsal (stereopairs); **C**, rostral; and **D**, caudal views. *Ceratosaurus magnicornis* (MWC 1.1; c.f. *C. nasicornis*) in **E**, lateral (stereopairs); **F**, dorsal (stereopairs); **G**, rostral; and **H**, caudal views. The four-pointed star in **C** indicates that the lagena is incompletely preserved. Scale bar equals 10 mm. See Appendix 1 for abbreviations.

The final identifiable brain part is the pituitary (hypophysis cerebri), and even here little can be said definitively about the pituitary itself. The endocast preserves the hypophyseal fossa (Figs. 15, 18), which undoubtedly contained the pituitary, but how much of the fossa it occupied is an open question because other neural and vascular components pass through it. For example, as noted above in the basisphenoid description, the cerebral carotid arteries entered the endocranial cavity to supply the brain via foramina in the floor of the hypophyseal fossa. Likewise, the sphenopalatine arteries branched off the cerebral carotids within the hypophyseal fossa on their way to the floor of the orbit (Figs. 14, 15, 18). Similarly, cranial nerves and associated veins also passed laterally through the fossa, as will be discussed shortly. Nevertheless, the hypophyseal fossa is probably a fair representation of the relative size and shape of the pituitary (Edinger, 1942). The hypophyseal fossa in the endocast is not particularly remarkable and generally resembles that of other midsized theropods (Hopson, 1979; Franzosa, 2004; Witmer and Ridgely, unpubl. data).

Size of the cranial endocast is often used as a proxy for the brain in scaling studies of relative brain size in vertebrates (e.g., Jerison, 1973; Hopson, 1977, 1980; Hurlburt, 1996; Larsson, 2001). We calculated the endocast volume for *Majungasaurus* based on FMNH PR 2100. Our methods differed from the classic graphical double-integration methods of Jerison, Hurlburt, and Larsson, and instead, following Witmer and colleagues (2003) and Franzosa (2004), used the more exact measuring tools within the 3D visualization software. We also depart from previous authors in what we measured; that is, we included the full olfactory tract cavity and bulbs, which, along with the cerebrum, comprise the telencephalon, rather than truncating the endocast somewhere within the olfactory tract cavity as advocated by Jerison (1973) and Larsson (2001); this inclusion allows comparison of relative olfactory bulb size among taxa. Also, we digitally 'sheared off' the cranial nerve trunks and vascular elements so that, as much as possible, only the dural envelope of the brain was measured (measurements with these structures intact overestimated the volume by more than 7%).

Measured in this way, endocast volume for *Majungasaurus*, based on FMNH PR 2100, is 106.4 cm^3. Following Witmer and colleagues (2003), endocast volume was multiplied by the density of brain tissue (1.036 g cm^{-3}) to yield a mass of 110.2 g. Based on the assumption that roughly half of the endocast volume is occupied by the brain (Jerison, 1973; Hopson, 1977, 1980), we divided endocast mass by 2 to yield an estimated brain mass of 55.1 g. Using this mass and an estimated body mass of 1130 kg (estimated using the femoral circumference method of Anderson et al., 1985), we calculated the Encephalization Quotient (EQ), which is a simple metric devised by Jerison (1973) for comparison of relative brain size. We further used Hurlburt's (1996) modification of Jerison's equations for reptiles (Reptile EQ or REQ), yielding an REQ of 1.6. This number is smaller than any of the 16 theropods included in Franzosa's (2004) analysis (which did not include *Majungasaurus*), perhaps suggesting that *Majungasaurus* had a remarkably small brain. There is no question that, by any measure, this animal was 'small-brained,' but many of the above numbers are suspect and represent 'dated' science. For example, Jerison's (1973) '50% rule' whereby endocast masses

are simply halved to yield a brain mass is very coarse indeed. Likewise, none of the statistical analyses of relative brain size from which the (R)EQ equations were derived (e.g., Jerison, 1973; Hurlburt, 1996) took potential phylogenetic effects into account (e.g., by using independent contrasts). The calculations above are presented as a link to the past—that is, for comparison with previous brain scaling studies. A collaborative project by Witmer, Hurlburt, and Ridgely is ongoing and directed at ameliorating these problems to provide better estimates of relative brain size.

The trunks of the cranial nerves and their paths through the braincase are visible in the cranial endocast, which has provided important confirmation of the identifications of foramina presented in previous sections (Figs. 14, 15, 17, 18). In many if not all cases, it can be safely assumed that veins also passed through the cranial nerve foramina, because such is the case in extant archosaurs (Sedlmayr, 2002). The olfactory nerve trunks (CN I) are not visible on this (or any) endocast, but the cavity for the olfactory bulb and tracts is present and has been described above. The optic nerve trunks (CN II) are separated rostrally by the mineralized interorbital septum and orbitosphenoid but unite within the endocranial cavity forming the optic chiasm. The oculomotor nerve trunk (CN III) is located dorsally and the abducens nerve trunk (CN VI) ventrally within the elongate vertical fissure between the laterosphenoid and orbitosphenoid described above (Fig. 14B, C). This fissure almost certainly conveyed substantial veins from the orbit into the lateral part of the hypophyseal fossa. Thus, this arrangement can be regarded as a 'cavernous sinus' similar to that in birds and mammals, in that there is an endocranial sub-cavity that receives or drains into veins from the facial region and through which pass the oculomotor and abducens nerves and the cerebral carotid artery. The oculomotor nerve trunk and venous elements pass caudally into the endocast, after which they can no longer be traced. The abducens nerve trunk, however, tunnels through the basisphenoid toward the brainstem, and so in the endocast it forms a canal suspended between the cavernous sinus and brainstem (Fig. 18C, I). The trochlear nerve trunk (CN IV) is also located within the laterosphenoid-orbitosphenoid suture, but does not pass through the cavernous sinus (as in birds but not crocodilians; Sedlmayr, 2002), instead coursing below the cerebral hemisphere toward the dorsal aspect of the brainstem.

The trigeminal nerve trunk (CN V) is clearly visible on both sides of the cranial endocast, but its peripheral structure is clearer on the right side where the bony components are better preserved (Figs. 14, 15, 17, 18). The trigeminal nerve roots emerge as a relatively narrow trunk from the cerebellar region (i.e., caudal to the transverse sinus and middle cerebral vein), which then expands near the external foramen. This peripheral swelling represents the trigeminal (Gasserian) ganglion for the cell bodies of the sensory neurons. As noted above, this swelling confirms that the trigeminal ganglion has the primitive, extracranial position. Also significant here is that all three divisions of the trigeminal nerve clearly remain unified through the bone and the split into maxillomandibular nerve (CN V_{2-3}) and ophthalmic (profundus, CN V_1) nerve occurs outside the braincase (i.e., there is no separate ophthalmic nerve foramen). Both the maxillomandibular and ophthalmic trunks are quite large and, again as in extant archosaurs (Sedlmayr, 2002), it is virtually certain that large veins (and probably arteries, as well) ran with the trigeminal nerve branches.

The facial nerve trunk (CN VII) is relatively unremarkable, being a simple twig exiting the brainstem region of the endocast between the trigeminal roots and osseous labyrinth. The facial trunk does bear a peripheral dilatation, representing the geniculate ganglion. The branches of the vestibulocochlear nerve (CN VIII) are not visible in the endocast because of damage. The glossopharyngeal, vagus, and accessory nerve trunks (CN IX, X, and XI, respectively) are presumably united within a common canal, as in many amniotes, which is typically called the vagal canal or, if an encephalic vein is also transmitted, the jugular canal. The relationship of the vagal canal to the otic region in general has been discussed above in the section on the otoccipital. A key conclusion of that discussion is that the vagal canal in *Majungasaurus* clearly was diverted to the occiput (the derived condition), passing just caudomedial to the perilymphatic sac of the inner ear, a relationship made very clear in the endocast (Figs. 17, 18). Finally, the hypoglossal nerve trunk (CN XII) clearly is just a single, simple canal on both sides of FMNH PR 2100, and thus any branching of the hypoglossal nerve took place distal to the skull.

Some of the vascular elements visible on the cranial endocast have been discussed in previous paragraphs. As noted, it seems a certainty that many of the cranial nerve trunks also transmitted veins from the facial region. Relatively discrete vascular structures already mentioned include the cavernous sinuses adjacent to the hypophyseal fossa, the cerebral carotid and sphenopalatine arteries (both of which no doubt had accompanying veins; Sedlmayr, 2002), and the middle cerebral and transverse sinus system (Fig. 18). This last system merits further discussion.

The literature on the comparative anatomy of cerebral veins in sauropsids is very confused and often contradictory (Bruner, 1908; O'Donoghue, 1920; Goodrich, 1930; Oelrich, 1956; Sedlmayr, 2002). In an effort to keep the terminology as simple as possible, we will use as few names as possible. The transverse sinus of *Majungasaurus* is the dural venous sinus visible as a subtle elevation on the endocast (Fig. 18A, F, G). As in other amniotes, the transverse sinus separates the cerebrum and cerebellum. The transverse sinus drains rostrolaterally, exiting the endocranial cavity and ultimately the braincase as the middle cerebral vein, which is very clear on the endocast. The transverse sinus also exits caudally to the occiput where (unfortunately) it also is referred to as the middle cerebral vein (indeed, some sources call the transverse sinus the middle cerebral vein) or external occipital vein. As noted earlier, the foramen in the occiput is situated at the juncture of the parietal, otoccipital, and supraoccipital (Figs. 14G, 17C). Anastomosing with the middle cerebral vein within the skull roof is the dorsal head vein, the external foramen for which is located at the juncture of the parietal, laterosphenoid, and probably prootic (Fig. 17A, D). As noted above (but not illustrated in Figure 17), the dorsal head vein foramen leads to a groove on the paroccipital process that extends caudally to open on the occiput at the posttemporal fenestra. From there, there are occipital grooves indicative that the dorsal head vein and middle cerebral vein anastomose again on the occiput, thus forming a complete anastomotic loop.

With regard to the other dural venous sinuses, the occipital sinus and the dorsal longitudinal (sagittal) sinus are visible on the cranial endocast (Figs. 17, 18). Given the small size of the vagal canal and hence the presumably small size of the jugular (posterior cerebral) vein, it seems certain that *Majungasaurus*, like its extant archosaur relatives, emphasized the large occipital sinus as the major venous drainage of the brain and endocranial cavity. The dorsal longitudinal sinus is remarkable for the pronounced dural peak it makes dorsally in association with the pineal gland (Fig. 18A, B). There is also a ventral longitudinal sinus visible below the brainstem (Fig. 18C). A presumably venous, paired channel is present, originating in the orbit via a foramen between the laterosphenoid and orbitosphenoid and passing into the endocast, rostral to the cerebrum (Figs. 17, 18A–D). Although, as noted above, the cerebellar flocculi were small, there are clear vascular (presumably venous; Sedlmayr, 2002) structures that continue the course of the flocculi into the region of the osseous labyrinth.

The osseous labyrinth itself is illustrated in Figure 19 (A–D), along with the labyrinth of *Ceratosaurus* (MWC 1.1) for com-

parison. The complete left labyrinth of the inner ear of FMNH PR 2100 was digitally extracted from the CT data, with the exception of the lagena, the distal (ventral) end of which was lost in preparation. The right labyrinth was harder to extract in its entirety due to damage; in Figures 17 and 18 the left labyrinth has been mirrored and registered as the right labyrinth for reference. In general, the osseous labyrinth of *Majungasaurus* is quite conservative and not particularly remarkable. It is quite similar to that of *Ceratosaurus* in overall conformation (Fig. 19E–H) and likewise resembles the published inner ears of other midsized theropods (e.g., *Allosaurus* [Hopson, 1979; Rogers, 1998], *Acrocanthosaurus* [Franzosa and Rowe, 2005], *Carcharodontosaurus* [Larsson, 2001]).

As is typically the case in theropods (in fact, dinosaurs generally; Witmer and Ridgely, unpubl. data), the rostral semicircular canal is the longest of the three canals and roughly elliptical in shape (longest axis: 17.4 mm; shortest axis: 9.3 mm; radius of curvature: 6.7 mm). The lateral semicircular canal is the most circular of the three but is still elliptical (longest axis: 13.2 mm; shortest axis: 9.9 mm; radius of curvature: 5.8 mm). The caudal semicircular canal is the most strongly elliptical of the three (longest axis: 15.4 mm; shortest axis: 7.6 mm; radius of curvature: 5.7 mm). The rostral canal does not extend caudodorsally beyond the common crus such that the latter is not 'twisted;' *Majungasaurus* bears the primitive condition. Another plesiomorphy occurs in the caudal canal, which extends only slightly below the lateral canal such that, in caudal view (Fig. 19D), there is little distinction between the lateral canal and the caudal canal (and its ampulla). All of the canals are basically planar (i.e., each defines a flat plane) and, collectively, they do not strongly depart from being mutually orthogonal.

As in other archosaurs, the vestibule of the inner ear does not project dorsally much beyond the level of the lateral canal. The ventral portion of the vestibule is not entirely clear due to damage, but the position of the fenestra vestibuli is apparent and marks the location of the footplate of the columella. Likewise, the position of the perilymphatic sac is also more or less identifiable, although its full extent is not as clear. A 'fenestra cochleae' has been labeled in Figure 19, and we regard this identification of the position for the secondary tympanic membrane as being reasonable, but will reiterate that the anatomy of the 'metotic' region is complex and controversial (see discussion in otoccipital section above), and that *Majungasaurus* is somewhat damaged in this area. The base of the lagena is present, but its length is not known. However, given the overall similarities of the labyrinths of *Majungasaurus* and *Ceratosaurus* (Fig. 19), we see no reason to believe that the lagena of the former was significantly different from the latter.

One potentially interesting difference between *Majungasaurus* and *Ceratosaurus* is that the lateral semicircular canal is much longer in *Majungasaurus* (Fig. 19). Given that canals with greater radii of curvature in general should have greater sensitivity, it would seem that *Majungasaurus* might have had more sensitivity to lateral turning movements of the head. However, caution is warranted at this point, pending analysis of more taxa (Witmer and Ridgely, unpubl. data.). On the other hand, a fairly safe behavioral interpretation (Hullar, 2006) relates to the stereotypical 'alert' posture that *Majungasaurus* would have adopted when intending to maximize sensory awareness. Witmer and colleagues (2003 and references therein) discussed the planar orientation of the lateral canal as a rough behavioral measure of this alert posture such that a broad range of extant vertebrates adopt a posture that places the lateral canal basically level with the horizon. When the labyrinth of *Majungasaurus* is oriented such that the lateral canal is horizontal, the entire skull has the orientation shown in Figure 1—that is, roughly horizontal. This may not seem remarkable, but a variety of other theropods display an alert posture with a more strongly down-turned head (Witmer and Ridgely, in press, unpubl. data.). The significance of the horizontal posture in *Majungasaurus* may relate to elevating the snout to the point that the lacrimal rugosities no longer (or at least minimally) obstruct the field of view, perhaps enhancing the binocular field of view.

Palatoquadrate Complex

General—Most of the palate, excluding the vomer, has been recovered for *Majungasaurus*. The elements are particularly well preserved on the left side of FMNH PR 2100 and some palatal elements are preserved in UA 8709, allowing for a detailed assessment of palatal architecture (Fig. 1). Unfortunately, the bony palate is poorly known for most basal theropod taxa, and few detailed descriptions have been published (e.g., Currie and Zhao, 1994a, *Sinraptor*; Madsen, 1976a, *Allosaurus*), making comparisons problematic. Below is the first detailed description of the palate of an abelisauroid theropod.

Vomer—To date, the vomer has been definitively identified only in a handful of non-tetanuran theropods (e.g., *Herrerasaurus*, *Coelophysis*). No conclusive evidence of this gracile median palatal element has been recovered with any of the *Majungasaurus* specimens.

Palatine—A mostly complete left palatine and fragmentary right palatine are preserved with FMNH PR 2100 (Figs. 1, 20), as well as a right palatine fragment in UA 8709. As in many other theropods, the palatine of *Majungasaurus* contacts the maxilla and jugal laterally, and the pterygoid and (presumably) the vomer medially. Like the ectopterygoid, this element effectively braces the palate against the facial skeleton. The palatine of the Malagasy abelisaurid can be divided into three portions: (1) a triangular ventral body; (2) an elongate, rostromedially positioned vomeropterygoid process; and (3) a more abbreviated, caudomedially positioned pterygoid process. The two medial processes span the distance between the maxilla and the pterygoid, contributing to the formation of three palatal openings: rostral to the vomeropterygoid process is the choana; between the vomeropterygoid and pterygoid processes is the pterygopalatine fenestra (subsidiary palatal fenestra of some authors); and caudal to the pterygoid process is the suborbital fenestra (postpalatine fenestra of some authors; Figs. 1B, D, 20).

The palatine body, which is deepest caudally and tapers rostrally virtually to a point, forms the broad maxillary contact on its lateral side (Fig. 20B). This articulation extends over much of the caudomedial surface of the maxillary body, spanning alveoli 8 through 14. Laterally, the maxillary contact surface of the palatine transitions from being rugose and convoluted ventrally to virtually smooth dorsally. There is no indication of a palatine pneumatic recess or associated pneumatic chambers, which are present in certain more derived theropods (*Sinraptor*, *Acrocanthosaurus*; Witmer, 1997a; Harris, 1998). Contact with the jugal appears to have been minimal, marked by a shallow concavity with a robust margin at the caudodorsal corner of the body. This concavity apparently formed the medial boundary of a large neurovascular opening that penetrates the inner aspect of the jugal. Medially, the vomeropterygoid and pterygoid processes radiate from the palatine body rostral to the midpoint of the element. A pronounced, possibly pneumatic fossa occurs at the junction of these processes, terminating dorsally in two moderately sized foramina that pierce the element. A similarly positioned, blind fossa has also been reported in *Acrocanthosaurus* (Harris, 1998). A second, larger fossa is present along the caudal margin of the pterygoid process, though with no detectable associated foramen. A third, more diminutive fossa occurs dorsally at the base of the pterygoid process.

Of the two prominent palatine processes, the rostrally positioned vomeropterygoid process is significantly longer, more than twice the length of the pterygoid process as preserved in

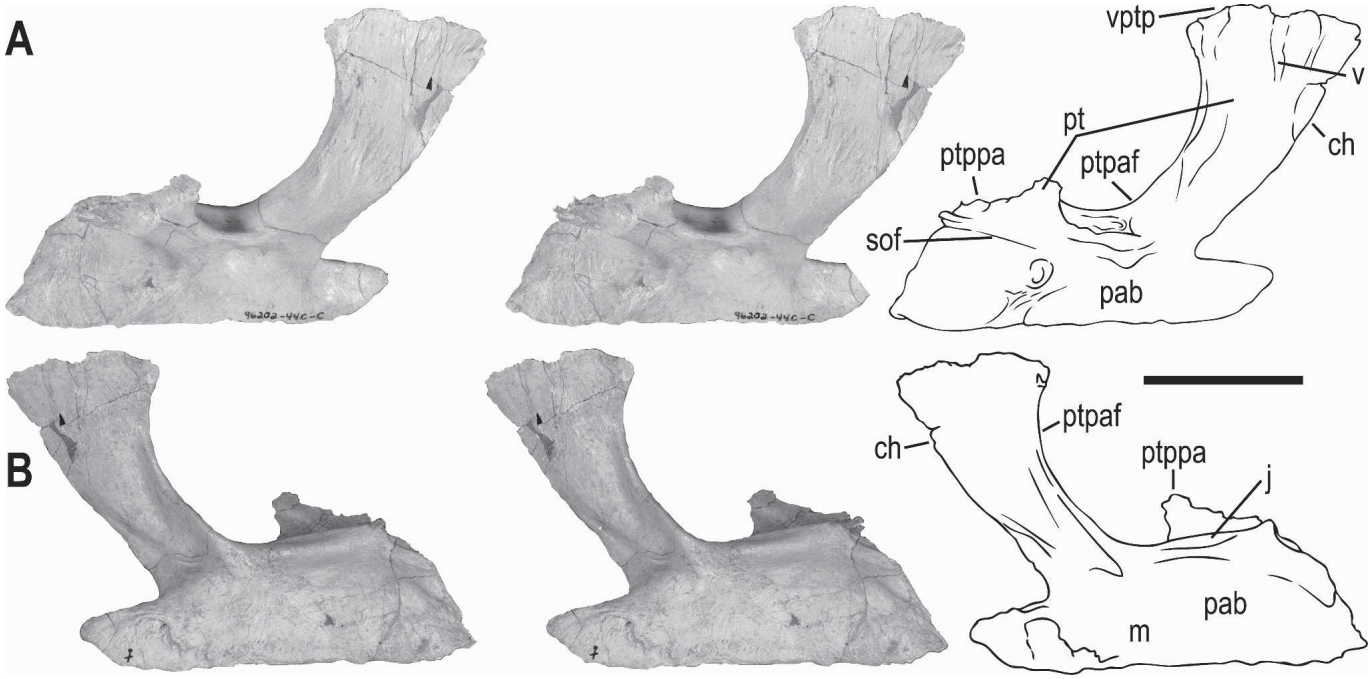

FIGURE 20. Stereopairs of left palatine of *Majungasaurus crenatissimus* (FMNH PR 2100) in **A**, lateral; and **B**, medial views. Scale bar equals 5 cm. See Appendix 1 for abbreviations.

FMNH PR 2100. This process is distinctly concave laterally and convex medially, particularly in the ventral portion. It partially serves as the attachment site of the M. pterygoideus, pars dorsalis as well as partitioning the oral, nasal, and antorbital cavities (Witmer, 1997a). Pneumatic invagination of the vomeropterygoid process is relatively common in theropods, and this concavity in *Majungasaurus* may be functionally related to a laterally positioned paranasal diverticulum (Fig. 20B). However, there are no foramina associated with this space. Moreover, palatine pneumatic recesses are otherwise unknown in 'ceratosaurs' (Witmer, 1997a) and, where present in theropods (e.g., *Sinraptor*, *Deinonychus*), tend to occur within the body of the palatine. The lateral vomeropterygoid fossa is directed mostly toward the choana, and thus it may have had more to do with the oronasal region than the antorbital and muscular domains. The more robust ventral half of the vomeropterygoid process is inclined dorsomedially, whereas the extremely thin dorsal half is vertical or nearly so. This gracile upper portion of the vomeropterygoid process expands rostrocaudally to form a somewhat rugose surface that likely contacted the vomer ventrally and the pterygoid more dorsally. The dorsal limit of the rostral process is missing in FMNH PR 2100, preventing accurate determination of its full extent.

The pterygoid process resembles its vomeropterygoid counterpart in possessing a distal expansion. This expansion, incompletely preserved in FMNH PR 2100 but more extensive in UA 8709, is demarcated ventrally by a distinct rim, which forms the lower margin of the pterygoid contact. A pair of parallel ridges and grooves on this articular surface slot into corresponding surfaces on the pterygoid. In contrast to the vomeropterygoid process, the ramus of the pterygoid process is more steeply angled, with a weakly convex lateral surface and a slight concavity on the medial side.

Overall, the palatine of *Majungasaurus* is relatively more abbreviated than that of non-abelisaurid basal theropods, likely reflecting the telescoping present in other facial elements. The elongate caudal portion of other taxa, often with a substantial overlapping jugal contact (e.g., *Sinraptor*, Currie and Zhao, 1994a; *Acrocanthosaurus*, Harris, 1998), is lacking, as is the elongate rostral extension of the vomeropterygoid process (also absent in *Carnotaurus* and *Allosaurus*). A similarly distinct pterygoid process with an expanded apex appears to be present in *Carnotaurus*, but otherwise we have not seen this feature in any other basal theropod taxon. A more elongate caudomedial process of the palatine is present in some maniraptorans (e.g., *Deinonychus*, Ostrom, 1969; *Dromaeosaurus*, Currie, 1995), presumably representing a parallel condition. The general basal theropod condition is for the pterygoid to contact the caudal portion of the palatine body. Moreover, in most theropod taxa (as well as in dinosaurs generally), there is a continuous contact between the pterygoid and palatine, and thus the pterygopalatine fenestra is absent (e.g., *Coelophysis*; see Witmer, 1997a, fig. 14). This fenestra appears to have evolved at least two or three times within theropods, since it is present in ornithomimosaurs, (at least some) tyrannosaurids, troodontids, and dromaeosaurids (Rauhut, 2003). Within ceratosaurs, it appears to be present in *Carnotaurus* and *Majungasaurus*, but absent in *Ceratosaurus*.

Pterygoid—The pterygoid (Figs. 1, 21) is a highly complex triradiate element with multiple facets for surrounding elements. FMNH PR 2100 includes a well preserved left pterygoid, and substantial portions of both pterygoids are preserved in UA 8709. The pterygoid contacts the palatine and presumably vomer rostrally, the quadrate caudally, the ectopterygoid laterally, the opposite pterygoid medially, the basisphenoid in its central portion, and probably the epipterygoid dorsally. For the purposes of description, it can be divided into four parts: a rostrally positioned vomeropalatine ramus, a ventral ectopterygoid ramus (ala pterygoideus of some authors), a caudal quadrate ramus, and a centrally located body effectively comprised of the confluence of the above three processes. Together, opposing pterygoids diverge ventrally, forming a vaulted, highly arched palatal roof.

As in other theropods, the body possesses a deep, caudally-facing slot that forms an articulation with the basipterygoid process of the basisphenoid. The basipterygoid articulation itself

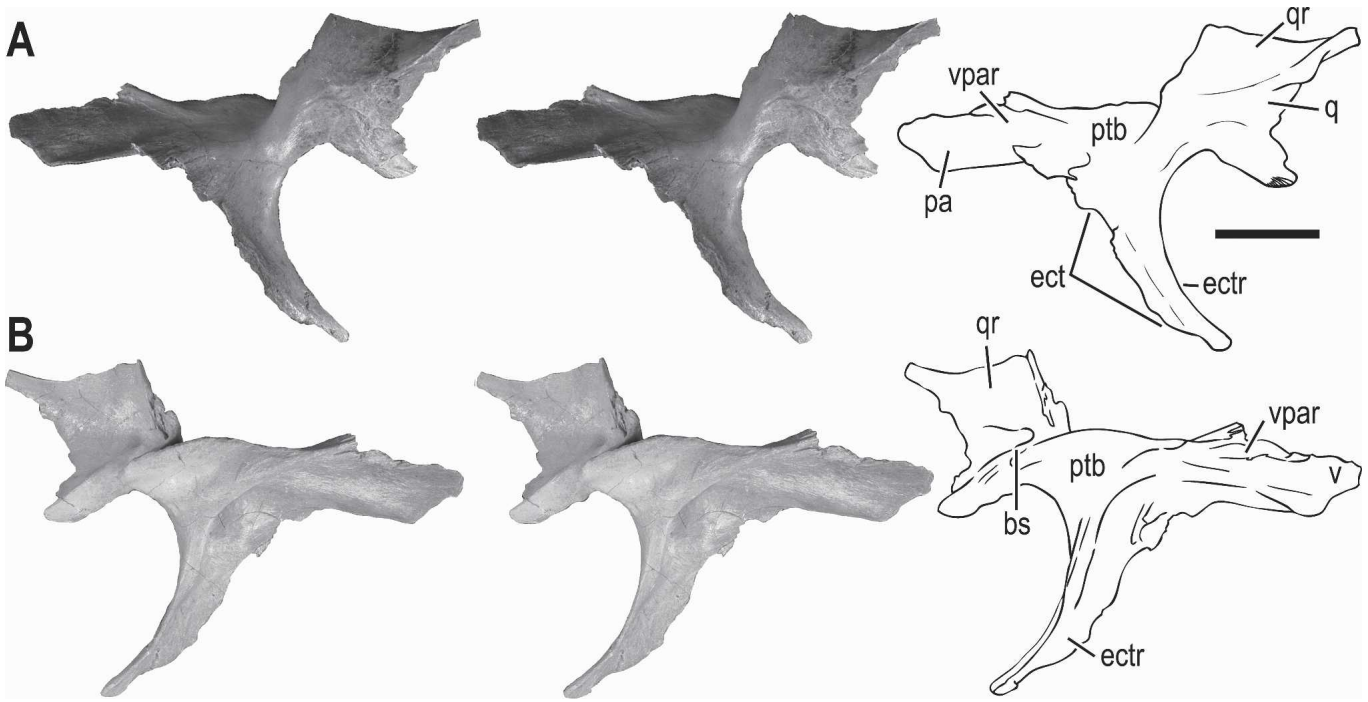

FIGURE 21. Stereopairs of left pterygoid of *Majungasaurus crenatissimus* (FMNH PR 2100) in **A**, lateral; and **B**, medial views. Scale bar equals 5 cm. See Appendix 1 for abbreviations.

takes the form of a broad groove that is open caudally and ventrally and inclined such that it runs caudoventrolaterally to rostrodorsomedially. The articular region is arranged as two discrete pads laterally and medially separated by a groove; the groove leads rostrodorsally to a cavity rimmed in front by a shell of bone. The overall structure has all the appearance of a well formed synovial articulation, with the rostral cavity and its groove perhaps housing the synovial membrane. The basicranial joint of tetrapods generally is regarded as a synovial joint. Thus the situation in *Majungasaurus* is no surprise, and there is no reason to believe that there was anything other than slight compensatory movements taking place at this joint.

The pterygoid bears a large ventromedial fossa that spans the ectopterygoid and vomeropalatine rami and is fairly clearly a pneumatic fossa or, at least, housed an oropharyngeal recess of some kind (Figs. 1B, D, I, L, 21). The margin of the fossa takes the form of a raised ridge that starts from almost the distal tip of the ectopterygoid ramus, sweeps around the body of the pterygoid, and then passes rostrally along the dorsomedial aspect of the vomeropalatine ramus. The apex of the fossa is deeply invasive in both FMNH PR 2100 and UA 8709, in both bearing foramina that lead up into the body of the pterygoid. This structure is characteristic of pneumatic systems in general, and a variety of theropods (e.g., *Syntarsus*, *Sinraptor*) have similar pneumatic recesses in their pterygoids, usually associated with ectopterygoid recesses (Witmer, 1997a). Pterygoid pneumaticity has not been previously reported in abelisaurids, although the basal ceratosaur *Ceratosaurus* (MWC 1.1) has a very similar fossa.

The full extent of the vomeropalatine ramus cannot be assessed on the basis of available specimens. However, the presence of a dorsoventrally deep facet on the vomeropterygoid process of the palatine, together with the conformation of the palate in other basal theropods, indicates that the pterygoid of *Majungasaurus* extended at least rostral to this point. Indeed, the complete pterygoid may well have been the most elongate element of the skull, as in some other basal theropods (Currie and Zhao, 1994a). As preserved in FMNH PR 2100, the lateral side of the vomeropalatine ramus possesses a pair of poorly defined ridges and grooves that articulate with corresponding surfaces on the pterygoid process of the palatine. Just caudal to this contact, at the junction with the ectopterygoid ramus, is another, slightly roughened contact surface, this one for the ectopterygoid. Between these palatine and ectopterygoid contacts, the vomeropalatine ramus of the pterygoid forms much of the medial margin of the suborbital fenestra.

The distinctly recurved, ventrolaterally directed ectopterygoid ramus tapers to a blunt point at the distal end. Its caudal surface is rounded, whereas the rostral margin tends to be sharp except in the central portion. The ectopterygoid contacts the rostral margin of this ramus virtually throughout its length, interlocking with the pterygoid in a complex manner. Dorsally, the ectopterygoid overlaps the pterygoid on the latter's dorsolateral surface. Ventral to this point, the ectopterygoid wraps around to form an extensive, slightly rugose and well-defined contact with the ventromedial surface of this ramus. Centrally, the otherwise thin rostral margin of the ectopterygoid ramus swells to form a flattened, crescentic process about 30 mm in length in FMNH PR 2100 that slots into a well developed notch of the ectopterygoid. The relative length of the ramus is greater in FMNH PR 2100 than in UA 8709, a difference that we ascribe to individual variation.

The subrectangular quadrate ramus of the pterygoid flares laterally and caudally from its base at the basipterygoid articulation. Other than its proximal portion, the quadrate ramus is extremely thin (about 1 mm), convex laterally and concave medially. A small, triangular facet, presumably for the epipterygoid, occurs laterally on the dorsal limit of this ramus. Also on the lateral side, the contact for the quadrate is clearly delimited, with a right-angled facet in the central region of this ramus. Medially, a well defined ventral ridge apparently reinforced contact with the quadrate and then sweeps dorsally to form a vertical ridge just dorsal to the basipterygoid articulation. This ridge system encloses a substantial fossa that is continuous with a similar fossa

on the pterygoid ramus of the quadrate. This fossa is smooth-walled and represents the lateral wall of the middle ear sac.

The triradiate pterygoid of *Majungasaurus* closely resembles that of most basal theropods, and stands in contrast to various coelurosaurs. Many maniraptorans (e.g., *Deinonychus*, Ostrom, 1969) lack the ventrally projecting ectopterygoid ramus. The ectopterygoid ramus is particularly elongate in *Majungasaurus*, closely resembling the condition in *Ceratosaurus* and *Sinraptor*, and in contrast to the more abbreviated condition in *Allosaurus*. The quadrate ramus is considerably more vertical in orientation in *Sinraptor* and particularly in *Allosaurus* relative to that of *Majungasaurus*, projecting well dorsal to the vomeropterygoid ramus in the allosauroid taxa. Most of the vomeropalatine ramus is missing or fragmentary on known specimens of *Majungasaurus*. However, the holotype of *Carnotaurus* appears to show that, at least in this Argentine abelisaurid, the process was relatively deep dorsoventrally, with a distinct lateral fossa.

Epipterygoid—No epipterygoid was recovered with any of the *Majungasaurus* specimens, but the presence of this element can be inferred from preserved contact surfaces on the latersphenoid and the pterygoid (see above; Fig. 14C, F). As in other basal theropods (e.g., *Herrerasaurus*, *Allosaurus*), there is a rugose region at the dorsal apex of the pterygoid's quadrate ramus on the lateral side (Fig. 21), indicating that this element would have been relatively small, thin-walled and triangular, probably very similar to that preserved in *Ceratosaurus* (Madsen and Welles, 2000:9).

Ectopterygoid—The ectopterygoid of *Majungasaurus*, like that of other basal theropods, is a U-shaped element that opens caudally, bracing the palate against the sidewall of the skull ventral to the orbit (Figs. 1, 22). In *Majungasaurus*, however, the ectopterygoid is perhaps the most robust bone of the palate. It contacts the jugal laterally and the pterygoid medially. Rostrally, the ectopterygoid borders the suborbital foramen, dorsally the orbital cavity, ventrally the oral cavity, and caudally the adductor chamber. The element can be subdivided into three parts: (1) a rostrally positioned body; (2) a lateral jugal process; and (3) a medial pterygoid process (Fig. 22). In the left ectopterygoid preserved with FMNH PR 2100, the lateral (jugal) side is about two-thirds the length of the medial (pterygoid) side. In contrast, the medial side of the ectopterygoids preserved with FMNH PR 2278 and UA 8709 is relatively broader and shorter than the lateral, variation that we presume to represent intraspecific differences, since the elements are otherwise closely similar. A gracile region of the ectopterygoid occurs rostrally on the body, where it tapers to a thin, arching lamina that forms a ventral concavity; this concavity takes the form of an invasive recess in the right ectopterygoid of UA 8709. Dorsally, the element is relatively smooth except for the strong notch and associated contact surface for the pterygoid. The jugal and pterygoid processes are relatively straight-margined and subparallel, giving the ectopterygoid a subrectangular appearance as viewed dorsally (Fig. 22).

Laterally, contact with the jugal occurs immediately ventral to the orbital margin via the broad and thickened jugal process. This process expands dorsoventrally in its mid-portion and tapers caudally. The jugal articular surface is divided into two parts by (in anatomical position) a horizontal sulcus (present in FMNH PR 2100 and UA 8709). As discussed above in the jugal description, this sulcus matches a similar one on the jugal, together forming a canal for the passage of a neurovascular bundle essentially right through the ectopterygoid-jugal contact. The portion of this contact below the sulcus is by far the more rugose and congruent one, and the ectopterygoid's jugal process is striate and ridged for a firm suture with the jugal. The articular surface dorsal to the neurovascular sulcus is much less marked, with the ectopterygoid presenting a simple smooth pad to the jugal. Medially, the ectopterygoid shares an elongate, complex contact with the pterygoid along the latter's ectopterygoid ramus and (to a far lesser extent) vomeropalatine ramus (see Pterygoid description above). The pterygoid process possesses a deep, steeply angled notch on its caudal surface that receives the ectopterygoid process of the pterygoid. The pterygoid process tapers to a point distally, terminating at approximately the same ventral level as the pterygoid.

The ectopterygoid of *Majungasaurus* differs significantly from that of non-abelisaurid theropods. In most dinosaurs, the ectopterygoid is a relatively simple element, with minimal expansion medially. However, the standard condition among nonavian theropods is strong expansion of the medial portion of the ectopterygoid, often with laminar portions that form a broad contact with the pterygoid. The theropod ectopterygoid also tends to be more triangular and triradiate in shape, with the jugal process curving away from the body at a relatively high angle together with a rostromedial expansion of the body (e.g., *Poekilopleurodon*?, Allain, 2002; *Dromaeosaurus*, Currie, 1995; Tyrannosauridae, Holtz, 2004). Although there is a small fossa on the underside of the rostral portion of the ectopterygoid in *Majungasaurus*, ventral fossae tend to be greatly elaborated in non-abelisaurid theropods, sometimes forming a broad, frequently pneumatic excavation that continues onto the pterygoid. The mode of ectopterygoid pneumatization, when present, varies considerably among theropods, limited to a deep pocket shared with the pterygoid in coelophysoids (e.g., *Syntarsus*; see Witmer, 1997a:fig. 35B), forming a ventral fossa and lateral groove in many allosauroids, and invading the element via a pronounced foramen in ornithomimosaurs, tyrannosaurids, troodontids, and dromaeosaurids (Gauthier, 1986; Witmer, 1997a, b; Rauhut,

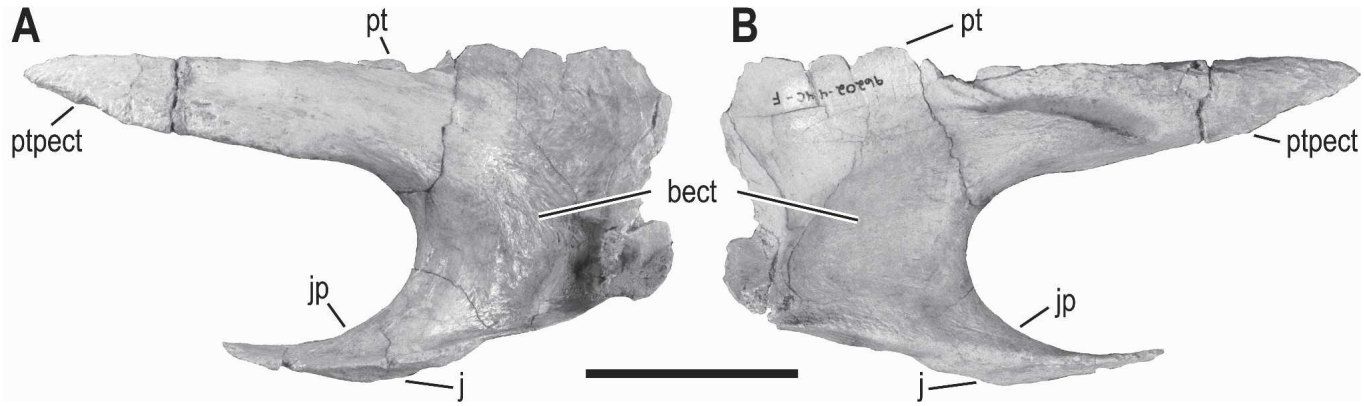

FIGURE 22. Left ectopterygoid of *Majungasaurus crenatissimus* (FMNH PR 2100) in **A**, caudodorsal; and **B**, rostroventral views. Scale bar equals 5 cm. See Appendix 1 for abbreviations.

2003). In *Majungasaurus*, the ectopterygoid's ventral fossa, although somewhat invasive in UA 8709, is not at all associated with the presumptive pneumatic fossa on the pterygoid (see above) but rather is directed more toward the suborbital fenestra (Fig. 1D, L). Although a pneumatic interpretation for the fossa is perhaps the most parsimonious, the fact remains that the situation is very different from that in other theropods and thus other explanations (e.g., vascular) remain viable.

In *Allosaurus*, the lateral and medial ectopterygoid processes are subparallel as in *Majungasaurus*, but the body and pterygoid process are more primitive, being expanded into a thin sheet that expands rostrally well beyond the origin of the jugal process. The ectopterygoid of *Ceratosaurus* (MWC 1.1) more closely resembles the *Majungasaurus* condition, with subparallel jugal and pterygoid processes and only moderate expansion of the body rostromedially. Not surprisingly, this element in *Majungasaurus* is most similar to that of other abelisaurids, such as *Carnotaurus* and an unidentified Lameta abelisaurid (GSI-IM K27/688), in which the ectopterygoid is robust, with nearly parallel lateral and medial processes, and a reduced to absent rostromedial extension of the body.

Quadrate—As in other basal theropods, the quadrate of *Majungasaurus* contacts the squamosal dorsally, the quadratojugal laterally, the pterygoid rostromedially, and the glenoid of the lower jaw ventrally (Figs. 1, 23). It can be divided into three major portions: (1) a thickened, prominent shaft running from the quadrate head dorsally to the mandibular condyles ventrally; (2) a laterally projecting quadratojugal ramus; and (3) a rostrally directed pterygoid ramus (Fig. 23). The quadratojugal and pterygoid rami are almost at right angles to each other. The quadrate of *Majungasaurus* is relatively tall and broad as viewed caudally. Viewed from either side, the caudal margin of the quadrate is distinctly concave. When placed in articulation with the skull, this caudal curvature results in the jaw joint being positioned behind the quadrate-squamosal contact.

The lateral ramus of the quadrate tapers in the dorsal one-third to terminate in the quadrate head that articulates with the squamosal. In proximal view, the head is quadrangular with a medially facing concavity. This concavity is variably developed, being poorly defined in FMNH PR 2100 and more evident in FMNH PR 2278. The articular surface of the head possesses a pronounced ventral expansion on the rostral aspect, which appears to be standard among basal theropods. Beneath the tapered region, the quadratojugal ramus projects somewhat lateral to the mandibular condyles to form the contact surface for the quadratojugal. A distinct fossa occurs on the rostral surface of the quadratojugal ramus dorsal to the lateral condyle (Fig. 23A). Another, less well defined fossa, occurs on the caudal surface of the quadratojugal ramus dorsal to this position. In most basal tetanuran theropods, the quadratojugal ramus of the quadrate is either significantly reduced (e.g., *Allosaurus*, *Sinraptor*) or virtually absent (*Baryonyx*), such that it does not project lateral to the mandibular condyles, but rather terminates more medially, dorsal to the condyles.

The large, triangular pterygoid ramus projects rostrally from the inner margin, forming a broad overlapping contact with the pterygoid on the quadrate's medial side. There is a large, shallow fossa on the medial side of the pterygoid ramus, bounded ventrally by a thickened region (Fig. 23C). As mentioned above in the pterygoid description, this smooth medial fossa is continuous with a similar fossa on the pterygoid's quadrate ramus, such that the two fossae together form the lateral wall of the epithelial middle ear sac. The ventral margin of the pterygoid ramus terminates in a medially projecting shelf that aided in securing the pterygoid and partially floored the middle ear sac. The ventral limit of the pterygoid ramus on the shaft occurs well above the medial condyle. In contrast, this ramus extends somewhat more ventrally in *Allosaurus*, virtually to the condyle in *Sinraptor*, and literally contacts the condyle in *Baryonyx*. Allosauroids also tend to have a strongly developed, rugose ventral facet for the quadratojugal, whereas this contact is overlapping and less well demarcated in *Majungasaurus*.

Ventrally, the medial and lateral mandibular condyles of the quadrate are distinctly asymmetrical (Figs. 1, 23). The lateral condyle is broader and more abbreviated rostrocaudally, whereas the medial condyle is transversely narrower and more elongate rostrocaudally. As viewed ventrally, then, the combined condylar surfaces are narrowest laterally and expand medially, with the medial condyle directed at an acute rostromedial-caudolateral angle (Fig. 1D, L). Both medial and lateral condylar surfaces (but particularly the lateral) extend onto the rostral and caudal surfaces of the quadrate shaft, suggesting a pronounced excursion of the mandible (Fig. 23).

The quadrate of *Majungasaurus* lacks a paraquadrate foramen. This opening along the quadrate-quadratojugal junction is a characteristic of a wide range of sauropsids and is routinely found in most clades of archosaurs. It is present in *Herrerasaurus*, *Liliensternus*, *Dilophosaurus*, and a variety of basal tetanurans, including *Allosaurus* and *Sinraptor*, where it is typically formed almost entirely within the quadrate and the quadratojugal makes just a glancing contact. However, this feature is absent in *Ceratosaurus* and abelisaurids, indicating a secondary loss in this clade. The paraquadrate foramen transmitted neurovasculature between the occiput and the adductor chamber (probably branches of the maxillomandibular vessels; Sedlmayr, 2002). Assuming that the soft-tissue structures were not lost in ceratosaurs, the absence of a foramen raises the question of a derived passage for this neurovascular bundle. The most likely pathway is ventrolateral to the quadrate-quadratojugal contact, as in extant crocodilians (Sedlmayr, 2002).

In most theropods, and indeed most dinosaurs, the quadrate is relatively straight and vertically positioned such that the mandibular joint lies almost directly below the quadrate head (Rauhut, 2003). Quadrate curvature and caudal displacement of the mandibular joint relative to the quadrate head occurs in several basal theropods, including *Herrerasaurus* and various allosauroids (*Monolophosaurus*, *Allosaurus*, *Sinraptor*), as well as in *Ceratosaurus* and abelisauroids. This curvature appears to be somewhat more pronounced in *Majungasaurus* and other abelisauroids (e.g., *Noasaurus*) than in non-abelisaurid theropods (Fig. 2). In a number of other taxa—including spinosaurs, ornithomimosaurs, and various birds—the reverse condition occurs, with the quadrate rostrally inclined such that the jaw joint occurs in front of the quadrate head (Rauhut, 2003).

Overall, the quadrate of *Majungasaurus* closely resembles that of *Ceratosaurus*. Differences include the fossae on the quadratojugal ramus; the fossa on the rostral surface is much more developed in *Ceratosaurus*, whereas the caudal fossa is more developed in *Majungasaurus*. In addition, the medial margin of the quadrate, as viewed caudally, is relatively straight in *Majungasaurus*, whereas it is notably concave in *Ceratosaurus*. The rostral and caudal extensions of the condylar articular surfaces, described above, are also present in other abelisaurids (e.g., *Ilokelesia*, *Carnotaurus*); they are lacking in *Ceratosaurus* (e.g., UMNH VP 5278) and apparently in non-abelisaurid basal theropods generally.

Lower Jaw

General—The lower jaw of *Majungasaurus* mirrors the skull in being relatively broad and U-shaped, the typical abelisaurid condition, rather than narrow and V-shaped as in most other basal theropods (Fig. 1). Much of the external surface, particularly of the dentary, is covered with the same rugose, subcutaneous bone texture present on the skull (Figs. 1, 24). Otherwise, the most notable feature is the hypertrophied external mandibu-

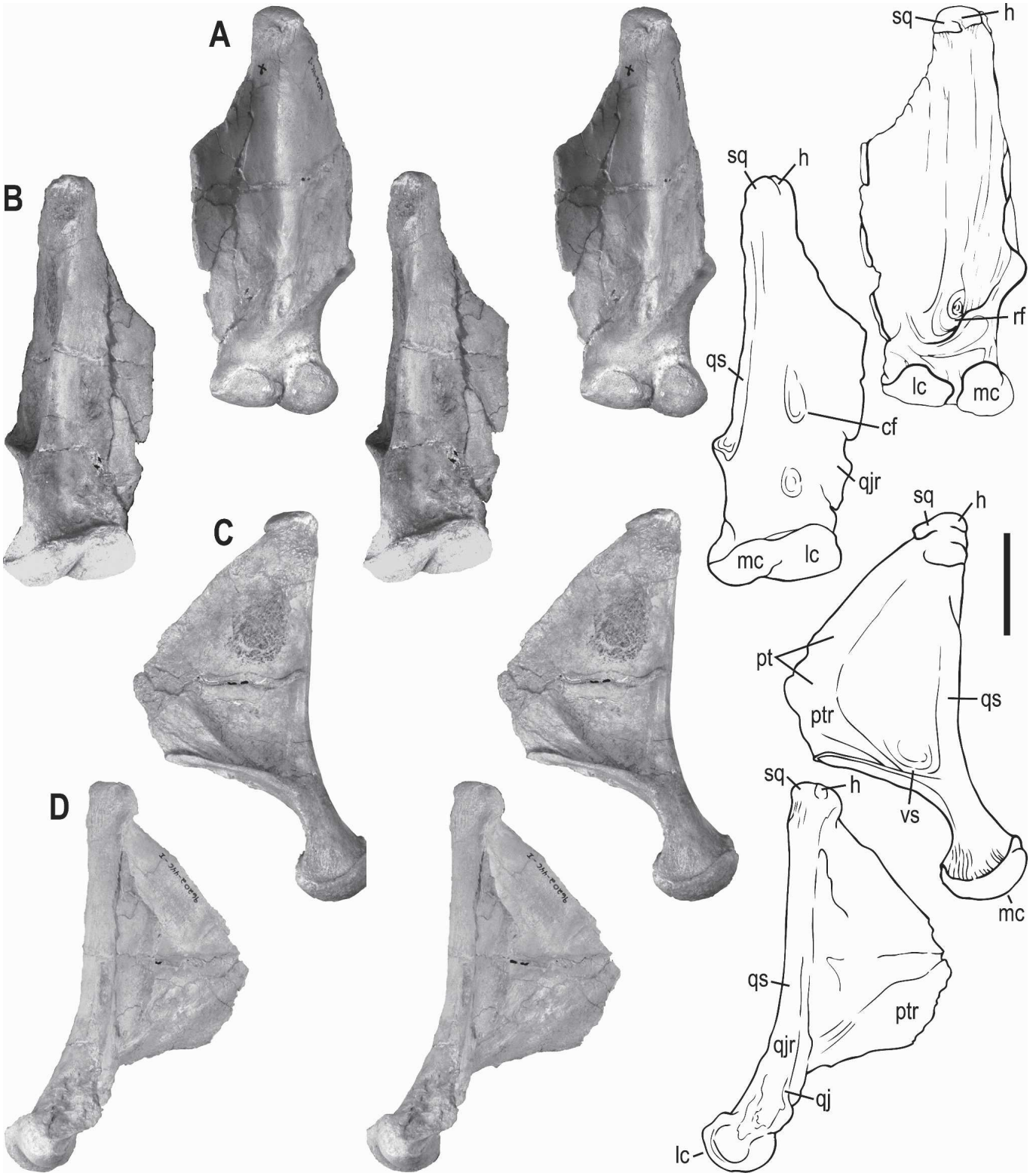

FIGURE 23. Stereopairs of right quadrate of *Majungasaurus crenatissimus* (FMNH PR 2100) in **A**, rostral; **B**, caudal; **C**, medial; and **D**, lateral views. Scale bar equals 5 cm. See Appendix 1 for abbreviations.

lar fenestra—bordered by the dentary, angular, and surangular (Figs. 1, 25)—which is also characteristic of abelisaurids (Fig. 2). As described above for the skull, there is some degree of telescoping evident in the lower jaws. In particular, the dentary and splenial are both foreshortened somewhat relative to non-abelisauroid basal theropods (see below). Also notable is the expanded retroarticular process, which is significantly more elongate than the standard theropod condition. Overall, the con-

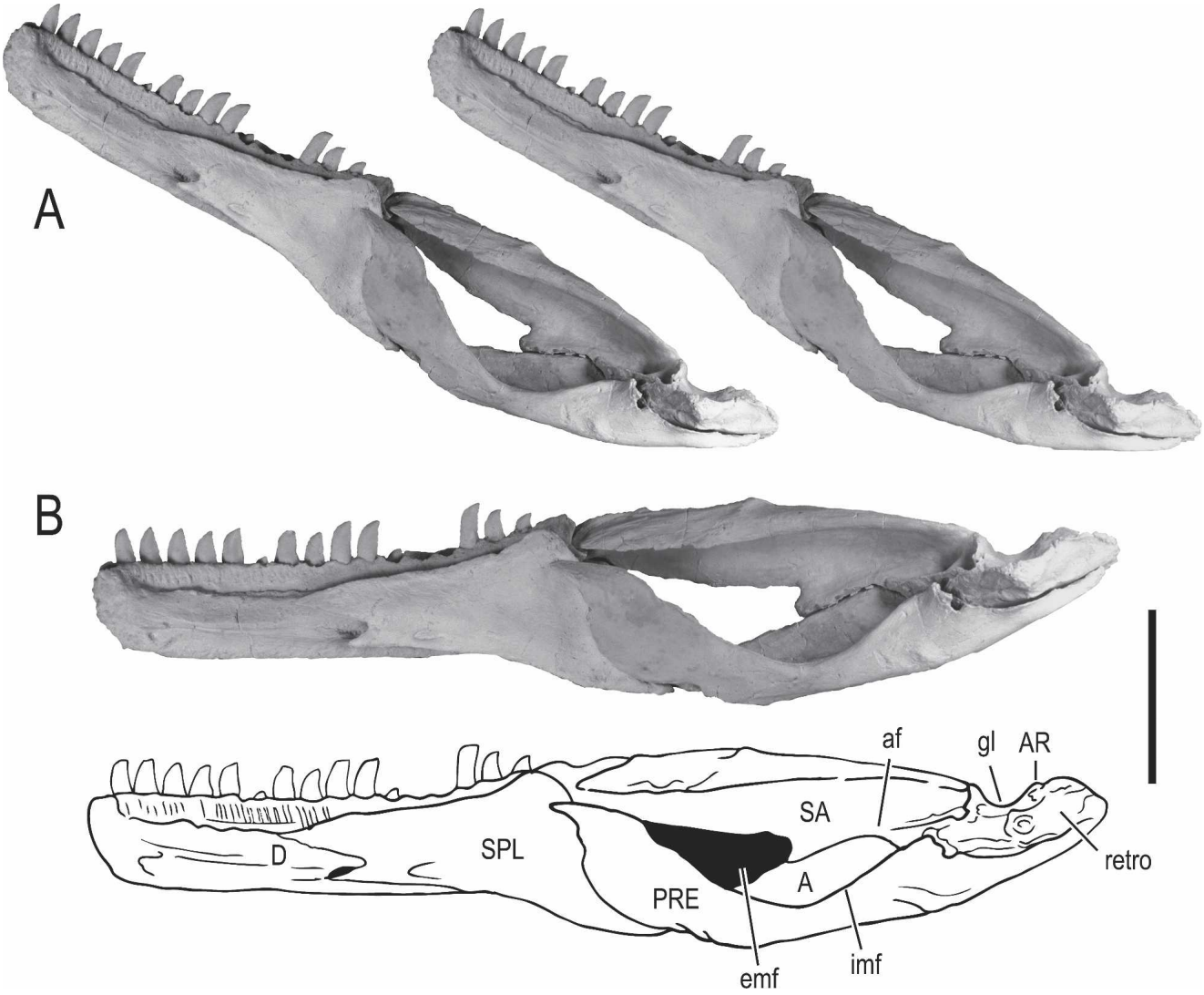

FIGURE 24. Right mandible of *Majungasaurus crenatissimus* (FMNH PR 2100) in medial view. **A**, Stereopairs. **B**, Photograph and interpretive drawing. Scale bar equals 5 cm. See Appendix 1 for abbreviations.

formation of the lower jaws is closely similar to that of the derived abelisaurid *Carnotaurus*, although the ventral margin is somewhat less curved in lateral view than is that of the Argentine taxon (Fig. 2).

The following description is based predominantly on FMNH PR 2100, which preserves nearly complete left and right jaws, lacking only the coronoids (Figs. 1, 24). The other particularly pertinent *Majungasaurus* specimens are MNHN.MAJ 1, the nearly complete right dentary of a subadult individual that comprises the type specimen of *Majungasaurus crenatissimus* and which was described by Lavocat (1955), UA 8709, which includes fragmentary remains of both mandibles, and FMNH PR 2278, which includes most of the post-dentary lower jaw from the left side. It bears noting that detailed comparisons of MNHN.MAJ 1 with the dentary of FMNH PR 2100 revealed no notable differences other than size (MNHN.MAJ 1 being approximately 25% smaller).

Dentary—Complete, well-preserved dentaries are preserved with FMNH PR 2100. Both left and right sides of this specimen possess 17 alveoli, most with erupted and/or unerupted teeth in place. The alveoli, like those of the upper jaws, are subrectangular in cross-section, as in other abelisaurids.

The dentary (Figs. 1, 24–26) contacts the splenial medially, the surangular caudodorsally, and the opposite dentary rostromedially. Viewed dorsally, the dentary is significantly bowed laterally, reflecting the considerable breadth of the lower jaws (Fig. 1J). Viewed laterally, the most notable characteristic is the relative reduction in the post-alveolar portion of the dentary, associated with development of the greatly enlarged external mandibular fenestra. The ventral margin is relatively straight though gently sigmoidal, whereas the dorsal margin is weakly concave.

Laterally, the dentary possesses a pronounced sulcus, with several associated foramina that, as confirmed by CT, lead to neurovascular canals arising from within the adductor fossa/canal and derive from the mandibular (ventral alveolar) nerves and vessels (Fig. 26A). These foramina vary in number and size, but tend to be smallest rostrally and largest caudally. In the midportion of the dentary, the region dorsal to the sulcus is deeper than the corresponding ventral region (deepest at level of tooth position 8). Although other theropods typically possess a serial arrangement of foramina on the lateral surface of the dentary, this sulcus is generally much less pronounced and more dorsally positioned. *Carnotaurus* closely resembles *Majungasaurus* in having a deep, ventrally placed lateral sulcus of the dentary.

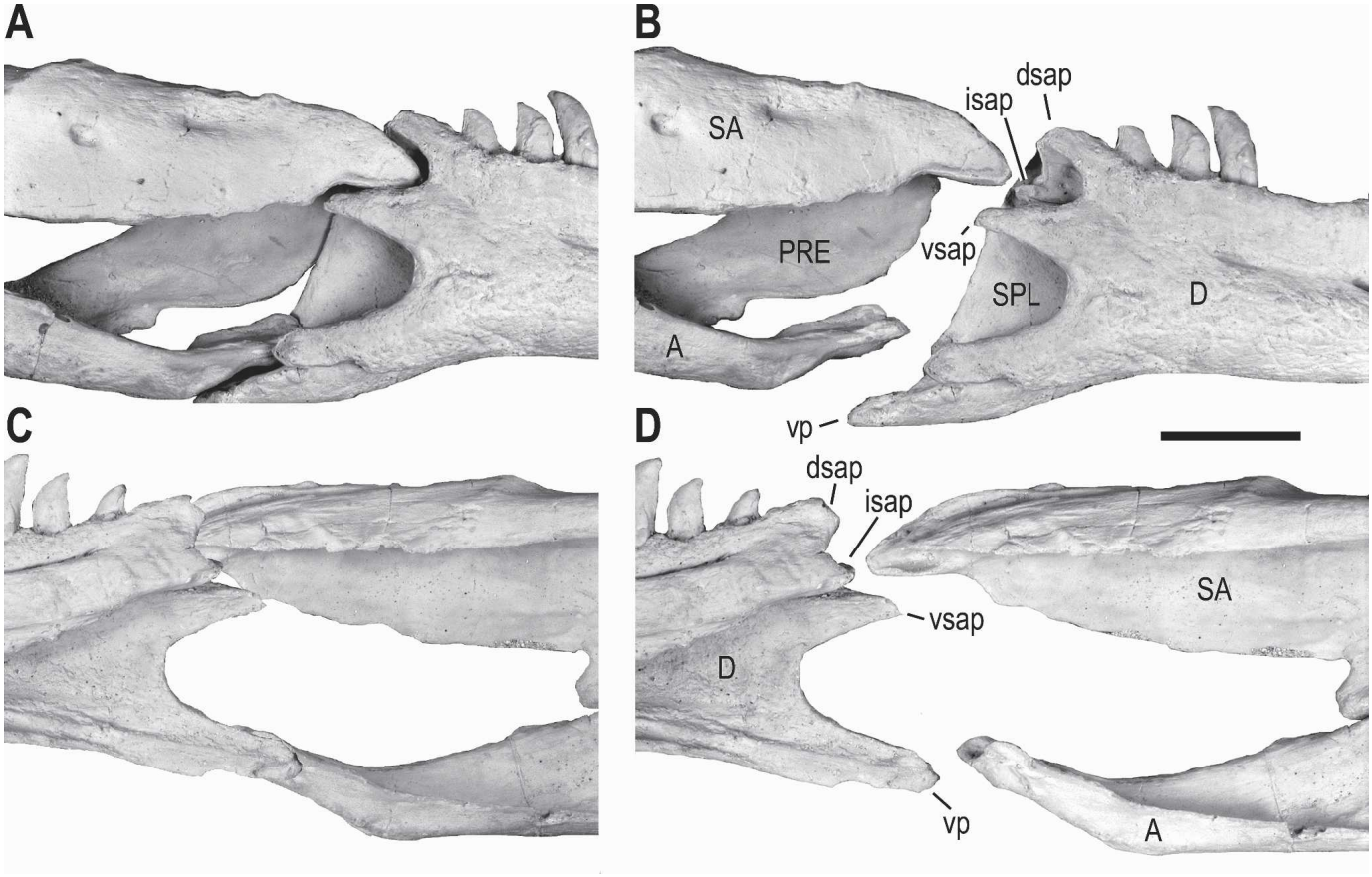

FIGURE 25. Intramandibular region of the lower jaw of *Majungasaurus crenatissimus* (FMNH PR 2100) in the following views: **A**, lateral, with intramandibular joints in articulation; **B**, lateral, disarticulated; **C**, medial, in articulation; and **D**, medial, disarticulated. Splenial and prearticular were removed in **C** & **D** in order to show joint contacts. Scale bar equals 5 cm. See Appendix 1 for abbreviations.

Although the deep sulcus also appears to be present on a dentary from the Lameta abelisaurid collection (GSI-IM K27–550), it is positioned relatively more dorsal, as is typical of other basal theropods.

Ventral to the longitudinal sulcus, the lateral surface of the dentary is covered with a highly rugose surface texture similar to that described above for many of the facial elements, with numerous relatively small foramina, many with associated neurovascular sulci (Fig. 26A). The texture is generally more similar to that of the ventrolateral elements of the skull (e.g., maxilla, jugal, quadratojugal), and has less of the raised, tubercular structure of the dorsal elements (e.g., nasal, frontal, lacrimal). Dorsal to the longitudinal sulcus, the bone texture is relatively smooth except for a series of shallow grooves emanating dorsally from the above-mentioned foramina. Thus the longitudinal sulcus appears to demarcate two soft tissue regimes: a lower, subcutaneous region covered with dermis and epidermis, and an upper alveolar region covered with gingival tissues. The nature of the oral tissues is still in question, but given that this region comes directly in contact with teeth from the upper jaw, it seems probable that the associated region on the dentary would have had some sort of keratinized gingival covering, as in crocodilians.

Caudally, the dentary bears several rearward-projecting processes (Fig. 26). There are three dorsal surangular processes and one ventral angular process, the last being the longest of the four. The three upper processes together form the margin of a distinct fossa that receives the rostral process of the surangular. Of the three surangular processes, the lowermost is the longest, and the upper and lower processes occur lateral to the intermediate process. The ventral process, though elongate, shares an abbreviated and relatively weak contact with the angular, marked by a small, distally positioned concavity. The two lowermost processes contribute to the border of the greatly enlarged external mandibular fenestra. Hypertrophy of this fenestra is largely the result of a reduction in the post-alveolar length of the dentary. In contrast to most basal theropods, the dentary terminates caudally slightly behind the last alveolus, whereas it extends considerably further rearward in most taxa, including the closely allied *Ceratosaurus*.

The enlarged external mandibular fenestra and pronounced surangular fossa of the dentary are characteristic of abelisauroids (e.g., *Carnotaurus*, Bonaparte et al., 1990; Fig. 2; *Masiakasaurus*; Sampson et al., 2001; Carrano et al., 2002). In contrast, the dentary of other theropods typically extends further caudally below the surangular contact, resulting in a smaller external mandibular fenestra. There are minor taxonomic variations in this pattern within abelisauroids, however. In *Masiakasaurus* (UA 8680), for example, of the three surangular processes, the intermediate, medially positioned one is the longest, versus *Majungasaurus* in which the ventralmost of the three is longest.

Rostromedially, the dentary bears a weak symphysis with its opposite (Fig. 26B), as is typical of theropods. Exceptions to this pattern among basal theropods include the abelisauroid *Masiakasaurus* and spinosaurids, in which the mandibular symphysis is elongate. Medially, the splenial covers more than one half the length of the dentary (Figs. 1B, I, 24). The caudal two-thirds of the ventral contact for the splenial consist of a strong longitudinal ridge bordered by distinct grooves, which articulate with a corresponding complex of groove and ridges on the splenial (see

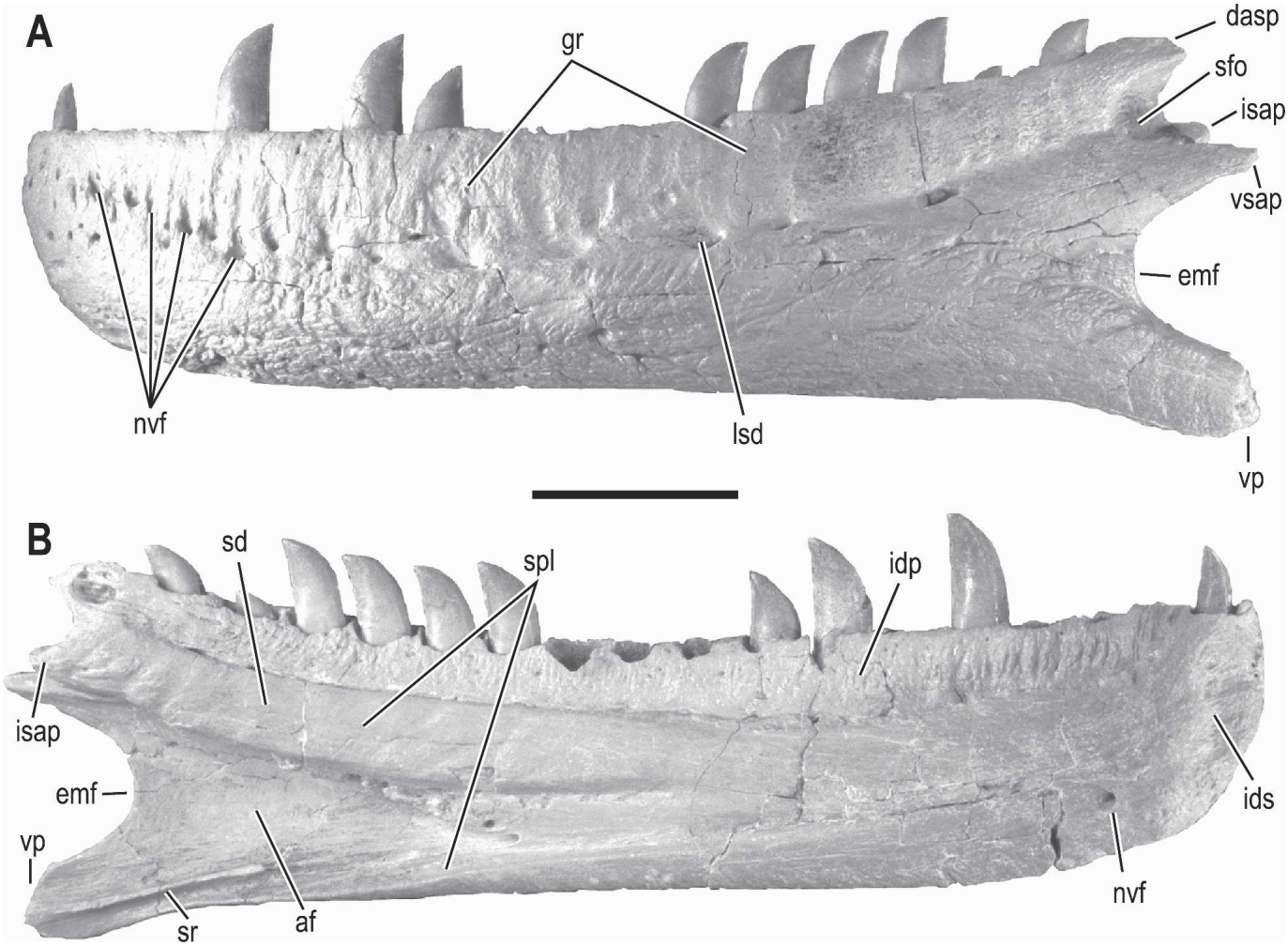

FIGURE 26. Left dentary of *Majungasaurus crenatissimus* (FMNH PR 2100) in **A**, lateral; and **B**, medial views. Scale bar equals 5 cm. See Appendix 1 for abbreviations.

below). The splenial ridge of the dentary extends from the 12th alveolus to the distal end of the angular process.

The interdental plates closely resemble those of the maxilla, being fused and covered with a rugose texture composed of vertically oriented ridges and grooves (Fig. 26B). The dorsal margin of the fused plates is horizontal, except caudally where there is a weak concavity associated with each alveolus, forming a series of shallow notches. This contrasts with the condition in many other basal theropods, in which the margin is more deeply notched (e.g., *Allosaurus*), or in which consecutive plates are separate (or almost separate) throughout their lengths (e.g., *Megalosaurus, Torvosaurus*, *Sinraptor*). The interdental plates are relatively broad throughout their length, though deepest (tallest) at the level of the sixth tooth position and narrowest at the front and rear of the element.

The highly rugose subcutaneous surface texture extends over the lower portion of the dentary onto the ventral margin of the internal surface, so as to be visible in medial view (Fig. 26B). As in many theropod taxa, a large rostral foramen pierces the dentary just caudal to the symphysis. This foramen is confluent with a shallow sulcus extending forward from the splenial contact surface, indicating the presence of neurovasculature passing within the adductor fossa on the medial side and exiting rostral to the splenial to enter the body of the dentary just inside the symphysis.

Supradentary (+ Coronoid?)—Several basal theropods (e.g., *Herrerasaurus*, *Dilophosaurus*, *Allosaurus*, *Monolophosaurus*), as well as basal sauropodomorphs, possess a thin, splint-like element covering the medial (lingual) surface of the interdental plates of the lower jaw throughout most of their length, and a pair of such elements was found with both FMNH PR 2100 and UA 8709 (Fig. 27). This bone has generally been referred to as the supradentary (Osborn, 1912; Gilmore, 1920; Madsen, 1976a; Zhao and Currie, 1994; Currie, 1995; Madsen and Welles, 2000). A valid question, however, relates to whether this bone actually should be regarded as a part of the coronoid (otherwise absent in known specimens of *Majungasaurus*, although a fragment may be present in UA 8709). The evolutionary history of the 'coronoid family' of bones is complicated, confusing, and beyond the scope here, but a variety of amniotes have multiple 'coronoids,' many of which have the appearance of the theropod supradentary (Romer, 1956). Hurum and Currie (2000) noted that the coronoid and supradentary bones were a single element in tyrannosaurids. Moreover, Currie (2003) suggested that perhaps in no theropod could a suture or line of fusion be demonstrated between these bones. Indeed, even more broadly, well preserved specimens of some ornithischians, such as the basal thyreophoran *Scelidosaurus* (BMNH R1111), exhibit what amounts to the tyrannosaurid condition, viz. a completely continuous coronoid-supradentary element. We will continue to use the terms supra-

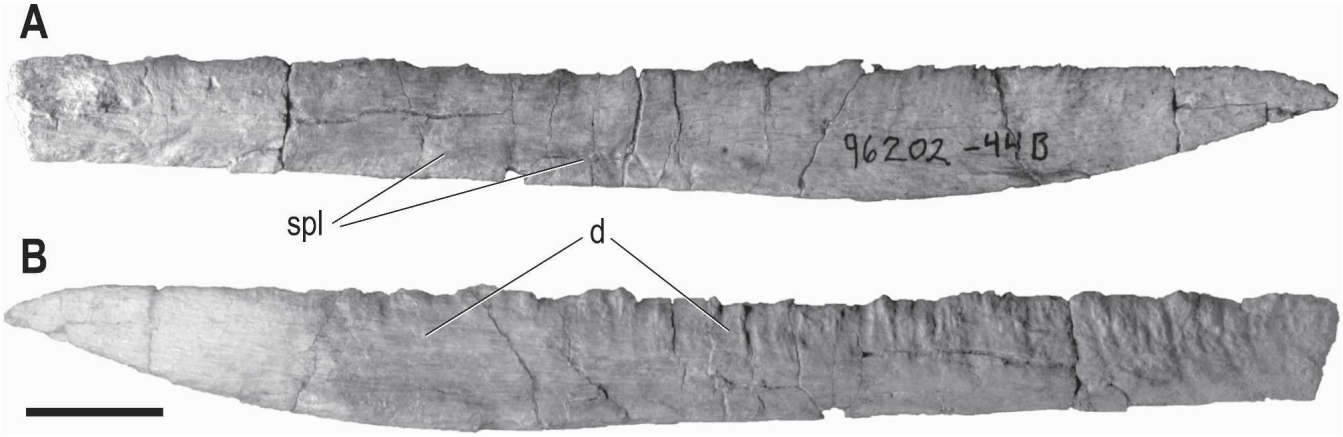

FIGURE 27. Left supradentary of *Majungasaurus crenatissimus* (FMNH PR 2100) in **A**, medial (lingual); and **B**, lateral (labial) views. Scale bar equals 2 cm. See Appendix 1 for abbreviations.

dentary and coronoid, but it is hoped the above discussion will raise the profile of this issue.

The supradentaries of *Majungasaurus* were recovered as isolated elements missing their caudal extremities in FMNH PR 2100, and are preserved in articulation in UA 8709. The supradentary in UA 8709 is interposed between the splenial and dentary caudally and progressively emerges more rostrally as the splenial pinches out. The dorsal margin is more or less straight and in line with the toothrow. The ventral margin, however, tapers rostrally, rising to a point. The supradentary does not reach the rostral end of the dentary, and, in fact, the rostralmost interdental plates are not covered by the supradentary. Although surprising, this assessment is supported by the in situ position of the element in UA 8709 and, additionally, by the curvature of the isolated supradentaries of FMNH PR 2100, which, although bowed, are not curved enough to cover the rostralmost interdental plates. The supradentary has its greatest dorsoventral height rostrally and becomes narrower (shorter) caudally. The medial surface is generally smooth (being covered by oral epithelium) although there is an elongate fossa ventrally for its articulation with the dorsolateral margin of the splenial. The lateral surface is characterized by a series of vertical ridges and grooves, essentially matching the texture of the adjacent fused interdental plates of the dentary.

As noted above, there is a fragment of bone on the left side of UA 8709, between the prearticular and surangular that may well represent the coronoid element. It is in line with but discontinuous with the supradentary in front, and so it is impossible to tell whether the elements were ever united. Given that this juncture crosses the intramandibular joint in not only *Majungasaurus* but theropods generally, it is perhaps no surprise that evidence of their continuity is so patchy. Despite the exceptional preservation and completeness of FMNH PR 2100, no coronoid bone was recovered. There is, however, a rostrodorsal slot on the surangular roughly corresponding to the coronoid contact surface described for *Allosaurus* (Madsen, 1976b) and *Sinraptor* (Currie and Zhao, 1994a). A somewhat rugose region on the rostrodorsal limit of the prearticular may represent the coronoid contact as well. It thus seems likely that a coronoid element was present in *Majungasaurus*. In support of this view, Bonaparte and colleagues (1990) describe the presence of a small coronoid in the abelisaurid *Carnotaurus*. Although not described by Bonaparte and colleagues (1990), a supradentary is preserved with the left lower jaw of *Carnotaurus*, and likewise has been identified in *Ceratosaurus* (Madsen and Welles, 2000) and *Genyodectes* (Rauhut, 2004b).

Splenial—The splenial (Figs. 1, 24, 25, 28) is a relatively flat, triangular element that covers much of the dentary on the lingual side and comprises most of the medial wall of the adductor canal. The splenial contacts the dentary laterally, the supradentary dorsolaterally, the angular caudoventrally, and the prearticular caudally. Overall, this element is thin and sheet-like, as in other theropods. The exception to this morphology occurs in the ventral portion, which progressively thickens caudally, terminating in a distinct platform that articulates with the angular. Rostrally, the splenial divides into two prongs separated by a shallow notch (Fig. 28). The notch undoubtedly provided passage of neurovasculature exiting the adductor canal to supply the rostral portion of the mandible. A rostroventrally positioned, completely enclosed splenial foramen (mylohyoid and/or Meckelian foramen of some authors) is present, confluent with a deep, lateral sulcus on the splenial. A pair of robust, ventromedially positioned, and longitudinally running ridges and grooves articulates with a corresponding ridge-groove complex on the dentary. Laterally (labially) in the dorsal portion, the splenial has a parallel series of pronounced and angled sulci that correspond to similar markings on the dentary (Fig. 28B); these features likely represent the osteological traces of neurovasculature exiting the adductor canal between the dentary and splenial to supply gingival tissues adhering to the interdental plates. The left splenial of FMNH PR 2100 has a small but distinct foramen in its mid-region, with associated sulci that parallel those noted above. This feature is absent on the right side.

The robust angular process of the splenial extends caudally to form a short, broad contact along its dorsum for the angular. In contrast to other basal theropods, this process projects well behind and ventral to the dentary, so as to be distinctly visible in lateral view (Fig. 1A). Although the splenial is visible laterally in other non-tetanuran basal theropods (e.g., *Herrerasaurus*, *Ceratosaurus*), and independently in dromaeosaurs (Currie, 1995), this hypertrophy of the angular process in *Majungasaurus* appears to be independently derived and exaggerated. Much of the thickened ventral region is covered with the same rugose texture present externally on other skull elements, indicating that this portion of the splenial was subcutaneous.

The splenial of most basal tetanurans (e.g., *Syntarsus*, *Allosaurus*, *Baryonyx*) tends to be a rather simple, flattened, triangular element with only a minor degree of thickening along the ventral margin. By comparison, the splenial of *Majungasaurus* most closely resembles that of *Carnotaurus* and *Ceratosaurus*, in particular the former. All three ceratosaur taxa possess two rostral prongs separated by a notch. In basal tetanurans with well-

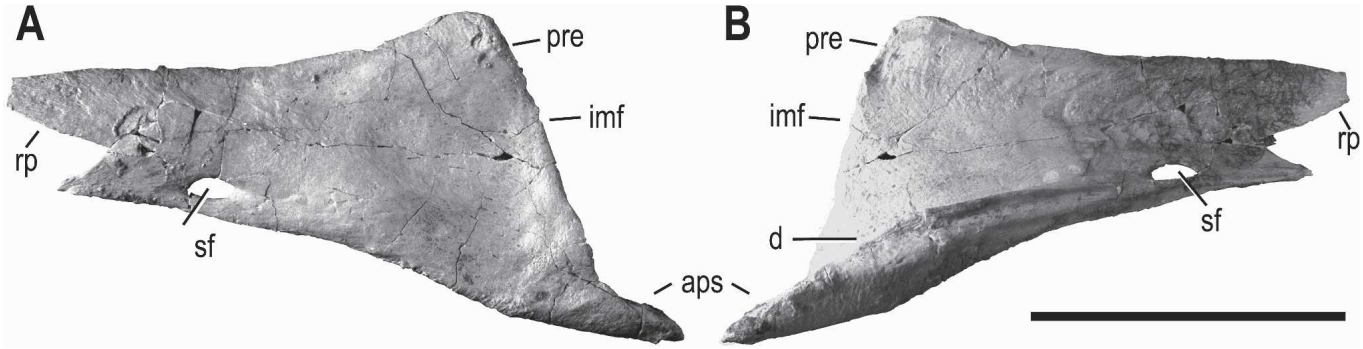

FIGURE 28. Right splenial of *Majungasaurus crenatissimus* (FMNH PR 2100) in **A**, medial; and **B**, lateral views. Rostralmost (pointed) portion of rostral process is absent on this specimen. Scale bar equals 5 cm. See Appendix 1 for abbreviations.

preserved splenials (e.g., *Syntarsus*, *Allosaurus*, *Baryonyx*), the dorsal of the two rostral prongs is absent, and the caudodorsal margin is lower, longer, and significantly more concave. The concave caudal margin is exaggerated in some basal tetanuran taxa (e.g., *Allosaurus*, Madsen, 1976a; *Sinraptor*, Currie and Zhao, 1994a; *Monolophosaurus*, Zhao and Currie, 1994; *Poekilopleuron*?, Allain, 2002), forming a distinct notch that effectively enlarges the internal mandibular fenestra. A caudally positioned apex is also present in *Carnotaurus* and *Ceratosaurus nasicornis* (USNM 4735), though it is more centrally positioned in the abelisauroid ceratosaur *Masiakasaurus* and the ceratosaur *Ceratosaurus dentisulcatus* (UMNH VP 5278), suggesting that this character is highly variable. The rostrocaudally elongate splenial foramen is similarly shaped and positioned in *Ceratosaurus*, *Carnotaurus*, and *Majungasaurus*. It is more centrally positioned in *Baryonyx*, reduced to a marginal notch in *Allosaurus* and *Monolophosaurus* (Zhao and Currie, 1994), and apparently absent in the coelophysoids *Dilophosaurus* and *Coelophysis*, as well as the abelisauroid *Masiakasaurus. Majungasaurus* and *Carnotaurus* are derived in having a straight, high-angled and relatively short caudodorsal margin, giving the splenial a more compact appearance. This conformation, resulting in an abbreviated and tall appearance, is another example of telescoping of skull elements in these derived abelisaurids.

The ceratosaurs *Carnotaurus*, *Majungasaurus*, and *Ceratosaurus* also share a laterally broadened, trough-shaped angular process that underlaps the angular. This feature appears to be primitive for theropods, since it is also present in *Herrerasaurus* (Sereno and Novas, 1993) and coelophysoids. In tetanurans generally, the splenial is secondarily reduced in thickness caudoventrally, forming a thin sheet that, with the dentary, sandwiches the equally thin angular and results in a mediolaterally restricted adductor fossa. Although the angular process is more elongate and pointed in *Ceratosaurus* (USNM 4735, UMNH VP 5278) than in *Majungasaurus*, it does not extend significantly caudal to the dentary as it does in the Malagasy taxon, due to secondary shortening of the post-alveolar dentary. Moreover, the ventralmost dentary contact of the splenial is smooth-walled and simple in *Ceratosaurus*, whereas *Majungasaurus* possesses the complex ridge-groove articulation described above. *Baryonyx* (BMNH R9951) also has the ridge and groove articulation between splenial and dentary, though different from that in *Majungasaurus* and apparently derived independently in this spinosaurid.

Surangular—As in other theropods, the surangular is an elongate, robust element forming the upper portion of the postdentary lower jaw. It contacts the dentary rostrally, the angular caudolaterally, and the articular and prearticular caudomedially (Figs. 1, 24, 25, 29, 32). The dorsal margin is thick and rounded, with an obliquely running ridge that marks the attachment of the M. adductor mandibulae externus superficialis. There is a pronounced lateral shelf over the caudal half of the element, with a well-defined muscular fossa beneath. Along the dorsum of this shelf, immediately lateral to the articular bone, is a small foramen. Rostrally, the surangular tapers to a narrow, blunt process that slots into the surangular fossa of the dentary. On the medial side of this process is a distinct pocket that receives a process from the dentary (Fig. 25). Caudally, the surangular abuts the lateral side of the articular and terminates in a thin lamina that extends rearward to the limit of the retroarticular process (Fig. 32).

A ventrally projecting prong, the angular process of the surangular, descends at an acute angle approximately at the midpoint of the element, marking the caudodorsal margin of an enlarged external mandibular fenestra (Fig. 29). Although not fully preserved on either the left or right surangular of FMNH PR 2100, this process is complete on FMNH PR 2278. The angular process tapers abruptly to a gracile point that covers a significant portion of the angular, thereby limiting the contribution of the latter element to the external mandibular fenestra. Its extent is also evidenced by a well-defined facet on the dorsum of the angular. The elongate, pointed angular process appears to be autapomorphic for *Majungasaurus*, associated with dramatic enlargement of the external mandibular fenestra in this taxon. The dorsal rim of this fenestra is formed by the surangular rostral to this process. The roughened external margin of the rim likely served as an attachment site for the intramandibularis portion of the M. adductor mandibulae internus. On the ventral surface, caudal to the angular process, is an extensive squamous suture for the angular, as in other theropods.

Internally, the surangular forms the dorsal portion of a large internal concavity, the adductor fossa (Meckelian fossa of some authors), which served as the attachment site of the intramandibularis portion of the M. adductor mandibulae internus (Fig. 29B). A short, relatively thick medial lamina of the surangular forms the medial wall of this adductor fossa. As in other theropods, a robust, triangular process of the surangular, here termed the articular process, projects medially to contact the articular, prearticular, and surangular. Most of this process forms a strong, angled contact with the articular. This process also forms about one-third of the glenoid. Immediately in front of the glenoid, the articular process forms a roughened, crescentic contact for the prearticular. Medial and slightly ventral to this contact surface is a deep fossa or pocket that makes up the caudalmost portion of the adductor fossa. The large caudal surangular foramen passes through the surangular on the lateral side of this fossa, and several smaller foramina occur at its base.

A small, rostrodorsally located foramen on the surangular (Fig. 29A) is likely homologous with the anterior surangular foramen described by Madsen (1976a) for *Allosaurus* and by Currie and Zhao (1994a) for *Sinraptor*. As in the latter taxon,

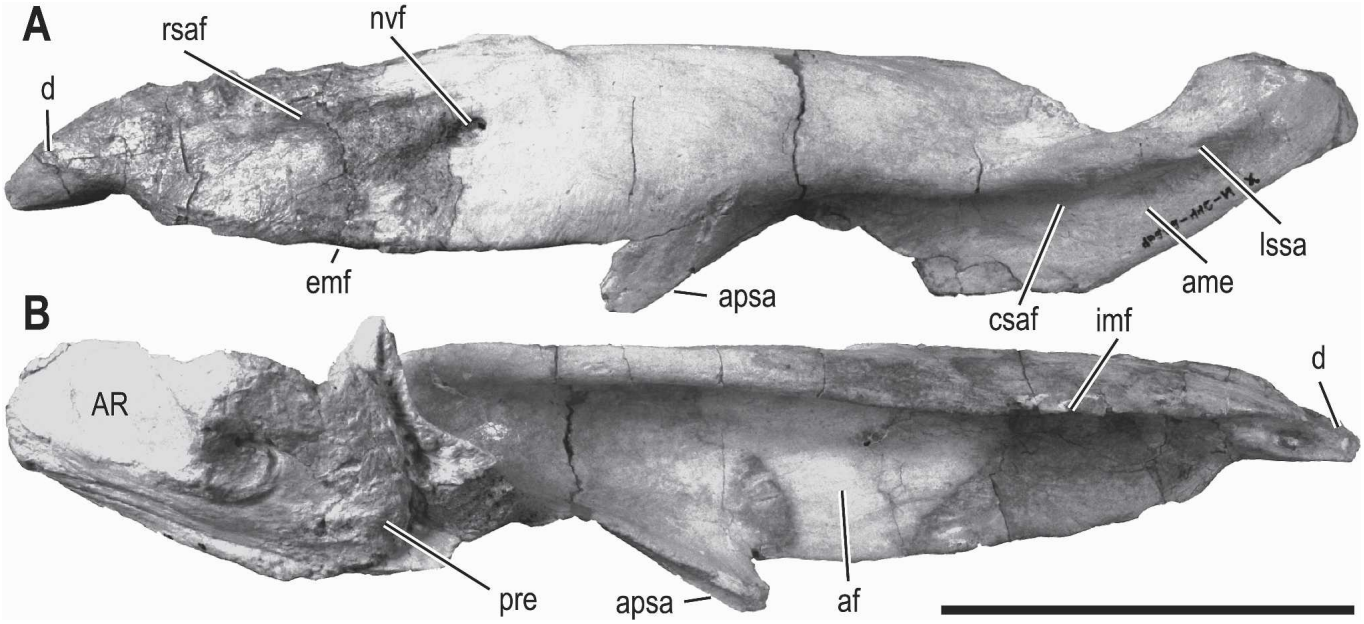

FIGURE 29. Left surangular and articular of *Majungasaurus crenatissimus* (FMNH PR 2100) in **A**, lateral; and **B**, medial views. Scale bar equals 5 cm. See Appendix 1 for abbreviations.

this foramen occurs virtually on the dorsum of the surangular and is associated with a rostrally directed sulcus that extends to the surangular-dentary contact. In *Majungasaurus*, the rostral surangular foramen is positioned relatively more forward and the associated sulcus is less well defined. The internal side of this foramen is visible along the dorsal surface of the adductor fossa, just caudal to the exterior opening. As in other theropods, the surangular of *Majungasaurus* possesses a relatively large caudal (posterior) surangular foramen located just ventral to the overhanging lateral shelf. A third, large foramen, not described in other theropods, is present on the lateral portion of the surangular of FMNH PR 2100 just rostral to the ventral projection. It is the largest of the surangular foramina in *Majungasaurus*, occurring within a pronounced recess, and lacks the rostrally-directed groove. This intermediate-positioned accessory foramen is paired in another surangular of *Majungasaurus* (FMNH PR 2278). The derived arrangement of rostral foramina is also present in *Carnotaurus*, whereas *Ceratosaurus* (USNM 4735) exhibits the *Allosaurus*/*Sinraptor* condition, lacking the accessory foramen. The rostral foramina of the surangular likely served as passages for cutaneous branches of the mandibular nerve (Oelrich, 1956).

Compared to the surangular of *Carnotaurus*, that of *Majungasaurus* is less derived in several respects. In particular, the dorsal margin is weakly convex in the Malagasy taxon (and in other theropods), whereas it is strongly convex in *Carnotaurus*. Also, the portion of the element rostral to the ventral prong is highly abbreviated in *Carnotaurus*. The surangular of *Majungasaurus* is notably broader than in other basal theropods, perhaps associated with an increased volume of jaw musculature housed within the adductor chamber.

Angular—The angular (Figs. 1, 24, 25, 30) is an elongate element, plate-like dorsally and thickened rostroventrally. It contacts the splenial rostrally, the prearticular dorsomedially, and the surangular caudodorsally. It also forms the floor of the relatively broad adductor fossa. The external surface is covered with a roughened subcutaneous texture similar to that of the dentary and many of the *Majungasaurus* skull elements. In this case, however, the texture is somewhat less distinct and more granular in nature (FMNH PR 2100), with evidence of vascular traces in the central portion. The textural exception on the external surface is the caudodorsal region, which has a smooth, shallow concavity confluent with the ventral concavity on the surangular, presumably for attachment of jaw musculature.

Notably, in contrast to other theropods, the angular apparently does not contact the dentary. Articulation between the splenial and dentary, and between the angular and splenial, can be defined quite precisely, and they show a distinct gap between the angular and dentary (Fig. 25). This conformation appears to be due once again to the dramatic reduction of the post-alveolar dentary. In contrast, the splenial shares a robust contact with the angular. A broad, well-defined, rostroventrally-facing contact surface on the angular articulates with a corresponding platform on the splenial. Other than the upturned splenial process, the ventral margin of the angular is relatively straight. This is in contrast to the continuously curved dorsal margin, which comprises a portion of the external mandibular fenestra.

Medially, a pronounced ridge contributes to an elongate contact with the prearticular that spans virtually the full length of the angular (Fig. 30). Together, these two elements comprise the trough-like floor and medial wall of the caudal part of the adductor fossa. This trough is interrupted rostrally by a thickening of the angular associated with the splenial process. Caudally, the element becomes increasingly sheet-like, overlapping the surangular laterally and extending behind the caudal surangular foramen. In addition, the surangular overhangs the angular, forming an elongate dorsal contact between the two elements. Specifically, a shallow, inverted trough on the caudoventral margin of the angular process of the surangular receives a rounded caudodorsal margin of the angular. The surangular tops more than half of the angular's total length. In contrast to articulations at the rostral end of the angular, the broadly overlapping contact with the surangular, as well as the complex contact with the prearticular (see below), makes it difficult to envision significant movement along the angular-surangular contact.

The angular of most basal theropods resembles that of *Majungasaurus* in having a relatively straight ventral margin. The principle exceptions occur among basal tetanurans (e.g., *Allosaurus*, *Sinraptor*, *Acrocanthosaurus*), which tend toward a continuously and distinctly curved ventral margin. The conformation of the

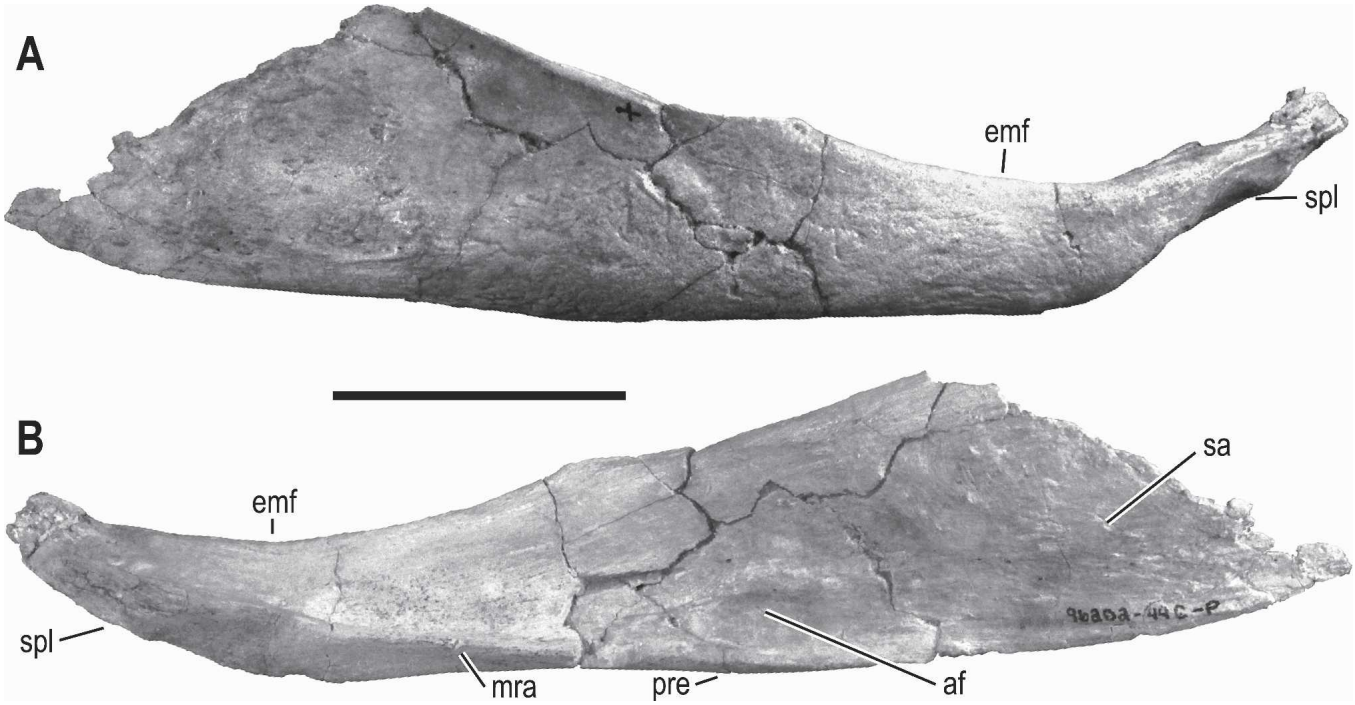

FIGURE 30. Right angular of *Majungasaurus crenatissimus* (FMNH PR 2100) in **A**, lateral; and **B**, medial views. Scale bar equals 5 cm. See Appendix 1 for abbreviations.

angular-dentary contact is unclear in *Carnotaurus*, but appears to closely mimic that of *Majungasaurus*. In contrast, *Ceratosaurus* and basal tetanurans such as *Allosaurus* are characterized by a much more extensive contact between the angular and dentary, largely because the dentary extends further caudal in these taxa. In the latter taxa, the angular extends virtually to the rostral limit of the external mandibular fenestra, whereas it terminates well behind this point in *Majungasaurus*. Like *Majungasaurus*, the angular of *Carnotaurus* extends caudally behind the caudal surangular foramen. This conformation is present in certain other basal theropods, including *Herrerasaurus* and *Allosaurus*, whereas in most taxa it terminates in front of or at the same level as this opening (e.g., *Acrocanthosaurus*, *Sinraptor*, *Ceratosaurus*).

Prearticular—The prearticular is a thin, elongate element, almost boomerang-like in overall shape, with expanded ends and a dorsoventrally constricted mid-portion (Figs. 1, 24, 25, 31). It contacts the splenial rostrally, the angular ventrally, the articular and surangular caudally, and (presumably) the coronoid rostrodorsally. The dorsal margin of the prearticular forms the lower border of the internal mandibular fenestra. Ventrally, a subtle but distinct contact surface for the angular extends more than half the length of the prearticular. This contact is weakly sinusoidal and somewhat complex; rostrally, a thin flange of the prearticular wraps around the lateral side of the angular whereas this conformation is reversed caudally, with the prearticular extending around the medial side of the angular. Laterally, a deep and robust groove in the central region of the prearticular represents most of this element's contribution to the adductor fossa (Fig. 31B). The rostral limit of the angular contact is marked by a weak notch along the ventral border. From this point the element thins to approximately 2 mm and hooks dorsally, terminating in a rostrally directed hook that likely contacted the coronoid. Caudally, the prearticular forks into articular and surangular processes. Caudoventrally, the thickened central portion thins to become the articular process, which underlies the articular and shares an extensive lateral contact with the surangular. The articular process is triangular in cross-section, due to a prominent ventral ridge running its length. As in theropods generally, the prearticular extends rearward virtually to the caudal limit of the retroarticular process. Caudodorsally, the prearticular terminates in an expanded surangular process that sutures with the crescent-shaped contact on the articular process of the surangular. The dorsalmost extent of the surangular process forms the medial wall of the glenoid.

There is considerable variation in the nature of contacts between the prearticular and surrounding elements. The contact for the angular is relatively smooth. The articular contact is somewhat more rugose, with a single low ridge fitting into a corresponding fossa on the articular, whereas that for the surangular (on the surangular process) is more rugose and convoluted. Currie and Zhao (1994a) described a similar pattern in *Sinraptor*.

The prearticular of theropods is not extensively described in the literature. Nonetheless, based on available comparisons, the prearticular of *Majungasaurus* closely resembles that of basal theropods generally, with a thin rostrodorsal process, extensive angular contact, and caudal processes for contacting the articular and surangular. The rostral limit of the angular contact is similarly marked in *Sinraptor* by a weak notch, whereas *Allosaurus* possesses a deep notch at this position. There is some variation in the shape of the rostrodorsal portion. In most basal theropods, this process is rounded and does not taper to a distinct point; it does taper to a point, however, in *Eoraptor* and apparently in *Carnotaurus*. This process is also much more developed and elongate in *Eoraptor* than in other theropods.

Articular—The diagonally positioned articular is a deep, robust element that contacts the prearticular ventrally and the surangular laterally, the latter being a strong interdigitating suture (Figs. 1J, 24, 32). The articular comprises more than half of the glenoid, including the interglenoid ridge and the bulk of the medial glenoid. It also forms a robust retroarticular process projecting caudally from the glenoid, for attachment of the jaw-opening M. depressor mandibulae. All of these characteristics are common to basal theropods generally. The most distinctive

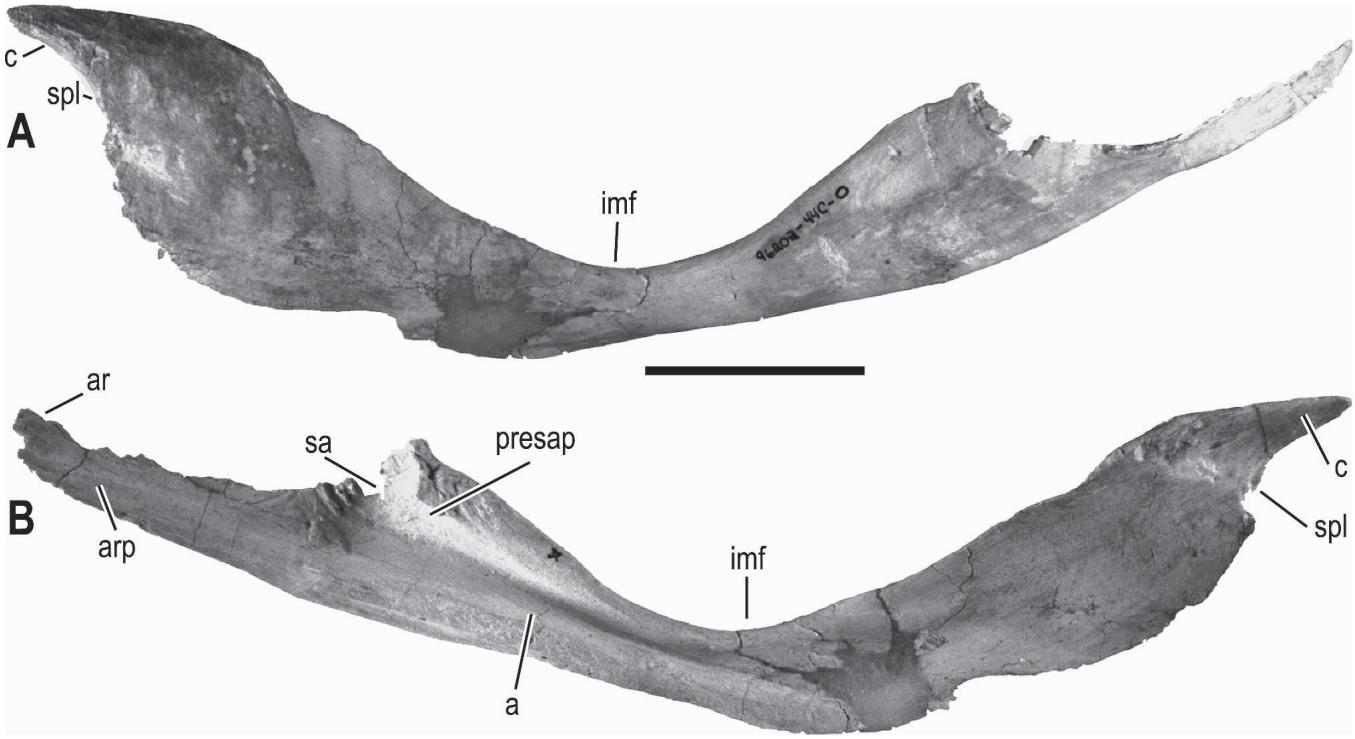

FIGURE 31. Right prearticular of *Majungasaurus crenatissimus* (FMNH PR 2100) in **A**, medial; and **B**, lateral views. Scale bar equals 5 cm. See Appendix 1 for abbreviations.

feature of the articular in *Majungasaurus* is an elongate retroarticular process housing a deep, circular retroarticular fossa. The floor of this fossa is pierced by numerous tiny foramina; the fossa walls are lowest rostrally and caudally and highest medially and laterally. Viewed from above, the articular has almost a dumbbell shape, with the medial glenoid and the retroarticular fossa making up the two ends and separated by a constriction on the medial side. The retroarticular process terminates caudally in a well developed, blunt tubercle. Also distinctive in *Majungasaurus* is a tall rostral wall of the glenoid, comprised largely of the

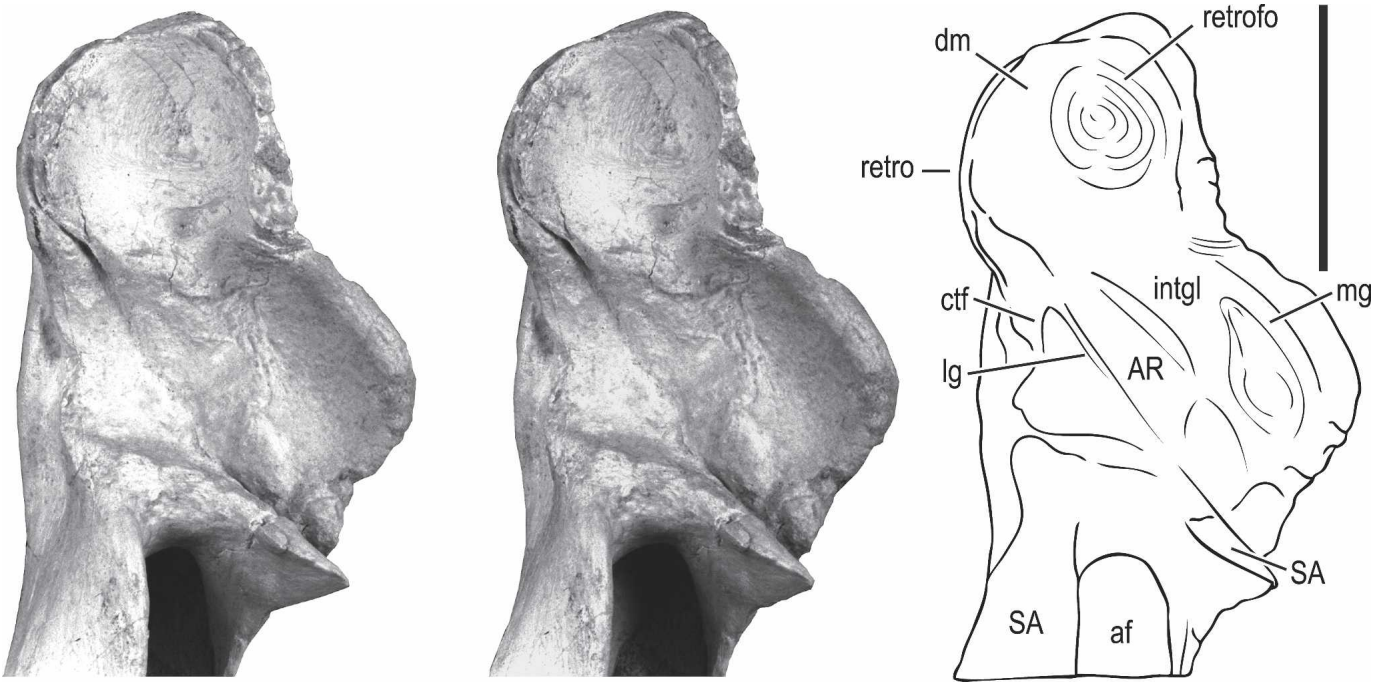

FIGURE 32. Stereopairs of articular region of left lower jaw of *Majungasaurus crenatissimus* (FMNH PR 2100) in dorsal view. Scale bar equals 5 cm. See Appendix 1 for abbreviations.

surangular process of the prearticular. This morphology is best seen in FMNH PR 2278, in which the prearticular is fused to the articular. The margin is notably higher than any other portion of the glenoid, approaching the dorsal limit of the surangular.

The retroarticular region of *Carnotaurus* closely resembles that of *Majungasaurus*, being elongate with a deep, circular fossa. In general, the retroarticular region of theropods (e.g., most allosaurids, tyrannosaurids, dromaeosaurids) tends to be relatively short. Among basalmost theropods, *Herrerasaurus* has an abbreviated, caudally facing retroarticular process whereas that of *Eoraptor* more closely resembles the abelisaurid condition, with a circular, dorsally directed retroarticular fossa. An elongate retroarticular process is present in *Sinraptor* (Currie and Zhao, 1994a), but the fossa is more rectangular than circular as viewed dorsally. Currie and Carpenter (2000) also reported an elongate, though medially oriented, retroarticular process in *Acrocanthosaurus*.

Dentition

A detailed description of the dentition of *Majungasaurus* is presented in Smith (this volume).

DISCUSSION

Mineralization of Cephalic Soft Tissues and Its Impact on Skull Form

Majungasaurus possesses a remarkably gnarled skull in the sense that it bears, among theropods at least, an unmatched array of bumps, grooves, tubercles, and foramina that generally give its surface a rugose, sculptured appearance. The details and patterns of the rugosity were outlined above in the descriptive sections for each element. As noted previously, the apparent distinctiveness of much of this rugose external bone texture may be at least partially the result of remarkable preservation rather than taxonomic uniqueness. Certainly such rugosity characterizes not just *Majungasaurus* but all abelisaurids to varying extents, and is also present in carcharodontosaurids. Nonetheless, this morphology is clearly apomorphic in comparison to immediate outgroups such as the smooth-skulled *Ceratosaurus*, and thus requires explanation. This highly sculptured morphology results from the induction of mineralization processes associated with specializations in the overlying dermis, such that the mineralized tissue comprising the rough surface texture represents mineralization of the bone's periosteum, overlying dermal fibers, or some combination of the two (Hieronymus and Witmer, 2003, 2004, unpubl. data). Technically, this mineralization would fall in the category of metaplastic ossification (Francillon-Vieillot et al., 1991). Such surface rugosity almost certainly indicates that the normal potential space between skin and bone has been obliterated, and that the integument is essentially fused to the skull bones in these areas.

The terms 'rugosity' and 'sculpture' do not adequately capture the varieties of surface textures throughout the skull. For example, the dorsal roofing elements (e.g., frontal, nasal, nasal process of the premaxilla) tend to have a more projecting, tuberculate, often cauliflower-like texture that mixes tangential vascular grooves and canals with more normal (i.e., perpendicular to the bone's surface) canals. The projecting tubercles often coalesce into mounds or ridges (Fig. 1). The nasal of FMNH PR 2100 itself has patches of different textures such that it would appear that the caudal area between the lacrimals has a different dermis and epidermis than does the more rostral part, which has very projecting, tuberculate sculpture (Fig. 5). On the other hand, the more lateral elements (e.g., quadratojugal, jugal, maxilla, dentary) tend to be characterized by a much higher percentage of tangential vascular canals and grooves, many of which branch and anastomose. Moreover, there are discrete patterns or fields that can be identified, such as the fields of tuberculate rugosity described above that flank a smoother 'groove' and extend from the postorbital, across the orbit, to the lacrimal and nasal beyond (Fig. 1). Other examples include the field of long vertical grooves and ridges that span the nasomaxillary contact just rostral to the antorbital cavity. Below this striate field is a distinctive field of very punctate bone (i.e., normal, not tangential canals) on the maxilla that extends forward onto the body of the premaxilla. All of these and other fields are generally very symmetrical.

Similar examples of dermal sculpturing abound in the extant realm, including the rugose texture on the skull elements of birds, crocodilians, many turtles, and even such mammals as giraffe, rhinoceros, and hippopotamus (Hieronymus and Witmer, 2003, 2004). How these different bony sculpture patterns and fields relate to differences in the overlying dermis and epidermis is currently under study (Hieronymus and Witmer, unpubl. data), but preliminary findings bear on the interpretation of *Majungasaurus*. For example, the projecting rugosity pattern on areas of the skull roof (e.g., nasal, frontal; Figs. 1, 5, 16) suggests that the dermis here was relatively thick, with collagen bundles of larger diameter that projected out into the overlying epidermis. The ventrolateral elements (e.g., maxilla; Fig. 4), with more tangentially arranged grooves, were covered with a thinner dermis probably overlain by larger scutes or scales. The cornual process on the frontal (Fig. 16), with its projecting tuberculate sculpture, was covered with a thick dermis, and potentially a small keratinized conical scute ('horn'), but there is no evidence (e.g., peripheral anchoring structures) for a tall projecting horn. The lacrimals of FMNH PR 2100 (Fig. 8) show evidence that they also may have sported a small hornlike scute; the dorsolaterally facing surface is relatively smooth (suggesting a thinner, tangentially organized dermis and an epidermal scute), but is surrounded by a peripherally projecting rugosity that may have supported fibers anchoring such an epidermal horn.

Apart from the clues provided by the rugosities with regard to the epidermis, the intersections between sculptured and nonsculptured bone can be used to delimit boundaries between soft-tissue regimes. For example, the smooth-textured bone of the antorbital fossa (in life lined by an epithelial air sac) abuts the strongly sculptured (subcutaneous) bone of the adjacent nasal and maxilla (Fig. 1). In fact, the relatively small antorbital fenestrae and bony naris are probably in part a reflection of the increased mineralization induced by the integument overlying the surrounding bones. That is, mineralization and metaplastic ossification of the skin overlying the rostral portion of the nasal bones encroaches on the narial region, restricting the size of the bony nasal aperture. Likewise, mineralization of the skin overlying the lacrimal bone encroaches on the antorbital fenestra. Other examples can be found in the dorsotemporal fenestra, indicating limits of the adductor musculature. A similar differentiation can be discerned on the lateral surface of the dentary, where a well developed, longitudinal bony ridge separates a subcutaneous sculptured ventral portion from a distinctive dorsal portion associated with the oral mucosa and gingiva.

In *Majungasaurus* and other abelisaurids, metaplastic ossification of the dermis and the resulting sculpturing may reflect a more general systemic propensity for the mineralization of soft tissues that extended to other systems. For example, the interorbital septum and sphenethmoid, largely cartilaginous and hence unpreserved in most theropods (indeed most dinosaurs), are mineralized in *Majungasaurus* and at least some other abelisaurids (Fig. 14). As discussed above in the descriptions of the interorbital septum and sphenethmoid, in *Majungasaurus* and other theropods preserving the septum, the mineralized interorbital septum (and often the sphenethmoid) bears a striate 'unfinished' texture that may reflect calcification of cartilage rather than normal endochondral ossification. Another example is the

suborbital processes of the postorbital (Fig. 10) and, to a lesser extent, lacrimal (Fig. 8). The postorbital's suborbital process almost certainly represents mineralization of the suborbital ligament and membrane that passed below the eyeball between these two bones. Likewise, the strong interdigitating union of the lacrimal and postorbital above the eyeball may also relate to mineralization of supraorbital soft tissues, in a sense 'adding' to the two bones (mostly the postorbital) to close the gap. In support of this notion, the basal abelisaurid *Rugops* clearly is tending toward the *Majungasaurus* condition but retains a gap in the dorsal wall of the orbit (Sereno et al., 2004).

The postorbital and lacrimal are not alone among the skull bones of *Majungasaurus* in displaying apomorphically enhanced contacts, and many of these may reflect increased mineralization of soft tissues. For example, the premaxilla-maxilla suture is a complex, highly congruent joint with bony lamina, pegs, and sockets (Figs. 3, 4). Likewise, the nasal-maxilla contact has the appearance of being 'overgrown' with bone, which again has the effect of reinforcing the articulation. In fact, many articulations between adjacent skull bones are apomorphically complicated, suggesting that sutural connective tissues were mineralized. It is even tempting to regard the fusions that occur between various of the skull bones (e.g., contralateral nasals, lacrimal and prefrontal, frontal and postorbital in some specimens, contralateral frontals in some specimens) as being simply an extension of this same phenomenon, carrying mineralization of the joint to the point that the tissues underwent bone remodeling, obliterating the suture. It is thus perhaps significant in this regard, given the overall strengthening of the skull joints, that the bones comprising the intramandibular joint show the opposite trend, retaining and enhancing an apparent high degree of synovial mobility.

Many of the attributes listed above for *Majungasaurus* that suggest enhanced mineralization of cephalic soft tissues pertain to other abelisaurids to varying extents (e.g., *Carnotaurus*, *Abelisaurus*). Interestingly, some other theropod groups, such as carcharodontosaurids, show some similar attributes, such as the dermal sculpturing, mineralized sphenethmoid and interorbital septum, and suborbital process of the postorbital bone, among others, suggesting that a systemic phenomenon may indeed be a valid hypothesis.

Braincase Pneumaticity and Soft-Tissue Inferences

One of the most unexpected morphological findings presented by Sampson and colleagues (1998) was the presence of 'hollow' frontals in FMNH PR 2100 (Figs. 14, 15, 16). Among saurischians, such frontal sinuses were previously unknown outside of Coelurosauria, and even then they are found only in some neornithine birds and oviraptorosaurs (Witmer, 1990, 1997a, b). Given the highly pneumatic condition of the adjacent nasal bone, it is natural to assume that the frontal sinuses also were produced by an air-filled, epithelial diverticulum. But whereas the nasal has a fairly 'normal' pneumatic foramen clearly indicating a diverticular source from the antorbital air sinus, the source of the frontal sinus, if indeed pneumatic, is more problematic. There are no obvious pneumatic foramina in the frontal bone, and the frontal does not directly border the antorbital cavity. The pneumatic chamber in the nasal does not communicate with the frontal sinus, and indeed CT shows that the nasal chamber pinches out caudally as it reaches the frontal (Fig. 6). Likewise, it is impossible to posit even indirect pneumatization from the tympanic cavity, because, although *Majungasaurus* clearly had paratympanic pneumaticity (see below), CT demonstrates that none of the diverticula come anywhere near the frontal. The status of the frontal sinuses and their mode of origin are taken up after an analysis of their morphology and variation, because these have bearing on their interpretation.

The considerable variation observed in these sinuses (Fig. 16) is consistent with a pneumatic interpretation, because pneumaticity among extant amniotes can often be highly variable. Nevertheless, it is necessary to determine if other soft-tissue systems or other processes could have created the unique frontal sinuses. Venous sinuses also can produce bony cavities, and the proximity of the frontal sinuses to the endocranial dural venous sinuses might make a venous interpretation plausible. However, as noted above, there is no significant communication between the endocranial cavity and the frontal sinuses in MNHN.MAJ 4 and FMNH PR 2099, which are well enough preserved to be definitive; again, the broad communication in FMNH PR 2100 (Fig. 15A) is obviously due to damage. Moreover, the frontal sinuses are not traversed by large vascular canals. Thus, a vascular explanation is not compelling. Nor does a pathological explanation seem tenable, because, although variable, the frontal sinuses are consistent enough (even across taxa, viz. *Ceratosaurus*; Fig. 16F) to be indicative of some normal biological process. For this same reason, some postmortem, perhaps diagenetic, process seems unlikely, because, although some of the sinuses seem to have been the site of a 'geode-like' mineral precipitate, the internal bone structure is not disrupted, and the sinus walls are generally smooth. Thus, a pneumatic interpretation remains the best explanation.

The problem of the source of the pneumaticity remains, however, because of the morphogenetic requirement that pneumatic sinuses be formed and maintained by air-filled diverticula (see Witmer, 1997a, and references therein). The frontals of FMNH PR 2100 do possess a pair of apertures that broadly communicate with the frontal sinus, and these are the articular slots for the long prefrontal prongs (Figs. 14B, E, 16B, arrow). In fact, the prefrontal slots either demonstrably communicate with the sinuses or are very close in MNHN.MAJ 4 and FMNH PR 2099; they may communicate in all cases, but sometimes the subtle density distinctions between matrix and bone in these fossils make it difficult to be definitive. Moreover, in the last two named specimens, the frontal sinuses are clearly directly in line (e.g., in a horizontal or parasagittal section) with the prefrontal slot (Fig. 16), suggesting a causal, morphogenetic link. Thus, accepting this slot as the pneumatic conduit, the next questions become, how does a pneumatic diverticulum track along this narrow frontal-prefrontal articular surface, and from where does the diverticulum originate?

To address the latter question first, the only possible source of the frontal sinus diverticulum is ultimately from the antorbital sinus (itself lodged within the antorbital cavity), with the more proximate source being the air sinus within the lacrimal bone. As noted in the section on the lacrimal above, the frontal articular surface on the dorsomedial aspect of the lacrimal bears an irregular series of pits and foramina. CT shows that many of these apertures communicate internally with the pneumatic sinus within the body of the lacrimal (Fig. 9B, vertical arrow). It is thus possible that a diverticulum exited the lacrimal sinus and then tracked caudally within the sutural region to enter the frontal bone along with the fused prefrontal prong. It may be significant in this regard that some *Allosaurus* lacrimals display a similar aperture leading from the lacrimal sinus caudodorsally toward the prefrontal-frontal region of the orbit (Fig. 9D, vertical arrow); Witmer (1997a:12) earlier suggested that this same aperture transmitted the duct of a nasal gland, but, in light of the situation in *Majungasaurus*, it is possible that the opening is instead a pneumatic foramen for a diverticulum entering not the frontal bone but an orbital air sac (for which there already is independent evidence; Witmer 1997a:51). Two specimens of *Majungasaurus* (MNHN.MAJ 4 and UA 8709) retain at least some portion of the prefrontal prongs preserved in place. In both cases, the prong does not fill the slot and there might be adequate room to transmit a diverticulum into the frontal bone.

Although it is unusual to transmit a diverticulum along a suture, there are ample precedents; for example, in birds, the dorsal tympanic diverticulum tracks between the prootic and squamosal bones and, in some galliforms, the quadrate diverticulum actually traverses the synovial cavity of the quadratopterygoid articulation to pneumatize the pterygoid bone (Witmer, 1990). The variation in the frontal sinuses, both in terms of morphology and extent, is difficult to explain. A pneumatic interpretation, although perhaps the best supported, is by no means certain. The presence of similar frontal sinuses in *Ceratosaurus* suggests that this attribute is not just a peculiarity of *Majungasaurus* and likewise raises the prospect that study of frontal sinuses in other theropods will clarify the nature of the morphological patterns observed in the Malagasy form.

Another area of uncertainty pertains to the significance of the paired shallow fossae and foramina on the caudal surface of the basioccipital, described above (Fig. 14G). The foramina in the basioccipital could have transmitted vasculature, because extant archosaurs sometimes have nutrient vessels penetrating the bone in this region (Sedlmayr, 2002). However, the foramina open rostrally into a pneumatic cavity, and thus they could also be pneumatic foramina (Fig. 15A, double-headed arrow with asterisk). Interestingly, the pneumatic cavity with which they communicate is not the basioccipital diverticulum of the basisphenoid recess (see below), but rather the caudal diverticulum of the rostral tympanic recess noted above in the prootic description (Figs. 15, 17). In other words, the rostral tympanic recess, housed largely in the prootic and basisphenoid, expands caudally into the basioccipital to emerge on the occipital surface via the foramina within the fossae adjacent to the median keel. Such pneumatic features in the basioccipital have not been described previously in abelisaurids. In some ways, these features correspond to the subcondylar recesses of tyrannosaurids and ornithomimids (Witmer, 1997b; Makovicky and Norell, 1998; Currie, 2003; Witmer and Ridgley, in press), although in these coelurosaurs the subcondylar fossae and apertures are much larger. Perhaps more similar are the foramina in *Giganotosaurus* (Coria and Currie, 2002) and *Piatnitzkysaurus* (Rauhut, 2004a), which are in similar positions to those of *Majungasaurus*. Coria and Currie (2002) suggested that the foramina indicate that a tympanic air sac occupied the region below the condyle. This may be true for *Giganotosaurus* and all other theropods with pneumaticity in this region, including *Majungasaurus*, but Witmer (1997b) suggested another alternative—pulmonary diverticula in the cranial cervical vertebrae extending forward to invade the basioccipital and eventually communicate with the middle ear sac (Witmer 1997a). Rauhut (2004a) argued that a pulmonary source was not likely for the subcondylar recesses of *Piatnitzkysaurus* in that its axis (vertebra C2) is not pneumatic (although it is in *Majungasaurus*; see O'Connor, this volume). Instead, Rauhut (2004a) suggested that the source could have come from the basisphenoid recess, although in *Majungasaurus*, as noted above, the foramina within the subcondylar recesses communicate *not* with the basisphenoid recess but rather the rostral tympanic recesses. It is not presently possible to decide between these alternatives for *Majungasaurus*.

Less controversially, the basisphenoid houses pneumaticity associated with two systems: (1) the middle ear sac (tympanic cavity), and (2) the enigmatic median pharyngeal system. With regard to the former, the rostral tympanic recess has been discussed above with the prootic bone. Again, the rostral tympanic recess is a lateral pneumatic excavation within the dorsal portion of the basisphenoid and ventral portion of the prootic that strongly undercuts the otosphenoidal crest and extends caudally within the cranial base to emerge on the occiput via the pair of foramina within the basioccipital discussed in the previous paragraph. The cerebral carotid artery (and accompanying veins) passed through the middle ear sac and rostral tympanic recess to enter a short carotid canal in the basisphenoid that opens in the pituitary (hypophyseal) fossa (Figs. 14C, 15, 17). The paired carotid canals remain separate throughout their courses rather than uniting prior to opening into the pituitary fossa as in some other theropods (e.g., *Giganotosaurus*; Coria and Currie, 2002). Pneumatic recesses associated with the cerebral carotid are quite common among theropods (Currie and Zhao, 1994a; Chure and Madsen, 1996; Witmer, 1997b; Coria and Currie, 2002), and Wilson and colleagues (2003) described a probably homologous recess in *Rajasaurus*.

The basisphenoid recess of *Majungasaurus* certainly has the appearance of being pneumatic in origin, forming a roughly pyramidal space with communicating chambers (Figs. 14, 15, 17). The source of the pneumatic diverticulum for these median fossae in archosaurs has been problematic (Witmer, 1997b), and in *Majungasaurus* the basisphenoid recess does not seem to have clear access to or continuity with the middle ear space. Thus, it is perhaps better, as argued by Witmer (1997b), to regard this recess as deriving from a separate pneumatic diverticulum from the pharynx, the median pharyngeal system. In support of this interpretation, the basisphenoid recess does not communicate with the rostral tympanic recess within the body of the basisphenoid, as confirmed by CT of FMNH PR 2100. The recess has a caudal chamber extending back into the basioccipital bone. There is an apparent communication here with the caudal extension of the rostral tympanic recess, but this communication is probably artificial, resulting from damage (Fig. 15, star). As preserved, the basisphenoid recess of UA 8709 is larger than that of FMNH PR 2100, which is interesting given than the former is otherwise smaller than the latter. Indeed, Rauhut and Fechner (2005) suggested that, in some cases, pneumatic systems may be relatively more expansive in younger animals, which is in accord with progressive ontogenetic reduction of braincase pneumaticity in extant crocodilians (Witmer, pers. obs.). Regardless of its cause, considerable individual variation is a hallmark of pneumatic systems.

Craniofacial Structure and Function in *Majungasaurus*

Majungasaurus possesses a number of skull specializations, documented above, some of which are shared with at least some other abelisaurid theropods. Specifically, relative to basal ceratosaurs (e.g., *Ceratosaurus*), and perhaps noasaurids as well (Carrano et al., 2004), the skull proportions of *Majungasaurus* are derived in at least four major aspects. First, the skull is dorsoventrally deep; that is, it has undergone an increase in height relative to the 'long and low' primitive condition. This statement applies to several other abelisaurid taxa (e.g., *Rugops*, *Carnotaurus*, *Aucasaurus*), and even to some forms that do not exhibit a proportional decrease in overall skull length (e.g., *Abelisaurus*). Second, the skull of *Majungasaurus* is abbreviated in overall length (rostrocaudal dimension), as evidenced by telescoping of various elements, as well as by proportions of the mandible and comparisons with postcranial elements. This trend is perhaps even better exemplified in the Argentine forms *Carnotaurus* and, to a lesser extent, *Aucasaurus*. Third, in contrast to the relatively tapered snouts that characterize *Ceratosaurus* and most basal theropods, the skull of *Majungasaurus* has a broad, rounded snout. This characteristic, best seen in rostral and dorsal views (Figs. 1, 2), appears to have been present in some other abelisaurids (e.g., *Carnotaurus*, *Abelisaurus*), although perhaps not to the degree as is present in the Malagasy taxon. Fourth, *Majungasaurus* (and indeed all abelisaurids for which good skull materials are known) possesses a relatively tall and broad occiput, with an expanded, plate-like transverse nuchal crest composed largely of the parietal, supraoccipital, and squamosal. A pronounced sagittal nuchal crest, formed by the supraoccipital, clearly delimits this region into left and right sides. This expan-

sion of the occiput, along with enhanced muscle rugosities, likely pertains to an increase in muscle attachment area. These traits, when combined with the tendency toward hypermineralization/hyperossification and fusion of cranial elements (including more intricate and elaborate articulations, for example, between the premaxilla and maxilla), suggest that abelisaurid skulls were considerably more robust than among theropods generally. Notably, some of these features occur in parallel in other theropod clades—for example, some tyrannosaurids have relatively deep skulls, somewhat broadened snouts and expanded occipital regions—clearly indicating the independent evolution of this unique suite of features in *Majungasaurus* and a subset of other abelisaurids.

The dentition and jaws of *Majungasaurus* are also derived in several respects. The teeth tend to be relatively short-crowned, more so in the dentary than the maxilla and premaxilla (Smith, this volume). The premaxillary teeth are unusually robust, being significantly broader, somewhat more elongate, and less curved than those in the maxilla and dentary (Smith, this volume). Short-crowned dentitions are present to greater or lesser extents in all known abelisaurids (although less so in *Carnotaurus*), in stark contrast to the elongate tooth crowns present in the closely-related *Ceratosaurus*. The lower jaws of *Majungasaurus* and other abelisaurids possess a greatly enlarged external mandibular fenestra, with specialized contacts between the dentary and post-dentary elements (Fig. 25). Virtually all theropods possess an intramandibular joint, in which the dentary is 'hinged' to the postdentary elements. However, the degree of movement at this joint, as well as its function, is not clear for most theropods. It has been argued that this system allowed for "some flexion in multiple planes . . ." so as to serve ". . . as a shock absorber to dampen the forces generated by the acquisition, manipulation, and/or consumption of large prey" (Holtz, 2003:331). Yet most theropods tend to have overlapping, squamous type contacts between the dentary and postdentary elements, which seemingly would severely limit movement at these joints. In contrast, the lower jaws of *Majungasaurus* and other abelisaurids (and perhaps noasaurids; Carrano et al., 2002) appear better equipped for some form of intramandibular movement (Mazzetta et al., 2000). Morphology consistent with this interpretation includes: (1) greatly enlarged external mandibular fenestra, marked in particular by reduction of the dentary; (2) peg and socket articulation between the surangular and dentary, almost certainly involving synovial joints; (3) reduced contact between the dentary and angular; and (4) a broad, platform-like articulation between the splenial and angular largely caudal to the dentary. In postulating the potential for intramandibular movement, however, we are not suggesting that abelisaurids possessed the ability for active, muscle-powered kinesis across these joints; rather, the joint contacts suggest a more limited, passive mode of kinesis perhaps best regarded as accommodation.

Among extant canid carnivorans, increased snout breadth (vs. skull length) has been associated with the ability to acquire larger prey, particularly among larger-bodied carnivores (Van Valkenburgh and Molnar, 2002). Interestingly, within Late Cretaceous faunas that include the remains of abelisaurids, the dominant large-bodied herbivores tend to be titanosaurian sauropods, with adult body sizes far exceeding those of the coeval carnivores (Mazzetta et al., 2004). However, this correlation between predator snout breadth and prey size does not apply in a number of other Mesozoic terrestrial ecosystems; for example, the Late Jurassic Morrison Formation of western North America is dominated by a diversity of truly gigantic sauropod taxa (e.g., *Apatosaurus*, *Diplodocus*, *Brachiosaurus*) and several large-bodied theropods (e.g., *Allosaurus*, *Ceratosaurus*, *Torvosaurus*), with the latter group all possessing the standard narrow-snouted morphology. Moreover, as egg-layers, dinosaurs had much greater reproductive capacities than placental mammals, necessitating relatively high rates of infant mortality in order to maintain stable populations (Farlow and Holtz, 2002). Thus, (at least some) large-bodied theropods may have preyed preferentially upon younger individuals, a contention supported by the occurrence of juvenile ornithischian bones in the gut regions and coprolites of tyrannosaurids (Chin et al., 1998; Varricchio, 2001).

Nonetheless, despite uncertainties regarding absolute age (and thus size) of prey, the above morphologies described for *Majungasaurus* lead to certain functional inferences that, minimally, constrain higher-order hypotheses of behavior. The enlarged occipital region, and in particular the transverse nuchal crest, indicate an expansion of at least some components of the cervical musculature (e.g., M. complexus, M. biventer cervicis, and perhaps M. splenius capitus; see braincase description above). This contention is supported by the relatively short and broad cervical column, with extensive muscle attachment sites on the vertebrae, as well as the hypertrophied epipophyses characteristic of the group (O'Connor, this volume). Indeed, bony indicators throughout the vertebral column indicate that, in contrast to most other theropods, abelisaurids had enhanced epaxial dorsal musculature relative to that of the hypaxial region. The attachment sites for cervical muscles on the cranium indicate increased capacity for head stabilization. One possibility is that this suite of features is associated with increased overall neck strength; however, increased strength necessitates greater total cervical musculature, for which we have no direct evidence. The relatively broad and deep skull appears well designed to resist torsional bending moments, particularly as compared with most other theropod taxa, which tend toward narrow-snouted morphologies.

The derived suite of skull morphologies in *Majungasaurus* (e.g., the short, deep, broad skull with short-crowned dentition, robust premaxillary teeth, and enlarged external mandibular fenestrae) all point to apomorphic modifications of the feeding apparatus (Therrien et al., 2005). Likewise, the Malagasy taxon also has several presumably related specializations of the postcranium, including a relatively robust cervical region with expanded muscle attachment (O'Connor, this volume) and greatly reduced forelimbs (Carrano, this volume). Moreover, the hind limbs of *Majungasaurus* appear to be stout and secondarily shortened, particularly the tibia (Carrano, this volume). Available data suggest that this description may apply to some other abelisaurid taxa (e.g., *Lametasaurus*, *Quilmesaurus*) but not to others (*Carnotaurus*). Finally, reconstruction of the skeleton of *Majungasaurus* (the result of the combined research of contributors to this volume; see Krause et al., this volume:fig. 1) demonstrates that, in overall proportions, this animal was relatively short (for its body size), stout and robust, with this robustness particularly evident in the head, neck, and hind limbs. Considered in total, the osteological evidence raises the possibility of a divergent predatory habitus for *Majungasaurus* and perhaps other abelisaurids relative to other mid- to large-bodied theropods.

If *Majungasaurus* was divergent, then what were the 'standard' modes of predation in theropod dinosaurs? Van Valkenburgh and Molnar (2002) conducted a comparison of dinosaurian and mammalian predators, employing structure-function correlates in extant carnivorous mammals to explore and interpret function and behavior in theropods. They noted that extant large carnivores can be divided into two groups based on their predatory behavior: (1) ambush species that, following a short-distance sprint, employ muscular, well developed forelimbs and clawed hind limbs to grapple with prey while administering bites with the head (e.g., felids, some ursids); and (2) pursuit species that lack well-developed forelimbs, instead employing the jaws and teeth as the primary or sole killing weapon, frequently after a long distance chase (e.g., canids, hyaenids). Van Valkenburgh and Molnar (2002) then applied these modes to theropod dino-

saurs, describing members of the former as 'grappler-slashers' (e.g., dromaeosaurids) and members of the latter as 'head-hunters' (e.g., tyrannosaurids).

Of these two predation categories, *Majungasaurus* clearly fits better into the second, 'head-hunter' category, possessing a well-developed skull and neck and abbreviated forelimbs. However, the Malagasy theropod certainly cannot be regarded as long-legged, let alone cursorial. Indeed, paradoxically, it appears that there has been a secondary reduction in hind limb length, particularly of the distal limb segments, and, consequently, an apomorphic decrease in cursoriality. Thus, it is apparent that additional explanation is required. Importantly, the current range of ecomorphs among extant mammalian predators almost certainly does not represent the possible, and indeed previously achieved, morphological range. Thus, for example, Van Valkenburgh (1988) argued persuasively that extinct guilds of Cenozoic mammalian predators included predatory modes quite different from those of modern taxa. Nonetheless, assuming it was not an exclusive scavenger (a highly unlikely contention; see Farlow and Holtz, 2002, for a discussion of this hypothesis as it relates to *Tyrannosaurus rex*), *Majungasaurus* can confidently be regarded as having been a hypercarnivorous 'head hunter'—that is, an obligatory predator that used its head as the primary weapon for killing (Van Valkenburgh and Molnar, 2002; Holtz, 2003).

Another important structure-function study relating to theropod dinosaurs is that of Rayfield and colleagues (2001; see also Rayfield, 2005), who applied digital finite element analysis to assess biomechanical aspects of the skull of the Late Jurassic form *Allosaurus fragilis*. Their findings suggest that the skull of this taxon (and, by implication, many theropods) was strong in bilateral vertical compression—particularly if the lower jaws were not employed in the initial bite—but relatively weak in resisting torsional bending, in part because of narrow skull configuration and generally open design. This led the authors to postulate that *Allosaurus* did not bite and hold prey throughout the kill, but rather employed a 'strike-and-tear' bite to generate fatal wounds. Van Valkenburgh and Molnar (2002) noted that extant canids, which tend to be narrow-snouted, typically employ repeated, shallow bites to subdue prey, whereas the broader-snouted felids tend to kill with a single, strong bite to the neck or muzzle. In their study of theropod predation, which was limited to certain Laurasian forms and thus did not include abelisaurids, these authors supported the above findings, arguing that carnivorous dinosaurs were narrow-snouted and thus more like canids, utilizing multiple-bite attacks rather than the single, prolonged killing bites characteristic of many felids. Holtz (2003) concurred with this conclusion, arguing that theropod predators generally would have utilized a strike-and-tear mode of attack and avoided bite-and-hold behavior due to structural limitations of the skull.

Two other functional studies included specific reference to abelisaurids. The first, by Mazzetta et al. (2000), focused on *Carnotaurus* and colleagues. Many of their functional inferences are predicated on the presence of significant muscle-powered craniofacial kinesis, for which, as detailed above, we find no evidence in *Majungasaurus* (although we do accept some amount of passive intramandibular mobility). Moreover, they suggested that *Carnotaurus* emphasized a quick bite over a powerful one, and targeted prey smaller than themselves, which would then be swallowed whole. The second study, by Therrien and colleagues (2005), focused almost exclusively on biomechanical design of the mandible, but had a broad taxonomic scope among theropods. Their findings for *Majungasaurus* were almost the opposite of those of Mazzetta and colleagues (2000) for *Carnotaurus*. Therrien and colleagues (2005) suggested that the mandibular mechanics of *Majungasaurus*, coupled with its broad snout and short teeth, made it most similar to the largest extant reptilian predator, *Varanus komodoensis*, and, in fact, it was almost the only theropod in their large study to match the Komodo dragon. Thus, they argued, *Majungasaurus* likewise was a hunter of large prey and delivered slashing bites capable of removing sizeable portions of flesh. Moreover, their mechanical analyses suggested that *Majungasaurus* could deliver high bite forces (and that *Carnotaurus* could bite even harder, in contrast to the findings of Mazzetta et al. [2000]).

The character suite described above for *Majungasaurus* suggests that it may have utilized a predation strategy divergent from that of other theropods. Although a detailed functional morphological analysis is beyond the scope of this study, in the spirit of provoking further thought on the matter, we offer the following speculation. In contrast to most other theropod taxa, *Majungasaurus* (and perhaps certain other abelisaurids) was adapted for a mode of predation that entailed relatively few, penetrating bites accompanied by powerful neck retraction, as well as bite-and-hold behavior. This hypothesis is provisionally supported by the following skeletal features, possibly related to prolonged contact with struggling, large-bodied prey: (1) broad skull (resisting torsional bending); (2) abbreviated skull (reducing the moment arm of resistance at the atlanto-occipital joint caused by rostrally placed loads, and thereby facilitating stabilization of the head using neck musculature; this feature may also have reduced the moment arm of the lower jaw, permitting increased bite forces at the tip of the snout); (3) surprisingly high bite forces (based on the mandibular biomechanics of Therrien et al. [2005]); (4) tendency toward hypermineralization and fusion of skull elements, including more intricate and robust contacts between skull elements (thereby strengthening the skull so as to resist torsional forces); (5) fused and pneumatized nasals (transforming these elements from a relatively thin strut into an elongate tube that would have been more effective in resisting torsional forces); (6) expanded occiput and neck musculature (for stabilizing, and perhaps retracting, the head); (7) short-crowned teeth (given that longer-crowned teeth would be more prone to breakage during extended biting); (8) robust premaxillary teeth (necessary since these were likely the primary weapons in bite-and-hold behavior); (9) enlarged external mandibular fenestra (permitting intramandibular accommodation movements through reduction of squamous contacts and concentration of articular surfaces at well-formed, probably synovial joint surfaces); and (10) relatively short hind limbs (resulting in a low center of gravity). The decrease in cursoriality may thus be accounted for by the need for short, powerful hind limbs, in combination with the fact that these predators, though incapable of high speeds, would nonetheless have been able to run down their likely prey—titanosaurian sauropods. Indeed this hypothesis is predicated on the assumption that the primary prey species of *Majungasaurus* were titanosaurian sauropods, the only large herbivores thus far recovered from the Maevarano Formation. Although many smaller-bodied vertebrates (e.g., crocodilians, turtles, snakes, and mammals) have also been recovered from the formation, and could have formed a portion of the diet of these top predators, the putative functional attributes noted above do not appear to be consistent with swallowing animals whole. Therrien and colleagues (2005) suggested that *Majungasaurus* may have been an ambush predator, a speculation that is also consistent with available data.

Returning to extant analogues, predators that engage in bite-and-hold behavior tend (not surprisingly) to target particular regions of the body. Some, like certain raptorial birds, bite the top of the neck and head, particularly if the prey species is smaller-bodied. Others, including many felids, which often attack prey of equal or larger body size, tend to suffocate victims through bites to the throat region and/or muzzle (Van Valkenburgh and Molnar, 2002). Whether or not it employed suffocation as a killing technique, *Majungasaurus* is here postulated to have been able to dispatch large prey more rapidly than other basal theropods, employing a combination of relatively few, pro-

longed, penetrating bites and powerful neck retraction to produce massive wounds, which is in accord with the biomechanical findings of Therrien et al, (2005). In sum, although speculative, current evidence is consistent with the possibility that *Majungasaurus*, and perhaps some other abelisaurid theropods, diverged from the predatory 'norm' among theropods, specializing in felid-like predation using a strategy of fewer, deeper, more lethal bites.

The above predation hypothesis is of course difficult to test, given that it makes detailed postulates about the behavior of an extinct organism. Moreover, other functional interpretations of these morphologies could be conceived. For example, Rogers and colleagues (2003, this volume) provided compelling evidence that *Majungasaurus* regularly engaged in stripping flesh from relatively dry carcasses; this difficult endeavor could also have been facilitated by a robust skull and neck. And other cited morphologies (e.g., stout legs, hypermineralization/ossification) may represent adaptations unrelated to mode of predation. Nonetheless, the above predation hypothesis and many of its stated suppositions are founded on qualitative observations of morphology. In particular, the presence of a relatively broad, deep, abbreviated skull together with enhanced epaxial musculature stands in contrast to the vast majority of other theropod dinosaurs, and is at least suggestive of a fundamentally divergent feeding strategy. In the future, it would be valuable to subject these ideas to a detailed analysis that takes into account not only craniofacial and postcranial osteology, but also consideration of reconstructed soft tissues and biomechanical constraints founded on quantitative and experimental studies on extant predators.

ACKNOWLEDGMENTS

We thank D. Krause and all the participants of the Stony Brook University/Université d'Antananarivo 1993-2001 field expeditions to the Mahajanga Basin, Madagascar: R. Asher, G. Buckley, M. Getty, M. Gottfried, J. Hartman, C. Lockwood, M. Loewen, J. Miller, C. Norovelo, P. O'Connor, R. O'Keefe, Prosper, J. A. Rabarison, L. Rahantarisoa, L. L. Randriamiaramanana, N. H. S. Ravelomanantsoa, F. Ravoavy, K. Curry Rogers, R. Rogers, K. Samonds, N. Stevens, E. Roberts, R. Terry, C. Wall, N. Wells, R. Whatley, and R. Wunderlich. Particular thanks are due to A. Rasoamiaramanana, G. Ravololonarivo, and the late B. Rakotosamimanana (Université d'Antananarivo), B. Andriamihaja and P. Wright (Institute for the Conservation of Tropical Environments), and the villagers of Berivotra for invaluable logistical support throughout these expeditions. Sincere thanks also to K. Passaglia, V. Heisey, J. Holstein, Mike Getty, Monica Castro, and the volunteer fossil preparators at the Utah Museum of Natural History for specimen preparation.

For providing access to specimens in their care, we gratefully acknowledge S. Bandyopadhyay (Indian Statistical Institute, Calcutta); J. Bonaparte (Museo Aregentino de Ciencias Naturales, Buenos Aires); R. Coria (Museo Municipal Carmen Funes, Plaza Huincul), P. Currie (Royal Tyrrell Museum of Paleontology, Drumheller); P. J. Makovicky and W. Simpson (Field Museum of Natural History, Chicago); J. Foster (Museum of Western Colorado, Fruita); M. Goodwin, K. Padian , and P. Holroyd (University of California, Berkeley); J. Horner and P. Leiggi (Museum of the Rockies, Bozeman); A. Milner and P. Barrett (Natural History Museum, London); M. Norell (American Museum of Natural History, New York); O. Alcober (Museo de Paleontologia Vertebrados, San Juan); P. Powell (Oxford University Museum, Oxford); P. Sereno (University of Chicago); K. Stadtman and B. Britt (Brigham Young University, Provo); and P. Taquet (Muséum National de l'Histoire Naturelle, Paris).

Ryan Ridgely (Ohio University) deserves special thanks for his great skill and talent in the analysis and visualization of the CT scan data. Ridgely executed visualizations that comprise Figures 1, 5, 6, 7, 9, 16, 17, 18, and 19, and he also did the pencil and line art for Figures 2, 7, and 15. For additional assistance with figures, we thank Jude Higgins, Anna DeBeer, and Mark Loewen (UMNH). For assistance with CT scanning, we thank Heather Mayle at O'Bleness Memorial Hospital (Athens, OH) and Timothy Ryan and Avrami Grader at the Center for Quantitative Imaging, Pennsylvania State University (State College, PA). P. Taquet kindly provided a cast of MNHN.MAJ 4 for study, and H-D. Sues provided stereophotographs of this specimen. We gratefully acknowledge J. Lanzendorf for his generous support of paleoartists, including those who have illustrated *Majungasaurus*.

This manuscript was greatly improved as a result of discussions with a variety of people, many of whom graciously shared their unpublished findings: J. Bonaparte , G. Buckley, K. Carpenter, T. Carr, M. Carrano, S. Chatterjee, L. Chiappe, D. Chure, J. Clark, R. Coria, P. Currie, P. Dodson, G. Erickson, J. Farlow, C. Forster, J. Franzosa, N. Fraser, T. Gates, T. Hieronymus, C. Holliday, T. Holtz, J. Horner, G. Hurlburt, D. Krause, M. Lamanna, M. Loewen, M. Norell, F. Novas, P. O'Connor, G. Paul, T. Pinegar, E. Rickart, R. Ridgely, R. Rogers, J. Sedlmayr, P. Sereno, J. Sertich, J. A. Smith, J. B. Smith, H.-D. Sues, T. Tsuihiji, J. Wilson, B. Van Valkenburgh, and L. Zanno. For reviews of the manuscript, we sincerely thank M. Carrano, O. Rauhut, and an anonymous reviewer, whose comments greatly improved this paper. This research has been supported by the following grants: National Science Foundation (DEB-9224396; EAR-9418816, EAR-9706302, EAR-0106477, EAR-0116517, EAR-0446488 [to D. Krause], DEB-9904045 [to SDS and M. Carrano], IBN-9601174 [to L. M. W. and S. D. S.], IBN-0343744 [to L. M. W.], IOB-0517257 [to L. M. W., G. Hurlburt, and R. Ridgely]; the Dinosaur Society (1995; to D. Krause), and the National Geographic Society (1999, 2001, 2004; to D. Krause). L. M. W. also thanks the Ohio University College of Osteopathic Medicine for support.

LITERATURE CITED

Allain, R. 2002. Discovery of megalosaur (Dinosauria, Theropoda) in the Middle Bathonian of Normandy (France) and its implications for the phylogeny of basal Tetanurae. Journal of Vertebrate Paleontology 22:548–563.

Anderson, J. F., A. Hall-Martin, and D. A. Russell. 1985. Long-bone circumference and weight in mammals, birds and dinosaurs. Journal of Zoology, London (A) 207:53–61.

Bakker, R. T., M. Williams, and P. J. Currie. 1988. *Nanotyrannus*, a new genus of pygmy tyrannosaur, from the latest Cretaceous of Montana. Hunteria 1(5):1–30.

Bakker, R. T., D. Kralis, J. Seigwarth, and J. Filla. 1992. *Edmarka rex*, a new gigantic theropod dinosaur from the middle Morrison Formation, Late Jurassic of the Como Bluff outcrop region, with comments on the evolution of the chest region and shoulder in theropods and birds, and a discussion of the five cycles of origin and extinction among giant dinosaurian predators. Hunteria 2(9):1–24.

Baumel, J. J., and R. J. Raikow. 1993. Arthrologia; pp. 133–188 in J. J. Baumel (ed.), Handbook of Avian Anatomy: Nomina Anatomica Avium. Publications of the Nuttall Ornithological Club No. 23, Cambridge, England.

Baumel, J. J., and L. M. Witmer. 1993. Osteologia; pp. 45–132 in J. J. Baumel (ed.), Handbook of Avian Anatomy: Nomina Anatomica Avium. Publications of the Nuttall Ornithological Club No. 23, Cambridge, England.

Bellairs, A. d'A. 1958. The early development of the interorbital septum and the fate of the anterior orbital cartilages in birds. Journal of Embryology and Experimental Morphology 6:68–85.

Bennett, S. C. 1993. The ontogeny of *Pteranodon* and other pterosaurs. Paleobiology 19:92–106.

Benton, M. J. 1983. The Triassic reptile *Hyperodapedon* from Elgin: functional morphology and relationships. Philosophical Transactions of the Royal Society of London, Series B 302:605–717.

Bonaparte, J. F., and F. Novas. 1985. *Abelisaurus comahuensis*, n. gen., n. sp., Carnosauria del Cretacico tardio de Patagonia. Ameghiniana 21:259–265.

Bonaparte, J. F., and J. E. Powell. 1980. A continental assemblage of tetrapods from the Upper Cretaceous beds of El Brete, northwestern Argentina (Sauropoda-Coelurosauria-Carnosauria-Aves). Memoir Societé Géologique de France 139:19–28.

Bonaparte, J. F., F. E. Novas, and R. A. Coria. 1990. *Carnotaurus sastrei* Bonaparte, the horned, lightly built carnosaur from the Middle Cretaceous of Patagonia. Natural History Museum of Los Angeles County, Contributions in Science 416:1–41.

Breazile, J. E., and Hartwig, H.-G. 1989. Central nervous system; pp. 485–566 in A. S. King and J. McLelland (eds.), Form and Function in Birds, Volume 4. Academic Press, New York, New York.

Brochu, C. A. 2003. Osteology of *Tyrannosaurus rex*: insights from a nearly complete skeleton and high-resolution computed tomographic analysis of the skull. Journal of Vertebrate Paleontology Memoir 7:1–138.

Bruner, H. L. 1908. On the cephalic veins and sinuses of reptiles, with description of a mechanism for raising the venous blood-pressure in the head. American Journal of Anatomy 7:1–117.

Bubien Waluszewska, A. 1981. The cranial nerves; pp. 385–438 in A. S. King and J. McLelland (eds.), Form and Function in Birds, Volume 2. Academic Press, New York, New York.

Buchholtz, E. A., and E.-A. Seyfarth. 1999. The gospel of the fossil brain: Tilly Edinger and the science of paleoneurology. Brain Research Bulletin 48:351–361.

Burnham, D. A. 2004. New information on *Bambiraptor feinbergi* (Theropoda: Dromaeosauridae) from the Late Cretaceous of Montana; pp. 67–111 in P. J. Currie, E. B. Koppelhus, M. A. Shugar, and J. L. Wright (eds.), Feathered Dragons: Studies on the Transition from Dinosaurs to Birds. Indiana University Press, Indianapolis, Indiana.

Camp, C. L. 1930. A study of the phytosaurs, with description of new material from western North America. Memoirs of the University of California 10:1–174.

Carr, T. D. 1999. Craniofacial ontogeny in the Tyrannosauridae (Dinosauria, Coelurosauria). Journal of Vertebrate Paleontology 19: 497–520.

Carrano, M. T. 2007. The appendicular skeleton of *Majungasaurus crenatissimus* (Theropoda: Abelisauridae) from the Late Cretaceous of Madagascar; pp. 163–179 in S. D. Sampson and D. W. Krause (eds.), *Majungasaurus crenatissimus* from the Late Cretaceous of Madagascar. Society of Vertebrate Paleontology Memoir 8.

Carrano, M. T., S. D. Sampson, and C. A. Forster. 2002. The osteology of *Masiakasaurus knopfleri*, a new abelisauroid (Dinosauria: Theropoda) from the Late Cretaceous of Madagascar. Journal of Vertebrate Paleontology 22:510–534.

Carrano, M. T., S. D. Sampson, and M. A. Loewen. 2004. New discoveries of *Masiakasaurus knopfleri* and the morphology of the Noasauridae (Dinosauria: Theropoda), Journal of Vertebrate Paleontology 24(3, Supplement):44A.

Case, E. C. 1921. On an endocranial cast from a reptile, *Desmatosuchus spurensis*, from the Upper Triassic of western Texas. Journal of Comparative Neurology 33:133–147.

Chatterjee, S. 1978a. *Indosuchus* and *Indosaurus*, Cretaceous carnosaurs from India. Journal of Paleontology 52:570–580.

Chatterjee, S. 1978b. A primitive parasuchid (phytosaur) from the Upper Triassic Maleri Formation of India. Palaeontology 21:83–127.

Chatterjee, S. 1991. Cranial anatomy and relationships of a new Triassic bird from Texas. Philosophical Transactions of the Royal Society of London B 332:277–342.

Chatterjee, S. 1993. *Shuvosaurus*, a new theropod. National Geographic Research and Exploration 9:274–285.

Chatterjee, S., and D. K. Rudra. 1996. KT events in India: Impact, rifting, volcanism, and dinosaur extinction; pp. 489–532 in F. E. Novas and R. E. Molnar (eds.), Proceedings of the Gondwanan Dinosaur Symposium. Memoir of the Queensland Museum No. 39.

Chatterjee, S., and Z. Zheng. 2002. Cranial anatomy of *Shunosaurus*, a basal sauropod dinosaur from the Middle Jurassic of China. Zoological Journal of the Linnean Society 136:145–169.

Chin, K., T. T. Tokaryk, G. M. Erickson, and L. C. Calk. 1998. A king-sized theropod coprolite. Nature 393: 680–682.

Chure, D. J. 2000a. On the orbit of theropod dinosaurs. Gaia 15:233–240.

Chure, D. J. 2000b. A new species of *Allosaurus* from the Morrison Formation of Dinosaur National Monument (Utah-Colorado) and a revision of the theropod family Allosauridae. Ph.D. dissertation, Columbia University, New York, New York, 964 pp.

Chure, D. J., and J. H. Madsen, Jr. 1996. Variation in aspects of the tympanic pneumatic system in a population of *Allosaurus fragilis* from the Morrison Formation (Upper Jurassic). Journal of Vertebrate Paleontology 16:573–577.

Chure, D. J., and J. H. Madsen, Jr. 1998. An unusual braincase (? *Stokesosaurus clevelandi*) from the Cleveland-Lloyd Dinosaur Quarry, Utah (Morrison Formation; Late Jurassic). Journal of Vertebrate Paleontology 18:115–125.

Colbert, E. H., and D. A. Russell. 1969. The small Cretaceous dinosaur *Dromaeosaurus*. American Museum Novitates 2380:1–49.

Coria, R. A., and P. J. Currie. 2002. The braincase of *Giganotosaurus carolinii* (Dinosauria: Theropoda) from the Upper Cretaceous of Argentina. Journal of Vertebrate Paleontology 22:802–811.

Coria, R. A., L. M. Chiappe, and L. Dingus. 2002. A new close relative of *Carnotaurus sastrei* Bonaparte 1985 (Theropoda: Abelisauridae) from the Late Cretaceous of Patagonia. Journal of Vertebrate Paleontology 22:460–465.

Currie, P. J. 1995. New information on the anatomy and relationships of *Dromaeosaurus albertensis* (Dinosauria: Theropoda). Journal of Vertebrate Paleontology 15:576–591.

Currie, P. J. 2003. Cranial anatomy of tyrannosaurid dinosaurs from the Late Cretaceous of Alberta, Canada. Acta Palaeontologica Polonica 48:191–226.

Currie, P. J., and K. Carpenter. 2000. A new specimen of *Acrocanthosaurus atokensis* (Dinosauria: Theropoda) from the Lower Cretaceous Antlers Formation (Lower Cretaceous, Aptian) of Oklahoma, USA. Geodiversitas 22:207–246.

Currie, P. J. and X.-J. Zhao. 1994a. A new carnosaur (Dinosauria, Theropoda) from the Jurassic of Xinjiang, People's Republic of China. Canadian Journal of Earth Sciences 30:2037–2081.

Currie, P. J., and X.-J. Zhao 1994b. A new troodontid (Dinosauria, Theropoda) braincase from the Dinosaur Park Formation (Campanian) of Alberta. Canadian Journal of Earth Sciences 30: 2231–2247.

de Beer, G. 1937. The Development of the Vertebrate Skull. Oxford University Press, Oxford, England, 552 pp.

Depéret, C. 1896. Note sur les Dinosauriens Sauropodes et Theropodes du Crétacé supérieur de Madagascar. Societé Géologique de France Bulletin 24:176–194.

Edinger, T. 1942. The pituitary body in giant animals fossil and living: a survey and a suggestion. Quarterly Review of Biology 17:31–45.

Edinger, T. 1975. Paleoneurology 1804–1966. An annotated bibliography. Advances in Anatomy, Embryology and Cell Biology 49:1–258.

Elzanowski, A. 1987. Cranial and eyelid muscles and ligaments of the tinamous (Aves: Tinamiformes). Zoologische Jahrbuch für Anatomie 116:63–118.

Evans, D. C. 2006. Nasal cavity homologies and cranial crest function in lambeosaurine dinosaurs. Paleobiology 32:109–125.

Farlow, J. O., and T. R. Holtz Jr. 2002. The fossil record of predation in dinosaurs; pp. 251–265 in M. Kowalewski and P. H. Kelley (eds.), The Fossil Record of Predation. Paleontological Society Paper 8.

Francillon-Vieillot, H. V. de Buffrenil, J. Castanet, J. Geraudie, F. J. Meunier, J. Y. Sire, L. Zylberberg, and A. de Ricqles. 1991. Microstructure and mineralization of vertebrate skeletal tissues; pp. 471–530 in J. G. Carter (ed.), Skeletal Biomineralization: Patterns, Processes and Evolutionary Trends. Volume 1. Van Nostrand Reinhold, New York, New York.

Franzosa, J. W. 2004. Evolution of the brain in Theropoda (Dinosauria). Ph.D. dissertation. University of Texas, Austin, Texas, 381 pp.

Franzosa, J., and T. Rowe. 2005. Cranial endocast of the Cretaceous theropod dinosaur *Acrocanthosaurus atokensis*. Journal of Vertebrate Paleontology 25:859–864.

Gauthier, J. 1986. Saurischian monophyly and the origin of birds; pp. 1–47 in K. Padian (ed.), The Origin of Birds and the Evolution of Flight. Memoirs of the California Academy of Sciences 8, San Francisco, California.

Gemmellaro, M. 1921. Rettili maëstrichtiani di Egitto. Giornale di Scienze Naturali ed Economiche 32:340–351.

Gilmore, C. W. 1920. Osteology of the carnivorous Dinosauria in the United States National Museum, with special reference to the genera *Antrodemus* (*Allosaurus*) and *Ceratosaurus*. Bulletin of the United States National Museum 110:1–159.

Goodrich, E. 1930. Studies on the Structure and Development of Vertebrates. Macmillan, London, England, 837 pp.
Gower, D. J., and E. Weber. 1998. The braincase of *Euparkeria*, and the evolutionary relationships of birds and crocodilians. Biological Reviews 73:367–411.
Harris, J. D. 1998. A reanalysis of *Acrocanthosaurus atokensis*, its phylogenetic status, and paleobiogeographic implications, based on a new specimen from Texas. New Mexico Museum of Natural History and Science Bulletin 13:1–75.
Hay, O. P. 1908. On certain genera and species of carnivorous dinosaurs, with special reference to *Ceratosaurus nasicornis* Marsh. Proceedings of the United States National Museum 35:351–366.
Hieronymus, T. L., and L. M. Witmer. 2003. Dermal enthesis: anatomy and histology of rhinoceros horn attachment. Integrative and Comparative Biology 43(6):874.
Hieronymus, T. L., and L. M. Witmer. 2004. Cranial rugosity and dinosaur 'horns:' rhino and giraffe as model systems for skin reconstruction in fossil taxa. Journal of Vertebrate Paleontology 24(3, Supplement):70A.
Holliday, C. M. 2006 Evolution and function of the jaw musculature and adductor chamber of archosaurs (crocodilians, dinosaurs, and birds). Ph.D. dissertation, Ohio University, Athens, Ohio, 325 pp.
Holtz, T. R., Jr. 1994. The phylogenetic position of the Tyrannosauridae: implications for theropod systematics. Journal of Paleontology 68: 1100–1117.
Holtz, T. R. Jr. 2000. A new phylogeny of the carnivorous dinosaurs. Gaia 15:5–61.
Holtz, T. R. Jr. 2003. Dinosaur predation: evidence and ecomorphology; pp. 325–340 in P. H. Kelley, M. Kowalewski, and T. A. Hansen (eds.), Predator-Prey Interactions in the Fossil Record. Kluwer Academic/Plenum, New York, New York.
Holtz, T.R., Jr. 2004. Tyrannosauroidea; pp. 111–136 in D.B. Weishampel, P. Dodson, and H. Osmólska (eds.), The Dinosauria. Second Edition. University of California Press, Berkeley, California.
Hopson, J. A. 1977. Relative brain size and behavior in archosaurian reptiles. Annual Review of Ecology and Systematics 8:429–448.
Hopson, J. A. 1979. Paleoneurology; pp. 39–146 in C. Gans (ed.), Biology of the Reptilia, Volume 9. Neurology A, Academic Press, New York, New York.
Hopson, J. A. 1980. Relative brain size in dinosaurs: Implications for dinosaurian endothermy; pp. 287–310 in R. D. K. Thomas and E. C. Olson (eds.), A Cold Look at the Warm Blooded Dinosaurs, American Association for the Advancement of Science, Washington, DC.
Huene, F. v., and C. A. Matley. 1933. The Cretaceous Saurischia and Ornithischia of the Central Provinces of India. Memoirs of the Geological Survey of India: Palaeontologica Indica 21:1–72.
Hullar, T. E. 2006. Semicircular canal geometry, afferent sensitivity, and animal behavior. Anatomical Record 288A:466–472.
Hurlburt, G. R. 1996. Relative brain size in Recent and fossil amniotes: determination and interpretation. Ph.D. dissertation, University of Toronto, Toronto, Ontario, Canada, 250 pp.
Hurum, J. H., and P. J. Currie. 2000. The crushing bite of tyrannosaurids. Journal of Vertebrate Paleontology 20:619–621.
Hurum, J. H., and K. Sabath. 2003. Giant theropod dinosaurs from Asia and North America: Skulls of *Tarbosaurus bataar* and *Tyrannosaurus rex* compared. Acta Paleontologica Polonica 48:161–190.
Janensch, W. 1935. Die Schädel der Sauropoden *Brachiosaurus*, *Barosaurus* und *Dicraeosaurus* aus den Tendaguru-Schichten Deutsch-Ostafrikas. Palaeontographica, Supplementum VII 1(2):147–297.
Jerison, H. J. 1973. Evolution of the Brain and Intelligence. Academic Press, New York, New York, 482 pp.
Jollie, M. T. 1957. The head skeleton of the chicken and remarks on the anatomy of this region in other birds. Journal of Morphology 100: 389–436.
Krause, D. W., S. D. Sampson, M. T. Carrano, and P. M. O'Connor. 2007. Overview of the history of discovery, taxonomy, phylogeny, and biogeography of *Majungasaurus crenatissimus* (Theropoda: Abelisauridae) from the Late Cretaceous of Madagascar; pp. 1–20 in S. D. Sampson and D. W. Krause (eds.), Majungasaurus crenatissimus from the Late Cretaceous of Madagascar. Society of Vertebrate Paleontology Memoir 8.
Kurzanov, S. M. 1976. Brain-case structure in the carnosaur *Itemirus* N. gen. and some aspects of the cranial anatomy of dinosaurs. Paleontological Journal 1976:361–369.
Lamanna, M. C., R. D. Martínez, and J. B. Smith. 2002. A definitive abelisaurid theropod dinosaur from the Early Cretaceous of Patagonia. Journal of Vertebrate Paleontology 22: 58–69.
Larsson, H. C. E. 2001. Endocranial anatomy of *Carcharodontosaurus saharicus* (Theropoda: Allosauroidea) and its implications for theropod brain evolution; pp. 19–33 in D. H. Tanke and K. Carpenter (eds.), Mesozoic Vertebrate Life. Indiana University Press, Indianapolis, Indiana.
Lavocat, R. 1955. Sur une portion de mandibule de Theropode provenant du Crétacé supérieur de Madagascar. Bulletin, Museum of Natural History, Paris 27:256–259.
Madsen, J. H. Jr. 1976a. *Allosaurus fragilis*: a revised osteology. Bulletin of the Utah Geological and Mineral Survey 109:1–163.
Madsen, J. H. Jr. 1976b. A second new theropod dinosaur from the Late Jurassic of East Central Utah. Utah Geology 3(1):51–60.
Madsen Jr., J. H., and S. P. Welles. 2000. *Ceratosaurus* (Dinosauria, Theropoda), a revised osteology. Utah Geological Survey Miscellaneous Publications MP-00–2:1–80.
Madsen, J. H., Jr., J. S. McIntosh, and D. S Berman. 1995. Skull and atlas-axis complex of the Upper Jurassic sauropod *Camarasaurus* Cope (Reptilia: Saurischia). Carnegie Museum of Natural History Bulletin 31:1–115.
Makovicky, P. J., and M. A. Norell. 1998. A partial ornithomimid braincase from Ukhaa Tolgod (Upper Cretaceous, Mongolia). American Museum Novitates 3247:1–16.
Mathur, U. B., and S. Srivastava. 1987. Dinosaur teeth from Lameta Group (Upper Cretaceous) of Kheda District, Gujarat. Journal of the Geological Society of India 29: 554–566.
Mazzetta, G. V., R. A. Fariña, and S. F. Vizcaíno. 2000. On the palaeobiology of the South American horned theropod *Carnotaurus sastrei* Bonaparte. Gaia 18:185–192.
Mazzetta, G. V., P. Christiansen, and R. A. Fariña. 2004. Giants and bizarres: body size of some southern South American Cretaceous dinosaurs. Historical Biology 2004:1–13.
Molnar, R. E. 1991. The cranial morphology of *Tyrannosaurus rex*. Palaeontographic Abteilung A 217: 137–176.
Norell, M. A., P. J. Makovicky, and J. M. Clark. 2004. The braincase of *Velociraptor*; pp. 133–143 in P. J. Currie, E. B. Koppelhus, M. A. Shugar, and J. L. Wright (eds.), Feathered Dragons: Studies on the Transition from Dinosaurs to Birds. Indiana University Press, Indianapolis, Indiana.
Novas, F. E. 1997. Abelisauridae; pp. 1–2 in P. J. Currie and K. Padian (eds.), Encyclopedia of Dinosaurs, Academic Press, San Diego, California.
Novas, F. E., F. L. Agnolin, and S. Bandyopadhyay. 2004. Cretaceous theropods from India: a review of specimens described by Huene and Matley (1933). Revista del Museo Argentino de Ciencias Naturales, Nueva Serie 6(1):67–103.
O'Connor, P. M., 2007. The postcranial axial skeleton of *Majungasaurus crenatissimus* (Theropoda: Abelisauridae) from the Late Cretaceous of Madagascar; pp. 127–162 in S. D. Sampson and D. W. Krause (eds.), *Majungasaurus crenatissimus* (Theropoda: Abelisauridae) from the Late Cretaceous of Madagascar. Society of Vertebrate Paleontology Memoir 8.
O'Donoghue, C. H. 1920. The blood vascular system of the Tuatara, *Sphenodon punctatus*. Philosophical Transactions of the Royal Society of London B 210:175–252.
Oelrich, T. M. 1956. The anatomy of the head of *Ctenosaurua pectinata* (Iguanidae). Miscellaneous Publications, Museum of Zoology, University of Michigan 94:1–122.
Osborn, H. F. 1912. Crania of *Tyrannosaurus* and *Allosaurus*. Memoirs of the American Museum of Natural History 1:1–30.
Ostrom, J. H. 1969. Osteology of *Deinonychus antirrhopus*, an unusual theropod from the Lower Cretaceous of Montana. Bulletin of the Yale Peabody Museum of Natural History 30:1–165.
Parker, W. K. 1866. On the structure and development of the skull in the ostrich tribe. Philosophical Transactions of the Royal Society of London B 156:113–183.
Parker, W. K. 1883. On the structure and development of the skull in the Crocodilia. Transactions of the Zoological Society of London 11: 253–311.
Quay, W. B. 1979. The parietal eye-pineal complex; pp. 245–406 in A, C. Gans (ed.), Biology of the Reptilia, Volume 9. Neurology. Academic Press, New York, New York.
Raath, M. A. 1985. The theropod *Syntarsus* and its bearings on the origin of birds; pp 219- 227 in M. K Hecht, J. H. Ostrom, G. Viohl, and P.

Wellnhofer (eds.), The Beginnings of Birds: Proceedings of the International *Archaeopteryx* Conference, Eichstadt. Freunde des Jura-Museums, Eichstätt, Germany.
Rauhut, O. W. M. 2003. The interrelationships and evolution of basal theropod dinosaurs. Special Papers in Palaeontology 69:1–213.
Rauhut, O. W. M. 2004a. Braincase structure of the Middle Jurassic theropod *Piatnitzkysaurus*. Canadian Journal of Earth Science 41: 1109–1122.
Rauhut, O. W. M. 2004b. Provenance and anatomy of *Genyodectes serus*, a large-toothed ceratosaur (Dinosauria: Theropoda) from Patagonia. Journal of Vertebrate Paleontology 24:894–902.
Rauhut, O. W. M., and R. Fechner. 2005. Early development of the facial region in a non-avian theropod dinosaur. Proceedings of the Royal Society B 272:1179–1183.
Rayfield, E. J. 2005. Aspects of comparative cranial mechanics in the theropod dinosaurs *Coelophysis*, *Allosaurus* and *Tyrannosaurus*. Zoological Journal of the Linnean Society 144:309–316.
Rayfield, E. J., D. B. Norman, C. C. Horner, J. R. Horner, P. M. Smith, J. J. Thomason, and P. Upchurch. 2001. Cranial design and function in a large theropod dinosaur. Nature 409:1033–1037.
Rogers, R. R., J. H. Hartman, and D. W. Krause. 2000. Stratigraphic analysis of Upper Cretaceous rocks in the Mahajanga Basin, northwestern Madagascar: implications for ancient and modern faunas. Journal of Geology 108:275–301.
Rogers, R. R., Krause, D. W., and Curry Rogers, K. 2003. Cannibalism in the Madagascan dinosaur *Majungasaurus crenatissimus*. Nature 422:515–518.
Rogers, R. R., D. W. Krause, K. Curry Rogers, A. H. Rasoamiaramanana, and L. Rahantarisoa. 2007. Paleoenvironment and paleoecology of *Majungasaurus crenatissimus* (Theropoda: Abelisauridae) from the Late Cretaceous of Madagascar; pp. 21–31 in S. D. Sampson and D. W. Krause (eds.), *Majungasaurus crenatissimus* (Theropoda: Abelisauridae) from the Late Cretaceous of Madagascar. Society of Vertebrate Paleontology Memoir 8.
Rogers, S. W. 1998. Exploring dinosaur neuropaleobiology: viewpoint computed tomography scanning and analysis of an *Allosaurus fragilis* endocast. Neuron 21:673–679.
Rogers, S. W. 1999. *Allosaurus*, crocodiles, and birds: evolutionary clues from spiral computed tomography of an endocast. Anatomical Record 257:162–173.
Romer, A. S. 1956. Osteology of the Reptiles. University of Chicago Press, Chicago, Illinois, 772 pp.
Rowe, T., and J. Gauthier. 1990. Ceratosauria; pp. 151–168 in D. B. Weishampel, P. Dodson, and H. Osmólska (eds.), The Dinosauria. University of California Press, Berkeley, California.
Russell, D., 1996. Isolated dinosaur bones from the Middle Cretaceous of the Tafilalt, Morocco. Bulletin Muséum National d'Histoire Naturelle. Paris, séries. 4, C 18:349–402.
Sampson, S. D., M. T. Carrano, and C. A. Forster. 2001. A bizarre predatory dinosaur from Madagascar: implications for the evolution of Gondwanan theropods. Nature 409:504–505.
Sampson, S. D., M. J. Ryan, and D. H. Tanke. 1997. Craniofacial ontogeny in centrosaurine dinosaurs (Ornithischia: Ceratopsidae): taxonomic and behavioral implications. Zoological Journal of the Linnean Society 121:293–337.
Sampson, S. D., C. A. Forster, D. W. Krause, and P. Dodson. 1996a. Non-avian theropod dinosaurs from the Late Cretaceous of Madagascar. Journal of Vertebrate Paleontology 16(3, Supplement):62A.
Sampson, S. D., C. A. Forster, D. W. Krause, and P. Dodson. 1996b. The premaxilla of *Majungasaurus* (Dinosauria: Theropoda), with implications for Gondwanan paleobiogeography. Journal of Vertebrate Paleontology 16:601–605.
Sampson, S. D., L. M. Witmer, C. A. Forster, D. W. Krause, P. M. O'Connor, P. Dodson, and F. Ravoavy. 1998. Predatory dinosaur remains from Madagascar: Implications for the Cretaceous biogeography of Gondwana. Science 280:1048–1051.
Sanders, R. K., and D. K. Smith. 2005. The endocranium of the theropod dinosaur *Ceratosaurus* studied with computed tomography. Acta Palaeontologica Polonica 50:601–616.
Save-Soderbergh, G. 1947. Notes on the brain-case in *Sphenodon* and certain Lacertilia. Zoologiska Bidrag, Uppsala 25:489–516.
Sedlmayr, J. C. 2002. Anatomy, evolution, and functional significance of cephalic vasculature in Archosauria. Ph.D. dissertation, Ohio University, Athens, Ohio, 398 pp.
Sedlmayr, J. C., S. J. Rehorek, E. Legenzoff, and J. Sanjur. 2004. Anatomy of the circadian clock in avesuchian archosaurs. Journal of Morphology 260:327.
Sereno, P. C. 1999. The evolution of dinosaurs. Science 284:2137–2147.
Sereno, P. C., and F. E. Novas 1993. The skull and neck of the basal theropod *Herrerasaurus ischigualastensis*. Journal of Vertebrate Paleontology 13:451–476.
Sereno, P. D., J. Conrad, and J. Wilson. 2002. Abelisaurid theropods from Africa: Phylogenetic and biogeographic implications. Journal of Vertebrate Paleontology 22(3, Supplement):106A.
Sereno, P. C., J. A. Wilson, and J. L. Conrad. 2004. New dinosaurs link southern landmasses in the Mid-Cretaceous. Proceedings of the Royal Society B 271:1325–1330.
Sereno, P. C., D. B. Dutheil, M. Iarochene, H. C. E. Larsson, G. H. Lyon, P. M. Magwene, C. A. Sidor, D. J. Varricchio, and J. A. Wilson. 1996. Predatory dinosaurs from the Sahara and Late Cretaceous faunal differentiation. Science 272:986–991.
Smith, J. B. 2007. Dental morphology and variation in *Majungasaurus crenatissimus* (Theropoda: Abelisauridae) from the Late Cretaceous of Madagascar; pp. 103–126 in S. D. Sampson and D. W. Krause (eds.), *Majungasaurus crenatissimus* (Theropoda: Abelisauridae) from the Late Cretaceous of Madagascar. Society of Vertebrate Paleontology Memoir 8.
Starck, D. 1979. Cranio-cerebral relationsin Recent reptiles; pp. 1–38 in C. Gans (ed.), Biology of the Reptilia, Volume 9, Neurology A. Academic Press, New York, New York.
Stromer, E., and W. Weiler. 1930. Ergebnisse der Forschungsreisen Prof. E. Stromers in den Wüsten Ägyptens. VI. Beschreibung von Wirbeltier-Resten aus dem nubischen Sandsteine Oberägyptens und aus ägyptischen Phosphaten nebst Bemerkungen über die Geologie der Umgegend von Mahamîd in Oberägypten. Abhandlungen der Bayerischen Akademie der Wissenschaften Mathematisch-naturwissenschaftliche Abteilung, Neue Folge 7: 1–42.
Sues, H.-D. 1980. A pachycephalosaurid dinosaur from the Upper Cretaceous of Madagascar and its paleobiogeographical implications. Journal of Paleontology 54:954–962.
Sues, H.-D., and P. Taquet. 1979. A pachycephalosaurid dinosaur from Madagascar and a Laurasia-Gondwanaland connection in the Cretaceous. Nature 279:633–635.
Tarsitano, S. F. 1985. Cranial metamorphosis and the origin of the Eusuchia. Neues Jahrbuch für Geologie und Paläontologie, Abhandlungen 170:27–44.
Therrien, F., D. M. Henderson, and C. B. Ruff. 2005. Bite me: biomechanical models of theropod mandibles and implications for feeding behavior; pp. 179–237 in K. Carpenter (ed.), The Carnivorous Dinosaurs. Indiana University Press, Indianapolis, Indiana.
Tsuihiji, T. 2004. The ligament system in the neck of *Rhea americana* and its implication for the bifurcated neural spines of sauropod dinosaurs. Journal of Vertebrate Paleontology 24:165–172.
Tsuihiji, T. 2005. Homologies of the transversospinalis muscles in the anterior presacral region of Sauria (crown Diapsida). Journal of Morphology 263:151–178.
Van Valkenburgh, B. 1988. Trophic diversity in past and present guilds of large predatory mammals. Paleobiology 2:155–173.
Van Valkenburgh, B., and R. E. Molnar. 2002. Dinosaurian and mammalian predators compared. Paleobiology 28:527–543.
Varricchio, D. J. 2001. Gut contents from a Cretaceous tyrannosaurid: implications for theropod digestive tracts. Journal of Paleontology 75:401–406.
Walker, A. D. 1961. Triassic reptiles from the Elgin Area: *Stagonolepis*, *Dasygnathus* and their allies. Philosophical Transactions of the Royal Society of London B 244:103–204.
Walker, A. D. 1990. A revision of *Sphenosuchus acutus* Haughton, a crocodylomorph reptile from the Elliot Formation (late Triassic or early Jurassic) of South Africa. Philosophical Transactions of the Royal Society of London B 330:1–120.
Welles, S. P. 1984. *Dilophosaurus wetherilli* (Dinosauria, Theropoda) osteology and comparisons. Palaeontographica Abteilung A 185(4–6):85–180.
Wettstein, O. von. 1954. Crocodilia; pp. 236–424 in W. Kükenthal, T. Krumbach, J.-G. Helmcke, and H. von Lengerken (eds.), Handbuch der Zoologie: eine Naturgeschichte der Stämme der Tierrieches, Volume 7: Sauropsida: Allgemeines Reptilia, Aves. de Gruyter, Berlin.
Wharton, D. S. 2002. The evolution of the avian brain. Ph.D. dissertation, University of Bristol, Bristol, England, 342 pp.

Wilson, J. A., P.C. Sereno, S. Srivastava, D. K. Bhatt, A. Khosla, and A. Sahni. 2003. A new abelisaurid (Dinosauria: Theropoda) from the Lameta Formation (Cretaceous, Maastrichtian) of India. Contributions to the Museum of Paleontology, University of Michigan 31(1): 1–42.

Witmer, L. M. 1990. The craniofacial air sac system of Mesozoic birds (Aves). Zoological Journal of the Linnean Society 100:327–378.

Witmer, L. M. 1995. Homology of facial structures in extant archosaurs (birds and crocodilians), with special reference to paranasal pneumaticity and nasal conchae. Journal of Morphology 225:269–327.

Witmer, L. M. 1997a. The evolution of the antorbital cavity of archosaurs: a study in soft-tissue reconstruction in the fossil record with an analysis of the function of pneumaticity. Society of Vertebrate Paleontology Memoir 3:1–73.

Witmer, L. M. 1997b. Craniofacial air sinus systems; pp. 151–159 in P. J. Currie and K. Padian (eds.), Encyclopedia of Dinosaurs. Academic Press, New York, New York.

Witmer, L. M., and W. D. Maxwell. 1996. The skull of *Deinonychus* (Dinosauria: Theropoda): new insights and implications. Journal of Vertebrate Paleontology 16(3, Supplement):73A.

Witmer, L. M., and R. C. Ridgely. In press. The Cleveland tyrannosaur skull (*Nanotyrannus* or *Tyrannosaurus*): new findings based on CT scanning, with special reference to the braincase. Kirtlandia.

Witmer, L. M., S. Chatterjee, J. Franzosa, and T. Rowe. 2003. Neuroanatomy of flying reptiles and implications for flight, posture and behavior. Nature 425:950–953.

Xu, X., and X.-C Wu. 2001. Cranial morphology of *Sinornithosaurus millenii* Xu et al. 1999 (Dinosauria: Theropoda: Dromaeosauridae) from the Yixian Formation of Liaoning, China. Canadian Journal of Earth Sciences 38:1939–1752.

Zhao, X-J., and P. J. Currie. 1994. A large crested theropod from the Jurassic of Xinjiang, People's Republic of China. Canadian Journal of Earth Sciences 30:2027–2036.

Submitted June 15, 2005; accepted January 5, 2007.

APPENDIX 1. List of abbreviations.

A, angular
a, angular contact
ac, adductor chamber
af, adductor fossa
al, alveolus
ame, attachment site of (M.) adductor mandibulae externus
aoc, antotic crest
aof, antorbital fossa
aofe, internal antorbital fenestra
ap, auricular process of nasal
aps, angular process of splenial
apsa, angular process of surangular
AR, articular
ar, articular contact
arp, articular process of prearticular
ascr, ascending ramus of maxilla
B, Basioccipital
bect, body of ectopterygoid
bpt, basipterygoid process
BS, basisphenoid
bs, basisphenoid contact
bsr, basisphenoid recess in skull or endocast
bt, basal tuber
c, coronoid contact(?)
cap, capitate process of laterosphenoid
car, endocast of cerebral carotid artery
cav, endocast of cavernous sinus (a venous sinus)
cc, cerebral carotid artery canal
cer, endocast of cerebral hemisphere
cf, caudal fossa of quadratojugal ramus of quadrate
ch, choanae
cmf, caudal median fossa
cor, columellar (stapedial) recess
cp, cornual process
crc, crus communis of osseous labyrinth
csc, caudal semicircular canal of osseous labyrinth
csca, ampulla of caudal semicircular canal of osseous labyrinth
csaf, caudal surangular foramen
ct, crista tuberalis of otoccipital
ctf, chorda tympani foramen
cup, cultriform process
cvl, crista ventrolateralis of basisphenoid
D, dentary
d, dentary contact
df, dental foramina
dg, dermal groove (separating distinct ornamentation fields)
dls, endocast of dorsal longitudinal (sagittal) sinus, a dural venous sinus
dm, attachment site of (M.) depressor mandibulae
dqjp, dorsal quadratojugal process
dqjr, dorsal quadratojugal ramus
dr, dermal rugosity
dsap, dorsal surangular process of dentary
dtf, dorsotemporal fenestra
dtfo, dorsotemporal fossa
eaof, margin of external antorbital fenestra
ecc, endocranial cavity
ECT, ectopterygoid
ect, ectopterygoid contact
ectr, ectopterygoid ramus of pterygoid
emf, external mandibular fenestra
epi, epipterygoid contact
F, frontal
f, frontal contact
fc, position of fenestra cochleae (pseudorotunda) in osseous labyrinth
fio, fonticulus interorbitalis
fl, endocast of flocculus (cerebellar auricle) and floccular vein
fm, foramen magnum
foa, fissure between oculomotor and abducens foramina leading to cavernous sinus
fr, frontal recess in skull or endocast
fv, position of fenestra vestibuli (ovalis) in osseous labyrinth
gl, glenoid of lower jaw
gr, gingival region of dentary
h, head of quadrate
iaof, margin of internal antorbital fenestra
idp, interdental plates
ids, interdentary symphysis
imf, internal mandibular fenestra
intgl, interglenoid ridge
ios, interorbital septum
ips, interpremaxillary symphysis
isap, intermediate surangular process of dentary
J, jugal
j, jugal contact
jp, jugal process of ectopterygoid
L, lacrimal
l, lacrimal contact
lab, osseous labyrinth
lag, lagena (cochlear duct) of osseous labyrinth
lc, lateral quadrate condyle
lg, lateral glenoid of mandible
lp, lacrimal process of jugal
lpr, lacrimal pneumatic recess
LS, laterosphenoid
ls, laterosphenoid contact
lsc, lateral semicircular canal of osseous labyrinth
lsca, ampulla of lateral semicircular canal of osseous labyrinth
lsd, lateral sulcus of dentary
lssa, surangular lateral shelf
ltf, laterotemporal fenestra
M, maxilla
m, maxilla contact
ma, muscle attachment surface
mc, medial quadrate condyle
mg, medial glenoid of mandible
mnf, medial nasal pneumatic fossa of lacrimal
mp, maxillary process of premaxilla
mr, median ridge of nasal
mra, medial ridge of angular
N, nasal
n, nasal contact
na, bony naris
nf, narial fossa
nlc, nasolacrimal canal
np, nasal process of premaxilla
nr, nasal pneumatic recess
nvf, neurovascular foramen
o, orbit
ob, endocast of olfactory bulb
oc, occipital condyle
ocs, endocast of occipital dural venous sinus
OS, orbitosphenoid
osc, otosphenoidal crest
OT, otoccipital (exoccipital-opisthotic)
ot, contact with paroccipital process of otoccipital
otc, olfactory tract cavity in skull or on cranial endocast
P, parietal
p, parietal contact
PA, palatine
pa, palatine contact
pab, body of palatine
paroc, paroccipital process of otoccipital
pb?, possible pathologic bone
pcr, paracondylar recess
pe, parietal eminence
PF, portion of lacrimal to which the prefrontal may be fused
pf, pneumatic fossa within medial nasal fossa of lacrimal
pfo, pituitary (hypophyseal) fossa
pin, endocast of dural peak probably marking the position of the pineal gland
pit, endocast of pituitary (hypophyseal) fossa
PM, premaxilla
pm, premaxilla contact
pmf, promaxillary fenestra
PO, postorbital
po, postorbital contact
pop, postorbital process of jugal
pos, preorbital strut
pp, parietal process of squamosal
ppm, palatal process of maxilla
ppp, palatal process of premaxilla
pqp, postquadratic process of squamosal
PR, prootic
PRE, prearticular
pre, prearticular contact
presap, surangular process of prearticular
prf, socket or contact for prefrontal prong
prp, preotic pendant (= ala basiphenoidalis)
PT, pterygoid
pt, pterygoid contact
ptb, body of pterygoid
ptf, posttemporal foramen
ptpaf, pterygopalatine fenestra
ptpect, pterygoid process of ectopterygoid
ptppa, pterygoid process of palatine
ptr, pterygoid ramus of quadrate
Q, quadrate
q, quadrate contact
qc, quadrate cotyle
QJ, quadratojugal
qj, quadratojugal contact
qjp, quadratojugal process (= ventral ramus) of squamosal
qjr, quadratojugal ramus of quadrate
qp, quadrate process of quadratojugal
qr, quadrate ramus of pterygoid
qs, quadrate shaft
reg, rostral groove on crista tuberalis of otoccipital
retro, retroarticular process
retrofo, retroarticular fossa
rf, rostral fossa of quadratojugal ramus of quadrate
rp, rostral processes of splenial
rqjr, rostral quadratojugal ramus
rr, rostral ramus of lacrimal
rsaf, rostral surangular foramen
rsc, rostral semicircular canal of osseous labyrinth
rsca, ampulla of rostral semicircular canal of osseous labyrinth
rtr, rostral tympanic recess in skull or endocast
rtrc, rostral tympanic recess, caudal chamber or diverticulum, in skull or endocast
S, squamosal
s, squamosal contact
SA, surangular
sa, surangular contact
sc, sagittal crest
sd, supradentary contact
sep, septum
sf, splenial foramen
sfo, fossa for reception of rostral process of surangular
sg, stapedial groove
sk, sagittal keel of nasal
snc, sagittal nuchal crest
SO, supraoccipital
sof, suborbital fenestra
sop, suborbital process
sot, supraoccipital tuberosity
sp, squamosal process of postorbital
SPH, sphenethmoid
spha, foramen for or endocast of sphenoidal artery
SPL, splenial
spl, splenial contact
sq, squamosal contact
sr, splenial ridge of dentary
ssr, subsellar recess in skull or endocast
sut, suture
tnc, transverse nuchal crest
toc, vertical crest on medial side of postorbital separating temporal and orbital regions
ts, endocast of transverse sinus, a dural venous sinus
tub, tuberosity on otosphenoidal crest
v, vomer contact(?)
vc, endocast of venous canal
vcd, foramen for or endocast of dorsal head vein (vena capitis dorsalis)
vcm, foramen for or endocast of middle cerebral vein (vena cerebralis media)
ve, vestibule of osseous labyrinth
vls, ventral longitudinal (sagittal) sinus
vp, ventral prong of surangular
vpar, vomeropalatine ramus
vptp, vomeropterygoid process
vqjp, ventral quadratojugal process
vs, ventral shelf of pterygoid ramus of quadrate
vsap, ventral surangular process of dentary